NIOSH

IC 9446 INFORMATION CIRCULAR/1997

Proceedings: New Technology for Ground Control in Retreat Mining

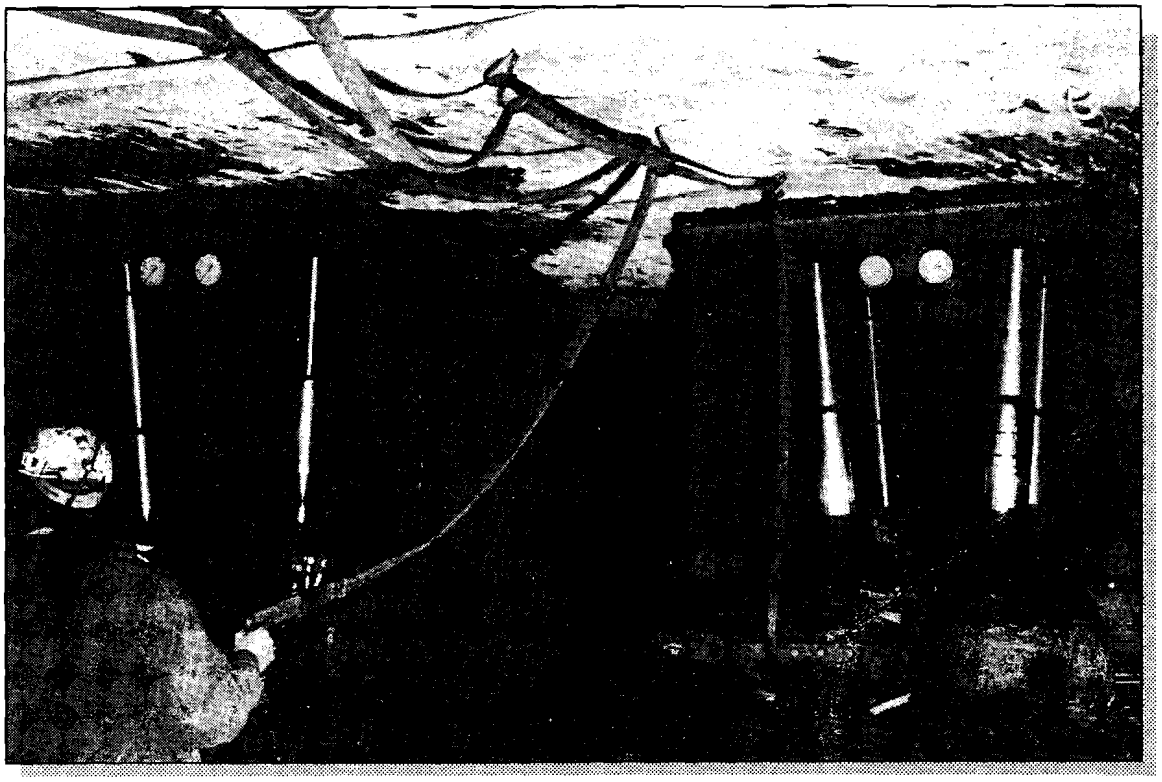

U.S. DEPARTMENT OF HEALTH AND HUMAN SERVICES
Public Health Service
Centers for Disease Control and Prevention
National Institute for Occupational Safety and Health

CDC
CENTERS FOR DISEASE CONTROL AND PREVENTION

Cover photo: Pillar extraction using mobile roof supports.

Information Circular 9446

Proceedings: New Technology for Ground Control in Retreat Mining

Christopher Mark, Ph.D., and Robert J. Tuchman

U.S. DEPARTMENT OF HEALTH AND HUMAN SERVICES
Public Health Service
Centers for Disease Control and Prevention
National Institute for Occupational Safety and Health
Pittsburgh, PA and Spokane, WA Research Centers

March 1997

International Standard Serial Number
ISSN 1066-5552

CONTENTS

Page

Abstract 1
A Statistical Overview of Retreat Mining of Coal Pillars in the United States, by C. Mark, Ph.D., F. E. McCall, and D. M. Pappas 2

PILLAR DESIGN

Analysis of Retreat Mining Pillar Stability (ARMPS), by C. Mark, Ph.D., and F. E. Chase 17
Preventing Massive Pillar Collapses in Coal Mines, by C. Mark, Ph.D., F. E. Chase, and R. K. Zipf, Jr., Ph.D. 35
Pillar Design and Coal Strength, by C. Mark, Ph.D., and T. M. Barton 49
A New Laminated Overburden Model for Coal Mine Design, by K. A. Heasley 60

MOBILE ROOF SUPPORTS

Retreat Mining With Mobile Roof Supports, by F. E. Chase, A. McComas, C. Mark, Ph.D., and C. D. Goble 74
Monitoring Mobile Roof Supports, by K. E. Hay, S. P. Signer, M. E. King, and J. K. Owens 89
Full-Scale Performance Evaluation of Mobile Roof Supports, by T. M. Barczak and D. F. Gearhart 99

UNIT OF MEASURE ABBREVIATIONS USED IN THIS REPORT

cm	centimeter	lbf	pound (force)
ft	foot	m	meter
ft/min	foot per minute	m/min	meter per minute
ft^2	square foot	m^2	square meter
ft^3	cubic foot	m^3	cubic meter
GPa	gigapascal	min	minute
ha	hectare	mm	millimeter
in	inch	MPa	megapascal
in^2	square inch	psi	pound (force) per square inch
kg	kilogram	st	short ton
kips/in	kips per inch	st/h	short ton per hour
kN	kilonewton	t	ton (metric)
kN/cm	kilonewton per centimeter	%	percent
kPa	kilopascal	°	degree
lb	pound		

Mention of any company name or product does not constitute endorsement by the National Institute for Occupational Safety and Health.

To receive other information about occupational safety and health problems, call
1-800-35-NIOSH (1-800-356-4674), or
visit the NIOSH Home Page on the World Wide Web at
http://www.cdc.gov/niosh/homepage.html

DISCLAIMER OF LIABILITY

The National Institute for Occupational Safety and Health expressly declares that there are no warranties, express or implied, that apply to the software described herein. By acceptance and use of said software, which is conveyed to the user without consideration by the National Institute for Occupational Safety and Health, the user hereof expressly waives any and all claims for damage and/or suits for or by reason of personal injury or property damage, including special, consequential, or other similar damages arising out of or in any way connected with the use of the software described herein.

PROCEEDINGS: NEW TECHNOLOGY FOR GROUND CONTROL IN RETREAT MINING

Compiled by Christopher Mark, Ph.D.,[1] and Robert J. Tuchman[2]

ABSTRACT

This proceedings volume contains papers presented at technology transfer seminars sponsored by the National Institute for Occupational Safety and Health (NIOSH) on New Technology for Ground Control in Retreat Mining. The seminars were conducted at five locations: Uniontown, PA (March 26, 1997), Norton, VA (April 8, 1997), Pikeville, KY (April 10, 1997), Charleston, WV (April 17, 1997), and Evansville, IN (April 22, 1997).

The papers presented here describe several new, highly practical technologies developed by the NIOSH Pittsburgh and Spokane Research Centers[3] to improve safety during pillar retreat operations. Two central issues are addressed: pillar design and mobile roof supports (MRS's).

Proper pillar sizing is essential for safe pillar extraction. The Analysis of Retreat Mining Pillar Stability (ARMPS) program and its large data base of actual mining case histories are presented. LAMODEL, a second computer program, can be used for analysis of multiple-seam and other complex mining situations. Other papers address pillar design to avoid massive pillar collapses and the proper role of coal strength testing.

MRS's have greatly improved safety where they are used for pillar line support. We studied the application of MRS's at 20 mines throughout the Eastern United States. Conclusions regarding the most effective section layouts, cut sequences, and support placements are reported. Field and laboratory tests of MRS's are also described.

[1]Mining engineer.

[2]Technical writer-editor.

Pittsburgh Research Center, National Institute for Occupational Safety and Health, Pittsburgh, PA.

[3]The research described in these papers originated under the former U.S. Bureau of Mines prior to transferring to the National Institute for Occupational Safety and Health in 1996.

A STATISTICAL OVERVIEW OF RETREAT MINING OF COAL PILLARS IN THE UNITED STATES

By Christopher Mark, Ph.D.,[1] Frank E. McCall,[1] and Deno M. Pappas[2]

ABSTRACT

The demographics and safety record of the pillar retreat segment of the U.S. coal industry was analyzed using statistics collected by the Mine Safety and Health Administration. Pillar recovery is practiced primarily by mines in Appalachia and the Midwest. Using 1993 data, the accident rates and productivity of a large sample of pillar retreat mines were found to be similar to other room-and-pillar mines in the same geographic areas. Pillar recovery apparently accounts for about 10% of all U.S. underground production, but has been associated with about 25% of the roof and rib fatalities during 1989-96. However, of the 28 fatalities that were analyzed, only 4 occurred for which no citations were issued for violations of mining law. Nearly one-half of the fatal incidents occurred during the mining of the last lift or pushout. All four no-citation incidents occurred during the removal of the last lift during a "Christmas tree" extraction sequence.

[1]Mining engineer.
[2]Civil engineer.
Pittsburgh Research Center, National Institute for Occupational Safety and Health, Pittsburgh, PA.

INTRODUCTION

Pillar recovery has always been an integral part of U.S. underground coal mining. It can be a less capital-intensive, more flexible alternative to longwall mining for small, irregular reserves [Blaiklock 1992]. It is often employed in deeper, high-value seams where recovery rates would be unacceptably low if only development room-and-pillar mining was conducted.

The process of pillar recovery removes the main support to the overburden and allows the ground to cave. As a result, the pillar line is an extremely complex and high-stress rock mechanics environment. Historically, retreat mining has accounted for a large number of fatal roof fall accidents. During 1978-86, 67 roof fall fatalities were attributed to retreat mining, representing 29% of the total. Of the pillaring fatalities, 49% occurred during the mining of the final stump [Montague 1988]. Nevertheless, there has apparently never been a detailed study of the demographics and safety record of pillar retreat mining. This study attempts to fill the gap.

The overview presented here is based almost entirely on information collected by the Mine Safety and Health Administration (MSHA). Three primary sources were used:

- *MSHA Accident and Employment Data Base:* This data base contains information on the employment and production of all U.S. operating coal mines. It also contains information on all accidents reported to MSHA.
- *Data Base of Retreat Mines:* In 1993, MSHA formed the Mine Ventilation Bleeder and Gob Training Committee. Part of the committee's work was to survey the nine bituminous coal MSHA health and safety districts about the practices of their mines. The survey identified 186 nonlongwall mines that were maintaining an active gob and that produced more than 4,500 t (5,000 st) in 1993 [Urosek et al. 1995]. These mines were approximately evenly divided between those that practiced full-pillar recovery and those that were limited to partial pillar extraction. An additional 181 mines had ventilated, inactive gobs. Some had permanently ceased retreat mining, others were developing for pillar recovery operations when they were surveyed. Therefore, the 186 active gob mines represent a large sample of the total retreat mine population. The identification numbers of these mines were the key to making comparisons using the MSHA Accident and Employment Data Base.
- *Fatal Accident Reports:* Since 1988, a total of 25 accidents resulting in 33 fatalities have occurred during pillar recovery operations. MSHA prepared detailed Reports of Investigation on all but the most recent of these fatal incidents, and the reports were subjected to in-depth analyses.

DEMOGRAPHICS AND ACCIDENT RATES

Table 1 compares basic statistics for 1993 for three segments of the U.S. underground coal industry: (1) longwall mines, (2) all room-and-pillar mines, and (3) the sample of 186 room-and-pillar retreat mines.

Table 1 and figures 1-2 show that the sample of retreat mines employed 9,129 miners and produced 56 million t (61.7 million st) in 1993, representing 18% of the total underground production. The 56 million t (61.7 million st) includes both

Table 1.— Demographics and accident statistics for U.S. underground coal mines by mine type[1]

Mine type	No. of mines	No. of employees	Average mine size (employees)	Tons, thousand st	Productivity, st/h	Total accident rate [2]	Roof/rib accident rate [2]	Total days lost rate [3]	Roof/rib days lost rate [3]
Room-and-pillar [4] . . .	1,014	33,073	33	214,299	3.45	15.92	1.44	451	41
Retreat [5]	186	9,129	49	61,701	3.27	15.58	1.14	432	29
Longwall	69	15,419	223	133,132	4.16	13.39	1.00	410	29
Entire industry	1,083	48,491	45	347,430	3.69	15.06	1.29	437	37

[1]Excludes anthracite mines and mines producing less than 5,000 st.
[2]Accident rates are calculated as the total number of injury accidents (severity 1-6) per 200,000 hours worked.
[3]Days lost rates are calculated as the total number of days lost due to injury per 200,000 hours worked.
[4]Room-and-pillar mines include all nonlongwall mines.
[5]Retreat mines are the 186 nonlongwall mines with active gobs identified by Urosek et al. [1995].

Source: MSHA Accident and Employment Data Base for 1993.

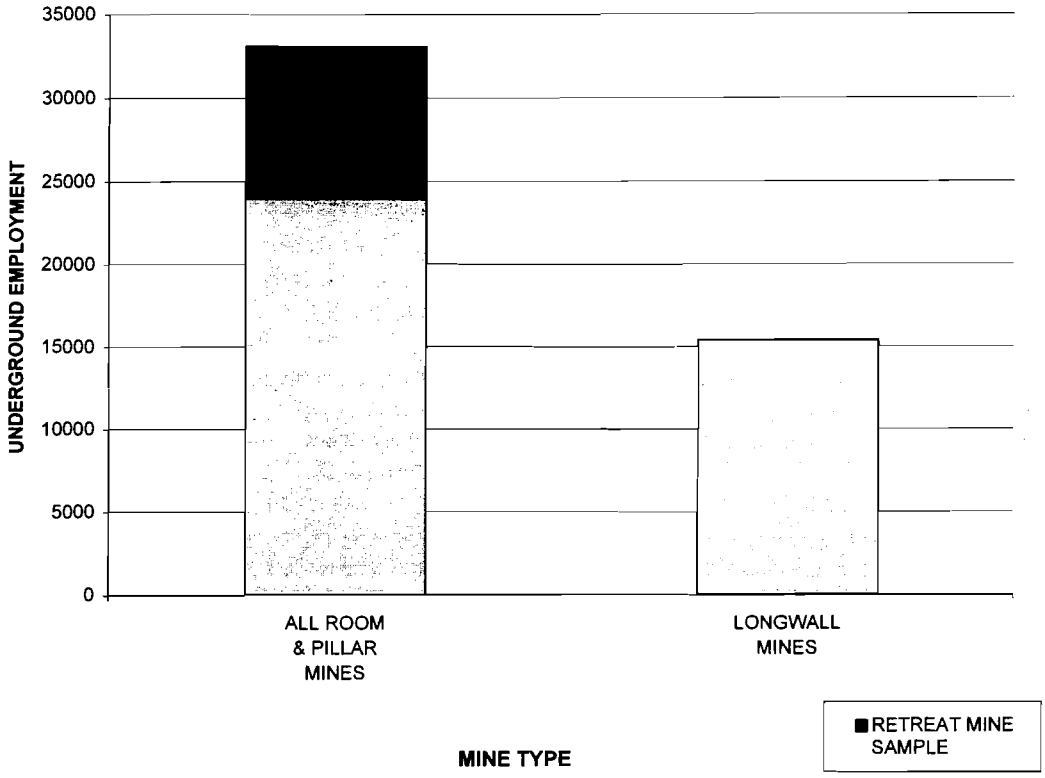

Figure 1.—Employment at U.S. underground coal mines in 1993, by mine type.

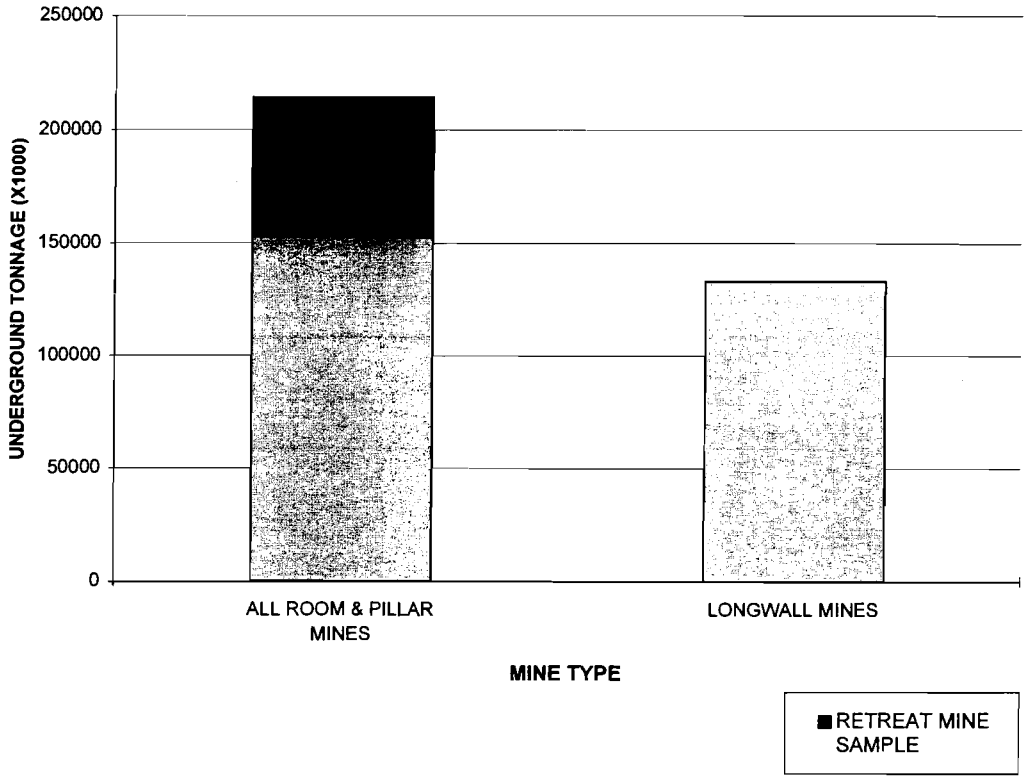

Figure 2.—Production at U.S. underground coal mines in 1993, by mine type.

development and retreat tonnage. A reasonable estimate is that pillar recovery operations account for about one-third of coal production from retreat mines [Reese et al. 1978]. Including some contribution from the mines with inactive ventilated gobs, it appears that pillar recovery may have accounted for about 10% of the 315 million t (347 million st) mined underground in 1993.

An average of 49 miners were employed at each pillar retreat mine, slightly more than at the typical room-and-pillar mine, but much less than at a longwall mine. The accident statistics in figure 3 show that, overall, the injury record of retreat mines was similar to that of other mining methods. Surprisingly, roof and rib accident rates in figure 4 were 21% *lower* at retreat mines than at other room-and-pillar mines. One possible explanation is that roof bolting, which is a significant source of roof fall injuries, is seldom employed during retreat mining. The rates for days lost from all accidents closely paralleled the overall accident rates.

Some regional trends are shown in table 2 and figures 5-6. It appears that retreat mining was widely practiced throughout the Appalachian and midwestern U.S. coal mining areas. The only MSHA districts with few active pillar recovery operations were District 3 (northern West Virginia), District 9 (primarily Colorado, Wyoming, and Utah), and District 10 (western Kentucky).

The largest number of retreat mines were found in the southern Appalachian coalfields (MSHA District 4 in southern West Virginia; District 5 in Virginia; District 6 in eastern Kentucky; and District 7 in eastern Kentucky and Alabama). These four MSHA districts accounted for 156 mines, or 85% of the sample. The retreat mines in this region were typically smaller than those in other districts, averaging 40 employees each, compared with 83 in the average mine outside the region.

Accident rates vary from MSHA district to district, as shown in figure 7. Within each district, they tend to be similar between the retreat mine sample and all room-and-pillar mines. Roof and rib accident rates were lower in 1993 at the retreat mines in six of the eight districts.

Table 3 and figure 8 show that retreat mines tended to be larger than the average room-and-pillar mines. Only 15% of all small mines were conducting active pillar recovery operations, whereas about 40% of all medium and large mines were recovering pillars.[3] Accident rates did not show any significant trends with regard to mine size.

[3]Small mines are those employing fewer than 50 workers; medium mines employ 50 to 150 workers; large mines employ more than 150 workers.

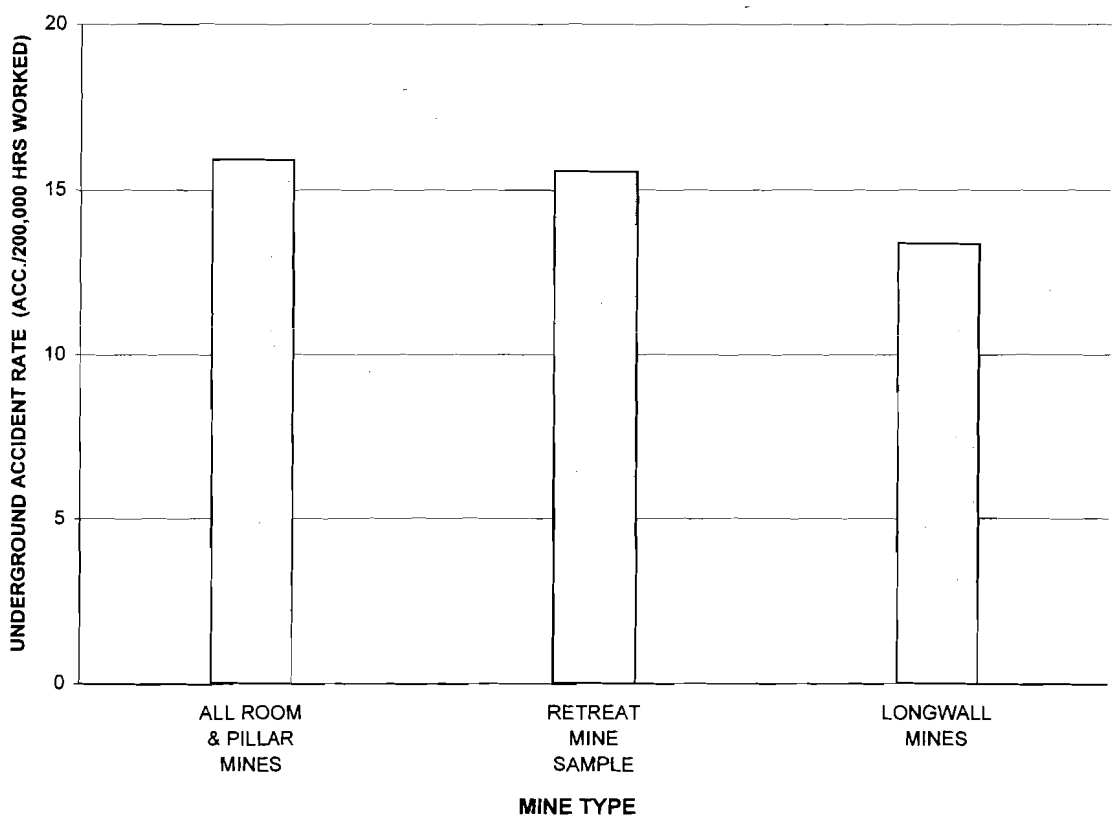

Figure 3.—Accident rate at U.S. underground coal mines in 1993, by mine type.

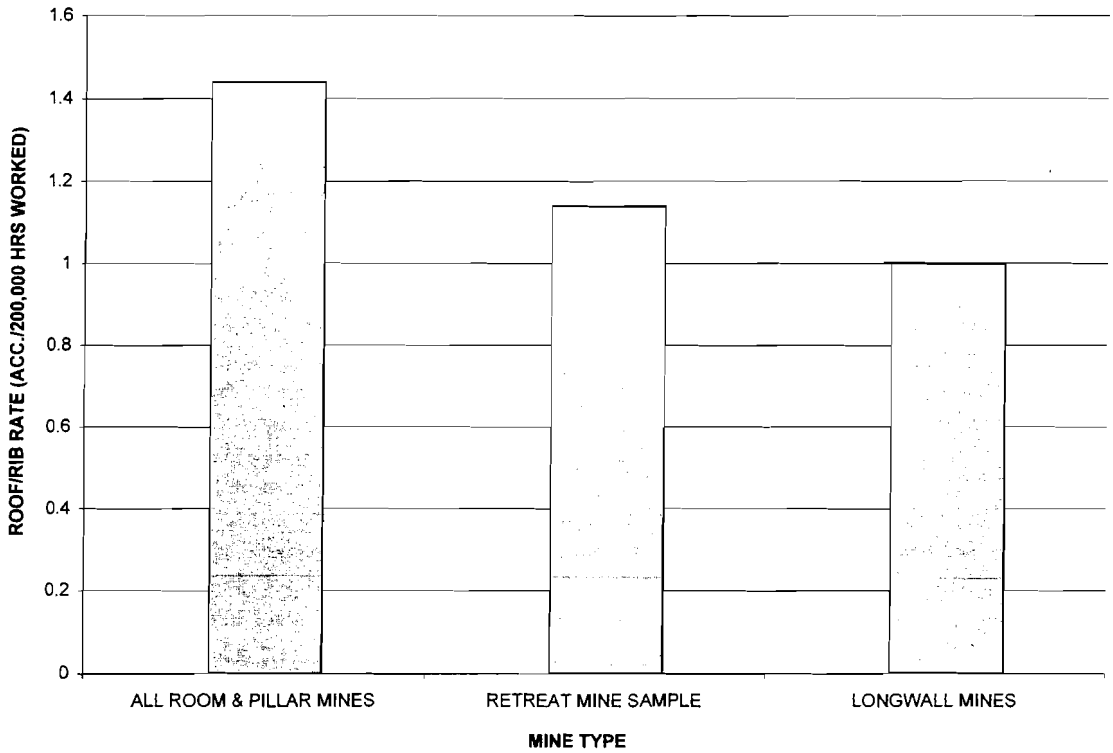

Figure 4.—Roof/rib accident rates at U.S. underground coal mines in 1993, by mine type.

Table 2.—Demographics and accident statistics for U.S. underground coal mines by MSHA district[1]

MSHA District No.	No. of mines	No. of employees	Average mine size (employees)	Tons, thousand st	Productivity, st/h	Total accident rate [2]	Roof/rib accident rate [2]	Total days lost rate [3]	Roof/rib days lost rate [3]
				RETREAT [4]					
2	13	1,029	79	4,495	2.10	27.40	1.31	942	24
3	7	240	34	1,702	3.46	10.15	0.41	145	11
4	57	2,184	38	15,260	3.60	15.91	1.37	592	47
5	37	1,215	33	7,504	2.91	11.64	0.78	230	13
6	28	948	34	7,525	3.74	15.22	1.49	302	21
7	34	1,878	55	12,069	2.99	13.31	0.84	271	15
8	8	1,323	165	9,755	3.64	16.48	1.42	387	38
9	7	314	45	3,388	4.83	6.56	0.86	330	78
10	0	0	0	0	0	0	0	0	0
				ROOM-AND-PILLAR [5]					
2	52	2,122	41	11,134	2.66	26.34	1.15	785	31
3	60	1,720	29	11,093	3.38	11.50	0.85	306	33
4	256	7,490	29	49,797	3.80	16.31	1.64	564	56
5	164	4,090	25	21,465	2.82	12.97	1.24	456	37
6	228	5,447	24	34,356	3.65	16.42	1.82	400	50
7	192	6,069	32	37,087	3.08	14.34	1.11	309	20
8	23	3,443	150	25,435	3.75	17.27	1.41	466	37
9	20	836	42	8,061	4.37	10.30	1.08	317	36
10	19	1,856	98	15,685	4.07	16.88	2.29	413	65

[1]Excludes anthracite mines and mines producing less than 5,000 st.
[2]Accident rates are calculated as the total number of injury accidents (severity 1-6) per 200,000 hours worked.
[3]Days lost rates are calculated as the total number of days lost due to injury per 200,000 hours worked.
[4]Retreat mines are the 186 nonlongwall mines with active gobs identified by Urosek et al. [1995].
[5]Room-and-pillar mines include all nonlongwall mines.

Source: MSHA Accident and Employment Data Base for 1993.

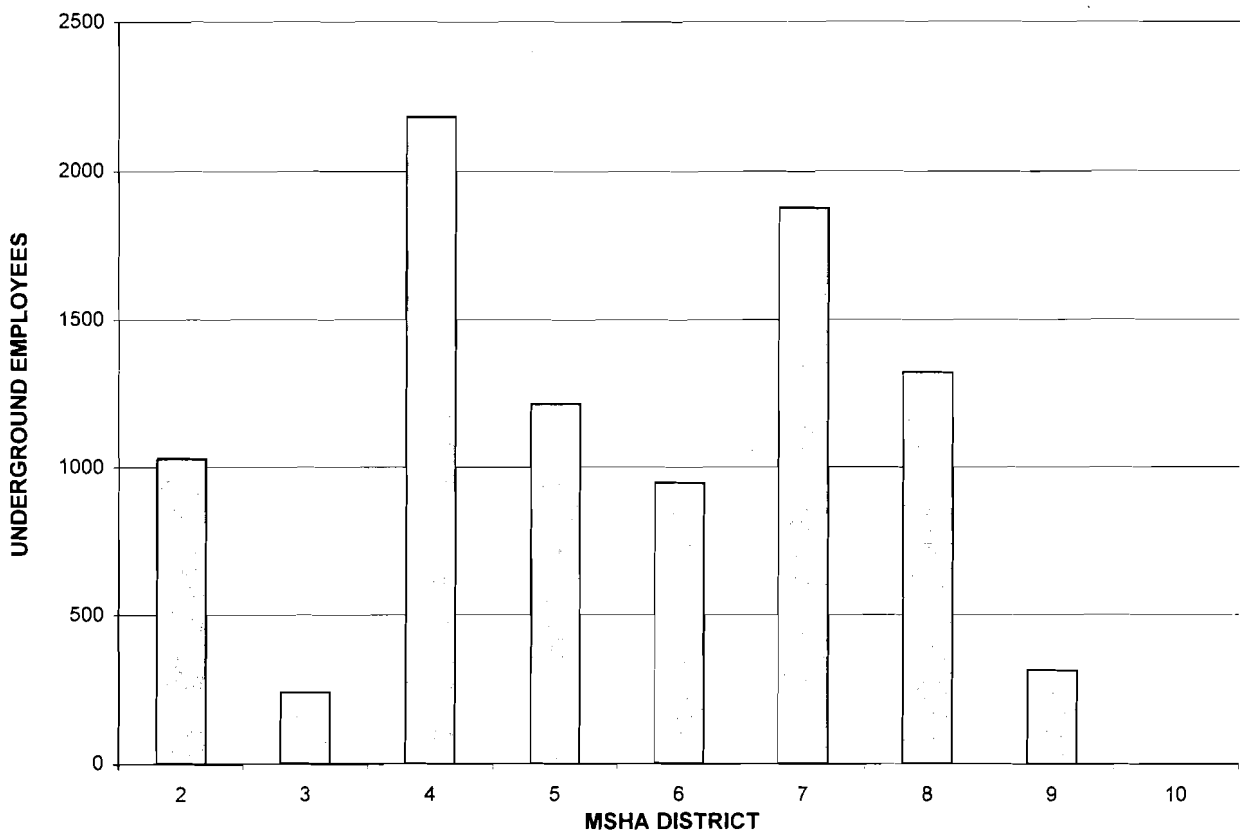

Figure 5.—Employment at sample retreat mines, by MSHA district.

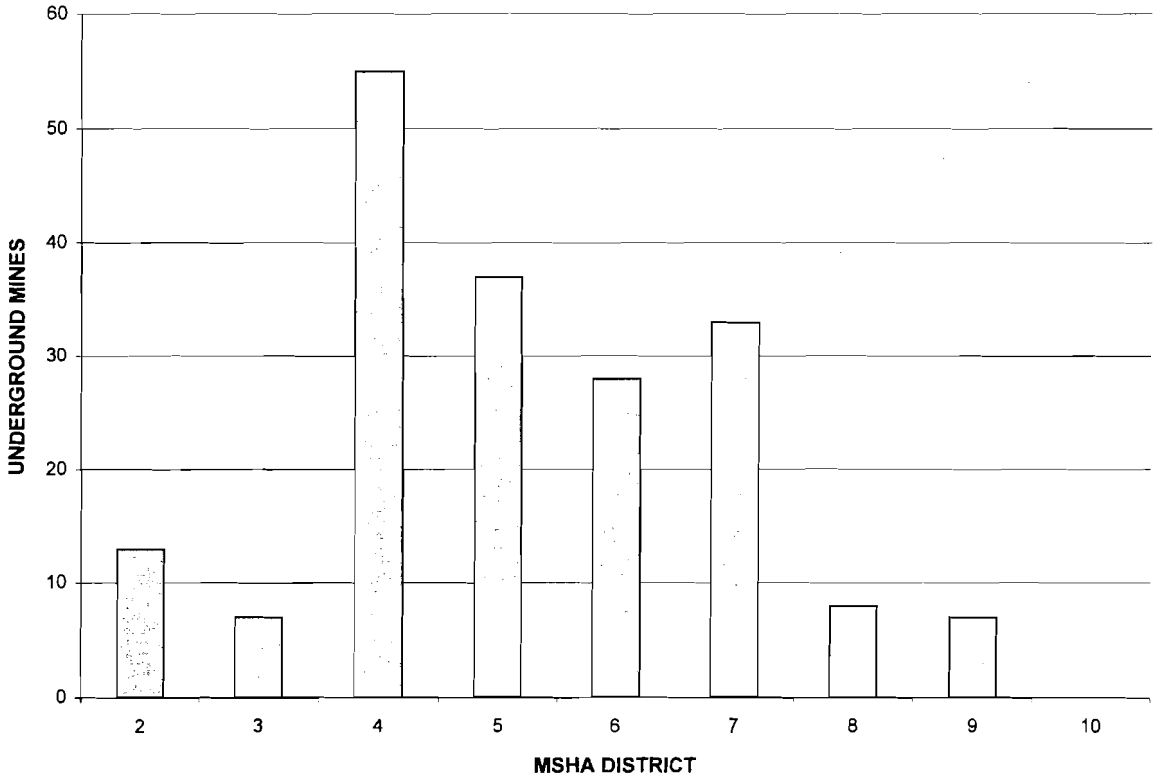

Figure 6.—Number of sample retreat mines, by MSHA district.

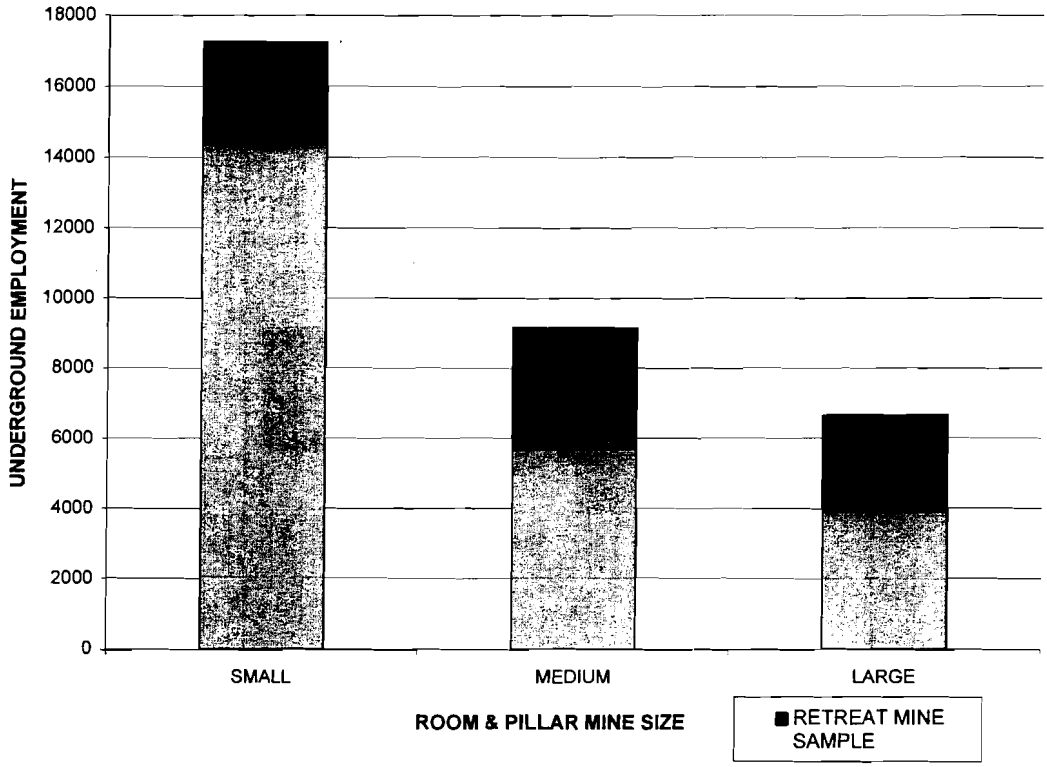

Figure 7.—Employment at retreat and all room-and-pillar mines, by mine size.

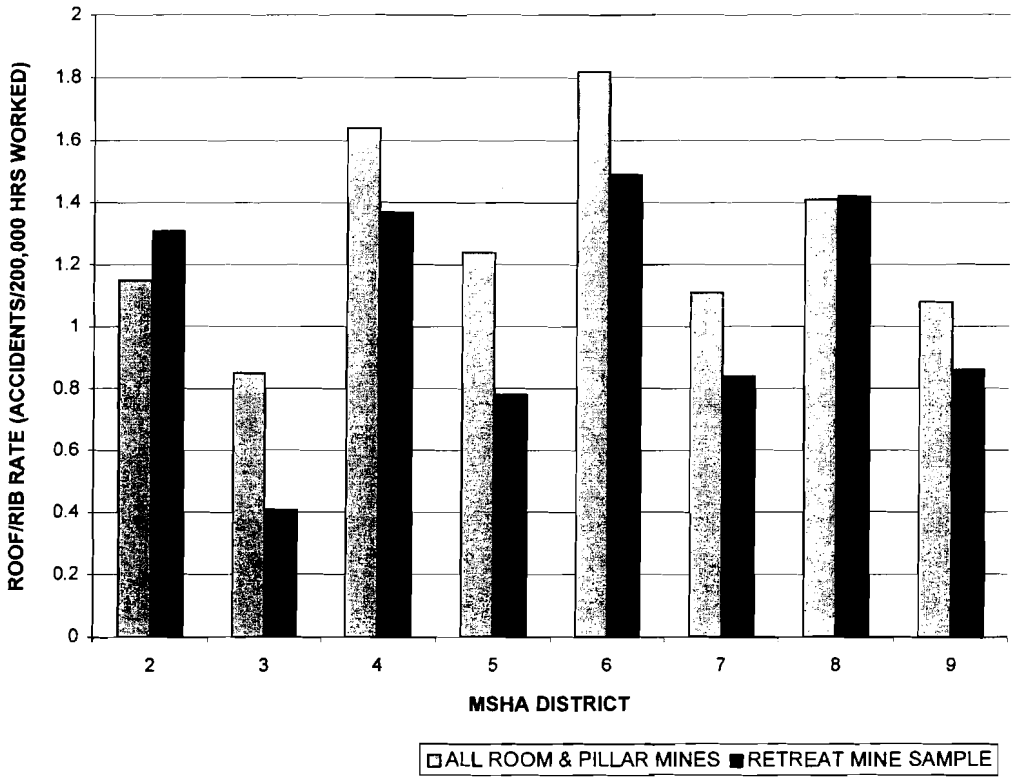

Figure 8.—Roof/rib accident rates at retreat and all room-and pillar mines, by MSHA district.

Table 3.—Demographics and accident statistics for U.S. underground coal mines by mine size[1]

Mine size	No. of mines	No. of employees	Average mine size (employees)	Tons, thousand st	Productivity, st/h	Total accident rate [2]	Roof/rib accident rate [2]	Total days lost rate [3]	Roof/rib days lost rate [3]
RETREAT [4]									
Small [5]	133	2,892	22	20,376	3.50	13.18	1.20	305	27
Medium [6]	41	3,481	85	23,785	3.25	17.30	1.04	466	26
Large [7]	12	2,756	230	17,539	3.06	15.83	1.22	519	35
ROOM-AND-PILLAR [8]									
Small [5]	873	17,253	20	103,912	3.50	14.76	1.44	353	37
Medium [6]	113	9,166	81	67,299	3.57	17.07	1.45	541	46
Large [7]	28	6,653	238	43,087	3.17	16.84	1.43	539	41

[1]Excludes anthracite mines and mines producing less than 5,000 st.
[2]Accident rates are calculated as the total number of injury accidents (severity 1-6) per 200,000 hours worked.
[3]Days lost rates are calculated as the total number of days lost due to injury per 200,000 hours worked.
[4]Retreat mines are the 186 nonlongwall mines with active gobs identified by Urosek et al. [1995].
[5]Small mines are those employing fewer than 50 workers.
[6]Medium mines are those employing 50 to 150 workers
[7]Large mines are those employing more than 150 workers.
[8]Room-and-pillar mines include all nonlongwall mines.

ANALYSIS OF FATAL INCIDENTS

A total of 25 fatal incidents, resulting in 33 deaths, have been attributed to retreat mining during 1989-96. These fatalities represent 25% of the 111 roof and rib fatalities that occurred during this period (figure 9). Four of the retreat mining fatal incidents (comprising five fatalities) occurred during room development with no apparent influence of a gob. A report by MSHA has not been completed on the most recent incident, a double fatality in Kentucky. The appendix to this paper summarizes the information collected on the 20 fatal incidents available for analysis.

Figure 10 shows that, in four incidents, no citations were issued for violations of mining law or the mine's roof control plan. The remaining 16 fatal incidents were divided into 2 categories, or classes. Class 1 includes eight incidents where gross violation of mining law (and often common sense) was deemed to be the chief factor. Class 2 incidents were those where a violation contributed to the fatality, but where other factors appeared to have played an important role as well. Class 3 incidents were those for which no citations were issued.

Figure 11 shows that the States of Kentucky, Tennessee, and West Virginia have accounted for 92% of all pillaring fatalities. Every incident in Kentucky and Tennessee involved a violation. All four of the no-citation incidents occurred in West Virginia.

Geologic factors were cited in eight instances as contributing to the fatal incidents. Roof slips and slickensides were the most common features. The no-citation incidents involved a first fall, a geologic feature, and a multiple-seam interaction (figure 12). High vertical stress was a factor in three of the class 2 fatal incidents. The types of violations cited in the other incidents are shown in figure 13. Mining sequence violations were most frequently cited in the class 2 fatal incidents.

The mining techniques employed to extract pillars are shown in figure 14. All five fatalities during slabbing operations occurred on conventional mining sections. Partial pillaring or "Christmas tree" methods were used in 82% of the incidents where continuous miners were employed.

In 45% of the fatal incidents, the pushout or last lift was being extracted at the time of the fall (figure 15). All four of the no-citation fatal incidents had two significant factors in common. All employed the Christmas tree extraction sequence, and in every case the continuous miner was extracting the last lift.

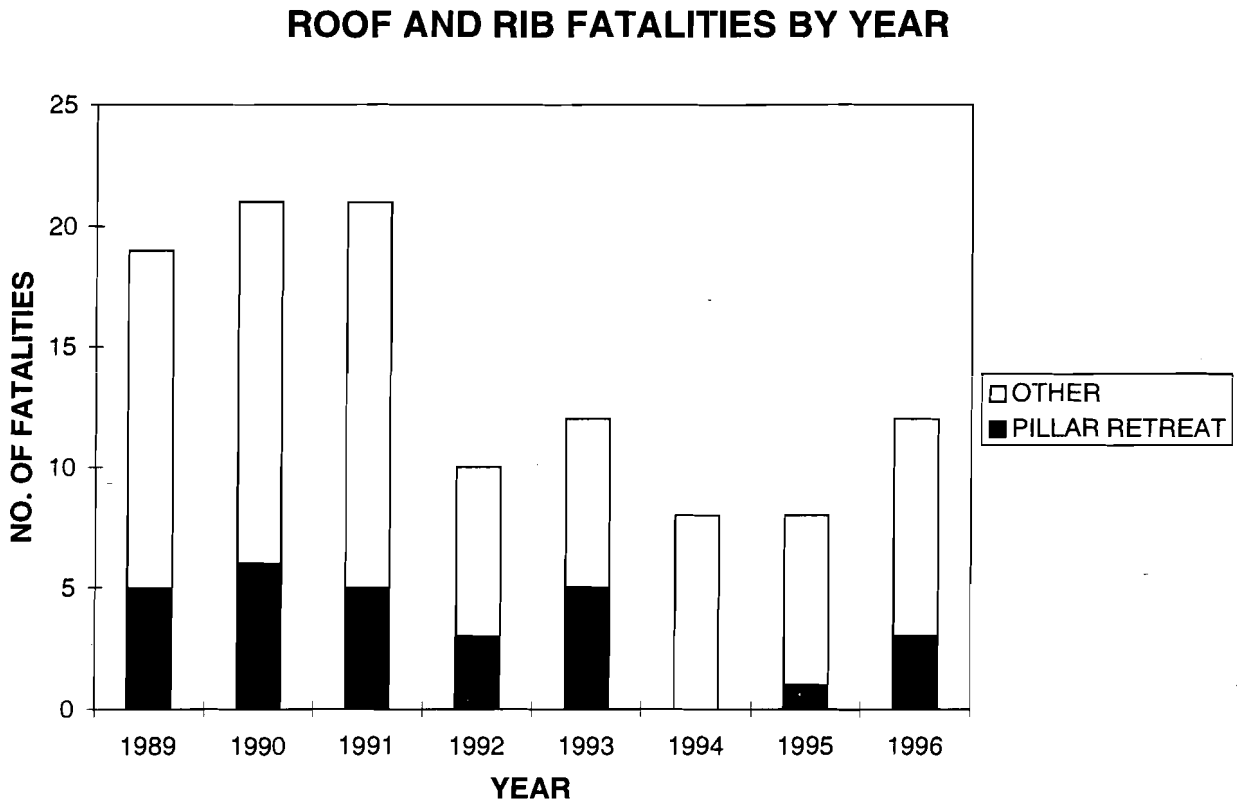

Figure 9.—Roof/rib fatalities, 1989-96.

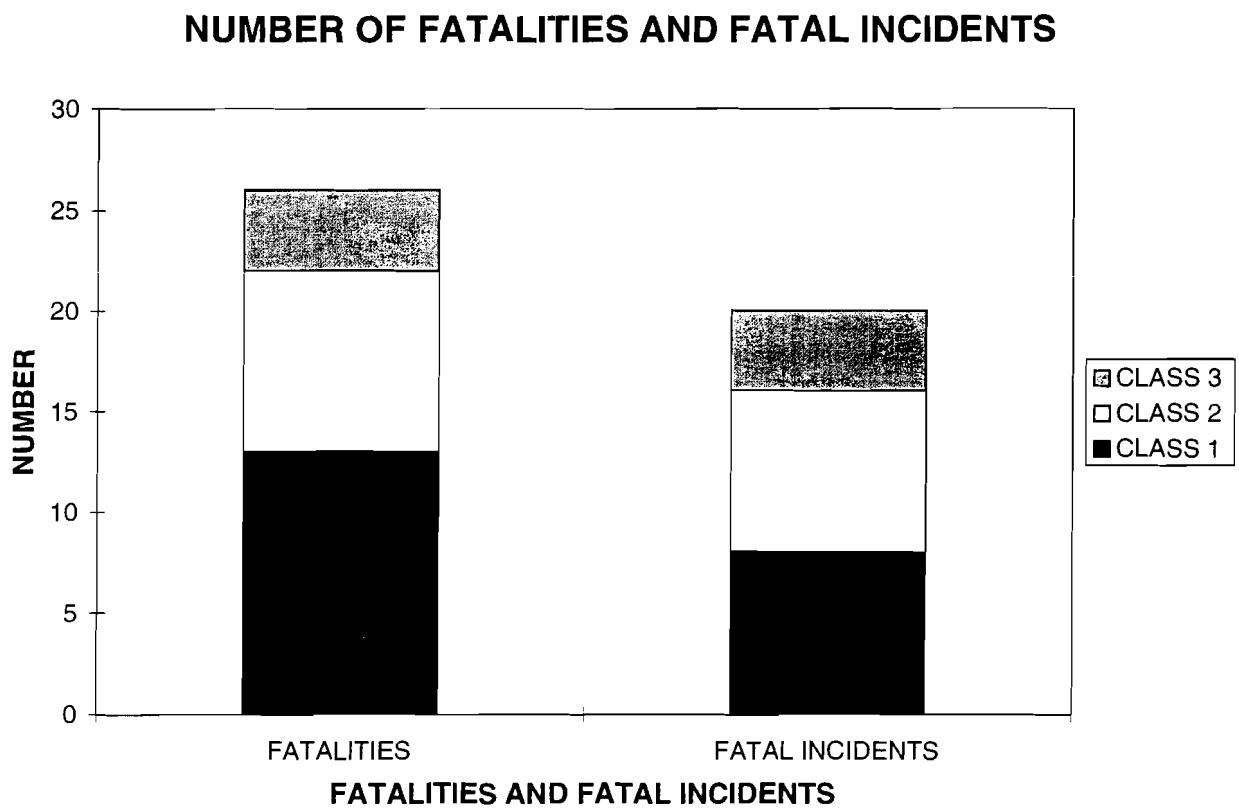

Figure 10.—Fatal roof/rib incidents and fatalities associated with retreat mining, 1989-96.

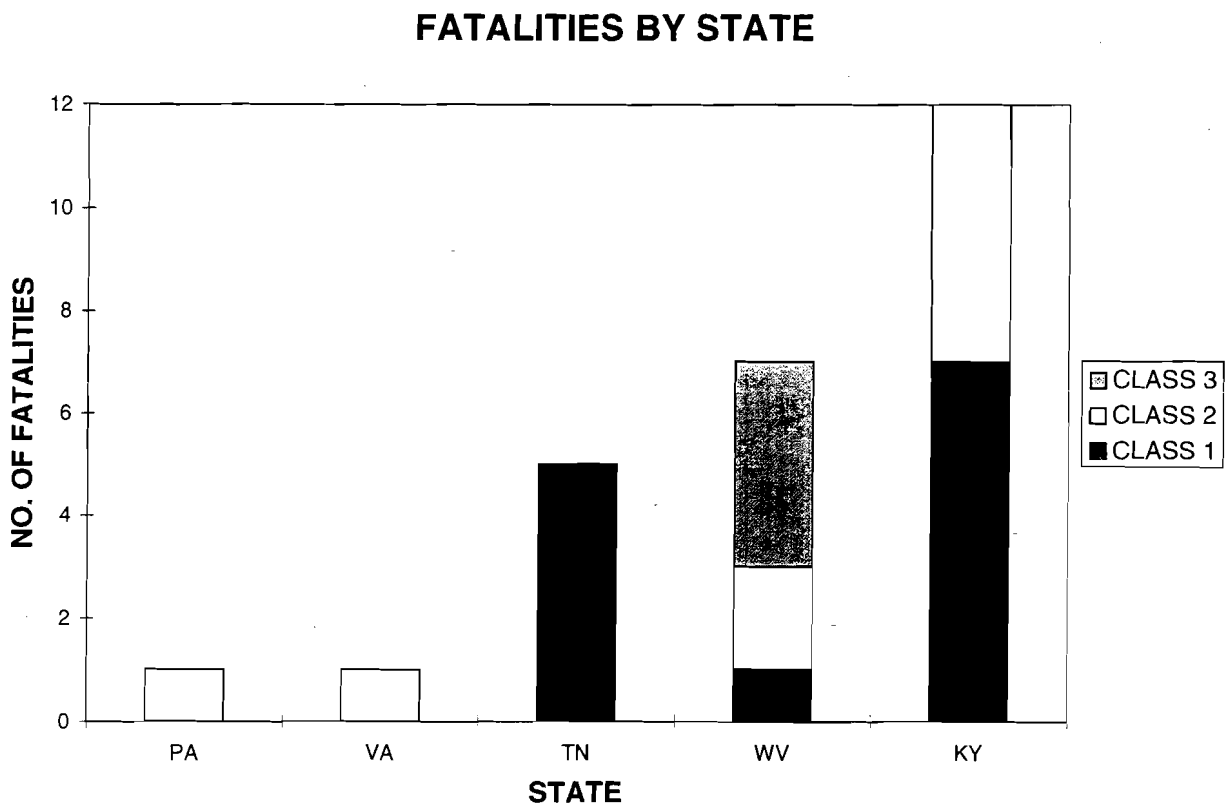

Figure 11.—Retreat mining fatal incidents, by State.

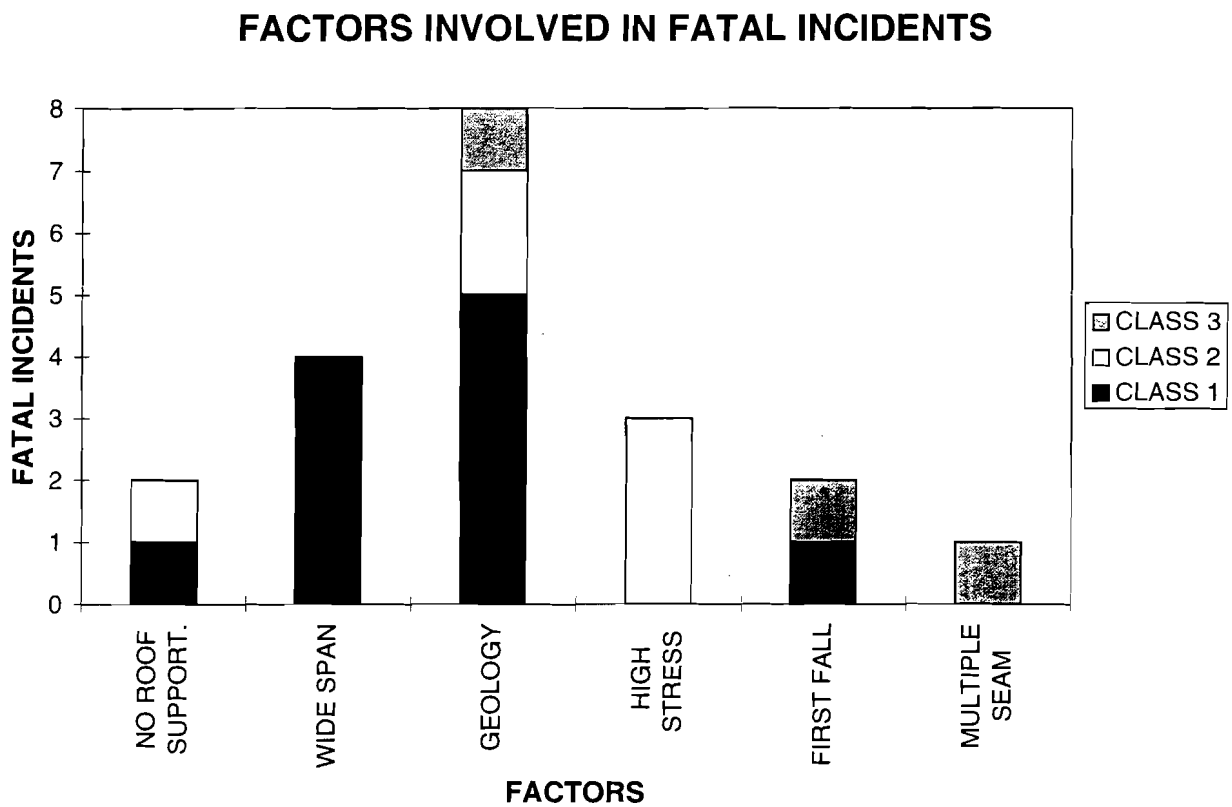

Figure 12.—Contributing factors cited in the retreat mining fatal roof/rib incidents.

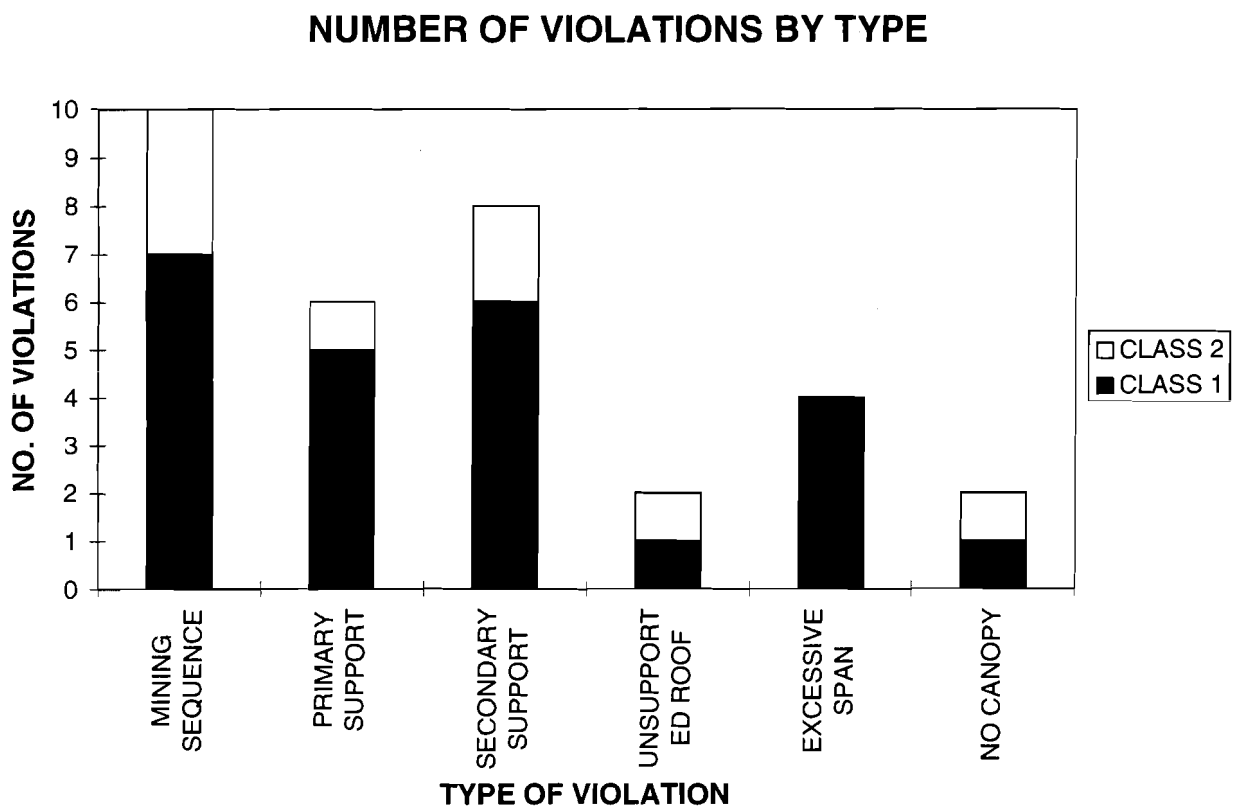

Figure 13.—Types of violations cited in the retreat mining fatal roof/rib incidents.

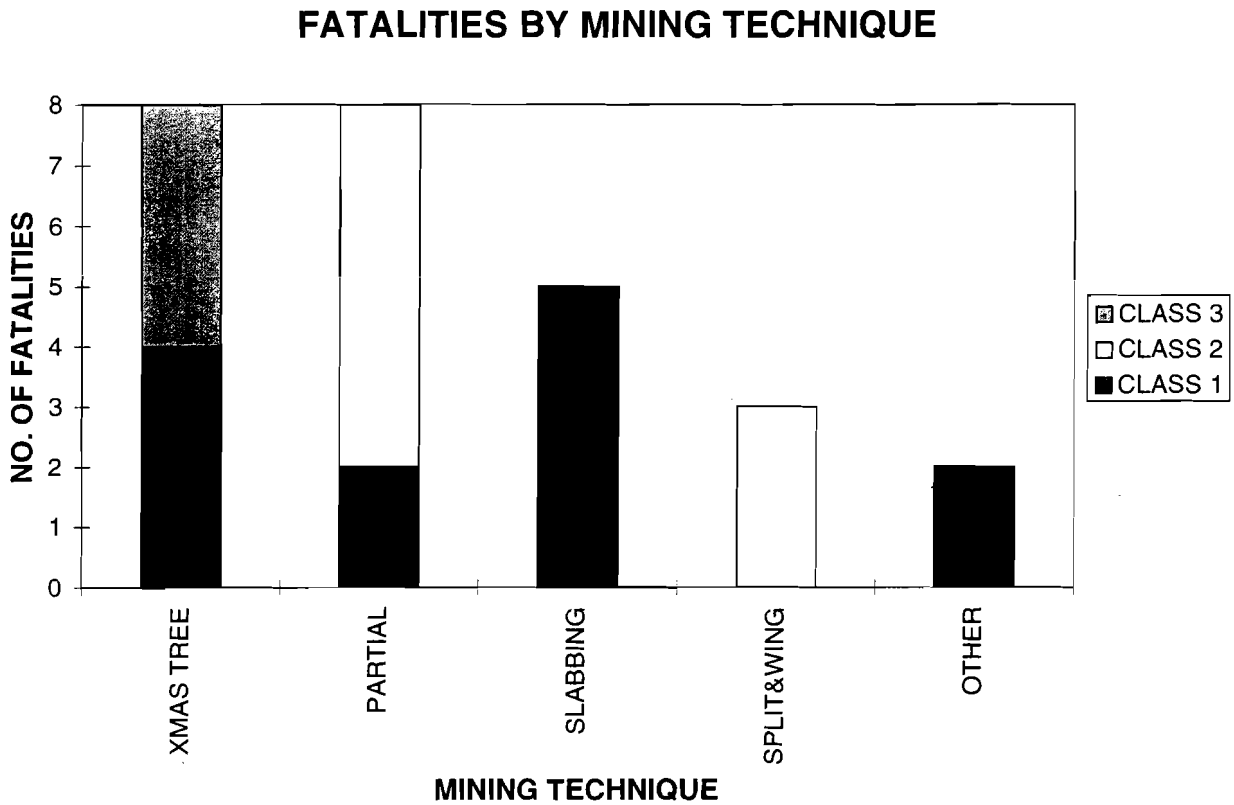

Figure 14.—Pillar extraction techniques employed in the retreat mining fatal roof/rib incidents.

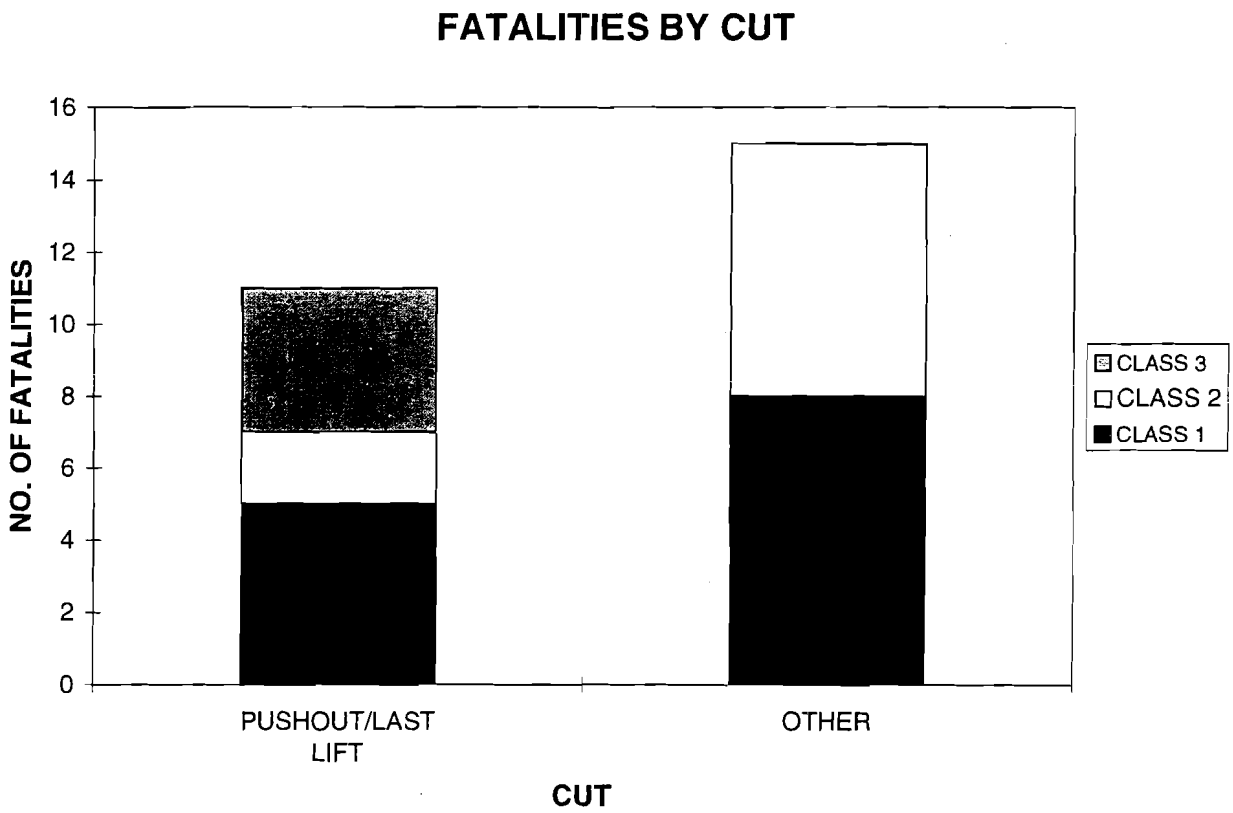

Figure 15.—Lift being extracted when fatal roof fall occurred.

CONCLUSIONS

Pillar recovery is employed in many U.S. coal regions. It is practiced primarily at many medium and some small mines. The overall accident rates for retreat mines appear to be similar to those of other room-and-pillar mines. The number of fatalities that have occurred during pillar recovery operations seems disproportionately high relative to coal production. Many fatalities that have occurred during retreat operations can be largely attributed to violations of existing mining law. Nearly 50% of fatal incidents have occurred during the recovery of the final lift (or pushout). Other potential problem areas include high stress/deep cover, first falls, geologic factors, mining sequence, and multiple-seam interactions.

REFERENCES

Blaiklock J [1992]. A Kentuckian vote for continuous mining. Mining Magazine *June*:365-366.

Montague PG [1988]. Pillar recovery—the lost art? In: Proceedings of the American Mining Congress. Chicago, IL: pp. 531-548.

Reese RG, Dash BB, Hamilton PA [1978]. Coal recovery from underground bituminous coal mines in the United States, by mining method. Washington, DC: U.S. Department of the Interior, Bureau of Mines, IC 8785.

Urosek JE, Zuchelli DR, Beiter DA [1995]. Gob ventilation and bleeder systems in U.S. coal mines. Soc Min Eng preprint 95-78.

APPENDIX.—INFORMATION ON FATAL PILLAR RECOVERY INCIDENTS

Table A-1.—Information on fatal pillar recovery incidents (from MSHA Reports of Investigation)

Year, State, and seam	Extraction technique	Equipment	Seam height, in	Roof geology	Entry width, ft	Cut	Fatality occupation	Compliance class	Mining sequence violation	Primary support violation	Secondary support violation
1989:											
Kentucky:											
Haddix	Slabbing	Conventional	54	Mod. - weak	17-25	Other	Cut. mach. oper.	1	Yes	Yes	Yes
Upper Hignite	Christmas tree	Cab CM	60	Mod. - weak	20	Pushout	Roof bolters (2), supplyman.	1	No	No	Yes
Virginia:											
Jawbone	Partial	Cab CM	84	Moderate	18-20	Other	Shuttle car oper.	2	No	No	No
1990:											
Kentucky:											
Creech	Other	Remote CM	36	Moderate	—	Pushout	Foreman	1	Yes	No	Yes
High Splint	Split-and-wing	Remote CM	60	Weak	18-19	Pushout	Foreman	2	No	No	Yes
Pond Creek	Partial	Remote CM	50	Weak	18	Other	CM helper	2	Yes	No	No
Pennsylvania:											
Pittsburgh	Split-and-wing	Cab CM	120	Strong	18	Pushout	Roof bolter	2	Yes	No	Yes
Tennessee:											
Jellico	Other	Remote CM	40	Moderate	—	Other	CM operator	1	Yes	Yes	No
West Virginia:											
Middle Kittanning	Split-and-wing	Cab CM	60	Weak	20	Other	Roof bolter	2	No	Yes	No
1991:											
Kentucky:											
Hazard No. 4	Partial	Remote CM	54	Mod. - weak	20	Other	CM operator, CM helper.	1	Yes	Yes	No
Pond Creek	Partial	Remote CM	56	Weak	20	Other	Timber setter	2	Yes	No	No
West Virginia:											
Dorothy	Partial	Remote CM	78	Weak	20	Other	Foreman	2	No	No	No
Hernshaw	Christmas tree	Remote CM	52	Weak	20	Pushout	Foreman	1	Yes	No	Yes
1992:											
Tennessee:											
Sewanee	Slabbing	Conventional	36	Weak	20	Other	Roof bolter, utility man.	1	Yes	Yes	Yes
West Virginia:											
Upper Dorothy	Christmas tree	Cab CM	74	Strong	18	Pushout	Foreman	3	No	No	No
1993:											
Kentucky:											
Hazard No. 4	Partial	Cab CM	44	Mod. - weak	20	Other	Roof bolter, scoop operator.	2	No	No	No
Tennessee:											
Sewanee	Slabbing	Conventional	36	Moderate	—	Other	Foreman, roof bolter.	1	Yes	Yes	Yes
West Virginia:											
Pocahontas No. 3	Christmas tree	Cab CM	60	Weak	20	Pushout	CM helper	3	No	No	No
1995:											
West Virginia:											
Coalburg	Christmas tree	Remote CM	72	Strong	20	Last cut	MRS operator	3	No	No	No
1996:											
West Virginia:											
Beckley	Christmas tree	Remote CM	84	Moderate	20	Pushout	CM operator	3	No	No	No

Table A-1.—Information on fatal pillar recovery incidents (from MSHA Reports of Investigation)—Continued

Year, State, and seam	Victim under unsupported roof	Excessive span	Geological factor	Excessive stress	First fall	Victim location	Saved by canopy	Killed with no canopy	Pillar length, ft	Pillar width, ft
1989:										
Kentucky:										
Haddix	No	Yes	No	No	No	Intersection	No	Yes	35	35
Upper Hignite	No	No	Slickenslided slip	No	No	Intersection	No	No	40	40
Virginia:										
Jawbone	No	No	No	Depth	No	Other	No	Yes	—	—
1990:										
Kentucky:										
Creech	No	No	No	No	Yes	Intersection	No	No	—	—
High Splint	No	No	No	No	No	Intersection	No	No	—	—
Pond Creek	No	No	No	No	No	Other	Yes	No	40	40
Pennsylvania:										
Pittsburgh	No	No	No	No	No	Other	No	No	80	50
Tennessee:										
Jellico	Yes	Yes	No	No	No	Other	No	No	—	—
West Virginia:										
Middle Kittanning	Yes	No	Slickenslided slip	No	No	Other	No	No	45	45
1991:										
Kentucky:										
Hazard No. 4	No	No	Hill seams; shale thickened	No	No	Other	No	No	40	40
Pond Creek	No	No	No	No	No	Intersection	No	No	40	40
West Virginia:										
Dorothy	No	No	Roof fractures (cutters)	Depth	No	Intersection	No	No	55	30
Hernshaw	No	No	Slickenslides	No	No	Other	No	No	50	35
1992:										
Tennessee:										
Sewanee	No	Yes	Slickenslided slip	No	No	Other; intersection	No	No	30	20
West Virginia:										
Upper Dorothy	No	No	No	Multiple seam	No	Intersection	Yes	No	62	32
1993:										
Kentucky:										
Hazard No. 4	No	No	No	Depth	No	Intersection	No	No	30	40
Tennessee:										
Sewanee	No	Yes	Slickenslided slip	No	No	Intersection	No	No	40	40
West Virginia:										
Pocahontas No. 3	No	No	Slickenslided horseback	No	No	Other	Yes	No	50	30
1995:										
West Virginia:										
Coalburg	No	No	No	No	Yes	Other	No	No	40	40
1996:										
West Virginia:										
Beckley	No	No	No	No	No	Intersection	No	No	50	70

Table A-1.—Information on fatal pillar recovery incidents (from MSHA Reports of Investigation)—Continued

Year, State, and seam	Remarks
1989:	
Kentucky:	
Haddix	The cutting machine did not have a protective canopy. Slabbing created a span that was about 30 ft at the accident site.
Upper Hignite	Victims in dangerous location during mining of pushout. No signs of weight on the section. Miner operator was 12 ft inby roof bolts during mining of pillar cuts.
Virginia:	
Jawbone	Rib sloughing caused fatal injuries to the shuttle car operator. The shuttle car did not have a car or canopy, as required when the mining height exceeds 42 in.
1990:	
Kentucky:	
Creech	Visible cracks in the mine roof in the intersection where the accident occurred prior to the day of the accident. Exceeded 20-ft cut by 18 ft at various locations.
High Splint	The victim was in a hazardous position while the continuous miner was being operated. The first pillar fall occurred 45 min before the fall that caused the accident.
PondCreek	Actual mining far exceeded the approval plan. The roof fell 5 to 6 ft to a plane of weakness above the roof line, which was above the anchorage of the 36-in roof bolts.
Pennsylvania:	
Pittsburgh	A sufficient amount of coal was not left in place to adequately support the roof or was not removed to allow the roof to fall in a controlled manner.
Tennessee:	
Jellico	Five employees were positioned 10 to 30 ft inby permanent roof support. Last cut extended 61 ft; only 20 ft was permitted by roof control plan.
West Virginia:	
Middle Kittanning	The canopy over the controls was for another model of roof bolter. No additional support was installed inby the edge of the slip.
1991:	
Kentucky:	
Hazard No. 4	The hill seams were not adequately supported. Not enough coal was left inby the cut in the No. 2 pillar; the cut in the No. 3 pillar was started too close to the corner.
Pond Creek	The cut taken out of the right side of pillar No. 4 measured 23 ft wide and 39 ft deep. The approved roof control plan states that no cut will be more than 20 ft wide and 20 ft deep.
West Virginia:	
Dorothy	Accident area was developed 6 years earlier. A fatality and roof falls occurred previously with this system of mining. MSHA deemed the roof support plan inadequate.
Hernshaw	Approved cut depths were exceeded. Several lifts had been extracted without any supports installed.
1992:	
Tennessee:	
Sewanee	Slabbing created wide unsupported spans. A slickensided slip was not properly supported. Employees routinely traveled inby permanent support when loading.
West Virginia:	
Upper Dorothy	Four coal seams had been mined underneath this mine. There were no violations. The shale below the sandstone concealed the cracks in the overlying sandstone.
1992:	
Kentucky:	
Hazard No. 4	High pressure was evident in the fall location. This resulted from stresses on the active pillar line and an adjacent pillar area. The size of the pillars on the active pillar line was not sufficient to prevent pressure from overriding the pillar line. Due to equipment design and pillar orientation, full and partial extraction were conducted on the same pillar line.
Tennessee:	
Sewanee	Instead of making splits and lifts, slabbing was done. Slabbing created a span of 30 by 50 ft in the intersection where the accident occurred. Turn and roadway posts were not set as required. Loader operator was inby permanent supports when loading lifts.
West Virginia:	
Pocahontas No. 3	There were no violations on the section. A large slickensided horseback fell, causing the accident. The miner operator was saved by a canopy.
1995:	
West Virginia:	
Coalburg	The pressure gauges on the MRS units are small and located in positions requiring operators to stand close to the MRS units to observe the pressure readings. Pillars were being extracted 150 ft from the coal outcrop. The hydraulic gauges took a sudden rise of several hundred pounds immediately before the fall.
1996:	
West Virginia:	
Beckley	Some of the pillars were partially mined; others were fully mined in the same row due to poor roof conditions. There was minor floor heave in the immediate area of the accident, but not elsewhere on the section.

ANALYSIS OF RETREAT MINING PILLAR STABILITY (ARMPS)

By Christopher Mark, Ph.D.,[1] and Frank E. Chase[2]

ABSTRACT

The prevention of pillar squeezes, massive pillar collapses, and bumps is critical to safe pillar recovery operations. To help prevent these underground safety problems, the Pittsburgh Research Center has developed the Analysis of Retreat Mining Pillar Stability (ARMPS) computer program. ARMPS calculates stability factors (SF) based on estimates of the loads applied to, and the load-bearing capacities of, pillars during retreat mining. The program can model the significant features of most retreat mining layouts, including angled crosscuts, varied spacings between entries, barrier pillars between the active section and old (side) gobs, and slab cuts in the barriers on retreat. It also features a pillar strength formula that considers the greater strength of rectangular pillars. The program may be used to evaluate bleeder designs, as well as active workings.

A data base of 140 pillar retreat case histories has been collected across the United States to verify the program. It was found that satisfactory conditions were very rare when the ARMPS SF was less than 0.75. Conversely, very few unsatisfactory designs were found where the ARMPS SF was greater than 1.5. Preliminary analyses also indicate that pillar failures are more likely beneath sandstone roof and that the ARMPS SF may be less meaningful when the depth of cover exceeds 230 m (750 ft).

[1]Mining engineer.
[2]Geologist.
Pittsburgh Research Center, National Institute for Occupational Safety and Health, Pittsburgh, PA.

INTRODUCTION

The use of remote-control continuous miners, extended cuts, and mobile roof supports has increased the productivity of room-and-pillar retreat mining (also referred to as "pillaring," "pillar recovery," "robbing," and "second mining"). In the southern Appalachian coalfields, many mines are choosing room-and-pillar retreat mining because of its lower capital cost and greater flexibility [Blaiklock 1992]. Unfortunately, between 1989 and 1996, 25% of all roof and rib fatalities occurred on pillar recovery sections.

Roof fall accidents are not the only problem associated with retreat mining. Millions of tons of coal are sterilized annually because of pillar squeezes, floor heave, pillar line roof falls, and pillar bumps. Traditional pillar design methods are of little help due to the complex mining geometries and abutment pressures that are present during pillar extraction. The Pittsburgh Research Center has developed the Analysis of Retreat Mining Pillar Stability (ARMPS) computer program to aid in the design of pillar recovery operations. This paper describes the program and presents the findings thus far.

THE ARMPS METHOD

The goal of ARMPS is to help ensure that the pillars developed for future extraction (production pillars) are of adequate size for all anticipated loading conditions. The key is to be able to estimate the magnitudes of the various loads that the pillars might experience throughout the mining process. The formulas used in ARMPS are based on those originally developed for the Analysis of Longwall Pillar Stability (ALPS) method, which is widely used for longwall pillar design [Mark 1990, 1992]. ALPS was initially derived from underground measurements of longwall abutment stresses and was later validated by the back-analysis of more than 100 case histories. In ARMPS, the formulas have been extensively modified for the variety of mining geometries typically found in pillar recovery operations.

USER INPUT

The first step in using the ARMPS program is to enter the dimensions of the pillars in the working section, as illustrated in figure 1. The program can accommodate angled crosscuts, varied spacings between the entries, and barrier pillars between the active section and old (side) gob areas. Slabbing of barriers

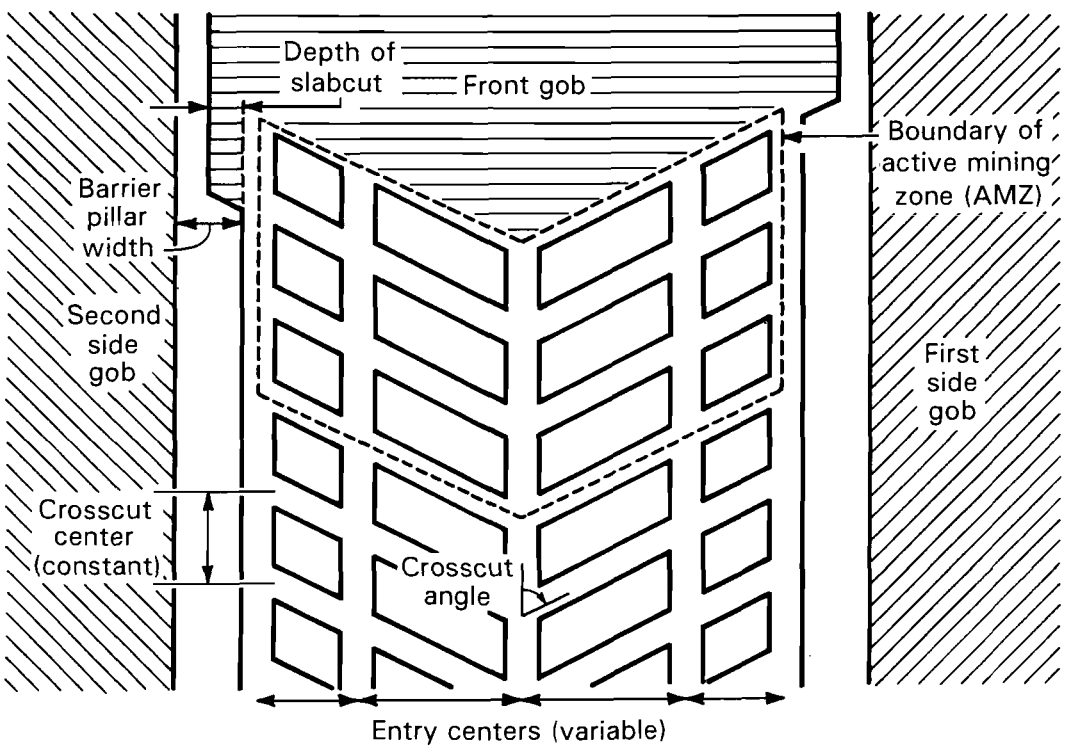

Figure 1.—Section layout parameters used in ARMPS.

on retreat can also be included. Other parameters that must be defined include depth of cover, mining height, entry width, and crosscut spacing. Finally, the user chooses one of four possible *loading conditions* (figure 2). The simplest, loading Condition 1, is development loading only. Loading condition 2 occurs when the active, or "front," panel is being fully retreated and there are no adjacent mined-out areas. The total applied load is the sum of the development loads and the front abutment load. Loading condition 3 occurs where the active mining zone (AMZ) is adjacent to an old (side) gob and the pillars are subjected to development, side abutment, and front abutment loads. Where the pillar line is surrounded by gob on three sides (sometimes referred to as "bottlenecking"), loading condition 4 is used. In every case, the extent of each gob is defined by the user.

ARMPS STABILITY FACTOR FOR THE ACTIVE MINING ZONE

The basic output from the ARMPS program is the stability factor (SF), defined as

$$\text{ARMPS SF} = \text{LBC/LT}, \qquad (1)$$

where LBC = the estimated total load-bearing capacity of the pillars within the AMZ,

and LT = the estimated total load applied to pillars within the AMZ.

Figure 3 illustrates the development and front abutment loads applied to the AMZ.

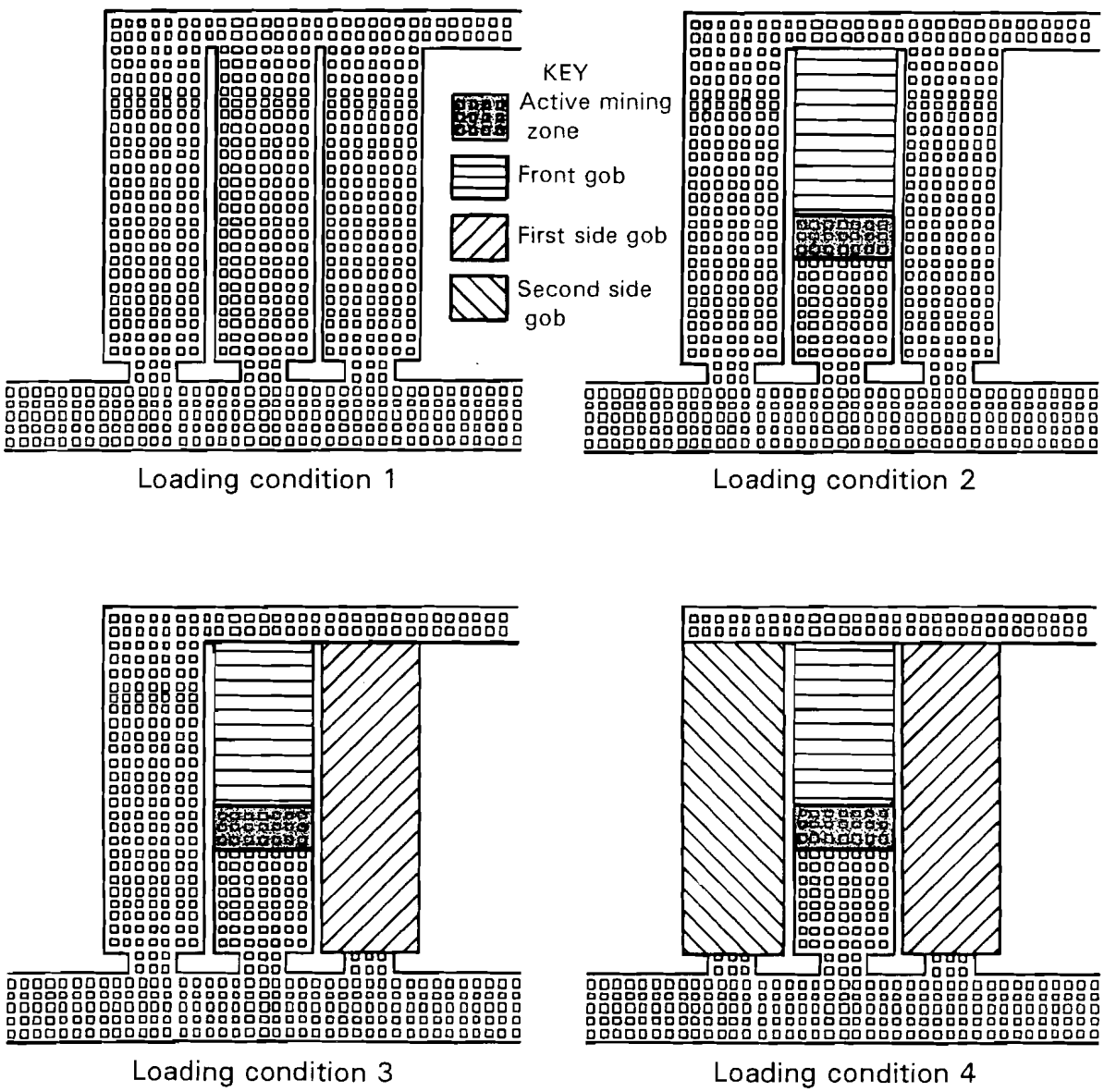

Figure 2.—The four loading conditions that can be evaluated with ARMPS.

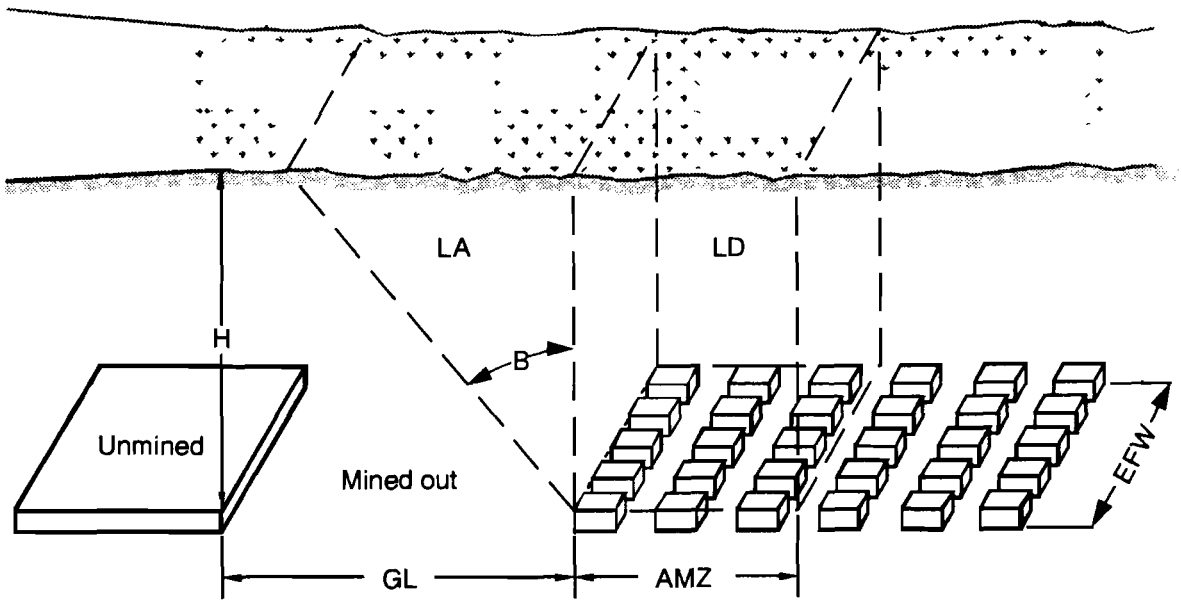

KEY

AMZ	Active mining zone	H	Depth of cover
B	Abutment angle	LA	Abutment load
EFW	Extraction front width	LD	Development load
GL	Mined out area		

Figure 3.—Schematic showing the active mining zone, the development load, and the front abutment load.

The AMZ includes all of the pillars on the extraction front (or "pillar line") and extends outby the pillar line a distance of five times the square root of the depth of cover ($5\sqrt{H}$). This distance was selected because measurements of abutment stress distributions [Mark 1990] show that 90% of the front abutment load falls within its boundaries (figure 4).

ARMPS calculates the SF for the entire AMZ, rather than stability factors for individual pillars, because experience has shown that the pillars within the AMZ typically behave as a *system*. If an individual pillar is overloaded, it will normally transfer its excess load to adjacent pillars. If those pillars are adequately sized, the process ends there. A pillar squeeze occurs only when the adjacent pillars are also undersized. They then fail in turn, resulting in a "domino" of load transfer and pillar failure. The ARMPS SF is therefore a measure of the overall stability of the pillar system.

PILLAR LOAD-BEARING CAPACITY

The load-bearing capacity of the AMZ is calculated by summing the load-bearing capacities of all of the pillars within its boundaries. The strength of an individual pillar (SP) is determined using a new pillar strength formula (the Mark-Bieniawski formula) that considers the effect of pillar length:

$$SP = S_1 [0.64 + (0.54 - 0.18 (w^2/hL))], \qquad (2)$$

where S_1 = in situ coal strength, assumed = 6.2 MPa (900 psi),

w = pillar width,

h = pillar height,

and L = pillar length.

The new pillar strength formula was needed because the pillars used in retreat mining are often much longer than they are wide. The strength of rectangular pillars can be significantly greater than square pillars due to the greater confinement generated within them. The Mark-Bieniawski formula was derived from analyses of the pillar stress distributions implied by empirical pillar strength formulas. A complete discussion of the Mark-Bieniawski formula is included in appendix A of this paper. The in situ coal strength is assumed to be 6.2 MPa (900 psi) in ARMPS; however, this value can be modified by the user.

The load-bearing capacity of the pillars is determined by multiplying their strength by their load-bearing area. When angled crosscuts are employed, the algorithm still calculates accurately each pillar's least dimension, length, and load-bearing area (A_p):

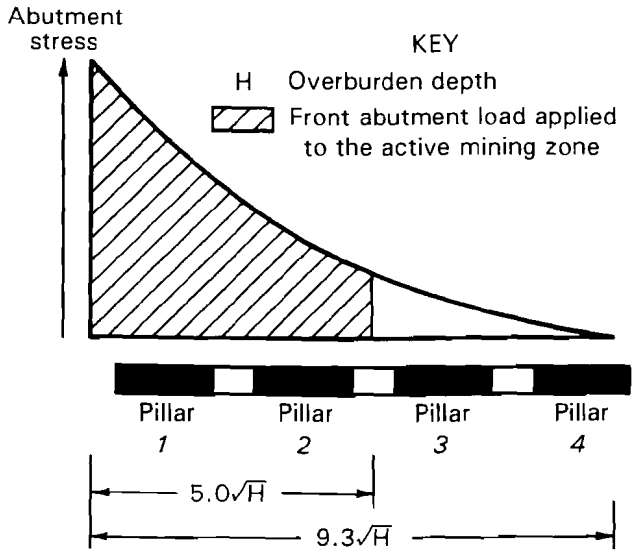

Figure 4.—Distribution of abutment stress, showing that 90% of the abutment falls within the distance of (5√H) from the gob edge.

$$A_p = [(XC)(ECTR) - (XC)(W_e) - (ECTR)(W_e)/(\sin \phi) + (W_e)^2/(\sin \phi)], \quad (3)$$

where XC = center-to-center crosscut spacing,

ECTR = center-to-center entry spacing,

W_e = entry width,

and ϕ = angle between the crosscut and the entry.

The load-bearing capacity of the pillar system is then obtained by summing the capacities of the individual pillars within the AMZ. ARMPS calculates the strength and load-bearing capacity of barrier pillars in the same manner as the panel pillars, except that their length is limited to the breadth of the AMZ.

PILLAR LOADINGS

The loadings applied to the AMZ include development loads, abutment loads, and loads transferred from barrier pillars. Table 1 shows the sources of loads and the loading conditions in which they occur.

Table 1.—Loads applied to the active mining zone in ARMPS

Source of load	Loading condition			
	1	2	3	4
Development	X	X	X	X
Front abutment		X	X	X
Side gob abutments			X	X
Transfer from barriers between active mining zone and side gobs			X	X
Transfer from remnant barriers between front gob and side gobs			X	X

Development loads are due to the weight of the overburden directly above the pillars before any retreat mining takes place. The tributary area theory is used in ARMPS to estimate development loads.

Abutment loads occur as a result of retreat mining and gob formation. They are determined by the depth of cover, the extent of the gobs, the width of the extraction front, and the abutment angles. These parameters are illustrated in two dimensions in figure 5. The abutment angle determines how much load is carried by gob. Measurements of longwall abutment stresses indicated that an abutment angle of 21° is appropriate for normal caving conditions [Mark 1992]. The ARMPS program initializes the abutment angles for all gobs to 21°; however, this can be changed by the user. For example, if it is known that no caving has occurred, then the abutment angle may be set to 90° to simulate zero load transfer to the gob [Chase and Mark 1993].

The abutment stresses are assumed to be distributed following the inverse-square function shown in figure 4. Abutment loads are also applied to barrier pillars; however, if a barrier is too small to carry its share, then some or all of the excess is transferred to the AMZ.

The front abutment load applied to the AMZ is calculated as follows. The volume of the overburden above the mined-out active gob is the depth of cover multiplied by the gob area. The portion of this volume whose weight is carried by the gob is determined by the tangent of the abutment angle, as shown in figure 5. This portion is subtracted, and the remainder is shared between the AMZ and the unmined coal on the other three sides of the gob. It is assumed that barrier pillars (or substantial production pillars) are present on the other three sides of the gob. Load applied to the barriers here may be transferred back to the AMZ if the barriers are removed later in the mining process.

The magnitude of the front abutment load applied to the AMZ is determined by the extent of the extraction zone and the depth of cover. The front abutment is considered fully developed if the gob area is large relative to the depth of cover (figure 6*A*). If only a few rows of pillars have been extracted (figure 6*B*), much of the load will be carried by the back barrier. If the full extraction zone is rather narrow (figure 6*C*), much of the load will be carried by the side barriers.

The side abutment loads are shared by the AMZ and, if it is present, the barrier pillar between the AMZ and the side gob. The inverse-square stress distribution (figure 4) again is used to apportion the load between the barrier and the AMZ. Next, if it is determined that the barriers are overloaded, some additional side abutment load is transferred to the AMZ.

To determine whether a barrier pillar can carry the load applied to it, ARMPS estimates the barrier's SF by dividing its load-bearing capacity by its load. The total load applied to a barrier pillar is the sum of the development load, the front abutment load due to any slabbing, and the side abutment load applied to the barrier. If the SF is greater than 1.5, the barrier is assumed to be stable. When the barrier's SF is between 1.5

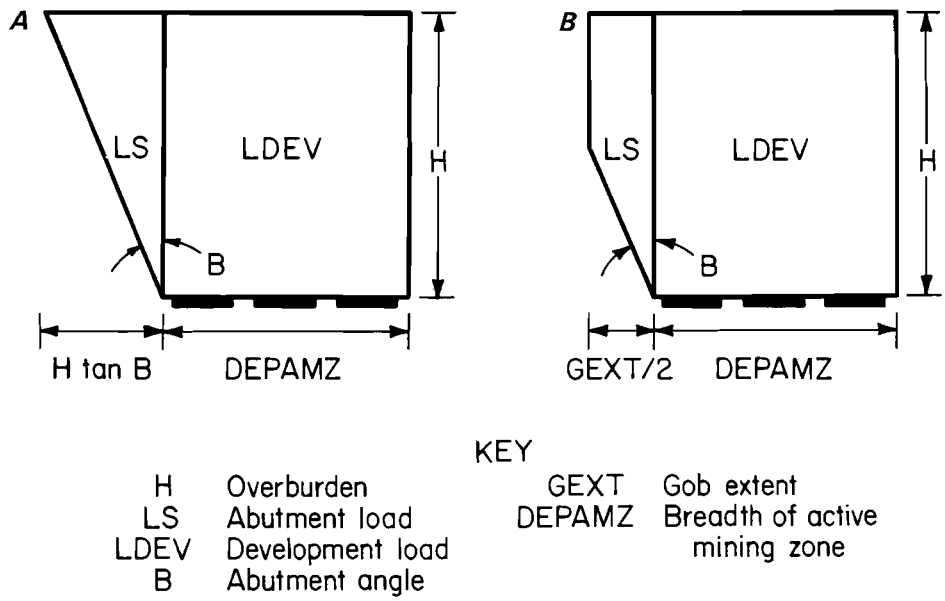

Figure 5.—Schematic showing the abutment load in two dimensions. *A*, supercritical gob; *B*, subcritical gob.

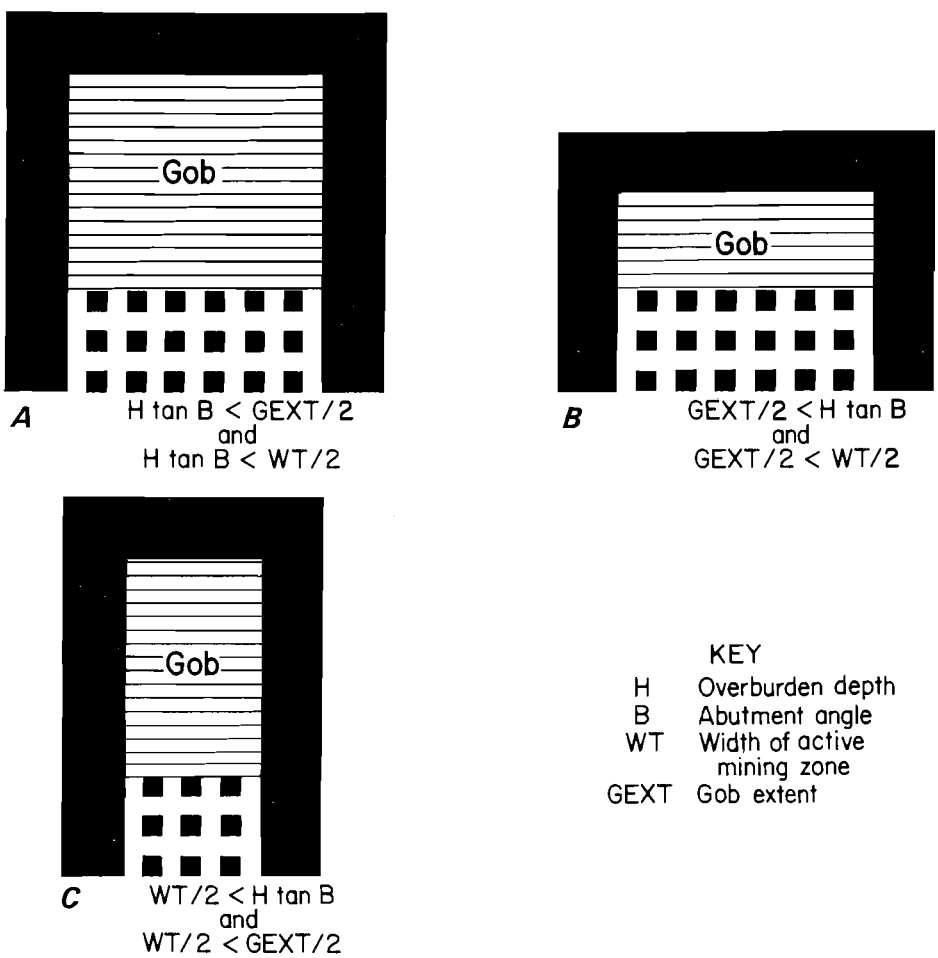

Figure 6.—Illustration of the effect of panel geometry on the front abutment loading in ARMPS. *A*, gob area is supercritical in both width and extent; *B*, gob area is subcritical in extent; *C*, gob area is subcritical in width.

and 0.5, a portion of its abutment load is transferred to the AMZ. If the SF is less than 0.5, all of the additional side abutment load (but not the development or front abutment load) is transferred to the AMZ.

The final sources of load on the AMZ are the remnant barrier pillars inby the pillar line (between the front and side gobs). If the remnant barriers are too small to carry their load, some part of it is returned to the AMZ. The decision to transfer the load and how much is based on the remnant barrier's SF. Slabbing of the remnant will also return some abutment load to the AMZ.

Further details on the formulas and calculations used in ARMPS loadings can be found in the "Help" text that accompanies version 4.0 of the program.

VERIFICATION OF THE ARMPS METHOD

The ARMPS method is being verified through back-analysis of pillar recovery case histories. To date, 140 case histories have been obtained from 10 States (see appendix B of this paper). They cover an extensive range of geologic conditions, roof rock cavability characteristics, extraction methods, depths of cover, and pillar geometries. Ground conditions in each case history have been categorized as either satisfactory or unsatisfactory. Pillar failures responsible for unsatisfactory conditions were found to include—

- Pillar squeezes, accompanied by significant entry closure and loss of reserves;
- Sudden collapses of groups of pillars, usually accompanied by airblasts; and/or
- Coal pillar bumps (violent failures of one or more pillars).

As figure 7 shows, pillar failures occurred in 93% of the cases where the ARMPS SF was less than 0.75. Where the ARMPS SF was greater than 1.5, 94% of the designs were satisfactory. SF values ranging from 0.75 to 1.50 form a "gray" area where both successful and unsuccessful cases are found.

Current research has begun to evaluate other factors that may contribute to satisfactory conditions when the ARMPS SF falls between 0.75 and 1.5. These include—

Coal strength: An extensive data base of laboratory tests of the strength of coal was compiled by Mark and Barton [1997]. When compared with the ARMPS data base, no correlation was found between coal strength and pillar strength.

Depth of cover: Figure 8 shows that there is a marked reduction in SF as depth of cover increases. When the depth exceeds 305 m (1,000 ft), the ARMPS SF was below 1.0 for 70% of the satisfactory designs. Highly unsatisfactory conditions have also been encountered under deep cover, which recently led to two fatalities. Pillar design for retreat mining under deep cover remains an important research issue.

Seam height: A plot of seam height against ARMPS SF shows no correlation (figure 9).

Roof geology: A detailed study of pillar performance was conducted at a mining complex in southern West Virginia. More than 50 case histories were collected. Analysis showed that satisfactory conditions were more likely to be encountered under shale roof than massive sandstone roof (figures 10-11). This implies that better caving occurs with shale, resulting in lower pillar loads.

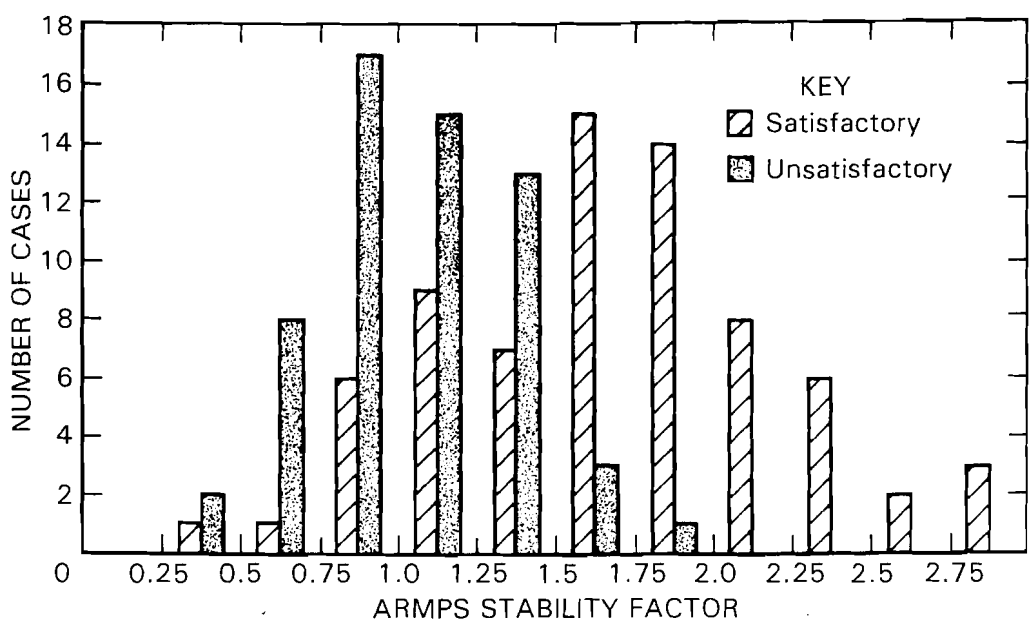

Figure 7.—ARMPS data base.

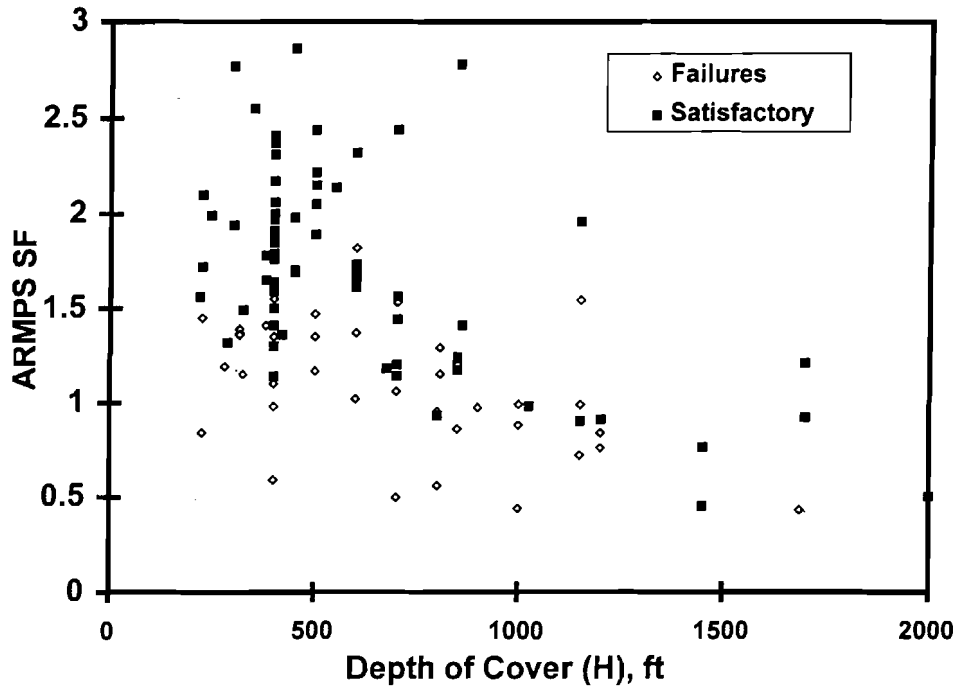

Figure 8.—Relationship between ARMPS SF and depth of cover within the case history data base.

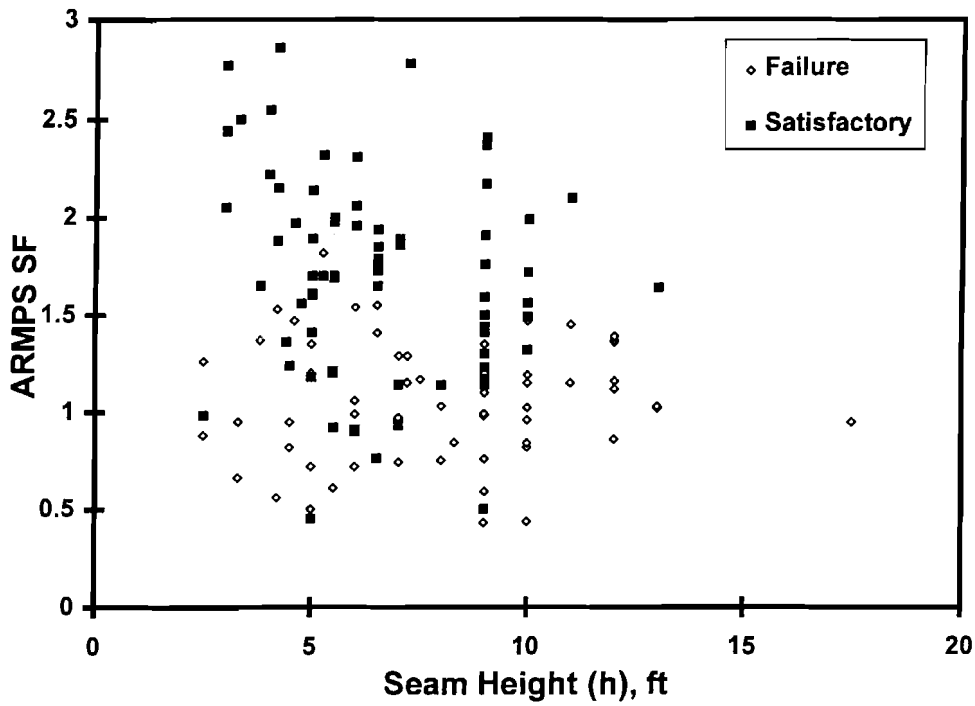

Figure 9.—Relationship between ARMPS SF and seam height within the case history data base.

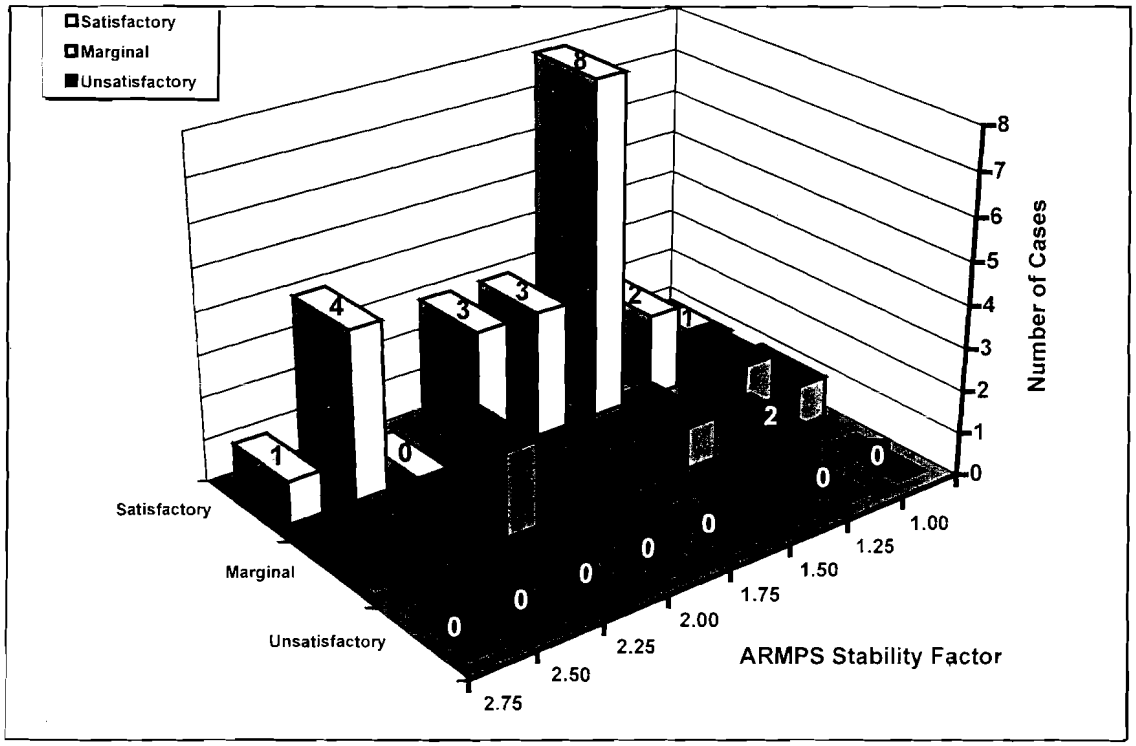

Figure 10.—Shale roof case histories from mining complex in southern West Virginia.

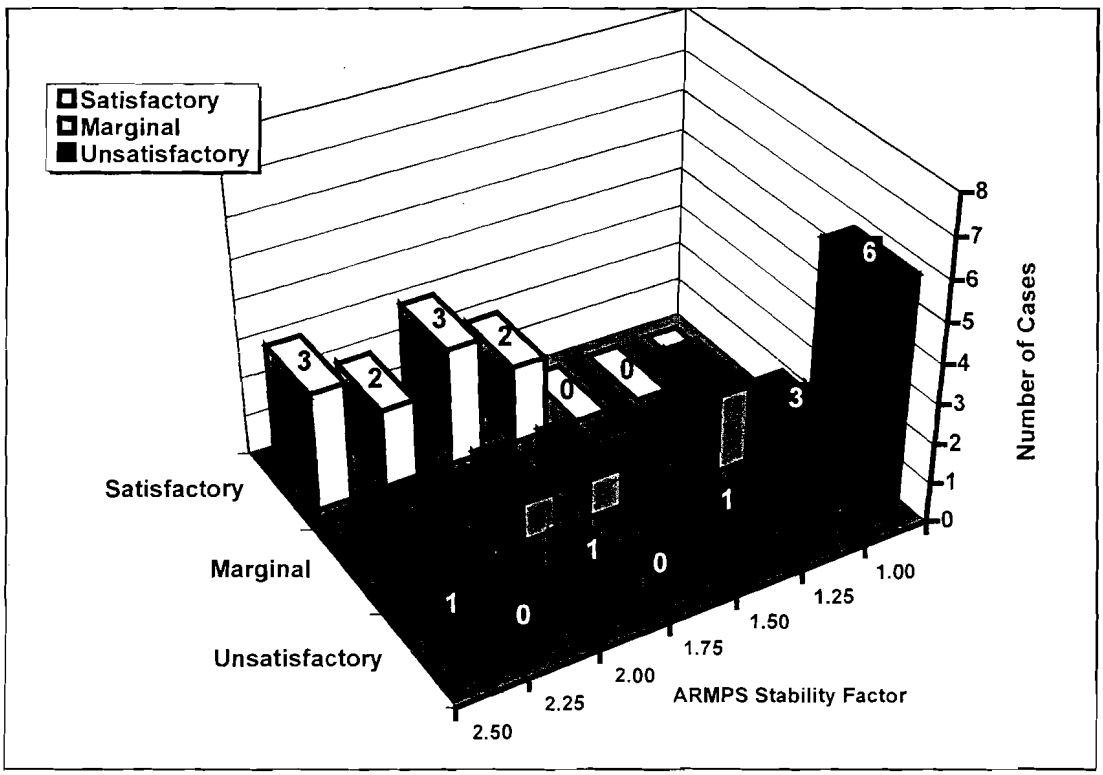

Figure 11.—Sandstone roof case histories from mining complex in southern West Virginia.

GUIDELINES FOR USING ARMPS

ARMPS appears to provide good first approximations of the pillar sizes required to prevent pillar failure during retreat mining. In an operating mine, past experience can be incorporated directly into ARMPS. ARMPS stability factors can be back-calculated for both successful and unsuccessful areas. Once a minimum ARMPS SF has been shown to provide adequate ground conditions, that minimum should be maintained in subsequent areas as changes occur in the depth of cover, coal thickness, or pillar layout. In this manner, ARMPS can be calibrated using site-specific experience.

ARMPS is also well suited for initial feasibility studies where no previous experience is available. Operators may begin with an SF near 1.5, then adjust as they observe pillar performance. ARMPS may also help in optimizing panel designs by identifying pillars that might be needlessly oversized.

ARMPS may be used to analyze a wide variety of mining geometries. For example, most bleeder designs can be analyzed by selecting loading condition 3, then setting the extent of the active gob to zero. The "Help" text included with version 4.0 of the program contains many tips on selecting the proper input parameters when using ARMPS.

In some cases, more detail may be desired than can be provided by ARMPS. Some complex situations, such as multiple-seam interactions, are beyond the capabilities of ARMPS. In these instances, the newly developed LAMODEL [Heasley 1997] may be the appropriate tool to use.

CONCLUSIONS

The ARMPS program has already proven to be a useful aid in planning pillar recovery operations. It is easy to use, and a large number of analyses can be run in a relatively short period. The program is sufficiently flexible to be applicable to a wide variety of mining geometries. If the user desires, it also provides a full range of intermediate calculations in addition to the SF. Many mines throughout the United States and abroad already use ARMPS, and the Mine Safety and Health Administration has also made extensive use of the program.

Current efforts are aimed at improving the interpretation of the ARMPS SF. Although pillar failures seem unlikely when the ARMPS SF is greater than 1.5, there are apparently many cases where SF values as low as 0.75 have been successful. Factors such as roof quality, floor strength, and mining method may determine whether a pillar design succeeds. These factors are now being included in the retreat mining case history data base and will be integrated into future design guidelines.

To obtain a single copy of the ARMPS computer program, version 4.0 for Windows, send three double-sided, high-density diskettes to: Christopher Mark, Ph.D., NIOSH, Pittsburgh Research Center, Cochrans Mills Rd., P.O. Box 18070, Pittsburgh, PA 15236-0070.

REFERENCES

Blaiklock J [1992]. A Kentuckian vote for continuous mining. Mining Magazine *June*:365-366.

Chase FE, Mark C [1993]. Ground control design for pillar extraction. Soc Min Eng AIME preprint 93-282.

Heasley KA [1997]. A new laminated overburden model for coal mine design. In: Mark C, Tuchman RJ, comp. Proceedings: New Technology for Ground Control in Retreat Mining. Pittsburgh, PA: U.S. Department of Health and Human Services, Public Health Service, Centers for Disease Control, National Institute for Occupational Safety and Health, IC 9446.

Mark C [1990]. Pillar design methods for longwall mining. Pittsburgh, PA: U.S. Department of the Interior, Bureau of Mines, IC 9247.

Mark C [1992]. Analysis of longwall pillar stability (ALPS): an update. In: Iannacchione AT, Mark C, Repsher RC, Tuchman RJ, Jones CC, comp. Proceedings of the Workshop on Coal Pillar Mechanics and Design. Pittsburgh, PA: U.S. Department of the Interior, Bureau of Mines, IC 9315, pp. 238-249.

Mark C, Barton TM [1997]. Pillar design and coal strength. In: Mark C, Tuchman RJ, comp. Proceedings: New Technology for Ground Control in Retreat Mining. Pittsburgh, PA: U.S. Department of Health and Human Services, Public Health Service, Centers for Disease Control, National Institute for Occupational Safety and Health, IC 9446.

APPENDIX A.—DERIVATION OF THE MARK-BIENIAWSKI PILLAR STRENGTH FORMULA

Early versions of the ARMPS program, following the ALPS program, used the Bieniawski formula to estimate pillar strength [Bieniawski 1992]:

$$S_p = S_1 [0.64 + (0.36\ w/h)], \qquad \text{(A-1)}$$

where S_p = pillar strength,

S_1 = in situ coal strength,

w = pillar width (or least plan dimension),

and h = pillar height.

The Bieniawski formula was originally developed in the 1960's from in situ testing of large-scale coal specimens. The specimen strengths were determined as the ultimate load-bearing capacity divided by the area. Bieniawski recognized that the formula underestimated the strength of rectangular pillars; however, because all of the specimens were square, there was no obvious way of estimating a "pillar length" effect.

It has been recognized that a major disadvantage of empirical formulas, like that of Bieniawski, is that they treat the pillar as a single structural element. In reality, the stress within even a relatively small pillar is highly nonuniform. Tests conducted by Wagner [1974] demonstrated this quite dramatically (figure A-1).

Modern *mechanics-based* approaches to coal pillars begin with stress distribution. Perhaps the best known is the approach proposed by Wilson [1973, 1983]. Wilson derived an expression for the vertical stress gradient within the yield zone, which he then integrated over the area of the pillar (figure A-2) to determine the ultimate pillar resistance (R). The "pillar strength" is simply the ultimate pillar resistance divided by the pillar area. Numerical models also provide stress distribution profiles, although not normally in the form of an equation. Mechanics-based approaches can be used to evaluate any pillar shape, because the stresses within the pillar are determined by laws that are independent of overall pillar geometry.

Although empirical formulas do not explicitly consider the effect of internal pillar mechanics, it is apparent that they imply a nonuniform stress distribution because of the shape effect. Once the implied stress gradient has been derived, the length effect can be readily determined. The derivation has been published previously [Mark et al. 1988; Mark and Iannacchione 1992] and is summarized below.

First, three assumptions are implicit in Wilson's and other analytical formulations:

1. The stress within the yield zone of a given pillar is a continuous function of the distance from the nearest rib.

2. The stress gradient within the yield zone of a given pillar does not change with time or load (i.e., the yielded coal is perfectly plastic).

3. The stress distribution is symmetric with respect to the center of the pillar.

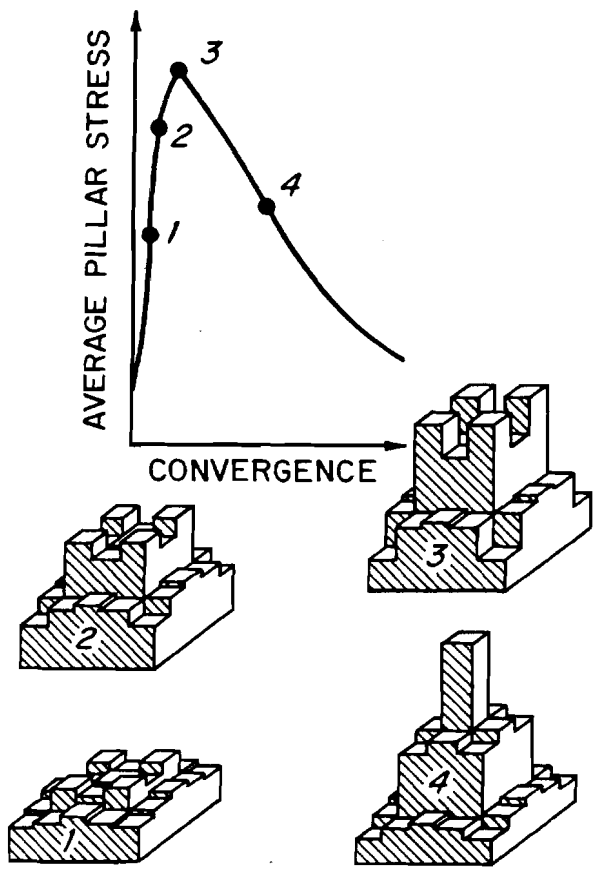

Figure A-1.—Pillar stress profiles measured in small coal pillars (after Wagner [1974]).

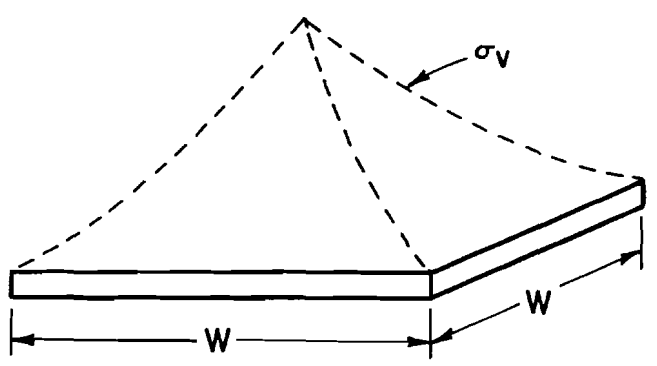

Figure A-2.—Determination of pillar load-bearing capacity as the integral of the pillar stress distribution.

The next step in the derivation is to calculate the ultimate resistance of a square pillar. Using the Bieniawski formula:

$$R = S_1 \left(0.64 + 0.36 \frac{w}{h} \right) w^2. \qquad \text{(A-2)}$$

Then, the increase in pillar resistance dR due to an increase in cross-sectional area dA = 2w dw (figure A-3*A*) may be calculated by taking the derivative of equation A-2 with respect to w:

$$dR = S_1 \left(1.28 + 1.08 \frac{w^2}{h} \right) dw. \qquad \text{(A-3)}$$

In the next step, the assumption that the vertical pillar stress is a continuous function of the rib distance (x) is applied. It may be seen (figure A-3*B*) that

$$dR = 4 \int_0^{\frac{w}{2}} \sigma_v \, dx \, dw. \qquad \text{(A-4)}$$

Equating A-3 and A-4 and simplifying, we have

$$S_1 = \left(0.32 \, w + 0.27 \frac{w^2}{h} \right) = \int_0^{\frac{w}{2}} \sigma_v \, dx. \qquad \text{(A-5)}$$

The function that satisfies equation A-5 is

$$\sigma_v = S_1 \left(0.64 + 2.16 \frac{x}{h} \right). \qquad \text{(A-6)}$$

Equation A-6 is the stress gradient in the yield zone predicted by the Bieniawski formula. Stress gradients have also been derived for several other common empirical pillar strength formulas [Mark and Iannacchione 1992].

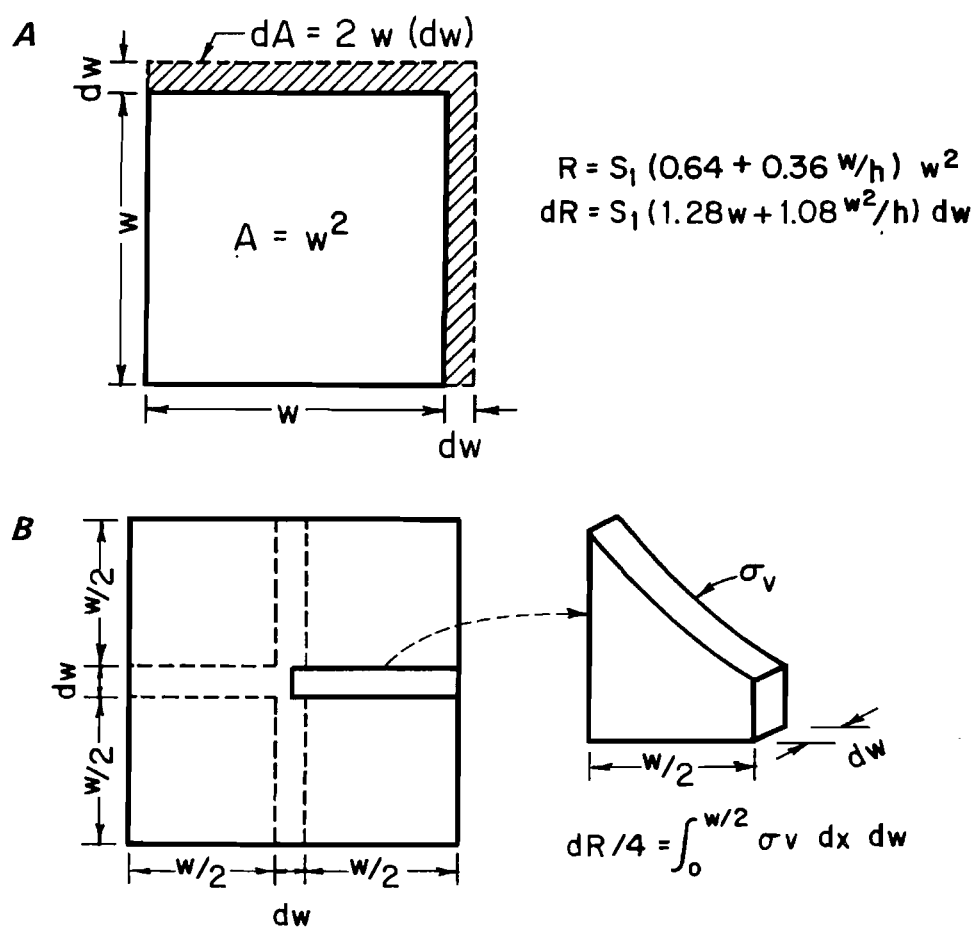

Figure A-3.—Determination of pillar stress gradients from a pillar strength formula. *A*, calculation of dR directly from the formula; *B*, calculation of dR in terms of the vertical stress gradient.

To determine the load-bearing capacity of any pillar shape, it is now only necessary to integrate equation A-6 over the load-bearing area of the pillar. For example, the load-bearing capacity of an extremely long strip pillar (R_s) is

$$R_s = 2L\int_0^{\frac{w}{2}} S_1 \left(0.64 + 2.16\frac{x}{h}\right) dx. \qquad \text{(A-7)}$$

Solving:

$$R_s = (Lw)\ S_1 \left(0.64 + 0.54\ \frac{w}{h}\right). \qquad \text{(A-8)}$$

Dividing by the pillar area (Lw) yields the strength of a strip pillar (S_s):

$$S_s = S_1 \left(0.64 + 0.54\ \frac{w}{h}\right). \qquad \text{(A-9)}$$

Equation A-9 implies that a strip pillar's strength can approach 150% that of a square pillar, but that the strength difference is reduced as the w/h ratio is reduced.

The ultimate load carried by a rectangular pillar is equivalent to the load carried by a square pillar of width w plus a section of a strip pillar of length (L − w), as shown in figure A-4. Combining equations A-6 and A-9, the ultimate load carried by a rectangular pillar (R_s) is

$$R_s = S_1 \left\{\left[w^2 \left(0.64 + 0.36\ \frac{w}{h}\right)\right] + \left[(w(L-w)) \left(0.64 + 0.54\ \frac{w}{h}\right)\right]\right\}. \qquad \text{(A-10)}$$

Simplifying:

$$R_s = S_1 \left[0.64\ wL + 0.54 \left(w^2\ \frac{L}{h}\right) - 0.18 \left(\frac{w^3}{H}\right)\right]. \qquad \text{(A-11)}$$

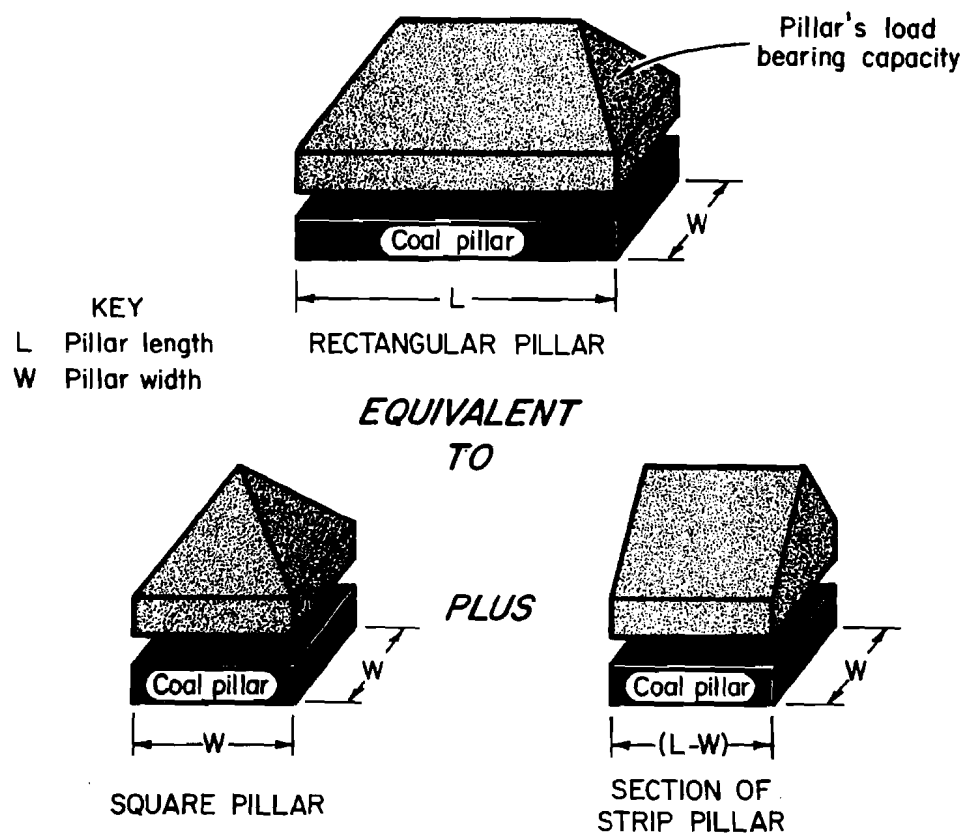

Figure A-4.—Pillar stress distributions for square, strip, and rectangular pillars.

Dividing by the load-bearing area (wL), the Mark-Bieniawski formula is obtained:

$$S_p = S_1 \left[0.64 + 0.54 \left(\frac{w}{H} \right) - 0.18 \frac{w^2}{Lh} \right]. \qquad \text{(A-12)}$$

Equation A-12 indicates that the increase in strength in a rectangular pillar depends on both (w/h) and (w/L). Table A-1 compares the pillar strengths determined by the Mark-Bieniawski formula with those obtained from the Bieniawski formula.

Table A-1.—Pillar strength from the Mark-Bieniawski formula, assuming the strength of a square pillar (original Bieniawski formula) as unity

Pillar L/w	Pillar w/h				
	1	2	4	10	20
1.5	1.06	1.09	1.12	1.14	1.16
2.0	1.09	1.13	1.18	1.21	1.23
4.0	1.14	1.23	1.32	1.41	1.45
10.0	1.16	1.25	1.34	1.42	1.46

REFERENCES

Bieniawski ZT [1992]. A method revisited: coal pillar strength formula based on field investigations. In: Iannacchione AT, Mark C, Repsher RC, Tuchman RJ, Jones CC, comp. Proceedings of the Workshop on Coal Pillar Mechanics and Design. Pittsburgh, PA: U.S. Department of the Interior, Bureau of Mines, IC 9315, pp. 158-165.

Mark C, Iannacchione AT [1992]. Coal pillar mechanics: theoretical models and field measurements compared. In: Iannacchione AT, Mark C, Repsher RC, Tuchman RJ, Jones CC, comp. Proceedings of the Workshop on Coal Pillar Mechanics and Design. Pittsburgh, PA: U.S. Department of the Interior, Bureau of Mines, IC 9315, pp. 78-93.

Mark C, Listak JM, Bieniawski ZT [1988]. Yielding coal pillars—field measurements and analysis of design methods. In: Proceedings of the 29th U.S. Symposium on Rock Mechanics. Minneapolis, MN: University of Minnesota, pp. 261-270.

Wagner H [1974]. Determination of the complete load-deformation characteristics of coal pillars. In: Proceedings of the 3rd International Society for Rock Mechanics Congress. Denver, CO: pp. 1076-1081.

Wilson AH [1973]. An hypothesis concerning pillar stability. Min Eng (London) *131*(141):409-417.

Wilson AH [1983]. The stability of underground workings in the soft rocks of the coal measures. Intl J Rock Mech Min Sci *1*:91-187.

APPENDIX B.—ARMPS CASE HISTORY DATA BASE

Table B-1.—Unsatisfactory pillar retreat case histories

State and coal seam	ARMPS SF	Seam thickness, m (ft)	Depth, m (ft)	Loading condition
Alabama:				
Blue Creek	1.54	1.8 (6.0)	350 (1,150)	2
Blue Creek	0.99	1.8 (6.0)	350 (1,150)	3
Colorado:				
Cameo	0.74	2.1 (7.0)	90 (300)	1
D	1.20	2.7 (9.0)	260 (850)	2
D	0.99	2.7 (9.0)	305 (1,000)	3
Kentucky:				
Harlan	1.16	3.7 (12)	285 (940)	1
Harlan	0.96	2.1 (7.0)	305 (1,000)	1
Harlan	0.86	3.7 (12)	260 (850)	2
Harlan	1.12	3.7 (12)	325 (1,070)	1
Hazard No. 4	0.44	3.0 (10)	305 (1,000)	4
Hazard No. 4	0.56	1.3 (4.2)	245 (800)	3
Hazard No. 4	0.50	1.5 (5.0)	215 (700)	3
Lower Elkhorn (No. 2 Gas)	1.03	4.0 (13.0)	245 (800)	1
Lower Elkhorn (No. 2 Gas)	1.02	4.0 (13.0)	185 (600)	3
Ohio:				
Lower Freeport	1.20	1.5 (5.0)	215 (700)	1
Mahoning	0.66	1.0 (3.3)	75 (250)	1
Mahoning	0.95	1.0 (3.3)	75 (250)	1
Pennsylvania:				
Lower Kittanning	1.41	2.0 (6.5)	115 (380)	2
Lower Kittanning	1.55	2.0 (6.5)	120 (400)	2
Lower Kittanning	1.29	2.1 (7.0)	75 (250)	1
Pittsburgh	0.97	2.1 (7.0)	275 (900)	3
Pittsburgh	1.17	2.3 (7.5)	150 (500)	3
Pittsburgh	1.29	2.2 (7.2)	245 (810)	4
Pittsburgh	1.15	2.2 (7.2)	245 (810)	4
Sewickley	1.82	1.6 (5.25)	185 (600)	3
Tennessee:				
Beach Grove	1.26	0.8 (2.5)	315 (1,025)	1
Beach Grove	0.88	0.8 (2.5)	305 (1,000)	3
Utah:				
Blind Canton	0.84	2.5 (8.3)	365 (1,200)	3
Gilson	0.76	2.7 (9.0)	365 (1,200)	3
Gilson	0.43	2.7 (9.0)	515 (1,690)	3
Lower O'Connor	0.95	5.3 (17.5)	170 (550)	1
Virginia:				
Blair	1.37	1.2 (3.8)	185 (600)	3
Glamorgan	1.06	1.8 (6.0)	215 (700)	3
Jawbone	1.53	1.3 (4.2)	215 (700)	3
Jawbone	1.47	1.4 (4.6)	150 (500)	3
Pocahontas No. 3	0.61	1.7 (5.5)	520 (1,700)	1
Pocahontas No. 3	1.35	1.5 (5.0)	150 (500)	3
Pocahontas No. 4	1.03	2.4 (8.0)	90 (300)	1
West Virginia:				
Beckley	0.72	1.8 (6.0)	350 (1,150)	4
Coalburg	0.75	2.4 (8.0)	90 (300)	1
Coalburg	0.59	2.7 (9.0)	120 (400)	NAp
Coalburg	0.98	2.7 (9.0)	120 (400)	NAp
Coalburg	1.10	2.7 (9.0)	120 (400)	NAp
Coalburg	1.35	2.7 (9.0)	120 (400)	NAp

See explanatory notes at end of table.

Table B-1.—Unsatisfactory pillar retreat case histories—Continued

State and coal seam	ARMPS SF	Seam thickness, m (ft)	Depth, m (ft)	Loading condition
West Virginia:—Continued				
Dorothy	1.36	3.7 (12.0)	95 (315)	3
Dorothy	1.37	3.7 (12.0)	95 (315)	2
Dorothy (Winifrede)	1.15	3.4 (11.0)	70 (225)	1
Dorothy (Winifrede)	1.45	3.4 (11.0)	70 (225)	4
Dorothy (Winifrede)	1.39	3.7 (12.0)	95 (315)	2
Dorothy (Winifrede)	1.02	3.0 (10.0)	55 (175)	1
Dorothy (Winifrede)	1.15	3.0 (10.0)	100 (325)	2
No. 2 Gas	0.95	1.4 (4.5)	245 (800)	4
Stockton	0.84	3.0 (10.0)	70 (225)	2
Stockton	0.96	3.0 (10.0)	75 (240)	1
Stockton	0.82	3.0 (10.0)	75 (245)	1
Stockton	1.47	3.0 (10.0)	85 (280)	1
Stockton	1.19	3.0 (10.0)	85 (280)	2
([1])	0.72	1.5 (5.0)	120 (400)	1
([1])	0.82	1.4 (4.5)	115 (375)	1

NAp Not applicable.
[1]Not provided by original reference.

Table B-2.—Satisfactory pillar retreat case histories

State and coal seam	ARMPS SF	Seam thickness, m (ft)	Depth, m (ft)	Loading condition
Alabama:				
Blue Creek	1.96	1.8 (6.0)	350 (1,150)	2
Colorado:				
Cameo	1.86	2.1 (7.0)	120 (400)	3
Cameo	1.14	2.1 (7.0)	215 (700)	2
Cameo	0.93	2.1 (7.0)	245 (800)	3
D	1.23	2.7 (9.0)	260 (850)	2
D	1.44	2.7 (9.0)	215 (700)	2
Illinois:				
Herrin No. 6	1.14	2.4 (8.0)	215 (700)	3
Kentucky:				
Harlan	1.94	2.0 (6.5)	90 (300)	3
Hazard No. 4	1.36	1.3 (4.4)	130 (420)	3
Kellioka	1.41	1.5 (5.0)	260 (860)	2
Kellioka	1.18	1.5 (5.0)	205 (675)	3
Kellioka	0.45	1.5 (5.0)	440 (1,450)	3
Kellioka	1.61	1.5 (5.0)	185 (600)	3
Lower Elkhorn (No. 6 Gas)	1.64	4.0 (13.0)	120 (400)	3
Pond Creek	1.20	1.7 (5.5)	215 (700)	2
Pond Creek	1.70	1.7 (5.5)	135 (450)	3
Pond Creek	2.0	1.7 (5.5)	120 (400)	2
Pond Creek	1.98	1.7 (5.5)	135 (450)	3
Pond Creek	1.69	1.7 (5.5)	135 (450)	2
Ohio:				
Lower Freeport	1.60	1.5 (5.0)	170 (550)	1
Lower Freeport	1.70	1.5 (5.0)	170 (550)	1
Mahoning	2.50	1.0 (3.3)	75 (250)	1
Pennsylvania:				
Lower Freeport	2.06	1.8 (6.0)	120 (400)	3
Lower Kittanning	1.65	2.0 (6.5)	115 (380)	3
Lower Kittanning	1.78	2.0 (6.5)	115 (380)	3
Lower Kittanning	1.79	2.0 (6.5)	120 (400)	3
Lower Kittanning	1.85	2.0 (6.5)	120 (400)	2
Lower Kittanning	2.14	1.5 (5.0)	170 (550)	3
Pittsburgh	1.89	2.1 (7.0)	150 (500)	3
Pittsburgh	2.78	2.2 (7.2)	260 (855)	2
Sewickley	1.70	1.6 (5.25)	185 (600)	3
Sewickley	2.32	1.6 (5.25)	185 (600)	2
Upper Freeport	1.88	1.3 (4.2)	65 (210)	1
Tennessee:				
Beach Grove	0.98	0.8 (2.5)	315 (1,025)	2
Utah:				
Gilson	0.50	2.7 (9.0)	610 (2,000)	2
Virginia:				
Blair	1.65	1.2 (3.8)	185 (600)	3
Glamorgan	2.31	1.8 (6.0)	120 (400)	3
Jawbone	2.86	1.3 (4.2)	135 (450)	2
Jawbone	2.15	1.3 (4.2)	150 (500)	3
Jawbone	1.97	1.4 (4.6)	120 (400)	3
Mossy-Haggy	2.05	0.9 (3.0)	150 (500)	3
Pocahontas No. 3	0.92	1.7 (5.5)	520 (1,700)	2
Pocahontas No. 3	1.21	1.7 (5.5)	520 (1,700)	3
Pocahontas No. 3	1.89	1.5 (5.0)	150 (500)	2
Pocahontas No. 4	0.91	1.8 (6.0)	365 (1,200)	3
Pocahontas No. 4	2.77	0.9 (3.0)	90 (300)	2
Pocahontas No. 4	0.76	2.0 (6.5)	440 (1,450)	3
Red Ash	2.44	0.9 (3.0)	150 (500)	2
Red Ash	2.44	0.9 (3.0)	215 (700)	3
Tiller	2.22	1.2 (4.0)	150 (500)	3

See explanatory notes at end of table.

Table B-2.—Satisfactory pillar retreat case histories—Continued

State and coal seam	ARMPS SF	Seam thickness, m (ft)	Depth, m (ft)	Loading condition
West Virginia:				
Beckley	0.90	1.8 (6.0)	350 (1,150)	4
Beckley	1.17	2.7 (9.0)	260 (850)	4
Coalburg	1.14	2.7 (9.0)	120 (400)	NAp
Coalburg	1.30	2.7 (9.0)	120 (400)	NAp
Coalburg	1.41	2.7 (9.0)	120 (400)	NAp
Coalburg	1.50	2.7 (9.0)	120 (400)	NAp
Coalburg	1.59	2.7 (9.0)	120 (400)	NAp
Coalburg	1.76	2.7 (9.0)	120 (400)	NAp
Coalburg	1.91	2.7 (9.0)	120 (400)	NAp
Coalburg	2.17	2.7 (9.0)	120 (400)	NAp
Coalburg	2.37	2.7 (9.0)	120 (400)	NAp
Coalburg	2.41	2.7 (9.0)	120 (400)	NAp
Dorothy (Winifrede)	2.10	3.4 (11.0)	70 (225)	2
Dorothy (Winifrede)	1.32	3.0 (10.0)	85 (285)	2
Dorothy (Winifrede)	1.49	3.0 (10.0)	100 (325)	2
Dorothy (Winifrede)	1.72	3.0 (10.0)	70 (225)	2
Fire Creek	1.24	1.4 (4.5)	260 (850)	2
Lower WInifrede	1.73	2.0 (6.5)	185 (600)	2
Peerless	1.56	1.4 (4.75)	215 (700)	2
Sewell	2.55	1.2 (4.0)	105 (350)	2
Stockton	1.56	3.0 (10.0)	65 (220)	2
Stockton	1.99	3.0 (10.0)	75 (245)	2

NAp Not applicable.

PREVENTING MASSIVE PILLAR COLLAPSES IN COAL MINES

By Christopher Mark, Ph.D,[1] Frank E. Chase,[2] and R. Karl Zipf, Jr., Ph.D.[3]

ABSTRACT

A massive pillar collapse occurs when undersized pillars fail and rapidly shed their load to adjacent pillars, which in turn fail. The consequences of these chain-reaction failures can be catastrophic. One effect of a massive pillar collapse can be a powerful, destructive, and potentially hazardous airblast. Thirteen recent massive pillar collapses have been documented in West Virginia, Ohio, Utah, and Colorado. Data collected at the failure sites indicate that all of the massive collapses occurred where the pillar width-to-height (w/h) ratio was 3.0 or less and where the Analysis of Retreat Mining Pillar Stability Factor was less than 1.5. The unique structural characteristics of these pillar systems apparently result in sudden, massive pillar failures, rather than the more common slow "squeezes." The field data, combined with theoretical analysis, provide the basis for two partial-extraction design approaches to control massive pillar collapses. These are the *containment* approach and the *prevention* approach; practical examples are provided of each.

[1]Mining engineer, Pittsburgh Research Center, National Institute for Occupational Safety and Health, Pittsburgh, PA.
[2]Geologist, Pittsburgh Research Center, National Institute for Occupational Safety and Health, Pittsburgh, PA.
[3]Lecturer, Department of Mining and Metallurgical Engineering, University of Queensland, Brisbane, Queensland, Australia.

INTRODUCTION

Massive pillar collapses in room-and-pillar mines have also been labeled "cascading pillar failures," "domino-type failures," or "pillar runs." In this type of failure, when one pillar collapses, the load that it carried transfers rapidly to its neighbors, causing them to fail, and so forth. This failure mechanism can lead to the rapid collapse of very large mine areas. In mild cases, only a few tens of pillars might fail; however, in extreme cases, hundreds, even thousands, of pillars can collapse.

Massive pillar collapses can have catastrophic effects on a mine. Sometimes these effects pose a greater safety risk than the underlying ground control problem. Usually, the collapse induces a devastating airblast due to the displacement of air from the collapsed area. An airblast can totally disrupt the ventilation system at a mine by destroying ventilation stoppings, seals, and fan housings. Flying debris can seriously injure or kill mining personnel. The collapse might also fracture a large volume of rock in the pillars and immediate roof and floor. In coal and other gassy mines, this fragmentation can lead to the sudden release of large quantities of methane gas into the mine atmosphere, creating an explosion hazard. Finally, a massive pillar collapse can release significant seismic energy that may be experienced on the surface as a small earthquake.

Fortunately, not all pillar failures are sudden, massive collapses. Most are slow "squeezes" that develop over days to weeks, and because of their slow progress, do not pose as great a danger to mining personnel. A central goal of the research described in this paper was to identify the physical characteristics that distinguish sudden collapses from other pillar failures.

CASE HISTORIES

The most infamous massive pillar collapse in history occurred in 1960 at Coalbrook North Colliery in South Africa. Thousands of 12- by 12- by 4.2-m (40- by 40- by 14-ft) pillars collapsed over a 305-ha (750-acre) area in 5 min, killing 437 miners [Bryan et al. 1966]. Numerous other, smaller collapses have been reported in South Africa since then [Madden 1991]. In Australia, the New South Wales Joint Coal Board reported eight massive pillar collapses between 1990 and 1993 [University of New South Wales School of Mines 1994].

Massive collapses have also occurred in metal and nonmetal mines. Zipf and Mark [1996] documented six examples from lead-zinc, copper, silica, and salt mines. The largest occurred at a Wyoming trona mine in 1995, where 160 ha (400 acres) of 4- by 29- by 6-m (13- by 95- by 19-ft) fenders collapsed, resulting in a Richter magnitude 5.3 earthquake and one fatality underground [Ferriter et al. 1996]. The ventilation system at the mine was heavily damaged, and an estimated 1 million m^3 (30 million ft^3) of methane was liberated on the day of the collapse. Methane release levels did not return to normal until 3 months later [Ferriter et al. 1996].

In 1992, the former U.S. Bureau of Mines (USBM) was asked to investigate a massive pillar collapse and resultant destructive airblast that had occurred in a coal mine in Mingo County, WV. Subsequent investigations found 12 other examples, which were documented by field investigations [Chase et al. 1994]. Geotechnical evaluations examined the competency of the immediate roof, as well as that of the main roof and its susceptibility to caving. The Analysis of Retreat Mining Pillar Stability (ARMPS) program [Mark and Chase 1997] was used to determine the pillar stability factors (SF). Four examples that illustrate different mining methods and effects are described in detail below.

PILLAR SPLITTING (MINE A)

Mine A is located in Mingo County, WV, and is extracting the 2.9-m (9.5-ft) thick Coalburg Coalbed. A 28-m (90-ft) thick massive sandstone unit with a compressive strength of 83 MPa (12,000 psi) formed the roof above the collapsed area. The Coal Mine Roof Rating (CMRR) of the immediate roof was calculated to be 74. Below the noncleated coalbed is 10.5 m (34 ft) of competent sandy shale and sandstone units. All roadways were 6 m (20 ft) wide.

In 1991, the panel shown in figure 1 was developed. All roadways were driven on 18-m (60-ft) centers and were under 85 m (275 ft) of cover. After the panel was completed, partial pillar recovery was begun. A 6-m (20-ft) wide split was mined through the middle of each pillar, and two 3- by 12-m (10- by 40-ft) fenders with an ARMPS SF of 0.75 remained. Because of the competency of the roof and the support provided by the regularly spaced uniform fenders, no caving occurred while the panel was being retreat mined. Three weeks after the panel had been abandoned, an area measuring approximately 140 by 155 m (450 by 500 ft) containing 107 fenders collapsed. Miners on a nearby section were knocked to the floor by the resultant airblast. One miner was bounced off of a steel rail and required 26 stitches to his head. Fortunately, no miners were near the collapse. However, if the failure had occurred 15 min later, two miners would have

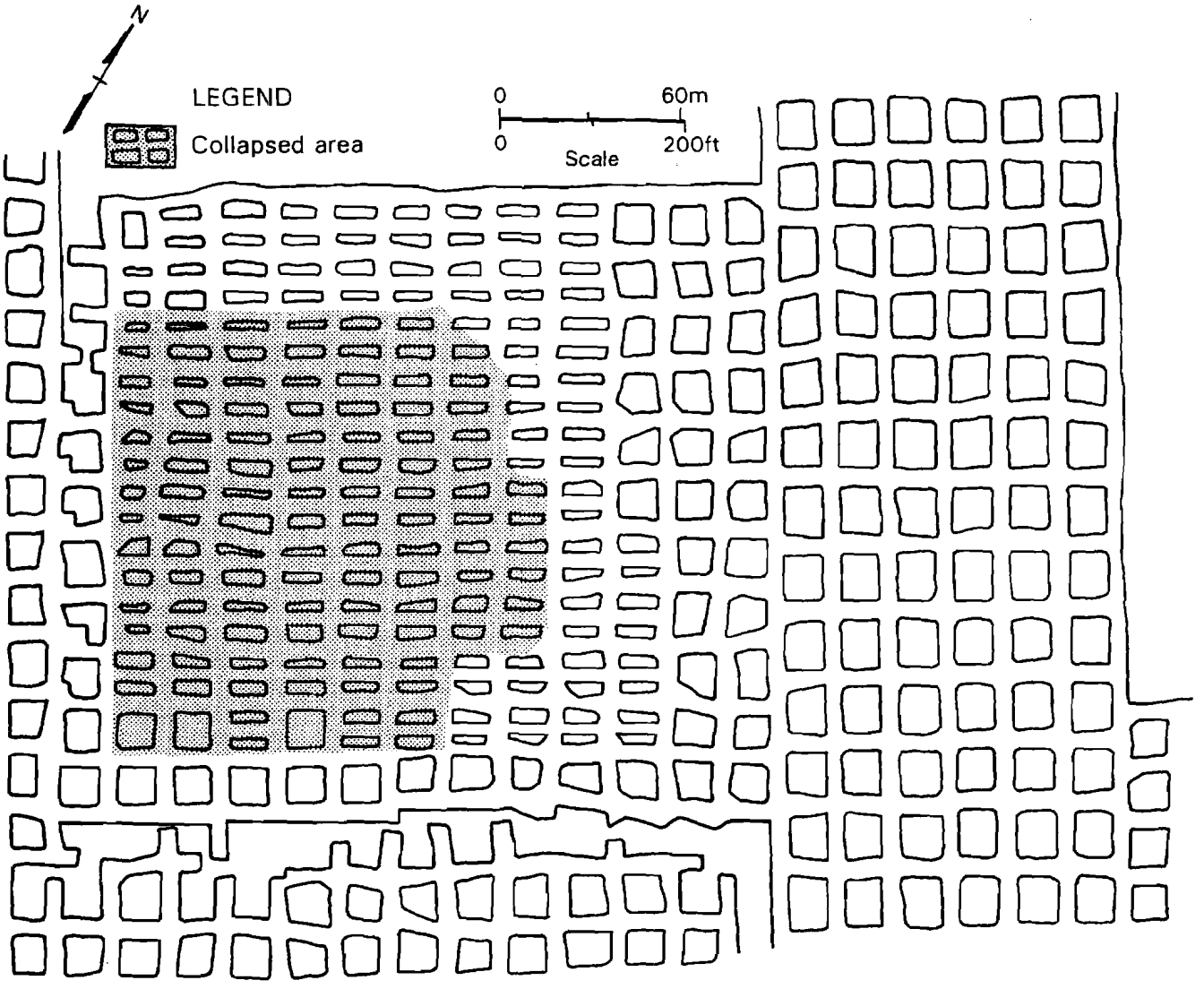

Figure 1.—Failed split-pillar workings in Mine A.

been rock dusting ribs immediately outby the area that collapsed. The airblast blew out 26 cinder block stoppings and the fan house weak wall, which closed the mine for days.

As was the case in many of the other collapses that were studied, a number of fenders near the edge of the collapse did not fail. There are two possible explanations for this: (1) The collapse might terminate as soon as the competent roof units were able to bridge the span, or (2) the collapse might terminate where the fenders were shielded from the full load by the adjacent abutment. In the second case, the 12- by 12-m (40- by 40-ft) pillars with an SF of 2.33 may have provided a hinge line, which allowed the roof to cantilever over the first several rows of fenders.

An earlier collapse had occurred at Mine A in partially pillared workings under very similar conditions. Damage was limited to blown out stoppings, and no one was injured. Complete documentation of this case was unavailable.

After the second collapse, the practice of pillar splitting was reexamined at the mine. Several sets of mobile roof supports were purchased, and retreat mining continued with full pillar extraction. Most recently, some pillar splitting has been conducted, with rows of unsplit pillars left as barriers to isolate retreated areas.

PILLAR SPLITTING/ABUTMENT LOAD OVERRIDE (MINE C)

Mine C is located in Logan County, WV, and is extracting the 3-m (10-ft) thick Dorothy Coalbed. The immediate and main roof throughout the mine is composed of a fine-grained,

semilaminated sandstone with a CMRR of 64; the floor was composed of an extremely firm sandstone. Coalbed cleating was nonexistent. All roadways in the mine were 6 m (20 ft) wide and were driven on 18-m (60-ft) centers in the relevant area.

In 1992, the operator was splitting pillars in the panel shown in figure 2. After the 6-m (20-ft) wide split, two 3- by 12-m (10- by 40-ft) fenders with an SF of 0.94-1.15 remained. When the operator began to mine the pillar row outby the last row split (figure 2), a massive collapse of the fenders in the gobbed-out area initiated. The roof bolter operator on the section indicated that he and his coworkers were knocked to the floor by the resulting airblast, and 103 stoppings were destroyed. The pillars where the collapse terminated had an SF of 1.97. Overburden in the collapsed area ranged from 53 to 66 m (175 to 215 ft).

A subsequent pillar collapse occurred at Mine C, apparently triggered by time deterioration and front abutment pressures generated by full pillar extraction. Roadways in the collapsed area were driven on 15-m (50-ft) centers, and 91 pillars with an SF of 1.08 failed. Pillars with an SF of 1.69 halted the collapse. These roadways were driven on 18-m (60-ft) centers. No stoppings were damaged, and the overburden in the area was 99 m (325 ft).

Mine C was visited in February 1994 to observe diagonal pillar splitting, which is not a common practice. Roadways were driven on 15-m (50-ft) centers, and the pillar splits were 5 m (16 ft) wide. The extraction percentage was 86%. The triangular remnant stumps were observed to routinely crush out after finishing the pillar row, and the roof caved immediately inby the breakers. The breakers and wedges showed no weight. Where the first pillar collapse occurred in Mine C using the traditional 6-m (20-ft) wide split through a 12- by 12-m (40- by 40-ft) pillar, 78% of the coal was extracted. This 8% increase in resource recovery, coupled with a less stable triangular stump with a smaller perimeter, probably explains why the roof caves more readily than in traditional pillar splitting.

SMALL-CENTER MINING (MINE D)

Mine D is located in Mingo County, WV, and is extracting the 3.4-m (11-ft) thick Dorothy Coalbed. The roof consisted of 76 cm (2.5 ft) of laminated fossiliferous shale and 7 cm (3 in) of rider coal, and 25 m (80 ft) of cross-bedded sandstone was observed in the highwall. The roof had a CMRR of 81. Below the noncleated coalbed was 1.5 m (5 ft) of sandy shale and 28 m (91 ft) of sandstone. All roadways in the mine were 6 m (20 ft) wide.

In 1992, ninety-four 6- by 6-m (20- by 20-ft) pillars with an SF of 1.15 and thirty-two 9- by 9-m (30- by 30-ft) pillars with an SF of 1.45 failed. As shown in figure 3, the pillar failures occurred in a panel driven off the mains. The resultant airblast blew out 37 stoppings. The only other stopping in the mine had a hole in it. Some of these stoppings were as far away as 244 m (800 ft) from the perimeter of the collapse. In one stopping, it was determined that some of its 14-kg (30-lb) cinder blocks had been hurled 152 m (500 ft). Fortunately, the occurrence was on an idle shift, and no one was in the mine. The collapse was halted by pillars in the main entries, which were 12- by 12-m (40- by 40-ft) and had an SF of 3.33. Cover over the collapsed area was 69 m (225 ft).

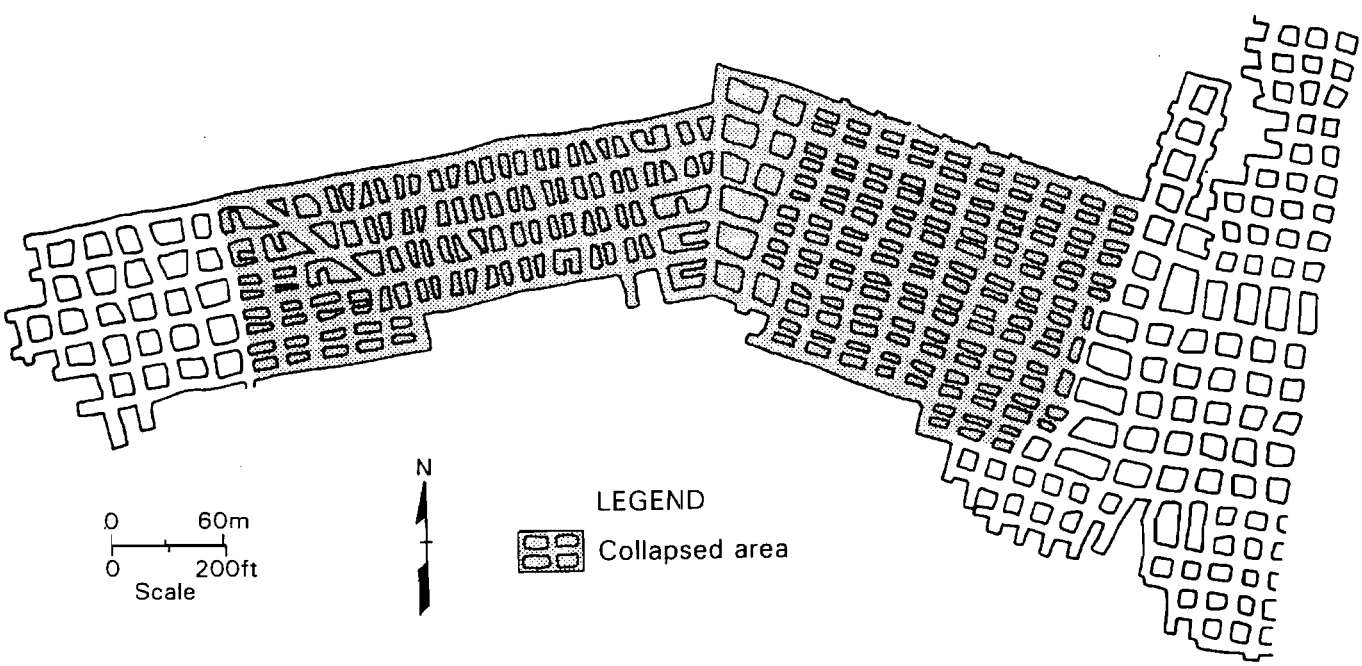

Figure 2.—Location of split-pillar collapse at Mine C.

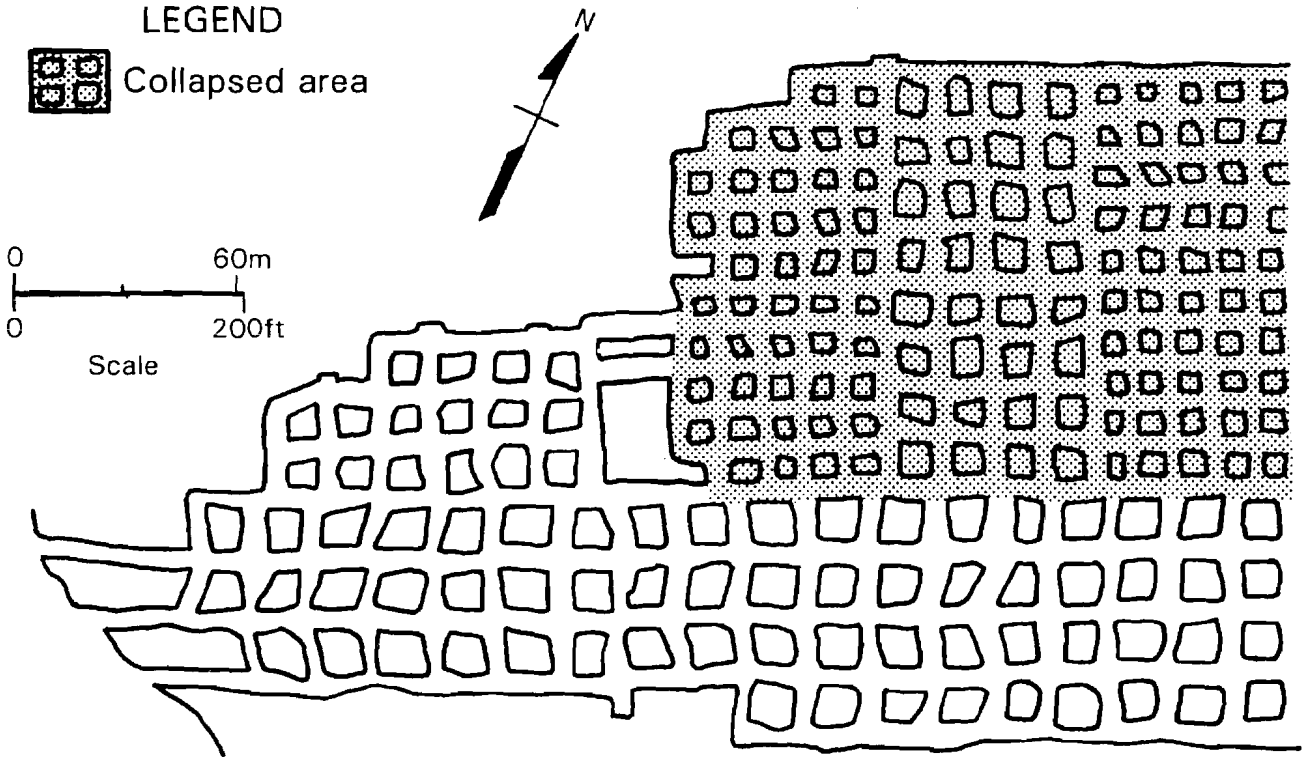

Figure 3.—Failed small-center development workings at Mine D.

FLOOR RECOVERY (MINE G)

Mine G is located in Utah and was extracting the 8-m (25-ft) thick Lower O'Connor Seam [Ropchan 1991]. There were previous workings in the Upper O'Connor above Mine G, separated by 18-23 m (60-80 ft) of overburden. The total overburden above the collapsed area was about 170 m (550 ft).

Room-and-pillar workings were advanced 2.4 m (8 ft) high on 18-m (60-ft) centers. The panel was developed nine entries wide and 535 m (1,740 ft) long. The pillars were not extracted on retreat, but an additional 3 m (10 ft) was removed from the floor, leaving 5.4-m (18-ft) high remnants. Mining the floor coal decreased the w/h ratio of the pillars from 5 to 2.2 and reduced their strength by about 45%.

The collapse occurred when the section was within two crosscuts of being completely retreated. The force of the airblast hurled three miners for distances of 12-30 m (40-100 ft), causing one severe head laceration. A 2-ton shop car was blown through a stopping. There was extensive damage to ventilation structures; concrete blocks from stoppings were scattered up to 30 m (100 ft). The main mine fan was stalled, and airflow in the mine was temporarily reversed. There was some speculation that a north-south trending fault that bordered the panel may have contributed to the collapse.

SUMMARY OF CASE HISTORIES

Table 1 summarizes the mining dimensions of 13 examples of massive pillar collapses in U.S. coal mines. All occurred during the 1980's and 1990's, and all happened suddenly or without significant warning. Most resulted in airblasts and damage to the ventilation system.

Analysis of the data reveals some important similarities. First, the ARMPS SF was less than 1.5 in every case and less than 1.2 in 81% of the cases. This implies that the pillars were not sized to carry the full overburden load. Pillar failures are not unusual; however, most are slow and nonviolent. What apparently distinguishes the sudden collapses from the slow squeezes is the pillar's w/h ratio. Every massive pillar collapse involved *slender* pillars with a w/h ratio of less than 3. Another common characteristic of the collapses is that the overburden was judged to be relatively strong in every case. Finally, the collapsed areas were all at least 1.6 ha (4 acres), and the minimum dimension of a collapsed panel suffering major damage was 110 m (350 ft).

Table 1.—Massive pillar collapses in coal mines

Case history	State	Depth, m (ft)	Pillar size, m (ft)	ARMPS SF	w/h ratio	Collapsed area, ha (acres)	Collapse size, m (ft)	Damage from airblast
A	WV	84 (275)	3 by 12 (10 by 40)	0.86	1.05	2.3 (5.7)	150 by 150 (500 by 500)	26 stoppings, 1 injury.
B1	WV	73 (240)	3 by 12 (10 by 40)	0.96	1.00	—	—	32 stoppings, fan wall out.
			3 by 18 (10 by 60)	1.10	1.00			
B2	WV	75 (245)	3 by 12 (10 by 40)	0.94	1.00	1.7 (4.1)	100 by 150 (350 by 500)	40 stoppings.
B3	WV	85 (280)	9 by 9 (30 by 30)	1.46	3.00	2.8 (6.8)	180 by 180 (600 by 600)	70 stoppings.
			6 by 12 (20 by 40)	1.47	2.00			
C1	WV	60 (195)	3 by 12 (10 by 40)	1.19	1.00	2.1 (5.2)	140 by 150 (450 by 500)	103 stoppings.
C2	WV	99 (325)	9 by 9 (30 by 30)	1.15	3.00	1.9 (4.8)	100 by 180 (350 by 600)	Minimal.
D	WV	69 (225)	6 by 6 (20 by 20)	1.15	1.82	1.7 (4.3)	100 by 160 (350 by 540)	37 stoppings.
			9 by 9 (30 by 30)	1.42	2.73			
E1	WV	91 (300)	3 by 12 (10 by 40)	0.79	1.42	7.4 (18.2)	240 by 290 (800 by 950)	Major damage.
E2	WV	91 (300)	3 by 12 (10 by 40)	0.71	1.11	6.7 (16.6)	220 by 275 (720 by 900)	Major damage.
F	OH	76 (250)	2 by 12 (7 by 39)	0.66	2.12	2.0 (4.9)	90 by 215 (300 by 700)	Minimal.
G	UT	168 (550)	12 by 12 (40 by 40)	0.95	2.29	7.9 (19.4)	150 by 490 (480 by 1,620)	Major damage, 1 injury.
O	WV	—	—	1.03	2.50	1.8 (4.5)	120 by 150 (400 by 500)	—
R	CO	120 (400)	4 by 24 (12 by 80)	0.57	1.71	2.8 (6.8)	180 by 150 (600 by 500)	Minor damage.

NOTE.—Dash indicates no data available.

MECHANICS OF MASSIVE PILLAR COLLAPSES

A conceptual model of a massive pillar collapse can be described as follows. Undersized, regularly spaced remnant pillars help the stiff and competent roof to bridge a relatively wide span. A pressure arch is created, with much of the overburden load being transferred by the stiff roof to the barrier pillars surrounding the extraction area. Within the pressure arch, the pillars are shielded from the full weight of the overburden. Eventually, any one of a number of mechanisms may cause the pressure arch to break down:

- The extraction area becomes so large that it exceeds the bridging capacity of the roof.
- Mining approaches a fault or other discontinuity.
- The roof weakens over time.
- The remnant pillars weaken over time.

Once the pressure arch breaks down and additional overburden load is shifted to the pillars, their structural characteristics are such that a sudden, massive collapse can occur. Slender pillars have little residual strength and shed load rapidly as they fail. When one fails, the weight it transfers can overload adjacent pillars, and a rapid "domino" failure of adjacent pillars can ensue. Pillars that are more squat retain most of their load even after failure. Such pillars will squeeze slowly, rather than collapse.

Laboratory tests have shown that the residual strength of coal specimens depends on their w/h ratio [Das 1986]. Specimens with a w/h ratio of less than 3 typically have little residual strength, which means that they shed almost their entire load when they fail (figure 4). As the specimens become more squat, their residual strength increases. Once the w/h ratio reaches 8-10, the specimens become "strain-hardening," which means that they never shed load, and sudden collapse is impossible.

Figure 5 summarizes available postfailure modulus data for large in situ coal specimens and full-scale coal pillars. The dashed line indicates a conservative envelope for these limited in situ data. In general, the laboratory postfailure moduli exceed the large-scale test values.

The importance of the postfailure stiffness is further explained by the theory of *local mine stiffness*, first proposed by Salamon [1970] and discussed by Zipf [1992, 1996]. The theory states that if the pillar's postfailure modulus (K_P) is less than the stiffness of the mine roof (the local mine stiffness, or K_M), the failure is stable and gradual (figure 6*B*). If K_P exceeds K_M, on the other hand, the failure is sudden and violent (figure 6*A*). The local mine stiffness depends on the modulus of the immediate roof; floor and pillar materials; and the layout of pillars, mine openings, and barrier pillars. The postfailure stiffness, K_P, depends on the w/h ratio of the coal pillar, as shown in figure 5. Using a boundary-element method program similar to the USBM's MULSIM/NL program, it is possible to simulate both massive pillar collapses and stable, progressive pillar failures [Zipf 1996]. The behavior of computer simulations changes depending on whether the model satisfies or violates the local mine stiffness stability criterion.

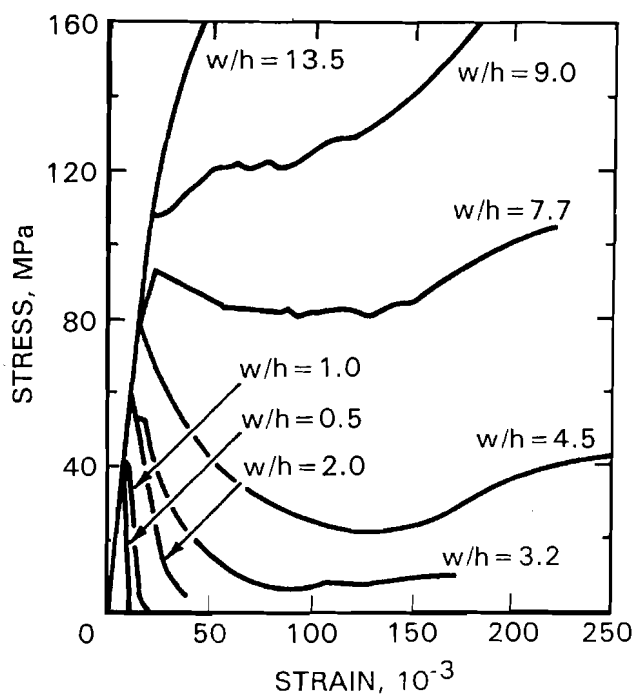

Figure 4.—Complete stress-strain curves for Indian coal specimens, showing increasing residual strength with increasing w/h ratio (after Das [1986]).

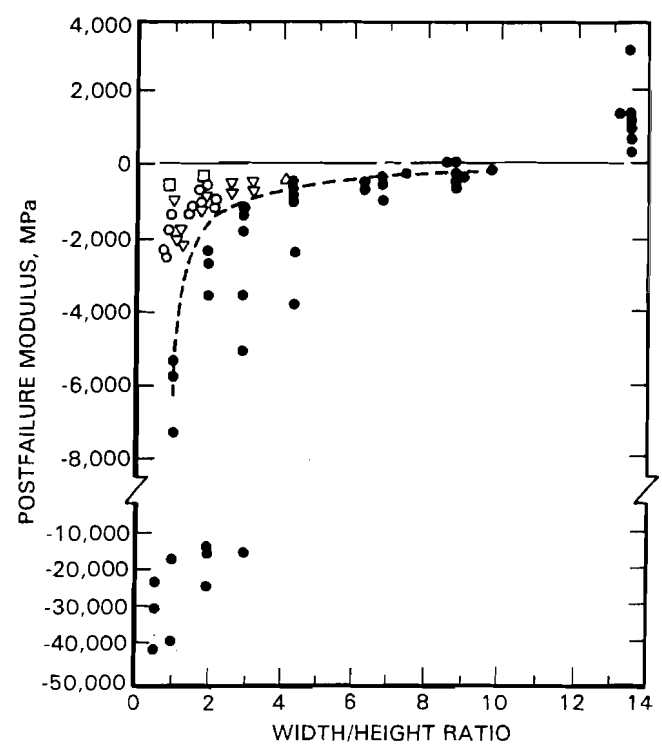

Figure 5.—Postfailure modulus of coal pillars, in situ coal specimens, and laboratory samples. Darkened circles represent laboratory tests, remaining symbols represent in situ tests [Chase et al. 1994].

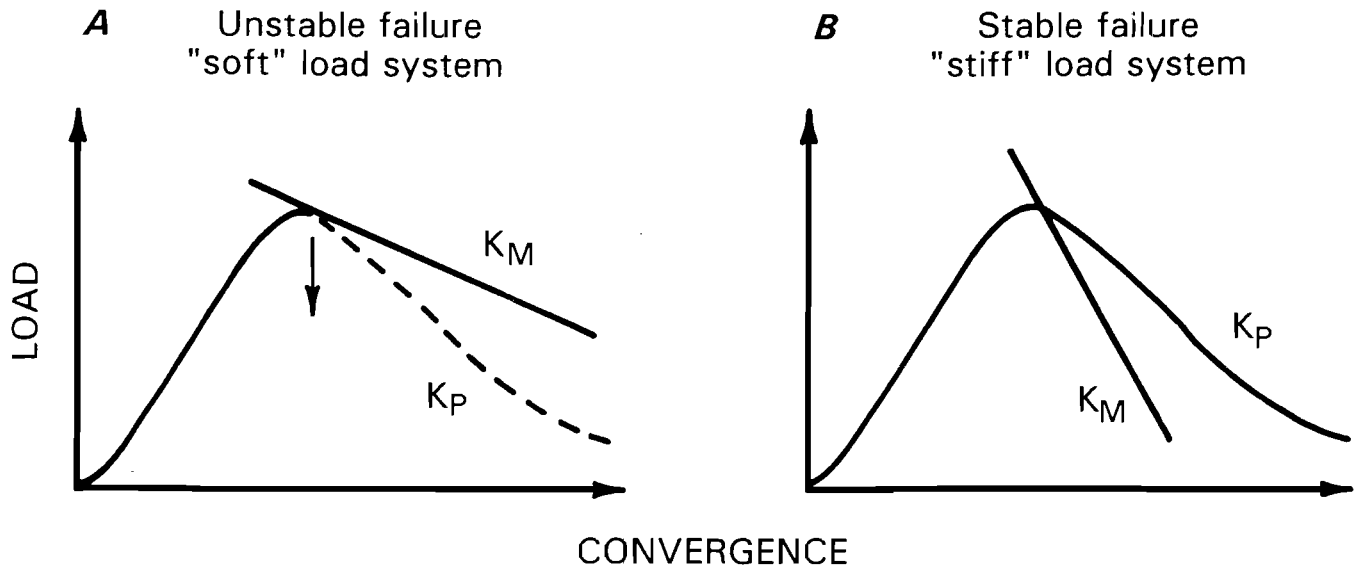

Figure 6.—Illustration of the local mine stiffness concept. *A*, local mine stiffness (K_m) is less than postfailure stiffness of the pillar (K_p), resulting in unstable failure. *B*, local mine stiffness (K_M) exceeds the pillar's postfailure stiffness (K_p), resulting in slow and stable failure.

DESIGN APPROACHES TO CONTROL MASSIVE PILLAR COLLAPSE

In coal mining, small-center mining and partial pillaring are methods to achieve high extraction without full pillar recovery. Both leave significant remnant pillars in the mined-out areas. For example, mining on 15-m (50-ft) centers using 6-m (20-ft) entries leaves about 35% of the coal in 9- by 9-m (30- by 30-ft) pillars. Splitting pillars developed on 18- by 18-m (60- by 60-ft) centers leaves about 22% of the coal. Both techniques can be adapted to avoid massive pillar collapses following the strategies of *prevention* or *containment.*

In the *prevention* approach, the panel pillars are designed so that collapse is highly unlikely. This can be accomplished by increasing either the SF of the pillars or their w/h ratio. In the *containment* approach, high extraction is practiced within individual compartments that are separated by barriers. The small pillars may collapse within a compartment; however, because the compartment size is limited, the consequences are not significant. The barriers may be true barrier pillars, or they may be rows of development pillars that are not split on retreat. The containment approach has been likened to the use of compartments on a submarine.

Full extraction can be another strategy to avoid massive pillar collapses. Mining all of the coal removes the support to the main roof, thereby limiting the potential width of the pressure arch. Although some "first falls" behind longwalls and other full-extraction systems have been destructive, they generally involve areas smaller than massive pillar collapses.

SMALL-CENTER MINING: A PREVENTION APPROACH

Square pillars are generally used in small-center mining. Table 1 indicates that three collapses involved 9-m (30-ft) square pillars, and one involved 12-m (40-ft) square pillars. Square pillars may be designed to be collapse-resistant in two ways. The first is to increase their w/h ratio. Because no collapses have been documented in which the w/h ratio was greater than 3.0, a design w/h ratio of 4.0 is suggested to provide an adequate margin of safety.

Pillar collapses may also be avoided by maintaining a sufficiently high SF. The ARMPS case history data base [Mark and Chase 1997] suggests that normally an ARMPS SF of 1.5 is sufficient to limit the probability of pillar failure. Where slender pillars are being employed and their failure may result in a massive collapse rather than a slow squeeze, it

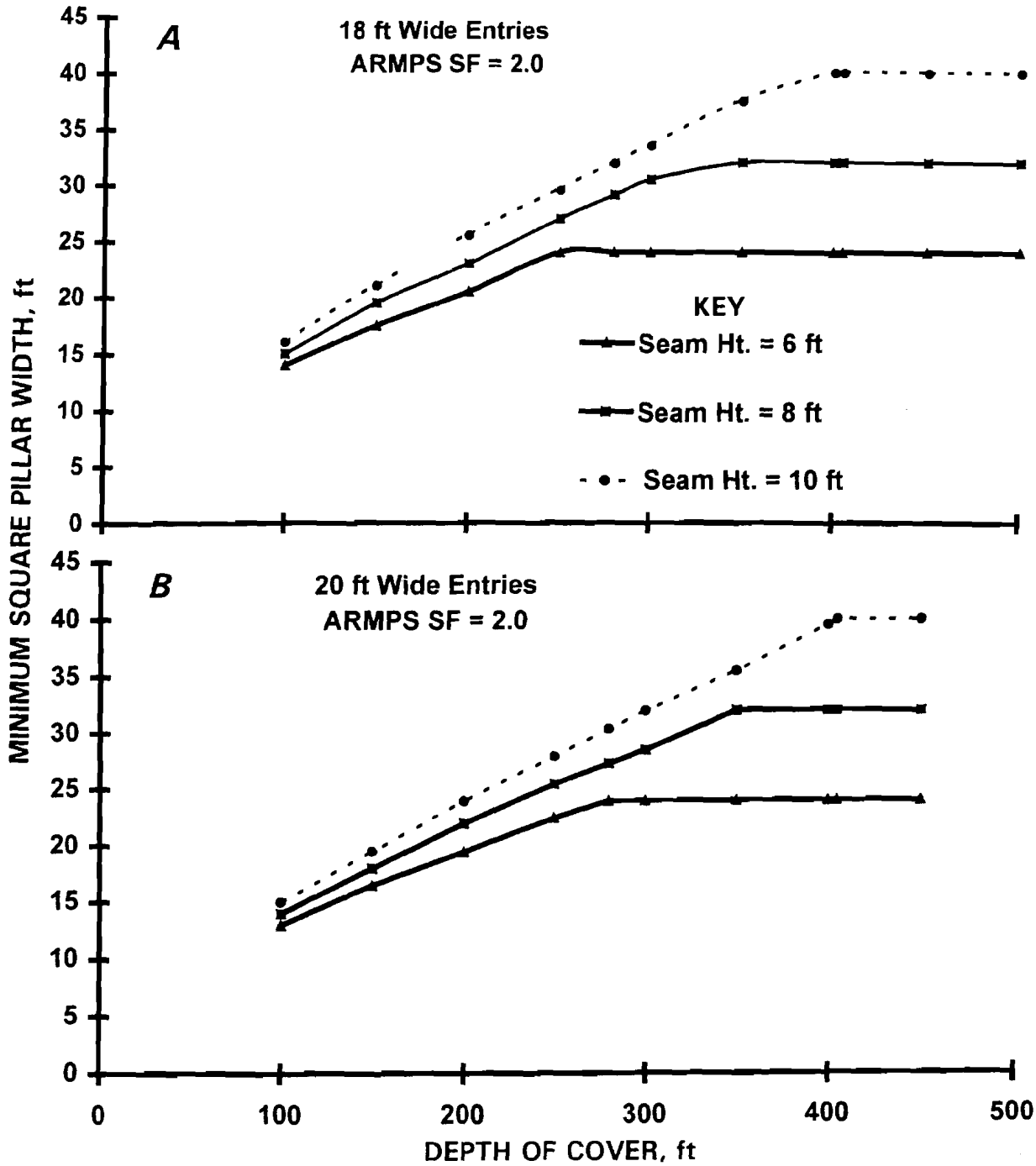

Figure 7.—Suggested minimum square pillar size to avoid massive pillar collapse. *A*, 5.5-m (18-ft) entries; *B*, 6-m (20-ft) entries.

might be prudent to increase the SF to 2.0. The SF can be increased by increasing the pillar width, decreasing the extraction ratio, or both. These two design criteria have been combined to develop guidelines for small-center mining. Figure 7 was developed assuming square pillars with an SF of 2.0 or a w/h ratio of 4.0.

When using 6-m (20-ft) wide entries, the minimum suggested pillar sizes are increased by about 6%. Also note that these design criteria are only for controlling massive pillar collapses. At greater depths, pillar sizes may need to be increased beyond a w/h ratio of 4 to maintain an adequate SF. The failure of pillars with a w/h ratio greater than 4 should be a slow squeeze rather than a sudden collapse.

PILLAR SPLITTING: A CONTAINMENT APPROACH

Fenders left from pillar-splitting operations have failed at even shallow depths. For example, 3- by 12-m (10- by 40-ft) fenders in a 3-m (10-ft) seam have an SF of 1.5 at only 55 m (180 ft) of cover. The potential for a destructive massive collapse can be reduced by limiting the size of the gob area. To separate the gob areas, rows of unsplit development pillars can be left as barriers. This strategy is based on two assumptions:

- By limiting the span above the mined-out area, a bridging failure of the strong overburden is less likely.
- By minimizing the size of the potential collapsed area, any airblast resulting from a collapse would be less powerful.

Table 1 shows that no major collapses have been documented in which the gob area was less than 1.5 ha (4 acres). In the five cases where the gob area was between 1.5 and 1.9 ha (4 and 5 acres), about 60% of the incidents resulted in major damage. Additionally, no damaging incidents occurred when the minimum dimension of the mined-out area was less than 100 m (350 ft). Using these data, acceptable dimensions of a pillar-splitting operation might be a maximum area of 1.2 ha (3.2 acres), with a minimum dimension of less than 90 m (300 ft). For example:

- Assuming 18- by 18-m (60- by 60-ft) centers in a nine-entry system with four rows split, the mined-out area would have a minimum dimension of 72 m (240 ft) and an area of about 1.1 ha (3 acres), as shown in figures 8*A* and 8*B*.
- Assuming the same pillar size in a six-entry system with five rows split, the minimum dimension would be 90 m (300 ft) and the area would be about 1 ha (2.5 acres), as shown in figures 8*C* and 8*D*.

The next question is: how many unsplit rows should be left between these mined-out areas? The goal is to leave enough of a "barrier" so that the failure of one gob area does not initiate failure in adjacent areas. ARMPS was used to evaluate the loading on unsplit pillars between two mined-out areas. The program was modified so that two "front" gobs could be applied to the unsplit pillars. The analyses were run with abutment angles of 90°, which assumes that none of the load is carried by the gob, but instead is transferred to the barriers.

In the first set of analyses, two rows of full-sized pillars were used as the barrier. An ARMPS SF of 1.5 was deemed necessary to prevent the collapse of one gob area triggering the collapse of an adjacent area. Three rows of pillars were used in the second set of analyses; the SF was reduced to 1.0 because of the greater stiffness of the barrier. Pillars on 18- by 18-m (60- by 60-ft) centers were used in all cases.

Other parameters that were varied included the number of rows that were split (three, four, and five), the entry width (5.5 and 6 m (18 and 20 ft)), the seam height (2, 2.5, and 3 m (6, 8, and 10 ft)), and the number of entries in the section (five, seven, and nine). The results are presented in figure 9, which shows the suggested maximum depth of cover for each combination of parameters. In general, considering 5.5-m (18-ft) entries in a 2.5-m (8-ft) seam, it appears that two rows of unsplit pillars are an adequate barrier at depths less than about 300 ft and that three rows are acceptable to about 170 m (550 ft) of cover.

Barriers must also be left between extracted panels. These can be unsplit development pillars or solid coal. If unsplit development pillars are used, the analysis in figure 9 should apply. For solid coal barriers, figure 10 shows the suggested widths, using the same loading assumptions. For a 2.5-m (8-ft) seam, a 17-m (55-ft) solid barrier appears to be appropriate at 75 m (250 ft) of cover, and 23 m (75 ft) might be needed at 120 m (400 ft).

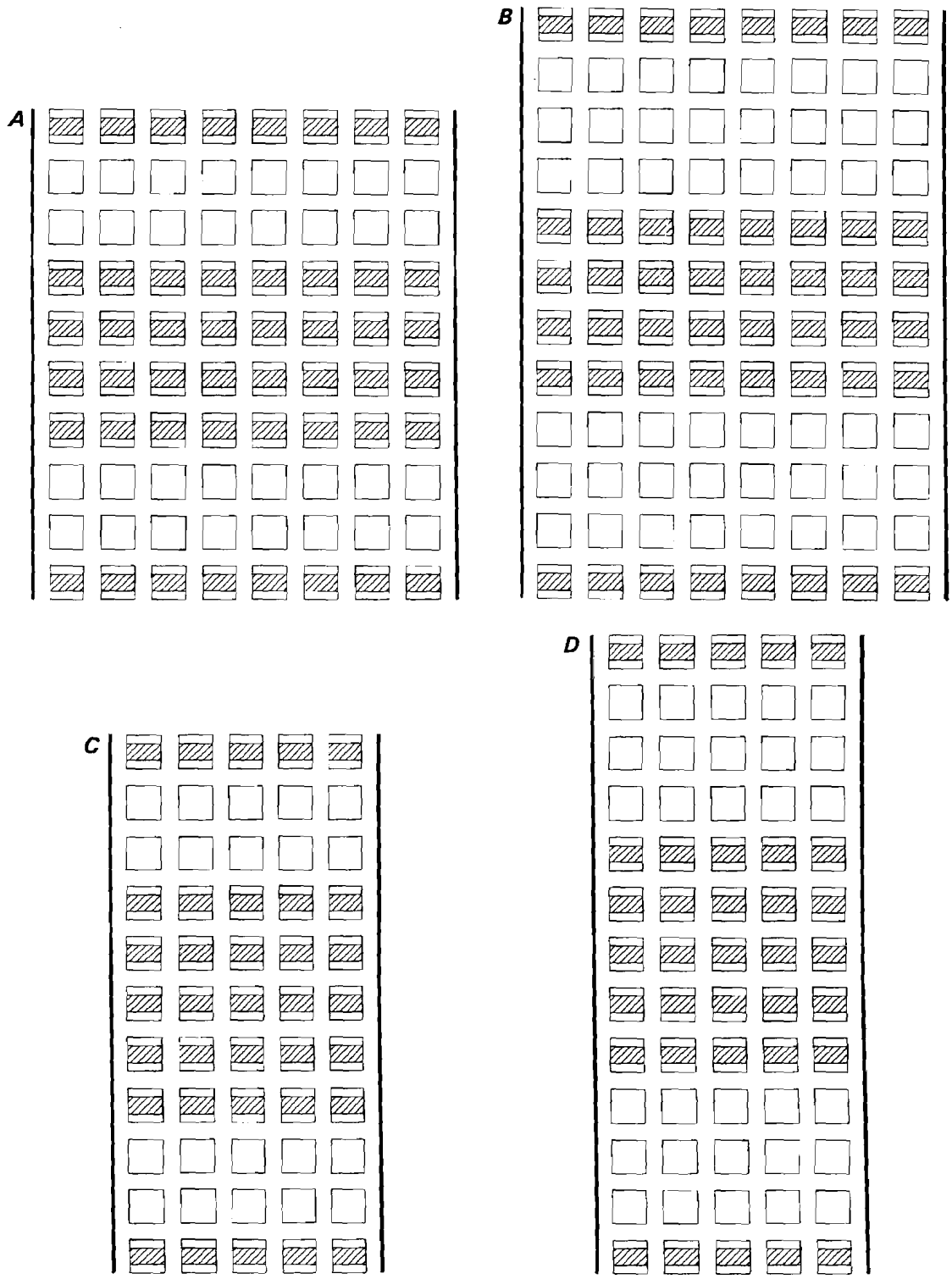

Figure 8.—Possible pillar-splitting plan for airblast control. *A*, nine-entry system, two rows of unsplit pillars for barrier. *B*, nine-entry system, three rows of unsplit pillars for barrier. *C*, six-entry system, two rows of unsplit pillars for barrier. *D*, six-entry system, three rows of unsplit pillars for barrier.

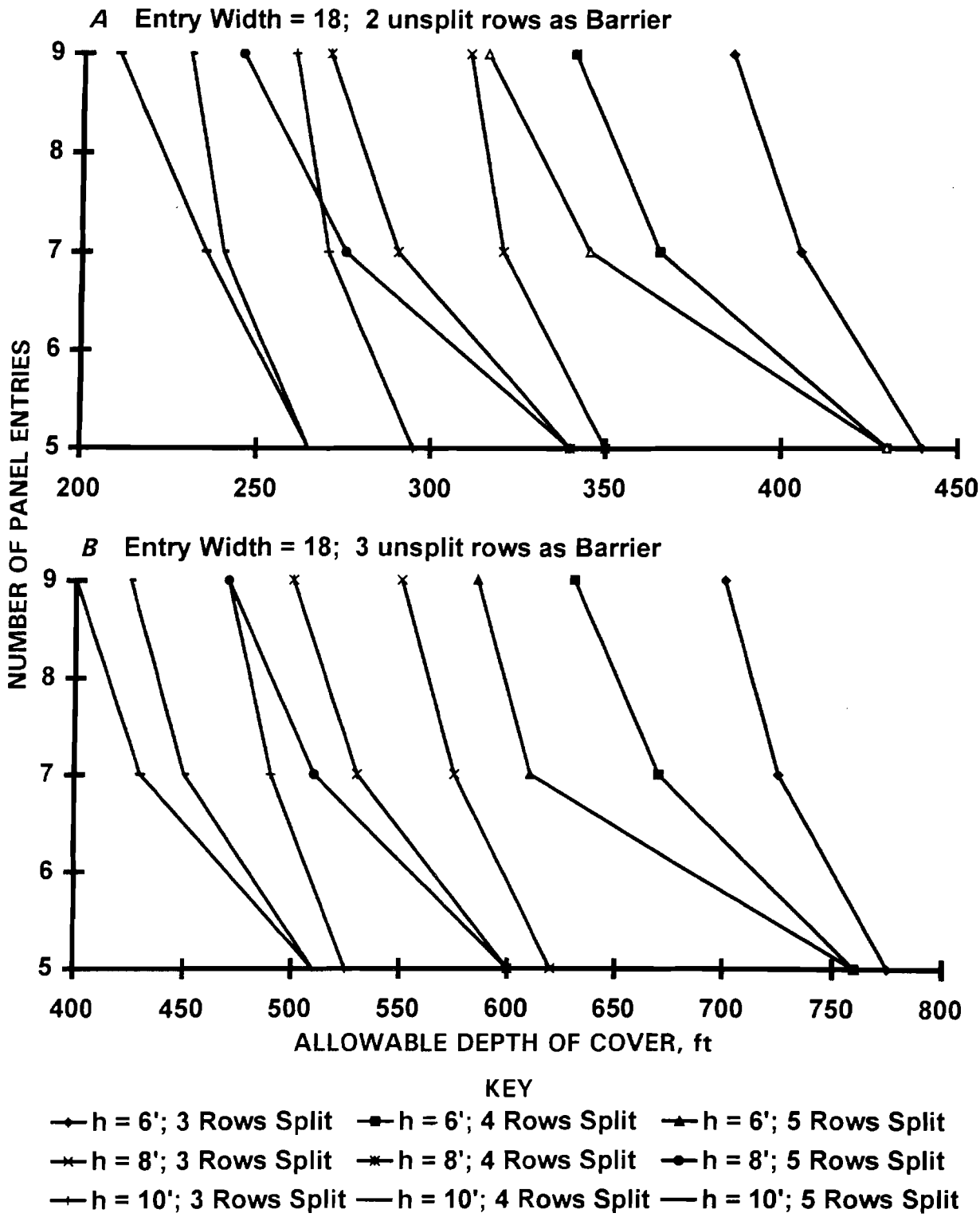

Figure 9.—*A*, suggested maximum depth for two rows of unsplit pillars as barrier between gob areas, 5.5-m (18-ft) entry, 18- by 18-m (60- by 60-ft) pillars. *B*, suggested maximum depth for three rows of unsplit pillars as barrier between gob areas, same entry and pillar sizes.

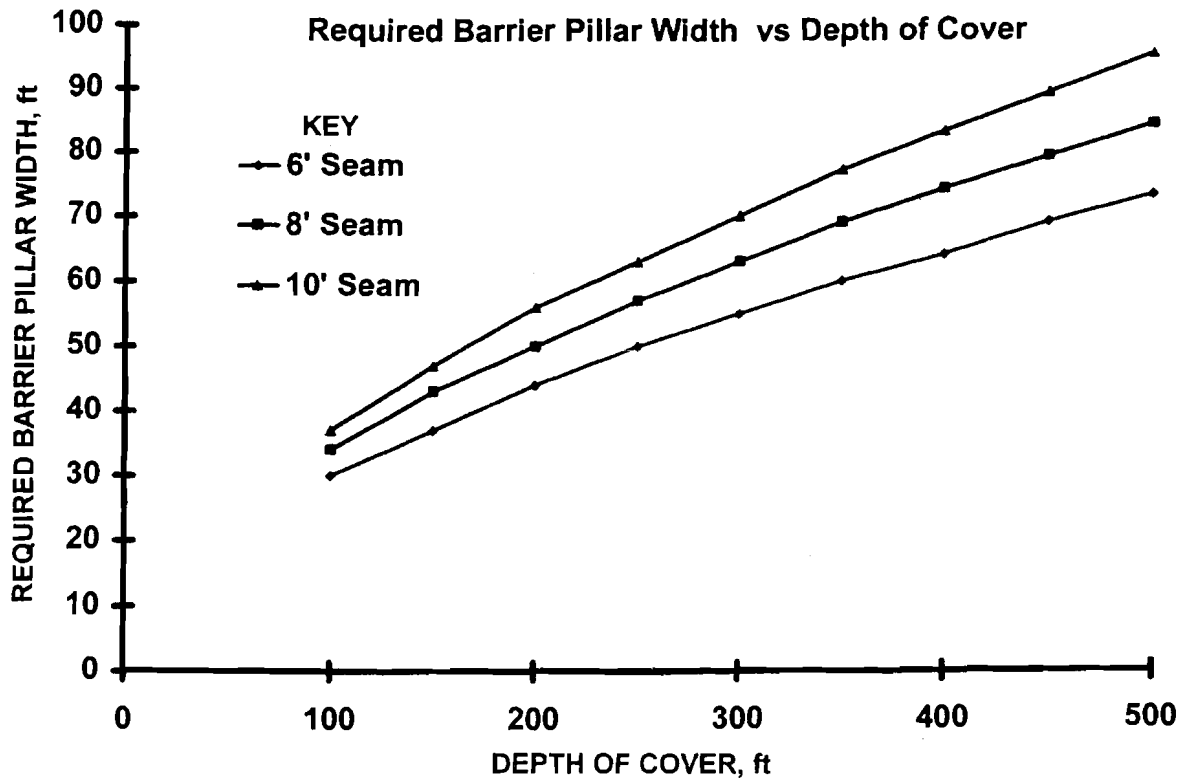

Figure 10.—Suggested solid coal barrier width between two areas where pillars have been split.

CONCLUSIONS

The potential for massive pillar collapses should always be considered when designing room-and-pillar mining operations. A collapse can occur when one pillar fails suddenly, overstresses its neighbors, causing them to fail, and so forth, in very rapid succession. Very large mining areas can collapse via this mechanism within seconds with little or no warning. The collapse itself can pose serious danger to nearby mining personnel. Additionally, the collapse can induce a violent airblast that disrupts or destroys the ventilation system. Further critical danger to miners exists if the mine atmosphere becomes explosive or contaminated as a result of the pillar collapse.

Research has found that massive collapses in coal mines have the following common characteristics:

- Slender pillars (w/h ratio less than 3.0).
- Low SF (less than 1.5).
- Competent roof strata.
- Collapsed area greater than 1.6 ha (4 acres).
- Minimum dimension of the collapsed areas greater than 110 m (350 ft).

Two alternative strategies may be successful in preventing massive pillar collapses. For small-center mining, *prevention* may be applied by increasing either the w/h ratio or the SF. *Containment* is appropriate for pillar splitting and requires leaving barriers or rows of unsplit pillars to limit the area of potential collapses. A final strategy is to go to full pillar extraction. By removing the support provided by the remnant fenders left during traditional pillar splitting, the bridging capacity of the roof should be substantially reduced.

Finally, it is important to note that the massive pillar collapses discussed in this paper are not to be confused with coal bumps or rock bursts. Although the outcomes may appear similar, the underlying mechanics are entirely different. Bumps are sudden, violent failures that occur near coal mine entries and expel large amounts of coal and rock into the excavation [Maleki 1995]. They occur at great depth, affect pillars (and longwall panels) with large w/h ratios, and are often associated with mining-induced seismicity. The design recommendations discussed here for massive pillar collapses do *not* apply to coal bump control.

REFERENCES

Bryan A, Bryan JG, Fouche J [1966]. Some problems of strata control and support in pillar workings. Min Eng (London) *123*:238-254.

Chase FE, Zipf RK, Mark C [1994]. The massive collapse of coal pillars - case histories from the United States. In: Proceedings of the 13th Conference on Ground Control in Mining. Morgantown, WV: West Virginia University, pp. 69-80.

Das MN [1986]. Influence of width/height ratio on postfailure behavior of coal. Intl J Min Geol Eng *4*:79-87.

Ferriter RL, Zipf RK, Ropchan DM, Davidson J [1996]. Report of technical investigation underground nonmetal mine collapse accident, Solvay Mine. U.S. Department of Labor, Mine Safety and Health Administration.

Madden BJ [1991]. A re-assessment of coal pillar design. J South Afr Inst Min Metall *91*(1):27-37.

Maleki H [1995]. An analysis of violent failure in U.S. coal mines—case studies. In: Maleki H, Wopat PF, Repsher RC, Tuchman RJ, eds. Proceedings: Mechanics and Mitigation of Violent Failure in Coal and Hard-Rock Mines. Pittsburgh, PA: U.S. Department of the Interior, Bureau of Mines, SP 01-95, pp. 5-25.

Mark C, Chase FE [1997]. Analysis of retreat mining pillar stability (ARMPS). In: Mark C, Tuchman RJ, comp. Proceedings: New Technology for Ground Control in Retreat Mining. Pittsburgh, PA: U.S. Department of Health and Human Services, Public Health Service, Centers for Disease Control, National Institute for Occupational Safety and Health, IC 9446.

Ropchan D [1991]. Ground support evaluation—Belina No. 2 Mine ID No. 42-01280. Denver, CO: U.S. Department of Labor, Mine Safety and Health Administration.

Salamon MDG [1970]. Stability, instability, and design of pillar workings. Intl J Rock Mech Min Sci *7*:613-631.

University of New South Wales School of Mines [1994]. Pillar performance. Strata Control for Coal Mine Design *Apr*:5.

Zipf RK Jr. [1992]. Analysis of stable and unstable pillar failure using a local mine stiffness method. In: Iannacchione AT, Mark C, Repsher RC, Tuchman RJ, Jones CC, comp. Proceedings of the Workshop on Coal Pillar Mechanics and Design. Pittsburgh, PA: U.S. Department of the Interior, Bureau of Mines, IC 9315, pp. 128-143.

Zipf RK [1996]. Analysis and design methods to control cascading pillar failure in room-and-pillar mines. In: Bieniawski ZT, ed. Milestones in Rock Engineering, Balkema, pp. 225-264.

Zipf RK, Mark C [1996]. Design methods to control violent pillar failures in room-and-pillar mines. In: Proceedings of the 15th Conference on Ground Control in Mining. Golden, CO: Colorado School of Mines, pp. 571-585.

PILLAR DESIGN AND COAL STRENGTH

By Christopher Mark, Ph.D.,[1] and Timothy M. Barton[1]

ABSTRACT

A comprehensive data base was created that includes more than 4,000 individual uniaxial compressive strength test results from more than 60 coal seams. These data were compared with 100 case studies of in-mine pillar performance from the Analysis of Retreat Mining Pillar Stability (ARMPS) data base.

Statistical analysis found no correlation between the ARMPS stability factor of failed pillars and coal specimen strength. Pillar design was much more reliable when a uniform coal strength of 6.2 MPa (900 psi) was used in all case histories. The conclusion is that laboratory testing should *not* be used to determine coal strength for ARMPS.

Other analyses provided evidence of why laboratory strength does not correlate with pillar strength. The data showed clearly that the "size effect" observed in laboratory testing is related to coal structure. The widely used Gaddy formula, which predicts a significant strength reduction as the specimen size is increased, was found to apply only to "blocky" coals. For friable coals, the size effect was much less pronounced, or even nonexistent. Laboratory tests do not account for large-scale discontinuities, such as roof and floor interfaces, which apparently have more effect on pillar strength than small-scale structure.

[1]Mining engineer, Pittsburgh Research Center, National Institute for Occupational Safety and Health, Pittsburgh, PA.

BACKGROUND

The uniaxial compressive strength of coal was one of the first issues addressed by early rock mechanics researchers. Bunting [1911] observed that "to mine without adequate pillar support will result, sooner or later, in a squeeze; the inherent effects of which are crushing of the pillars, the caving of the roof, and the heaving of the bottom." By testing anthracite specimens of various sizes and shapes in the laboratory, Bunting and his collaborators hoped to aid mine operators in "establishing the width of chambers and pillars." They soon found that "the crushing strength of small cubes is greater than that for large cubes; and, with a constant base area, the crushing strength becomes less as the height increases" [Daniels and Moore 1907]. Bunting apparently concluded that these two issues, the "size effect" and the "shape effect," prevented the direct use of laboratory strength results in design. His design equation was the first U.S. empirical coal pillar strength formula:

$$S_p = S_1 [0.70 + 0.30(w/h)], \quad (1)$$

where S_p = pillar strength,

S_1 = coal strength parameter,

w = pillar width,

and h = pillar height.

Bunting used the laboratory results to determine the *shape* of the formula (figure 1). The coal strength parameter was determined from analysis of in situ pillar failure ("actual squeezes" in figure 1). For anthracite pillars, it was set at 7 MPa (1,000 psi).

The basic approach employed by Bunting and his colleagues remained the state of the art for much of the 20th century. For example, Zern presented the following equation in the 1928 edition of the "Coal Miner's Pocketbook":

$$S_p = S_1 (w/h)^{0.5}. \quad (2)$$

Zern's suggested value of the coal strength parameter is 4.8-7 MPa (700-1,000 psi).

More than 20 years later, Gaddy [1956] attempted to provide the link between laboratory specimens and field strength. He attacked the size effect by testing coal cubes of various sizes from five seams. Gaddy concluded that the strength decrease with increasing specimen size could be expressed as

$$k = S_c (d)^{-0.5}, \quad (3)$$

where k = Gaddy constant
= estimated strength of a 2.5-cm (1-in) cube,

S = coal specimen strength,

and d = specimen dimension (in).

His work led to the widely used Holland-Gaddy pillar strength formula [Holland and Gaddy 1956]:

$$S_p = k (w)^{0.5}/h. \quad (4)$$

The Holland-Gaddy formula appears to have been the first in the United States to employ a seam-specific strength parameter determined from laboratory testing.

In situ testing of full-scale pillars in South Africa during the 1960's resulted in the concept of a "critical" specimen size beyond which the strength is constant [Bieniawski 1968]. The Bieniawski pillar strength formula below employed this concept:

$$S_p = S_1 [0.64 + 0.36(w/h)], \quad (5)$$

where S_1 = in situ coal strength.

Following Hustrulid [1976], Bieniawski recommended that the in situ strength be determined from laboratory tests and that the Gaddy formula be used to reduce the strength to that of a 1-m (36-in) critical-sized specimen [Bieniawski 1984].

Others proposed versions of the Holland-Gaddy and Obert-Duvall (Bauschinger) formulas that employed the in situ strength parameter [Bieniawski 1984]. It may be noted that the in situ coal strength in equation 5 is functionally equivalent to the "coal strength parameter" in equations 1 and 2.

Despite the fact that textbooks have considered laboratory testing an integral part of pillar design for nearly 30 years, it has remained controversial. One reason is that coal remains notoriously difficult to test. Coal contains many types of discontinuities, including microfractures, cleats, bedding planes, partings, shears, and small faults. Three sources of unreliability have been identified:

1. *Material variability within a particular seam:* Unrug et al. [1985] tested multiple layers of the Warfield and the Coalburg Seams and found that the strongest layers were *six times* stronger than the weakest in each seam. Newman and Hoelle [1993] reported similar results from the Harlan Seam.

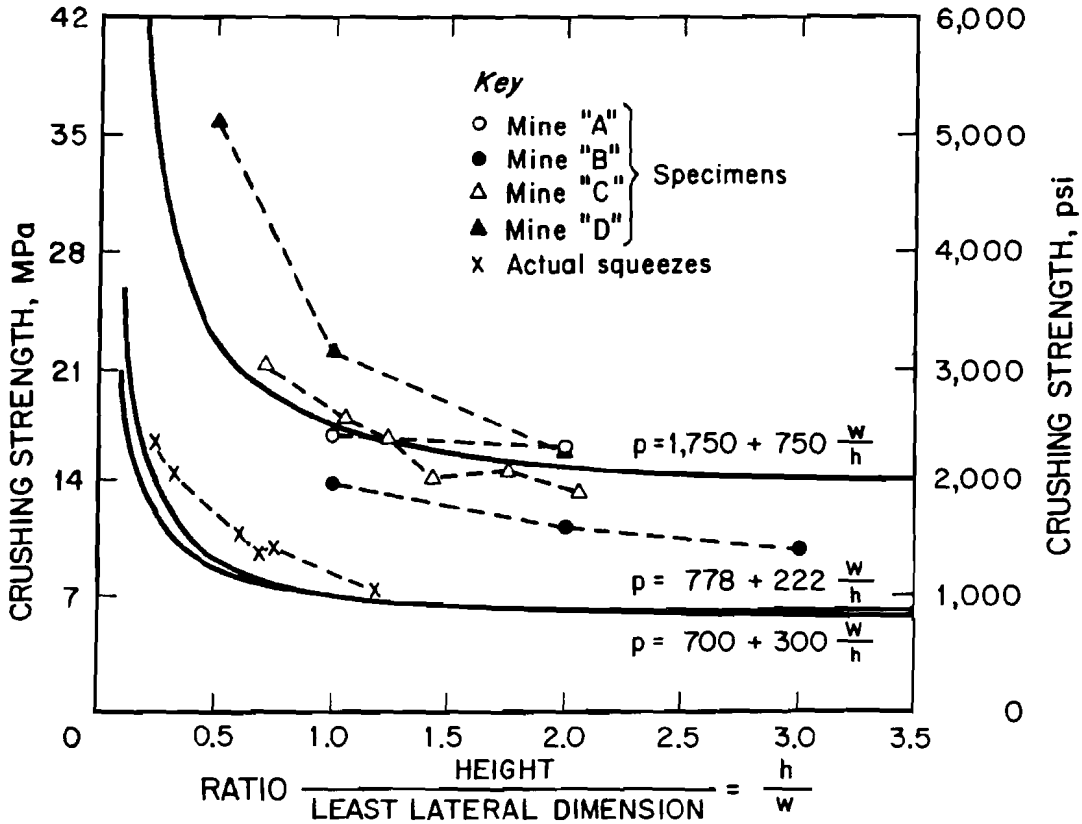

Figure 1.—Data used to develop the first U.S. pillar strength formula (after Bunting, [1911]).

2. *Variation in sampling, specimen preparation, and testing techniques:* Townsend et al. [1977] found that small cylindrical specimens were typically 30% weaker than cubical specimens of the same cross-sectional area. Khair [1968] documented large effects due to platen friction.

3. *Variation in size and shape effects between seams:* Panek [1994] and Mrugala and Belesky [1989], among others, have speculated that Gaddy's size effect exponent of -0.5 may be the *maximum* and not universally applicable. The shape effect has been the subject of numerous studies.

Some have held that these difficulties and the resulting high variability in results are enough to largely invalidate laboratory testing. Another school of researchers in the Republic of South Africa, Australia, and the United States have argued that, although the strength of laboratory-sized specimens varies widely, the in situ coal strength may fall within a narrow range [Salamon 1991; Galvin 1995; Mark 1990]. In each case, their conclusions were based on analysis of in-mine pillar failures. Salamon and Munro [1967] originally analyzed 27 pillar collapses and 92 intact cases. Their formula, perhaps the most widely used in the world, explained the data very well without reference to individual seam strengths. In 1991, Madden reanalyzed an updated version of their data set. Although he found some differences in strength between seams, he concluded again that the average strength could represent all seams. Galvin [1995] conducted a probabilistic analysis of 30 collapsed and stable bord-and-pillar workings from Queensland and New South Wales, Australia. He concluded that "pillar strength in the field is only marginally dependent on the seam strength once the w/h exceeds 2." In the United States, Mark and Chase [1997] presented data from 140 case histories, which were analyzed using the Analysis of Retreat Mining Pillar Stability (ARMPS). ARMPS estimates pillar strength using a slightly modified version of the Bieniawski formula; the analyses assumed a uniform in situ coal strength. Mark and Chase [1997] found that pillar failures occurred in 83% of cases when the ARMPS stability factor (SF) was less than 0.75, but only 8% of cases when it greater than 1.5 (figure 2).

These researchers have all determined that the value of the in situ coal strength falls between 5.4-7.4 MPa (780-1,070 psi). The range is remarkably small, considering that it was determined from three data sets that span the globe. On the other hand, at least one South African seam has been shown by back-calculation to be significantly weaker than the average [Van der Merwe 1993]. In India, researchers concluded from back-analysis of 43 pillar case histories that coal strength should be considered in design [Sheorey et al. 1987].

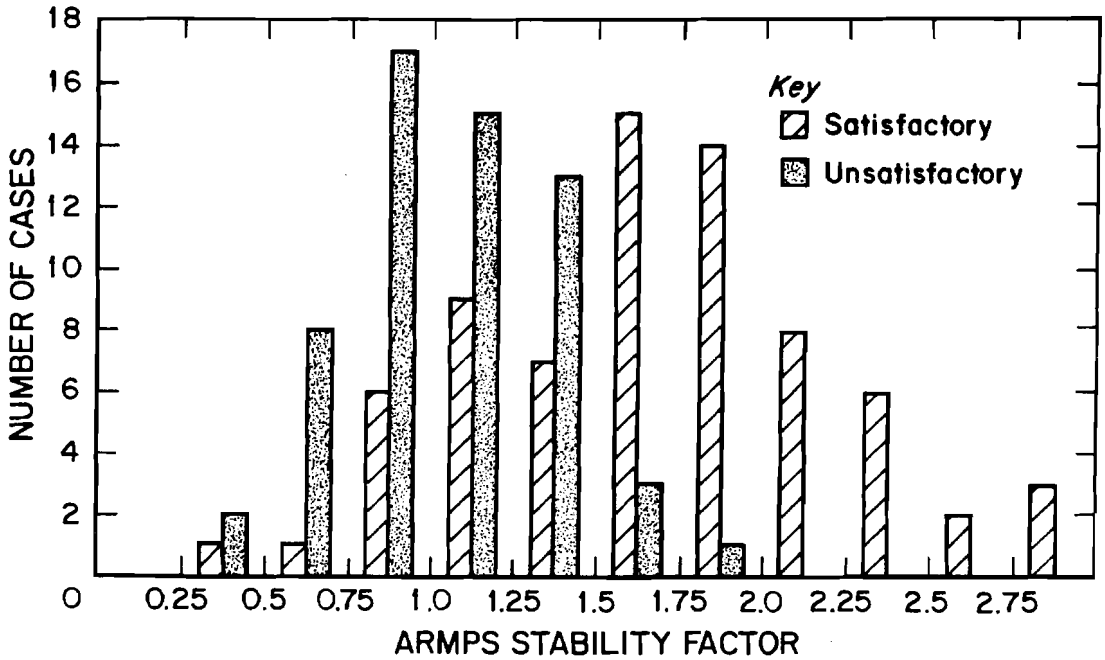

Figure 2.—ARMPS data base.

Interest in the uniaxial compressive strength of coal has also waned over the past 15 years because researchers have devoted their energy to analytic pillar strength formulas and numerical models. These theories are developed from the principles of mechanics rather than curve-fitting to test data. The shift in emphasis has been related to the recent focus on pillar design for longwall mining. Longwalls employ pillars that are much more "squat" than those traditionally used in room-and-pillar operations. Few compressive strength tests have ever been conducted where the specimen width-to-height (w/h) ratio exceeded 4; however, longwall pillars often employ w/h ratios of 10, 20, or greater.

Obviously, the very concept of pillar failure takes on a different meaning for squat pillars. The wide range of conflicting theories about the mechanics of squat pillars and the substantial difficulties with obtaining field data to confirm or disprove any of them have been described elsewhere [Mark and Iannacchione 1992]. On the other hand, Mark et al. [1994] have shown that longwall tailgate performance can be accurately predicted without reference to seam-specific coal strength. There is clearly overwhelming evidence, theoretical and empirical, that the uniaxial compressive strength is irrelevant to the strength of a squat pillar.

Longwall mines, however, account for only 45% of the coal mined underground in the United States. Much of the remainder comes from small room-and-pillar mines usually operating at relatively shallow cover. These mines use many "slender" pillars, and traditional pillar failures still occur. The ARMPS data base contains 60 instances of pillar squeezes, bumps, or collapses that have taken place in recent years. About one-half of these occurred at depths of less than 150 m (500 ft) and involved pillars whose w/h ratio was less than 5. The failures occurred in a variety of seams. Because some seams appear blocky and strong, and others seem weak and extremely friable, it is reasonable to expect that these obvious structural differences might affect pillar strength. As figure 2 shows, successful and unsuccessful designs occur in approximately equal proportions in the ARMPS SF range of 0.75 to 1.5. Might seam-specific laboratory coal strength data explain some of this variability? That was the question this research was initiated to answer.

DISCUSSION OF RESEARCH

Despite the large volume of coal strength testing reported in the literature, it had never been compiled into a single data base. The Pittsburgh Research Center, therefore, undertook the task. The Coal Strength Data Base now contains the results from more than 4,000 individual uniaxial compressive strength tests covering more than 60 seams and obtained from more than 30 references. All of the data have been entered into a spreadsheet and are readily accessible for a wide variety of statistical studies.

Two types of data are included. For about 2,300 tests, information was provided on single specimens. These data were entered individually, then grouped by reference, seam,

specimen geometry, and specimen size. Each group, or suite, of tests was placed on a separate page within the data base. A "summary line" containing the mean compressive strength and standard deviation for the suite was also generated. The summary lines were collected and placed in the summary table. The summary table also includes lines representing about 1,700 tests that were reported in summary form in the original reference. The summary table contains information on about 380 suites of tests. The structure of the Data Base of Uniaxial Coal Strength (DUCS) is illustrated in figure 3.

A single copy of the DUCS may be obtained by sending three formatted, double-sided, high-density diskettes to: Timothy M. Barton, NIOSH, Pittsburgh Research Center, Cochrans Mill Rd., P.O. Box 18070, Pittsburgh, PA 15236-0070. Please specify whether you prefer .xls, .wk3, or comma-separated values format.

A table of average U.S. coalbed strengths was derived from the summary statistics (table 1). To minimize size and shape effects, this table uses only specimens whose w/h ratio is approximately 1.0 and whose smallest dimension is approximately 5-8 cm (2-3 in). The average coalbed strength is calculated as the weighted mean of all of the summary lines for a particular seam that meet these geometric criteria. In addition to strength data, the Coal Strength Data Base also includes a variety of coal quality information for each seam tested. The most relevant is perhaps the Hardgrove Grindability Index (HGI), which is a measure of the relative grindability of coal. Larger HGI values imply easier grindability and greater friability. The HGI is almost universally required by utilities that purchase coal, so the information is readily accessible. Representative values of the rank, carbon content, volatile content, ash content, and heating value are also included. Because the coal quality data were collected independently of the coal strength data and from different sources, they are approximations for comparative purposes only.

During the past 6 years, coal samples measuring about 0.003 m^2 (0.1 ft^3) have also been collected from 45 seams. These were classified using the following simple system:

Composition:

Bright (>90% bright coal)
Semibright (60%-90% bright coal)
Intermediate (40%-60% bright coal)
Semidull (60%-90% dull coal)
Dull (>90% dull coal)

Structure:

Blocky (major cleat spacing > 8 cm (3 in))
Semiblocky (major cleat spacing 3-8 cm (1-3 in))
Friable (cleat spacing < 3 cm (1 in))

Shearing: Yes or no.

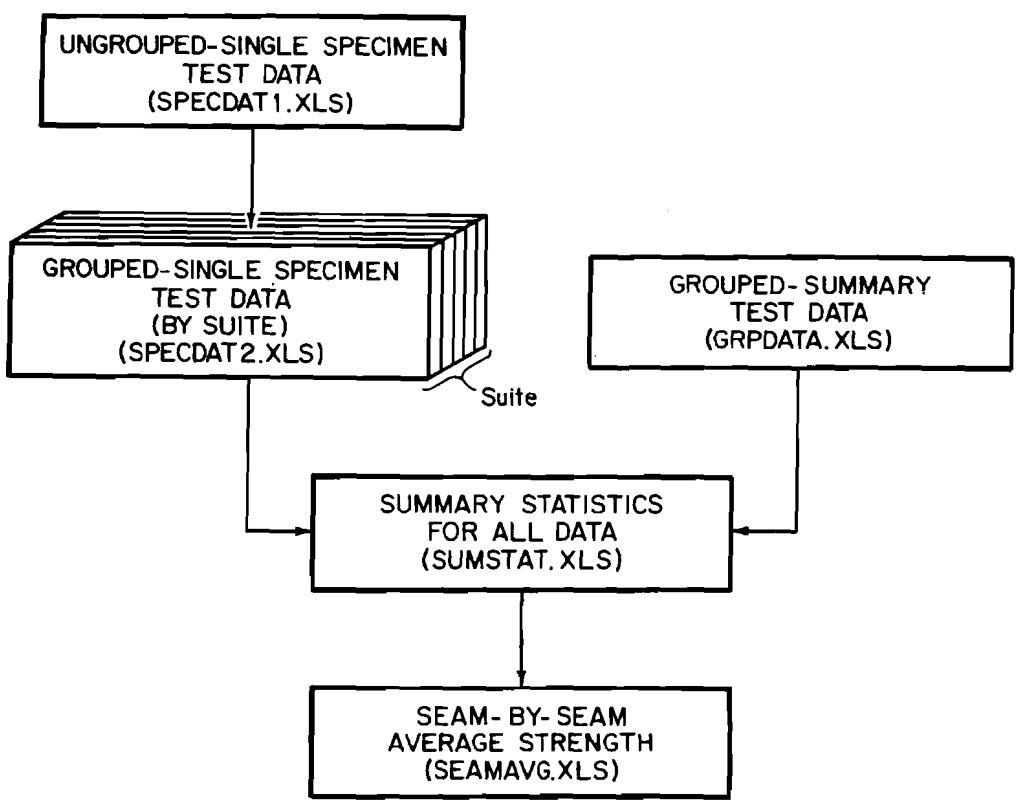

Figure 3.—Structure of the Coal Strength Data Base.

Table 1.—Unconfined compressive strength of U.S. coal seams (5- to 8-cm (2- to 3-in) specimens)

Coalbed	Seam average strength, MPa (psi)	Typical HGI	No. of tests	Coalbed	Seam average strength, MPa (psi)	Typical HGI	No. of tests
Allen	10.8 (1,570)	100	11	Kentucky No. 13	26.8 (3,890)	60	37
Alma	27.7 (4,024)	55	30	Lower Kittanning	14.6 (2,117)	90	96
B	25.1 (3,633)	95	61	Marker	44.9 (6,509)	47	24
Bakerstown	16.7 (2,420)	64	12	Mary Lee	7.8 (1,135)	76	10
Beckley	14.6 (2,121)	101	30	No. 2 Gas	12.4 (1,801)	52	50
Blind Canyon	38.9 (5,646)	46	54	Pittsburgh	160 (4,330)	56	160
Blue Creek	9.1 (1,324)	81	10	Pocahontas No. 3	10.5 (1,528)	110	85
Chilton	27.4 (3,973)	50	6	Pocahontas No. 4	19.9 (2,892)	90	31
Clintwood	19.2 (2,783)	63	40	Pocahontas No. 5	14.7 (2,127)	100	4
Coalburg	24.3 (3,521)	45	124	Pond Creek	32.0 (4,635)	39	13
D	18.2 (2,632)	46	10	Powellton	13.8 (2,008)	58	13
Darby	20.9 (3,907)	49	22	Redstone	20.2 (2,932)	65	10
Douglas	15.9 (2,300)	50	7	Sewell	16.5 (2,386)	65	30
E	24.2 (3,514)	47	4	Sewickley	27.6 (4,000)	60	72
Eagle	10.5 (1,526)	59	10	Stockton	47.2 (6,844)	45	10
Elkhorn No. 4	30.3 (4,393)	42	24	Sunnyside	26.6 (3,856)	50	48
Geneva	36.2 (5,250)	48	3	Tiller	15.3 (2,215)	54	12
Harlan	32.6 (4,728)	44	88	Upper Banner	9.6 (1,391)	84	30
Hazard No. 4	18.2 (2,644)	43	67	Upper D	46.5 (6,746)	50	36
Hemshaw	32.6 (4,727)	47	10	Upper Freeport	10.3 (1,493)	82	17
Herrin No. 6	24.7 (3,576)	57	102	Upper Hiawatha	37.6 (5,446)	46	20
Island Creek	32.6 (4,734)	42	8	Upper Kittanning	10.5 (1,519)	79	60
Jawbone	3.7 (539)	54	3	Warfield	22.7 (3,295)	50	93
Kellioka	21.8 (3,159)	44	49	Waynesburg	30.9 (4,474)	54	15
Kentucky No. 9	28.3 (4,102)	54	46	Welch	13.1 (1,902)	95	6
Kentucky No. 11	25.5 (3,693)	52	52	Winfrede	43.8 (6,345)	45	10
Kentucky No. 12	15.6 (2,268)	58	5	York	18.9 (2,735)	54	60

The ARMPS data base contains the best available information on the in situ strength of U.S. coal pillars. ARMPS SF have been back-calculated for 140 case histories (figure 2), covering an extensive range of geologic conditions, extraction methods, depths of cover, and pillar geometries [Mark and Chase 1997]. Ground conditions in each case history have been categorized as either satisfactory or unsatisfactory. Unsatisfactory conditions included—

- Pillar squeezes, with significant entry closure and loss of reserves.
- Sudden collapses of groups of pillars, usually accompanied by airblasts.
- Coal pillar bumps (violent failures of one or more pillars).

RESULTS

ARMPS CASE HISTORY DATA BASE

Coalbed specimen strength data were available for approximately 100 case histories in the ARMPS data base. The case histories are about evenly split between successes and failures. In figure 4, the ARMPS SF are plotted against coal strength. All ARMPS SF were calculated assuming the in situ strength was 6.2 MPa (900 psi). If pillar strength was related to specimen strength, low-strength seams would be expected to fail at greater SF than high-strength seams. Instead, no meaningful correlation between SF and coal strength is apparent in the data. The best discrimination is achieved at an ARMPS SF of 1.55, with a misclassification rate of 20%. Only one failure is included among the misclassifications, which is highly significant from a practical standpoint.

In a second analysis, the ARMPS SF were recalculated using individual seam strengths instead of the uniform in situ strength. The seam strengths were divided by 4, as suggested by the Gaddy formula for a 6.5-cm (2.5-in) specimen, resulting in a mean SF that is about the same as in the first analysis.

The results are shown in figure 5. Now there is a strong correlation between specimen strength and SF, with "stronger" coals requiring higher SF to avoid failure. The best misclassification rate, at an SF of about 1.7, is 37%. Also, the misclassifications now include 10 failures. In other words, when seam-specific strengths are used, the SF becomes almost meaningless.

A third analysis applied seam-specific size-effect exponents to the coal strength data, as defined later in the "Size Effect" section of this paper. The correlation between seam strength and SF was still apparent, as in figure 5. Although the misclassification rate improved to 33%, it was still 50% greater than in the uniform seam strength analysis.

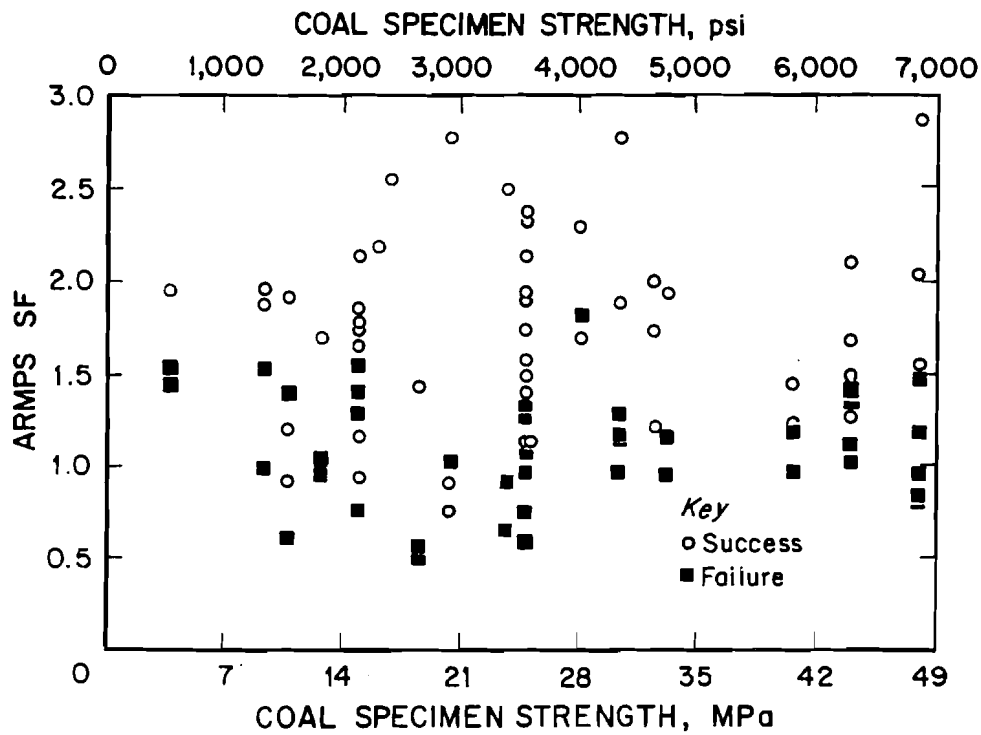

Figure 4.—ARMPS SF compared with specimen strength data.

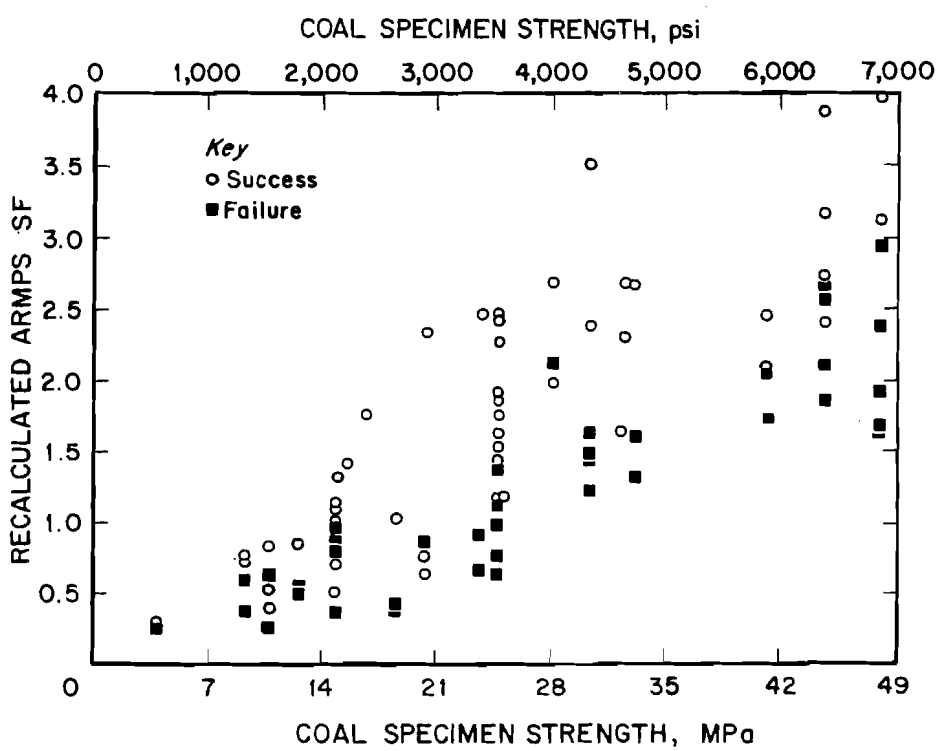

Figure 5.—Recalculated ARMPS SF compared using seam-specific coal strength data.

The data indicate that there is no meaningful correlation between the specimen strength and the in situ strength of U.S. coal seams. Knowledge of the specimen strength does not improve the accuracy of the design formula's prediction; it *reduces* it. A uniform coal strength provides a much more reliable prediction of pillar performance. Based on these results, laboratory test results are explicitly *not* recommended for use in ARMPS.

SIZE EFFECT

The Coal Strength Data Base contains information from 10 seams where a wide range of specimen sizes have been tested. Five of these were the seams originally tested by Gaddy.

To determine the size effect, only specimens with a w/h ratio of approximately 1:1 were used. Figures 6 and 7 show how power curves were fit to the data of the form:

$$S_c = k(d)^{\alpha}, \qquad (6)$$

where α = size effect exponent.

The results are summarized in table 2. Gaddy's α of -0.5 was found to apply to four seams: the Blind Canyon, Elkhorn, Pittsburgh, and Taggart-Marker. At the other extreme, the two Pocahontas Seams displayed negligible size effect. The other four seams had intermediate size effects. The r^2 values indicate that the size effect typically explains about 50% of the variability in the test results, which is higher than expected considering all of the potential sources of variation in these data. The explanation for the substantial range in size effect exponents is the different structure of the coalbeds. In a blocky coalbed, like the Pittsburgh (figure 6), a small sample will be largely free of cleats and fractures. As the specimen size increases, the density of cleating increases until it finally approaches in situ. In contrast, the fracture density of even a small sample of a friable seam like the Pocahontas No. 3 is nearly as great as in situ (figure 7). The following relationship between size effect and HGI was found (r^2 = 0.75):

$$\alpha = 0.0063\ \text{HGI} - 0.75. \qquad (7)$$

The implications of seam-specific size effects are quite important. It appears that the Gaddy equation underestimates the in situ strength of most seams, sometimes by a factor of 3 or more. Extremely costly and inefficient mining plans have certainly been the result.

COAL STRUCTURE

Several analyses explored the relationship between coal structure and specimen strength. Figure 8 shows U.S. coalbed strengths plotted against HGI. It shows that specimens from all seams with HGI > 70 have strengths less than 20 MPa (3,000 psi). These seams include all of the medium- and low-volatile seams in the data base. Likewise, 85% of seams with HGI < 50 have a strength exceeding 20 MPa (3,000 psi). For the large number of seams between these extremes, the HGI is a poor predictor of strength. Many of these intermediate HGI seams are high-volatile A in rank. The r^2 for the power curve fit to the entire data set is 0.33.

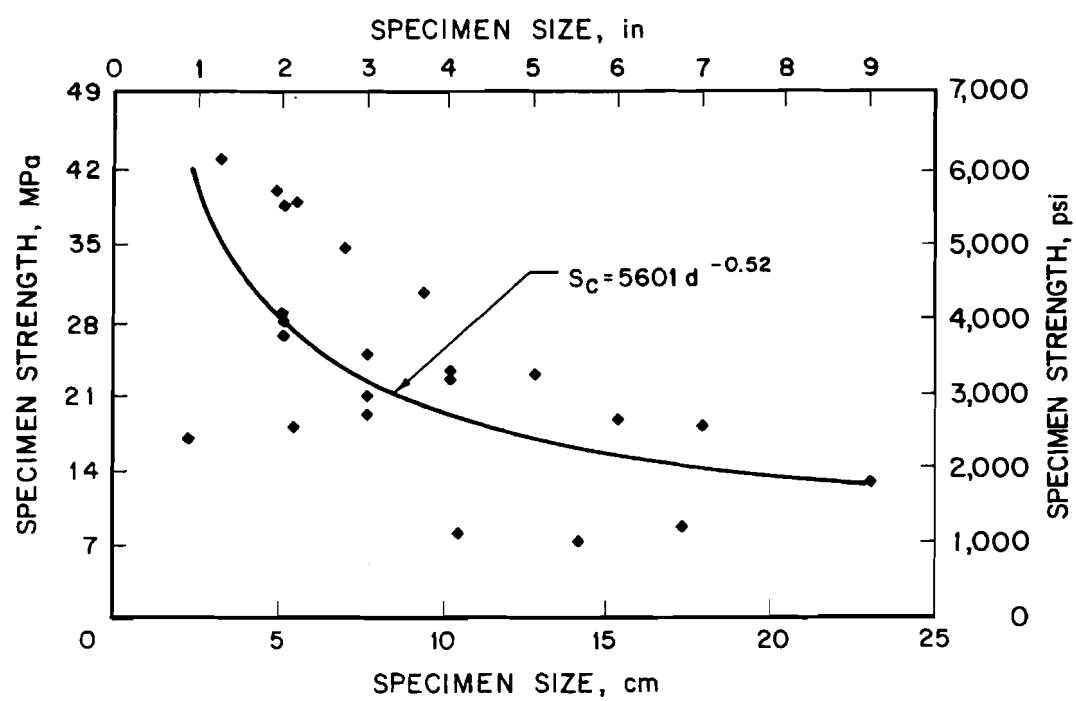

Figure 6.—Size effect in the blocky Pittsburgh Seam.

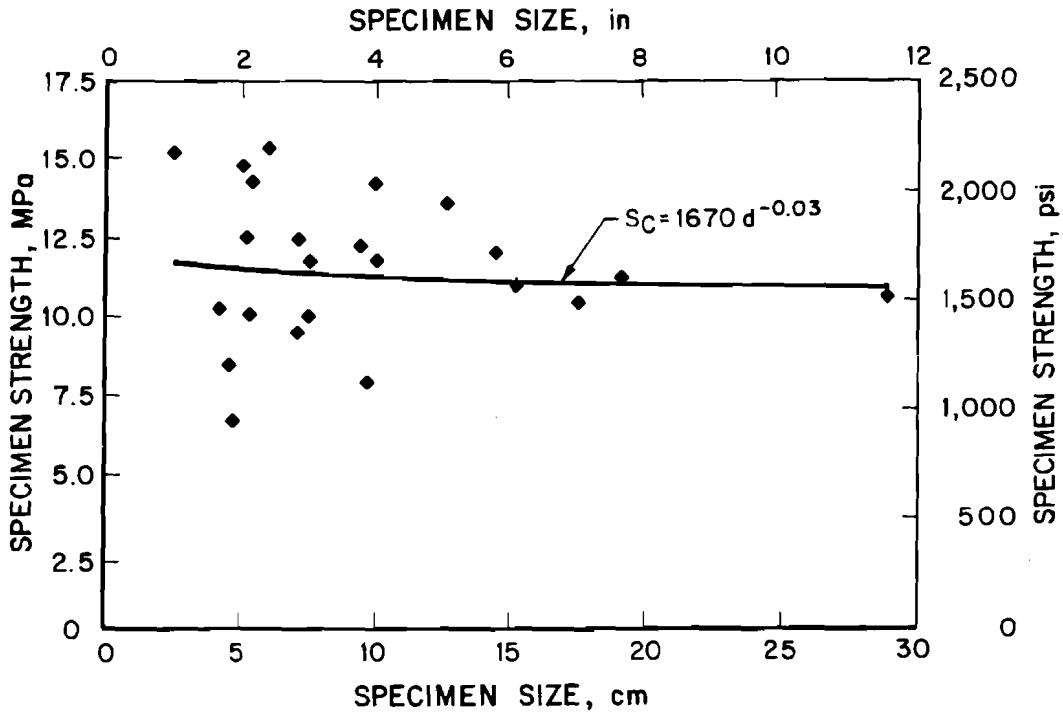

Figure 7.—Size effect in the friable Pocahontas No. 3 Seam.

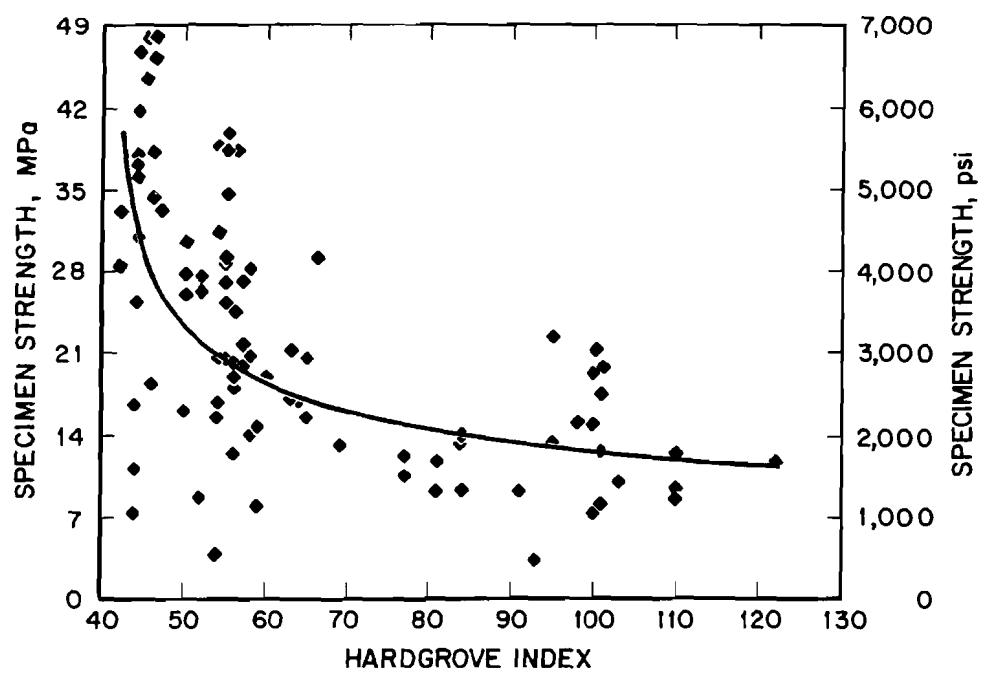

Figure 8.—Specimen strength and HGI of U.S. coalbeds.

Table 2.—Size effect exponents for 10 U.S. coal seams

Coalbed	No. of specimens	No. of references	Maximum specimen size, cm (in)	HGI	Size effect (α)	k	r^2
Blind Canyon	126	2	29.5 (11.6)	46	-0.54	7,045	0.90
Clintwood	88	1	18 (7)	63	-0.31	3,686	0.93
Elkhorn	69	1	16.0 (6.3)	42	-0.55	7,302	0.52
Harlan	129	2	18 (7)	44	-0.29	6,491	0.31
Herrin No. 6	150	5	34.5 (13.6)	56	-0.38	4,293	0.33
Taggart-Marker	60	1	18 (7)	47	-0.45	9,837	0.99
Pittsburgh	272	7	22.9 (9.0)	55	-0.52	5,601	0.48
Pocahontas No. 3 ...	140	5	29.5 (11.6)	110	-0.03	1,670	0.01
Pocahontas No. 4 ...	74	1	18 (7)	100	-0.13	3,238	0.58
Upper Banner	78	1	20.8 (8.2)	84	-0.29	1,730	0.34

The second analysis compared the structure of the hand samples obtained from the mines with the HGI. In this case, every seam rated "blocky" had an HGI less than 60. The HGI of the "semiblocky" seams was less than 80. "Friable" seams were found throughout the range of HGI.

Compressive strength and sample structure data were available for 26 seams. The specimen strength of all eight blocky seams exceeded 23 MPa (3,500 psi), but so did that of four friable and one semiblocky seam. Another 13 friable and semiblocky seams were intermixed below 23 MPa (3,500 psi).

CONCLUSIONS

The results of this study cast doubt on many textbook assumptions about the value of coal strength testing. The data clearly show that specimen strength and the "size effect" are highly seam-specific and related to coal structure. The widely used Gaddy formula, which applies a uniform strength reduction for all seams as specimen size is increased, only applies to "blocky" coals with cleats spaced more than 8 cm (3 in) apart. For friable coals, the size effect was much less pronounced, or even nonexistent.

Case histories of failed pillars are the best available data on in situ coal strength. This study found no correlation between the ARMPS SF of failed pillars and coal specimen strength in the ARMPS data base. In current ARMPS practice, pillars are designed assuming an in situ strength of 6.2 MPa (900 psi) for all seams. When the specimen strength was used instead, the reliability of the ARMPS design method decreased substantially. Australian and South African studies have also found that pillar strength in the field is largely independent of specimen strength.

It should be noted that the coal strength tests were only matched with the seams in the case histories, not with the individual mines. It is also possible that some of the case histories involved roof or floor failure rather than pillar failures. Using a different pillar strength formula might also have changed the results somewhat. However, the data base is so large and the trends so strong that it is highly unlikely that the study is unrepresentative.

The most likely explanation for the results of the study is that specimen and in situ strengths are determined by different parameters. Laboratory tests, particularly those of blocky coals, require a significant amount of fracturing of intact coal. Pillars contain so many cleats and other discontinuities that their failure can occur almost entirely along preexisting fractures. The laboratory tests measure a parameter—the intact coal strength—that is apparently irrelevant to the in situ strength.

The study did not prove that the in situ strength of all U.S. coals is uniform. It only showed that a uniform strength is a better approximation than one based on laboratory testing. There is still significant variability in the ARMPS SF range of 0.75 to 1.5. Recent model studies have indicated that features such as roof and floor interfaces, bedding planes, partings, or weak coal layers have the greatest effects on in situ strength [Iannacchione 1990; Su and Hasenfus 1996]. A rock mass classification, such as the one proposed by Kalamaras and Bieniawski [1993], may prove to be an effective way of evaluating these effects in the field. In the meantime, laboratory uniaxial coal strength test results should not be used for pillar design with ARMPS.

REFERENCES

Bieniawski ZT [1968]. The effects of specimen size on the compressive strength of coal. Intl J Rock Mech Min Sci *5*:325-335.

Bieniawski ZT [1984]. Rock mechanics design in mining and tunneling. Balkema, Rotterdam, pp. 55-92.

Bunting D [1911]. Chamber pillars in deep anthracite mines. Trans AIME *42*:236-245.

Daniels J, Moore LD [1907]. The ultimate crushing strength of coal. Eng Min J, *Aug 10*:263-268.

Gaddy FL [1956]. A study of the ultimate strength of coal as related to the absolute size of cubical specimens tested. VA Polytechnic Bull 112, *Aug*:1-27.

Galvin JM [1995]. Roadway and pillar mechanics workshop: stage 2 - design principles and practice (Course notes). Sydney, New South Wales, Australia: University of New South Wales.

Holland CT, Gaddy FL [1956]. Some aspects of permanent support of overburden on coal beds. In: Proceedings of the West Virginia Coal Mining Institute, pp. 43-65.

Hustrulid WA [1976]. A review of coal pillar strength formulas. Rock Mechanics *8*:115-145.

Iannacchione AT [1990]. The effects of roof and floor interface slip on coal pillar behavior. In: Hustrulid WA, Johnson GA, eds. Proceedings of the 31st U.S. Symposium on Rock Mechanics. Golden, CO: Colorado School of Mines, pp. 153-160.

Kalamaras GS, Bieniawski ZT [1993]. A rock mass strength concept for coal seams. In: Proceedings of the 12th Conference on Ground Control in Mining. Morgantown, WV: West Virginia University, pp. 274-283.

Khair AW [1968]. The effects of coefficient of friction on strength of model coal pillar [Thesis]. Morgantown, WV: West Virginia University, Department of Mining Engineering.

Madden BJ [1991]. A re-assessment of coal-pillar design. J South Afr Inst Min Metall *91*:27-37.

Mark C [1990]. Pillar design methods for longwall mining. Pittsburgh, PA: U.S. Department of the Interior, Bureau of Mines, IC 9247.

Mark C, Iannacchione AT [1992]. Coal pillar mechanics: theoretical models and field measurements compared. In: Iannacchione AT, Mark C, Repsher RC, Tuchman RJ, Jones CC, comp. Proceedings of the Workshop on Coal Pillar Mechanics and Design. Pittsburgh, PA: U.S. Department of the Interior, Bureau of Mines, IC 9315, pp. 78-93.

Mark C, Chase FE, Molinda GM [1994]. Design of longwall gate entry systems using roof classification. In: Mark C, Tuchman RJ, Repsher RC, Simon CL, comp. New Technology for Longwall Ground Control; Proceedings: U.S. Bureau of Mines Technology Transfer Seminar. Pittsburgh, PA: U.S. Department of the Interior, Bureau of Mines, SP 01-94, pp. 5-18.

Mark C, Chase FE [1997]. Analysis of retreat mining pillar stability (ARMPS). In: Mark C, Tuchman RJ, comp. Proceedings: New Technology for Ground Control in Retreat Mining. Pittsburgh, PA: U.S. Department of Health and Human Services, Public Health Service, Centers for Disease Control, National Institute for Occupational Safety and Health, IC 9446.

Mrugala MJ, Belesky RM [1989]. Pillar sizing. In: Proceedings of the 30th U.S. Symposium on Rock Mechanics. Morgantown, WV: West Virginia University, pp. 395-402.

Newman DA, Hoelle JL [1993]. The impact of variability in coal strength on mine planing and design - a case history. In: 12th Conference on Ground Control in Mining. Morgantown, WV: West Virginia University, pp. 237-243.

Panek LA [1994]. Scaling mine pillars' size and shape with the psi function. Soc Min Eng AIME preprint 94-52, pp. 1277-1280.

Salamon MDG [1991]. Behavior and design of coal pillars. Australian Coal J *32*:11-22.

Salamon MDG, Munro AH [1967]. A study of the strength of coal pillars. J South Afr Inst Min Metall, *Sept*:55-67.

Sheorey PR, Das MN, Barat D, Prasad RK, Singh B [1987]. Coal pillar strength estimation from failed and stable cases. Intl J Rock Mech Min Sci Geomech Abstr *24*(6):347-355.

Su DWH, Hasenfus GJ [1996]. Practical coal pillar design considerations based on numerical modeling. In: 15th Conference on Ground Control in Mining. Golden, CO: Colorado School of Mines.

Townsend JM, Jennings WC, Haycocks C, Neall GM, Johnson, LP [1977]. A relationship between the ultimate compressive strength of cubes and cylinders for coal specimens. In: Symposium for Rock Mechanics, Keystone, CO, pp. 4A6-1 to 4A6-6.

Unrug KF, Nandy S, Thompson E [1985]. Evaluation of the coal strength for pillar calculations. SME AIME preprint 85-314.

Van der Merwe JN [1993]. Revised strength factor for coal in the Vaal basin. J South Afr Inst Min Metall *93*(3), pp. 71-77.

Zern EN [1928]. Coal miner's pocketbook. McGraw-Hill, NY, 12th ed., pp. 641-645.

A NEW LAMINATED OVERBURDEN MODEL FOR COAL MINE DESIGN

By Keith A. Heasley[1]

ABSTRACT

In the past, numerous boundary-element models of stratified rock masses have been proposed using a homogeneous isotropic elastic overburden. In this paper, it is postulated that a laminated overburden model might be more accurate for describing the displacements and stresses in these stratified deposits. In order to investigate the utility of using a laminated overburden in a boundary-element model, the fundamental mathematical basis of the laminated model is presented and graphically compared with the fundamental behavior of homogeneous isotropic elastic overburden and with field data. Specifically, the stresses and displacements surrounding an idealized longwall panel as determined from the laminated overburden model are presented and compared with results from the homogeneous isotropic overburden and with measured abutment stress data. Additionally, the remote displacements and surface subsidence as calculated by the laminated overburden model are compared with homogeneous isotropic calculations and with measured subsidence data. Finally, the new laminated boundary-element program, LAMODEL, is used to model the underground stresses and displacements, the topographic stresses, and the interseam interactions at a field site. The results of this investigation show that the laminated overburden is more supple, apt to propagate displacements and stress further, and better able to fit observed data than the classic homogeneous isotropic overburden. Ultimately, it is suggested that the laminated model has the potential to increase the accuracy of displacement and stress calculations for a variety of mining situations.

[1]Mining engineer, Pittsburgh Research Center, National Institute for Occupational Safety and Health, Pittsburgh, PA.

INTRODUCTION

If one wishes to perform a mechanical analysis of the geologic structure of a mining operation, there are several broad mathematical techniques available. For instance, one may choose finite-element, boundary-element, discrete-element, finite-difference techniques, and/or hybrid combinations of these techniques. In general, these mathematical techniques have strengths and weaknesses when applied to a specific geologic environment, mining geometry, and material behavior. Naturally, in each practical application the mathematical technique best suited to the prevailing conditions should be applied.

To analyze the displacements and stresses associated with the extraction of tabular deposits, such as coal, potash, and other thin vein-type deposits, the displacement-discontinuity version of the boundary-element technique is frequently the method of choice. In the displacement-discontinuity approach, the mining horizon is treated mathematically as a discontinuity in the displacement of the surrounding media. Thus, only the planar area of the seam is discretized in order to obtain the solution. Often this limited analysis is sufficient, because in many applications only the distributions of stress and convergence on the seam horizon are of interest. In addition, by limiting the detailed analysis to only the seam, the displacement-discontinuity method provides considerable computational savings compared with other techniques that discretize the entire body (such as finite-element, discrete-element, or finite-difference). It is a direct result of this computational efficiency that the displacement-discontinuity method is able to handle problems involving large areas of tabular excavations.

In the original mathematical formulations [Berry 1960; Salamon 1962] and computer implementations [Plewman et al. 1969; Crouch and Fairhurst 1973; Sinha 1979] of the displacement-discontinuity variation of the boundary-element method, the media surrounding the seam were assumed to be homogeneous, isotropic, or transversely isotropic elastic. This basic behavior of the surrounding media provided fairly good seam-level displacement and stress results for South African gold mines [Salamon 1964; Cook et al. 1966] and for U.S. coal mines [Kripakov et al. 1988; Zipf and Heasley 1990; Heasley and Zclanko 1992]. However, it was noted early in the application of the displacement-discontinuity method that the homogeneous isotropic overburden model does not fit measured subsidence data [Berry and Sales 1961]. As an alternative, it was proposed that a laminated model might be more suitable for describing the behavior of stratified coal-measure rocks [Salamon 1961, 1963]. Recently, a laminated overburden model was found to give good results for predicting surface subsidence [Salamon 1989a; Yang 1992]. Because the source of surface subsidence is convergence in the seam, it seems reasonable that a laminated overburden model might also be able to provide more accurate predictions of in-seam displacements and stresses.

If the utility of using a laminated overburden in a displacement-discontinuity model is to be determined, the fundamental mechanical behavior of the laminated model needs to be investigated and compared with both the classic homogeneous isotropic model and field data. In this paper, the stresses and displacements surrounding an idealized longwall panel as determined from the laminated overburden model, the homogeneous isotropic overburden model, and field data are presented and compared. In addition, the remote displacements and surface subsidence as calculated by the two overburden models are compared with measured subsidence data. Lastly, the laminated overburden model is applied to a site study.

FUNDAMENTAL BEHAVIOR

MATHEMATICAL FOUNDATION

The mathematical basis for the laminated model was originally proposed by Salamon in 1961-62 and more recently updated in 1991. Conceptually, the media in the laminated model consist of a horizontal stack of homogeneous isotropic layers where the interfaces between the layers are parallel and free of shear and cohesive stresses, and the vertical stresses and displacements are continuous across the layers. In the "homogeneous stratification" version of the model, all layers have the same elastic modulus (E), Poisson's ratio (v), and thickness (t). Thus, the homogeneous stratification formulation does not allow (or need) the specification of the properties for each individual layer, yet it provides the desired suppleness of the basic laminated model (compared with a homogeneous isotropic elastic model). In addition, the behavior of the rock mass in the laminated model is effectively characterized by two parameters, the elastic modulus and the lamination thickness, whereas the homogeneous isotropic model only has a single effective parameter, the rock mass modulus (the Poisson's ratio has a minor effect in both models).

The mathematical foundation of the laminated model is the theory of thin plates [Salamon 1991]. From this theory, the relationship between the vertical deflection (w) of the middle plane of a horizontal plate and the resultant transverse pressure (p) acting on the plate is defined by

$$D \nabla^4 w(x,y) = p(x,y), \tag{1}$$

where D is the flexural rigidity of a plate:

$$D = \frac{E t^3}{12 (1 - \nu^2)}, \tag{2}$$

and ∇^4 denotes the biharmonic operator in the xy plane, specifically:

$$\nabla^4 = \left(\frac{\partial^4}{\partial x^4} + 2 \frac{\partial^4}{\partial x^2 \partial y^2} + \frac{\partial^4}{\partial y^4} \right). \tag{3}$$

From equation 1, the convergence in the seam (S) can be related to the induced stress (σ_i) in the overburden laminae by the following second-order, partial differential equation [Salamon 1991]:

$$\frac{\partial^2 S}{\partial x^2} + \frac{\partial^2 S}{\partial y^2} = \frac{2}{E \lambda} \sigma_i, \tag{4}$$

where the laminae-related value, λ, is defined as

$$\lambda = \sqrt{\frac{t^2}{12 (1 - \nu^2)}}, \tag{5}$$

and σ_i is the vertical, or transverse, stress on the laminae at seam level induced by mining.

PANEL CONVERGENCE

The first step in investigating the fundamental behavior of the laminated model was to analyze the convergence across a two-dimensional slot. This slot can be viewed as an idealized longwall panel with no gob support and rigid ribs. From equation 4, the seam convergence across a two-dimensional slot for the laminated model (S_ℓ) as a function of the distance from the panel centerline (X) can be determined as

$$S_\ell(X) = \frac{\sqrt{12 (1 - \nu^2)}}{t} \frac{q}{E} (L^2 - X^2). \tag{6}$$

Here, L is the half-width of the slot; q is the primitive vertical stress at the mining horizon, which for an open panel is equal to the induced stress (σ_i). In solving equation 4, it was assumed that the convergence value at the rib side is zero and that the convergence distribution is symmetric about the panel centerline. Also, in this result and the result in equation 7, the stress-free ground surface was ignored.

Jaeger and Cook [1979] provide a comparable equation for the roof-to-floor convergence across a two-dimensional slot with homogeneous isotropic elastic overburden (S_h):

$$S_h(X) = 4 (1 - \nu^2) \frac{q}{E} (L^2 - X^2)^{1/2}. \tag{7}$$

The fundamental difference between these two equations is that the convergence in the laminated model is proportional to the square of the panel span, while the convergence in the homogeneous model is linearly proportional to the span.

In order to plot and compare the convergence computed from equations 6 and 7, some "typical" values were assumed for the geometric and rock mass parameters: a panel width of 200 m (656 ft)(L = 100), an overburden depth (H) of 160 m (525 ft)(q = 4 MPa (580 psi)), a seam height (M) of 2 m (6.6 ft), an elastic modulus of the rock mass (E) of 20 GPa (2.9 million psi), a Poisson's ratio (ν) of the rock mass of 0.25, and a lamination thickness (t) of 15 m (49 ft). Using these values for the parameters, the convergence across the slot for both the laminated and the homogeneous overburden is plotted in figure 1. As expected from the nature of the equations, the laminated overburden is considerably more flexible. In fact, with the given parameters, the laminated overburden exhibits six times the convergence of the homogeneous isotropic overburden.

ABUTMENT STRESS

The next step in investigating the fundamental behavior of the laminated model was to analyze the abutment stress at the edge of a two-dimensional slot. If the seam is assumed to be linear elastic with a modulus of E_s and Poisson's effect is ignored, then the induced stress in the seam for the laminated model is

$$\sigma_i = E_s \frac{S_\ell}{M}. \tag{8}$$

Then, from equation 4, the in-seam convergence in the laminated model is defined by

$$\frac{d^2 S_\ell}{d x^2} - \frac{2 E_s}{E \lambda M} S_\ell = 0, \tag{9}$$

which has a solution (for positive X values):

$$S_\ell(X) = q L \sqrt{\frac{2 M}{E \lambda E_s}} \, e^{\sqrt{\frac{2 E_s}{E \lambda M}} (X - L)}. \tag{10}$$

The associated induced vertical abutment stress (σ_ℓ) in the unmined seam bounding the panel is

$$\sigma_\ell(X) = q L \sqrt{\frac{2 E_s}{E \lambda M}} \, e^{\sqrt{\frac{2 E_s}{E \lambda M}} (X - L)}. \tag{11}$$

The total abutment stress at the edge of a two-dimensional slot in a homogeneous isotropic elastic model (σ_h) is given by [Salamon 1974]:

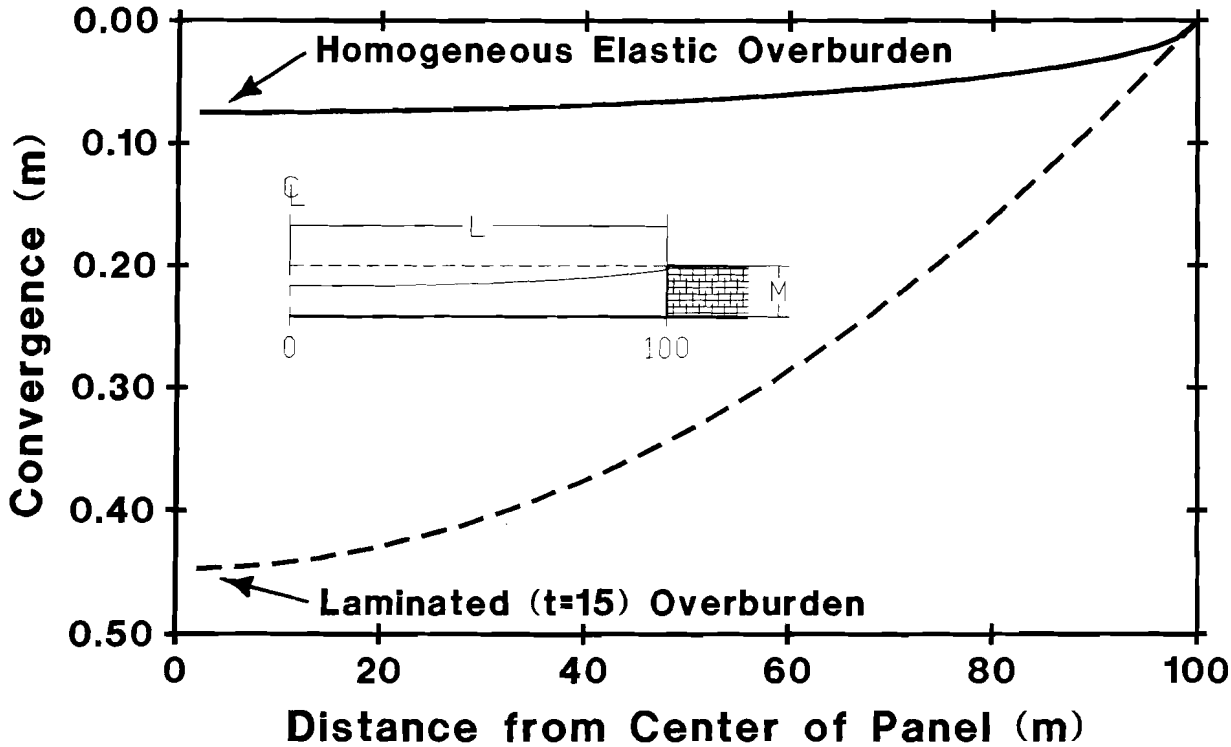

Figure 1.—Comparison of longwall convergence computed from the laminated and homogeneous isotropic models.

$$\sigma_h(X) = \frac{Xq}{\sqrt{X^2 - L^2}} . \tag{12}$$

It is noteworthy that this equation is independent of material properties. During its derivation, it was assumed that the seam material was identical to the surrounding media. Thus, to be consistent, the elastic modulus of the seam (E_s) in equation 11 is assumed to be equal to the modulus of the overburden (E), 20 GPa (2.9 million psi).

In addition, numerous field measurements of abutment load have been tabulated by Mark [1990], where he found that the measured distribution of induced abutment stress (σ_f) follows the equation:

$$\sigma_f(X) = \frac{3L_s}{(D - L)^3}(D - X)^2 , \tag{13}$$

where L_s is the total side abutment load (which in our case without any gob load is equal to qL), and D is the maximum horizontal extent of the abutment stress from the panel edge, which was determined from field measurements [Mark 1990]:

$$D = L + \sqrt{0.3048}\,(9.3\sqrt{H}) . \tag{14}$$

The total abutment stress curves, as calculated from the laminated and homogeneous isotropic models and from the empirical formula (equations 11, 12, and 13), are plotted in figure 2. (It should be noted that equations 11 and 13 calculate induced stresses and equation 12 calculates the total stress. Therefore, in the following plots, the virgin overburden stress (q) has been added to the results from equations 11 and 13 to provide a valid comparison with the total abutment stress values from equation 12.) In figure 2, it can be seen that the homogeneous isotropic abutment stress has a relatively sharp, infinite peak at the edge and approaches zero asymptotically with increasing distance from the panel. In contrast, the abutment stress in the laminated overburden is finite at the panel edge and approaches virgin overburden stress (q) rapidly. Neither of these mathematical models (using the assumed parameters) comes very close to matching the empirical abutment stress.

However, if the abutment stress level in the laminated model and that obtained from the empirical formula are equated at the edge of the seam (X = L), then the lamination thickness (t) that ensures this equality can be determined:

$$t = 20.29\sqrt{1 - v^2}\,\frac{E_s H}{M E} . \tag{15}$$

For a typical seam modulus (E_s) of 2 GPa (290,000 psi) in the laminated model, equation 15 provides a fitted lamination thickness of 157 m (515 ft). The plot of the abutment stress curve for the laminated overburden model with a fitted lamination thickness of 157 m (515 ft) is shown together with the empirically determined abutment stress in figure 3. The degree of agreement between the two curves is very good and serves to

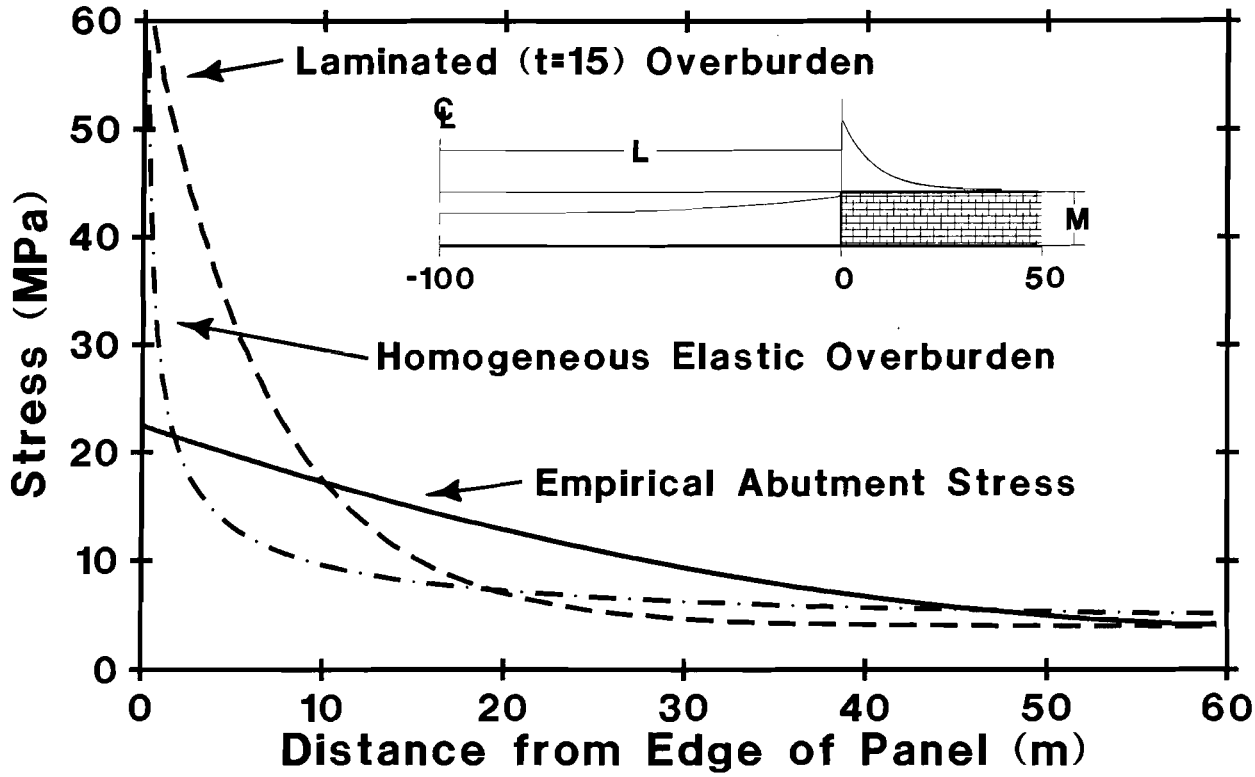

Figure 2.—Comparison of longwall abutment stress computed from the laminated and homogeneous isotropic models and from the empirical formula.

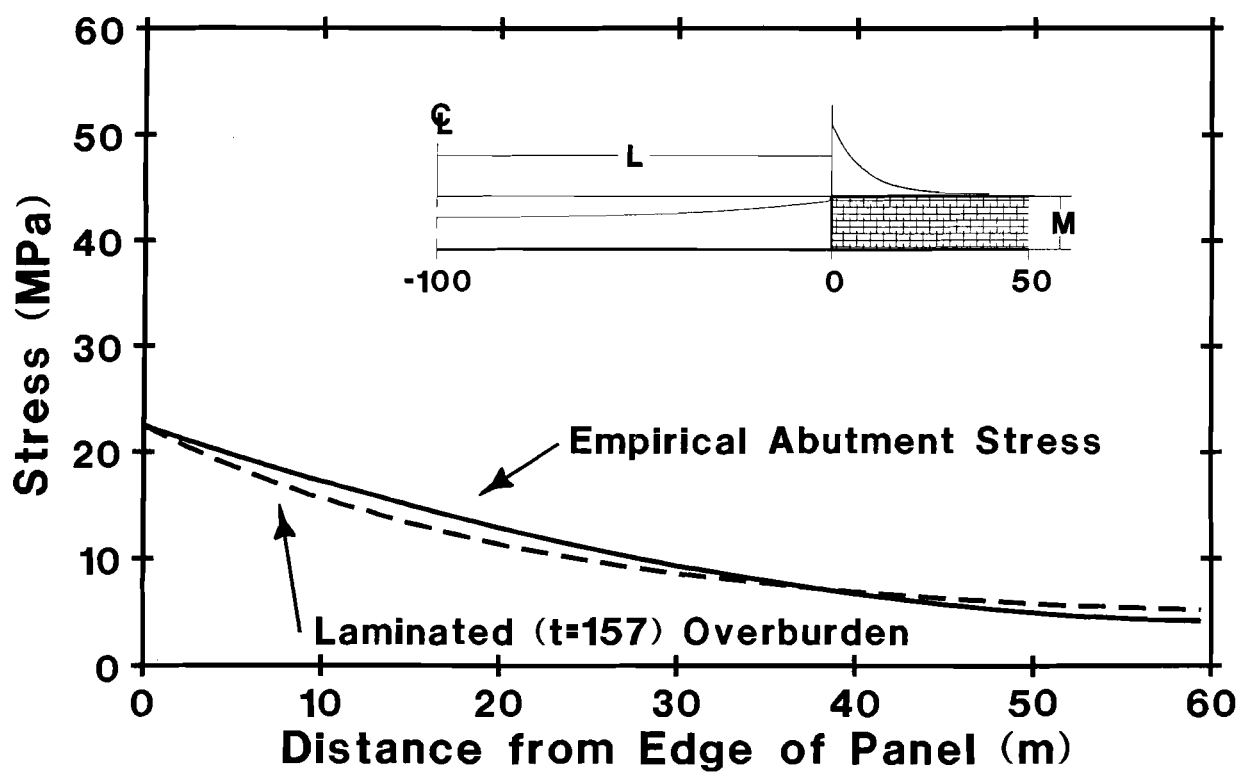

Figure 3.—Plot of the laminated abutment stress fitted to the empirical formula.

highlight the numerical flexibility provided by a variable lamination thickness parameter in the laminated model. (If a compressible seam is used, it may be possible to fit the abutment stress distribution in the homogeneous isotropic overburden to the empirical curve by varying the seam and overburden moduli. However, that calculation is beyond the scope of this paper.)

REMOTE DISPLACEMENTS

The next step was to analyze the remote displacements in the overburden generated by seam convergence. For the laminated overburden model, the kernel, or influence function, which relates the seam convergence (S_ℓ) to the vertical displacement (W_ℓ) of the overburden, was derived by Salamon [1962, 1989b] and Yang [1992]:

$$W_\ell(X,Y) = \frac{S_\ell}{4\sqrt{\pi \lambda Y}}\, e^{\frac{X^2}{4\lambda |Y|}} . \qquad (16)$$

Here, the magnitude of the convergence, S_ℓ, is assumed to occur over a unit element of the seam; the values of X and Y are the horizontal and vertical distances between the centroid of the converged seam element and the point in the overburden at which the displacement is desired.

Similarly, the kernel for the homogeneous isotropic overburden, which relates the seam convergence (S_h) to the vertical displacement (W_h) of the overburden, was derived by Crouch [1976] (see equation 17). Again, the magnitude of the convergence, S_h, is assumed to occur over a unit element of the seam, and the coordinates X and Y were defined previously in conjunction with equation 16. Note that the expression in equation 17 is again independent of elastic moduli.

Plots of the overburden displacements generated by these models are depicted in figure 4 for Y = 20 m (66 ft) and Y = 50 m (164 ft). In computing this illustration, a unit convergence spread over a seam element of unit length was assumed. Thus, the volume of convergence is identical in the two models. However, consistent with the greater suppleness of the laminated model, the stratified overburden (with a 15-m (49-ft) lamination thickness) appears to concentrate the displacement more tightly over the panel. This feature is particularly noticeable as the distance from the seam is increased.

This difference in remote displacement behavior is even more obvious in figure 5, which shows the 1-cm (0.39-in) displacement contours for both models generated above a unit volume convergence in a seam element. In this figure, the 1-cm (0.39-in) contour, or displacement "bulb," for the laminated model (with a 15-m (49-ft) lamination thickness) is broader and extends almost twice the distance into the overburden as the contour from the homogeneous elastic model. However, if the lamination thickness in the laminated model is increased to 28 m (92 ft)(as shown in figure 5), then the vertical extent of the 1-cm (0.39-in) displacement contour is equal between the two models, although the laminated displacement bulb is still broader. For most practical purposes (lower lamination thicknesses), both figures 4 and 5 indicate that seam displacements and stresses for a laminated overburden would propagate further and in a tighter pattern than the displacements and stresses from the homogeneous overburden. This greater remote response, coupled with the tendency for the laminated model to produce greater seam convergence, should greatly increase the remote displacements and stresses associated with a laminated displacement-discontinuity model.

SURFACE SUBSIDENCE

The final step in investigating the fundamental behavior of the laminated model was to analyze the surface subsidence over a longwall panel. In this analysis, the surface subsidence curves for the laminated and homogeneous isotropic models were calculated by taking the panel convergence from equations 6 and 7 and numerically integrating the surface subsidence using equations 16 and 17. These calculated subsidence curves are then compared in figure 6 with the results of the U.S. Bureau of Mines subsidence model [Jeran et al. 1986], which essentially represents an empirically derived "average" of 11 different subsidence curves from the Northern Appalachian Coal Basin.

For the subsidence curve of the laminated model in figure 6, the lamination thickness was optimized to provide the best fit with the empirical curve. This resulted in a lamination thickness of 5.3 m (17 ft), and from the figure, it can be seen that the laminated model provides a good fit to the empirical

$$W_h(X,Y) = \frac{S_h}{2\pi}\left(\arctan\left(\frac{Y}{X-0.5}\right) - \arctan\left(\frac{Y}{X+0.5}\right)\right) + \frac{S_h}{2\pi}\left(\frac{Y}{2(1-\nu)}\left(\frac{X+0.5}{(X+0.5)^2+Y^2} - \frac{X-0.5}{(X-0.5)^2+Y^2}\right)\right), \qquad (17)$$

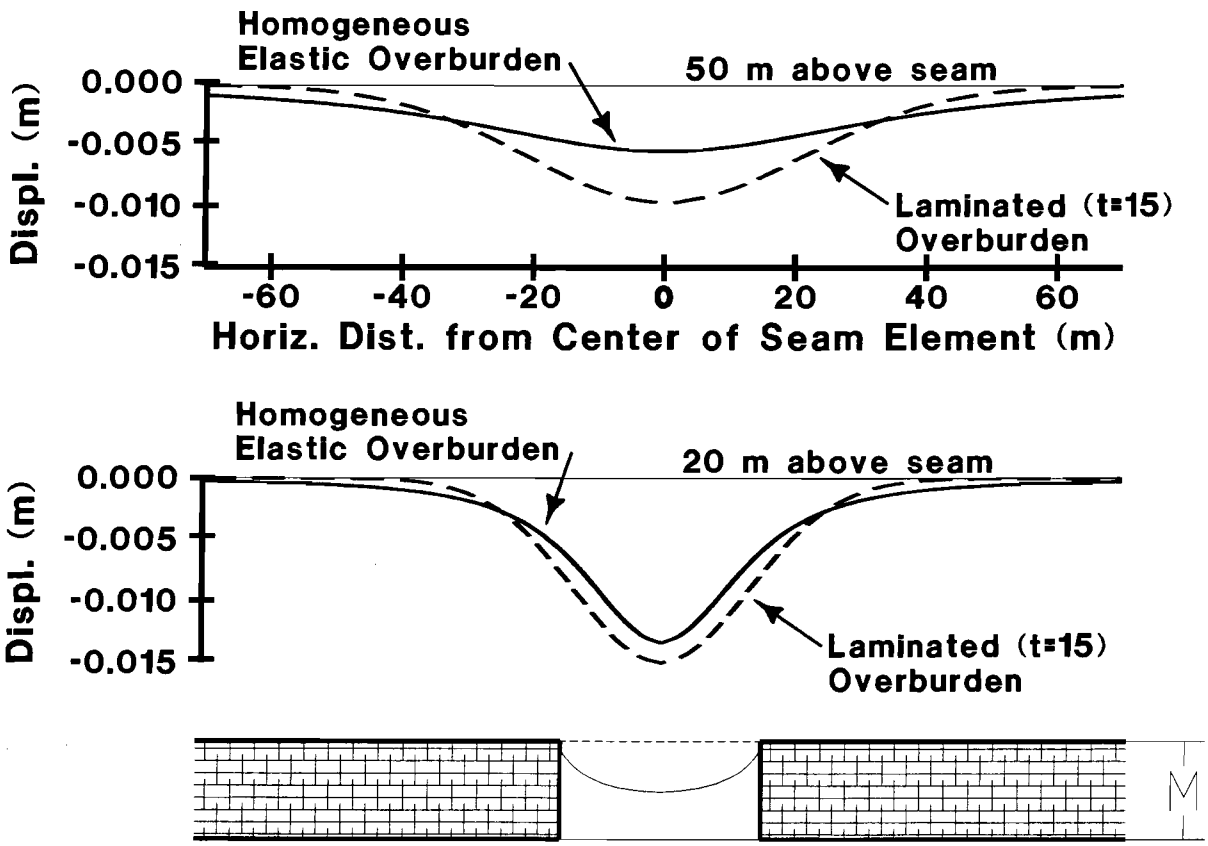

Figure 4.—Remote displacement due to a unit volume displacement.

curve. In earlier work where the laminated model was fit to several different individual sets of subsidence data [Yang 1992], a factor, ω:

$$\omega = \sqrt{\frac{H}{2\lambda}}, \tag{18}$$

was found to be fairly constant at an average of 6.9. (Here, H is the overburden depth, and λ is defined in equation 5.) For the fitted subsidence curve from the laminated model in figure 6, the value of ω is 7.1, which agrees very well with this previous work.

For the subsidence curve from the homogeneous elastic overburden, the elastic modulus was lowered in an attempt to fit the empirical curve. However, long before the maximum surface subsidence from the model matched the maximum empirical surface subsidence, the convergence in the seam exceeded the seam thickness. The homogeneous elastic surface subsidence actually plotted in figure 6 was determined using an elastic modulus of 1 GPa (145,000 psi). From this curve, it is clear that the homogeneous isotropic surface subsidence is naturally much shallower and broader than the empirical data, and with only one effective variable parameter (E), the homogeneous isotropic model cannot be accurately fitted to the Northern Appalachian data. This result further confirms earlier indications that the homogeneous isotropic elastic overburden could not be made to fit subsidence data in the United Kingdom [Berry and Sales 1961; Salamon 1963].

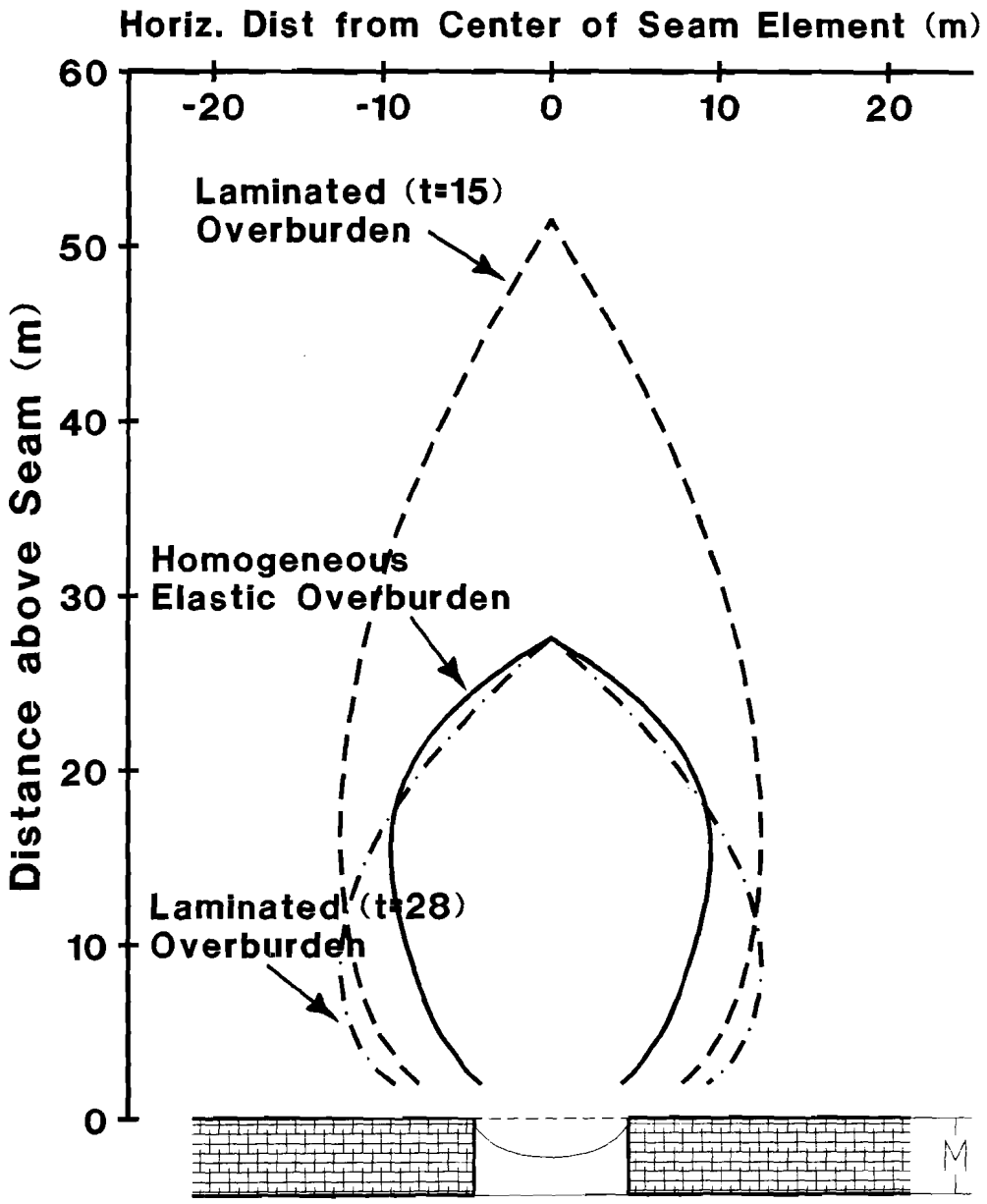

Figure 5.—1-cm (0.39-in) displacement contours associated with a unit volume displacement.

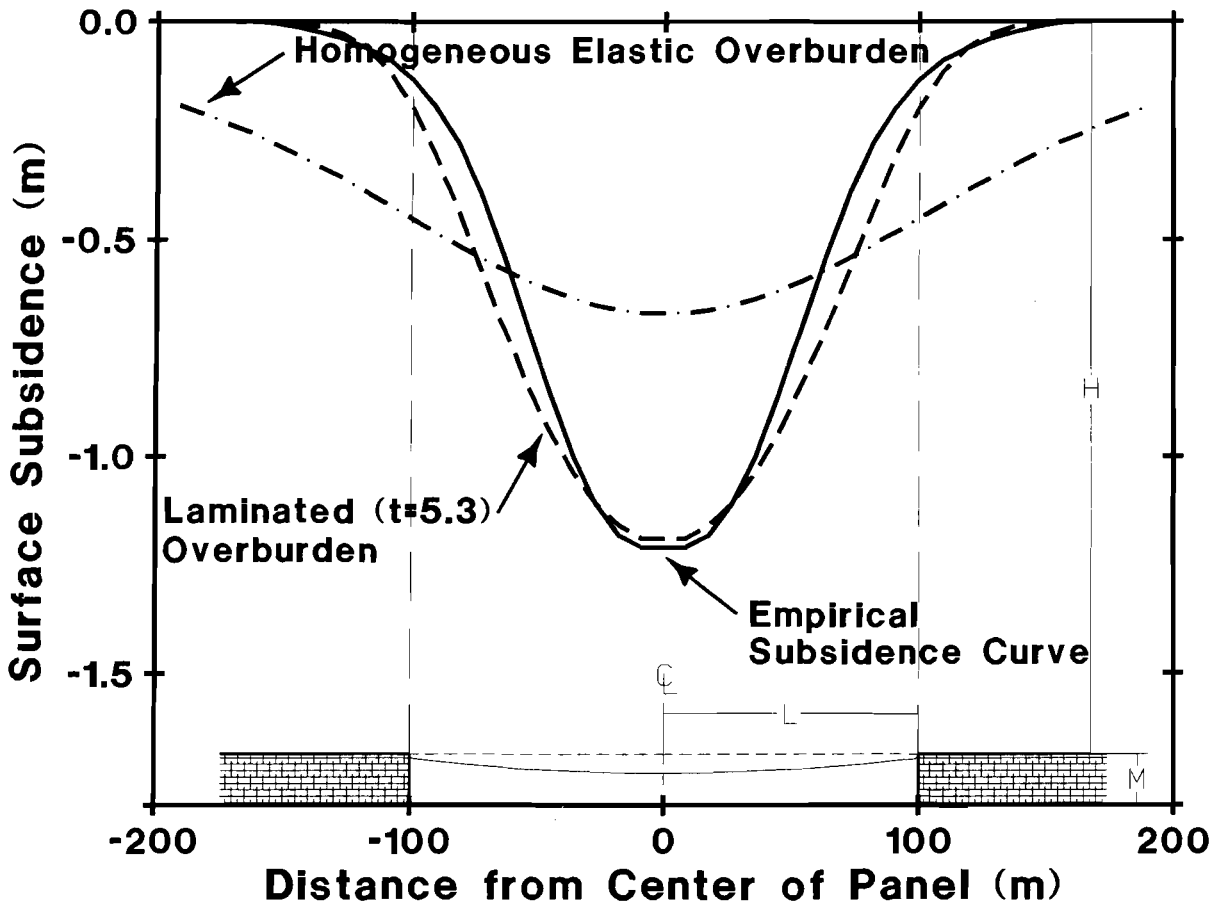

Figure 6.—Plot of the laminated and homogeneous isotropic subsidence fitted to the empirical curve.

THE LAMINATED MODEL PROGRAM, LAMODEL

IMPLEMENTATION FEATURES

The laminated overburden model, as presented in the previous sections of this paper, has been implemented into a modern boundary-element computer program called LAMODEL. This implementation has numerous practical features, including—

- Single- and multiple-seam simulations.
- Numerous individual excavation steps.
- Infinite media or surface effects for shallow seams.
- A constant overburden or a variable topography.
- Seam-level convergence and stress calculation, with each of the individual stress components (overburden, material, interseam, and surface) separately tabulated.
- User-defined laminae properties (elastic modulus, Poisson's ratio, and thickness).
- Up to 26 different in-seam materials can be specified from a selection of material models, which include elastic, elastic-plastic, strain-softening, bilinear strain-hardening, and exponential strain-hardening.
- User-defined convergence criteria.
- Grid sizes limited solely by the computation requirements (practical limit: 300 by 300).
- Either rigid or symmetric boundary conditions.
- Graphical pre- and postprocessors for simplified input entry and output analysis.

CASE STUDY

As part of the initial investigation and validation of this new implementation, the underground stresses, displacements, topographic stresses, and interseam interactions were modeled at a field site. This case study site is a multiple-seam situation

in eastern Kentucky. The geology in this area is fairly typical of the Southern Appalachian Coal Basin, with various sedimentary layers of sandstones, siltstones, shales, and numerous coal seams. The topography in the area is very rugged, with various steep ridges and valleys that have a topographic relief of over 600 m (2,000 ft). At the case study site, the overburden averages about 240 m (800 ft), but ranges from 90 m (300 ft) at the southeastern corner of the site to over 360 m (1,200 ft) at the northwestern corner (figure 7). (Because of the steep topography, it was critical to include the

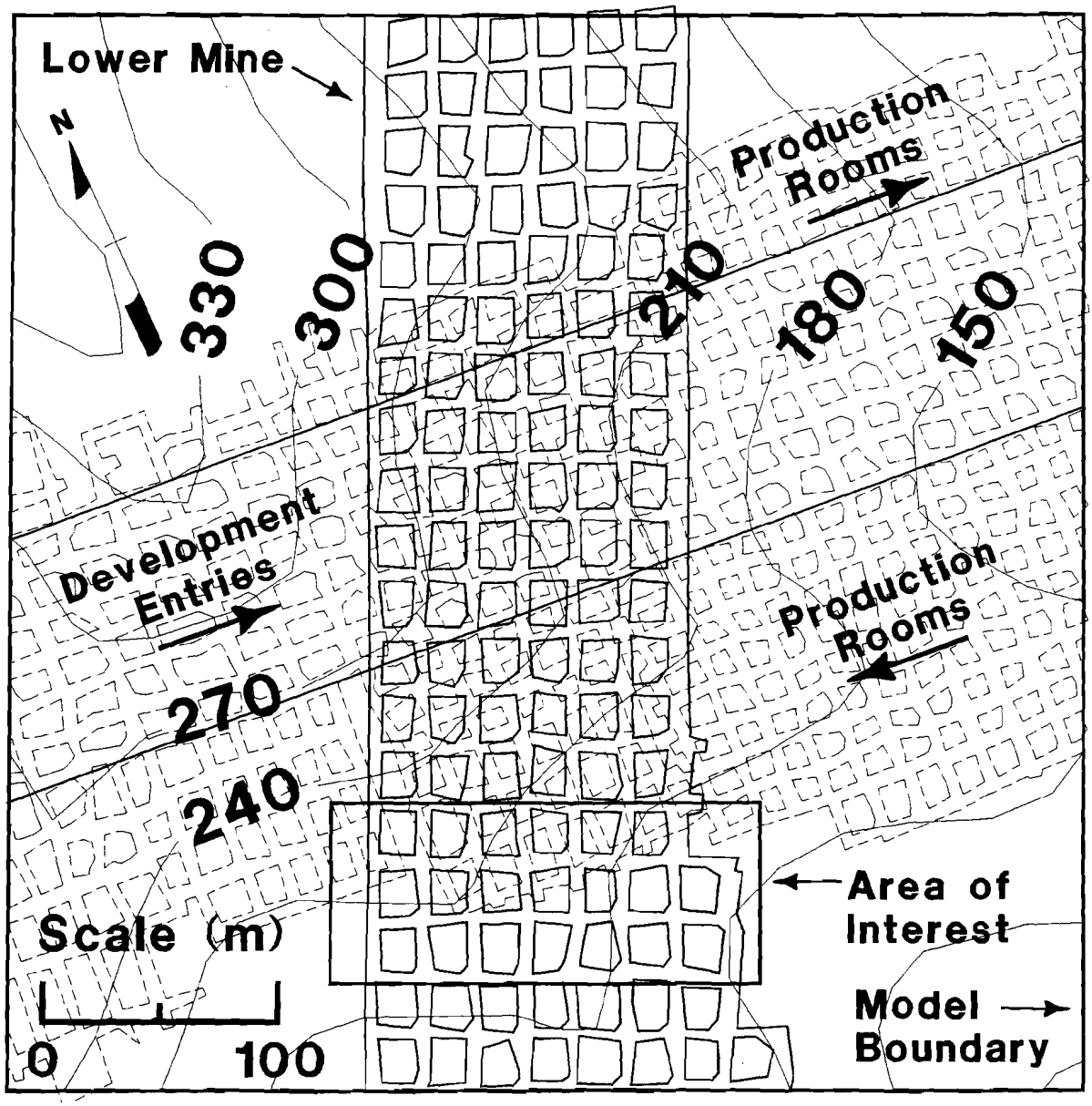

Figure 7.—Map of case study mines in eastern Kentucky.

topographic stress effects in the model to obtain accurate results.)

The overlying mine operates in the Upper Darby Seam, which typically averages about 2.0 m (6.5 ft) thick; however, in the model area, the extraction thickness had increased to over 2.7 m (9 ft). The lower mine operates in the Kellioka Seam, which averaged about 1.5 m (5.0 ft) thick in the study area. The interburden between the mines averages around 14 m (45 ft) and consists of interbedded sandstones and shales. The core logs nearest to the study site indicate about 3.5 to 5 m (12 to 15 ft) of thinly laminated shaley/carbonaceous sandstone (stack rock) directly over the Kellioka Seam. This is then overlain by 7.5 to 10.5 m (25 to 35 ft) of interbedded sandstones and shales, with shale primarily forming the floor of the Upper Darby Seam.

Both mines are room-and-pillar drift mines and utilize continuous miners for coal extraction. In some production sections, depending on local mining conditions, the mines remove the pillars on retreat for full extraction. In the study area, the lower mine had driven a seven-entry-wide set of main entries from north to south with pillars on 21- by 24-m (70- by 80-ft) centers and 6-m (20-ft) wide entries. Subsequently, the upper mine drove a seven-entry-wide set of panel development entries roughly perpendicular across the lower mains (figure 7). Relatively short (one- to two-crosscut) production rooms were driven to the north of the upper mine development entries during advance. At this point, no appreciable stress interaction was observed. Then, as the upper mine was pulling out of the section, long (seven- to eight-crosscut) production rooms with pillars on 18- by 18-m (60- by 60-ft), and smaller, centers were driven on the south side of the development entries (figure 7). At the extent of mining shown in figure 7, the upper mine began to experience major problems with pillar failure and floor heave and was forced to abandon the section.

Coincident with the failures in the upper mine, the lower mine experienced ground control problems in areas directly underlying the boundaries of the upper panel. These problems were primarily manifested as increased pillar spalling for approximately 30 m (100 ft) of entry and major roof cracking at overmined intersections. Both of these ground control problems were mitigated by supplemental bolting and cribbing.

The new laminated model, LAMODEL, was applied at this site to both quantify the magnitude of the stress interaction between the seams and to correlate the model results with in-mine ground control problems for subsequent predictions of mining conditions in future mine planning analysis. In the model, the seams were discretized with 3-m (10-ft) elements on 150-by-150 grids with the extent as shown in figure 7. Symmetrical seam boundary conditions were set, and no free-surface effects were included. The interburden was set at 14 m (45 ft), and the rock mass was simulated with a modulus of 20,700 MPa (3 million psi) and 15-m (50-ft) thick laminations. A strain-softening material was used for the in-seam coal, and the peak strength of the coal was varied until the pillars in the upper seam had just reached failure.

Additionally, because of the high topographic relief at the site, the topography was discretized with 15-m (50-ft) elements for an area extending 300 m (1,000 ft) beyond the limits of the displacement-discontinuity grids. The importance of including the topographic stress effects in the model is clearly evident in figure 8, which shows the topographic stress at the level of the upper mine. It is interesting to note in this figure the amount to which the topographic stress is "smoothed" with depth in comparison with the original topography shown in figure 7. Also, it should be observed in figure 8 that near the boundary of the upper mine (the area of interest) the topographic stress varies about 1.4 MPa (200 psi), or 30%, across the pillars in the lower mine.

The primary results of this multiple-seam modeling effort are shown in figure 9. Figure 9*C* shows the stress concentrations on the lower seam resulting from the pillar failure in the upper seam. In this image, stress concentrations up to 4.5 MPa (650 psi) and with functional widths of between 9 to 37 m (30 to 120 ft) can be seen. This model response correlates well with the underground observations. The calculated seam interaction stress results in increases of the average pillar stress in the lower mine up to 55% (figures 9*A* and 9*B*). By correlating this 55% increase in pillar stress with the observed ground control problems underground (figure 9), the magnitude of future ground control problems at this site can now be more accurately determined using LAMODEL.

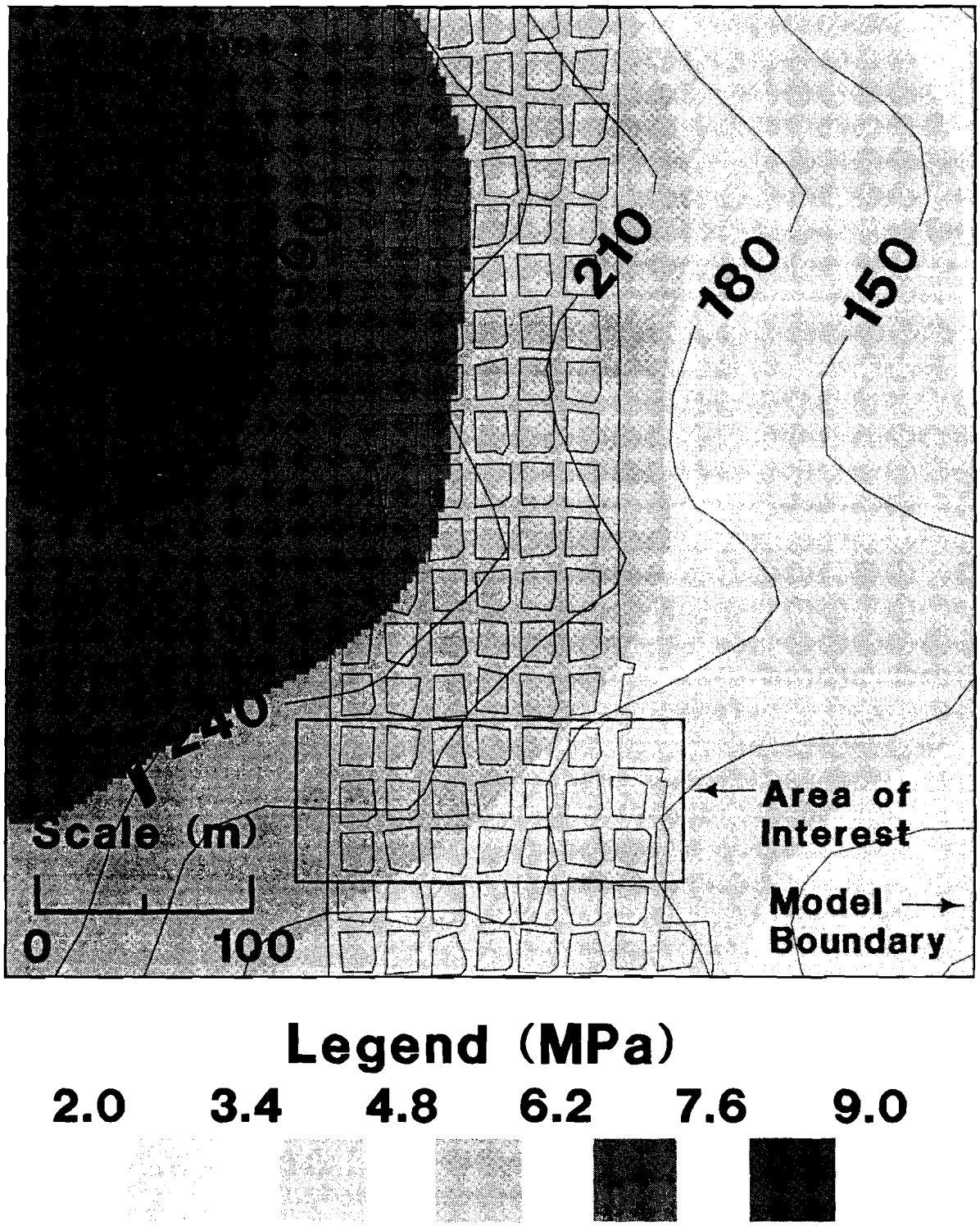

Figure 8.—Topographic stress on lower seam.

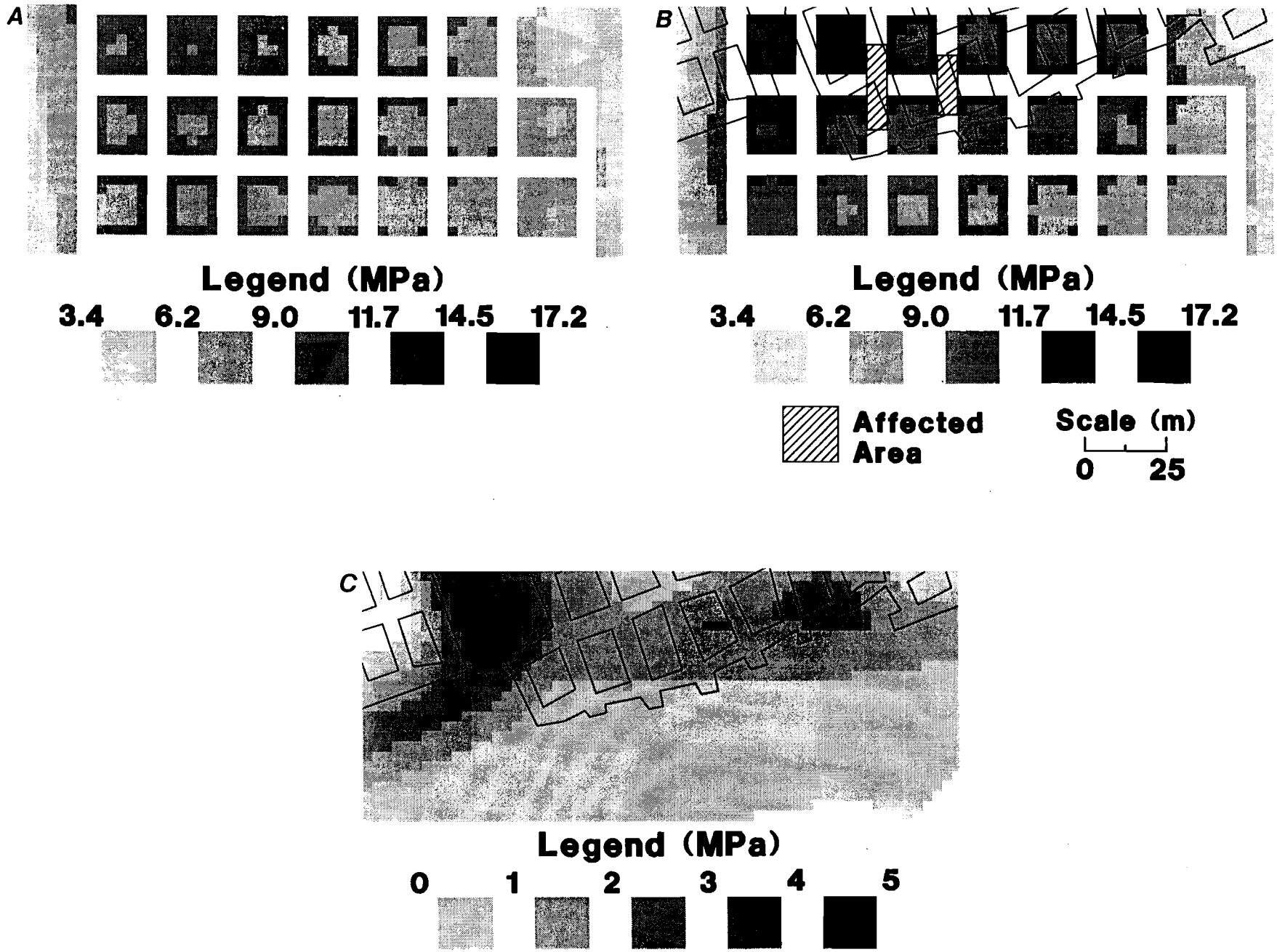

Figure 9.—Stress analysis on lower mine. *A*, single-seam stress; *B*, multiple-seam stress; *C*, additional stress from upper seam.

SUMMARY AND CONCLUSIONS

The investigation of the fundamental behavior of the laminated overburden presented in the first part of this paper has produced a number of significant results. First, it is clear that the laminated overburden (with a low lamination thickness) is more flexible or supple than the homogeneous isotropic overburden. This increased suppleness is evident in the greater convergence across a longwall panel, in the larger extent of the remote displacement contours, and in the nature of the surface subsidence. Second, due to the larger extent of the remote displacement contours, it is clear that a multiple-seam mine model using the laminated overburden will show increased interseam displacements and stresses compared with a homogeneous isotropic overburden. Third, because the overburden in the laminated model is effectively described with two parameters (as opposed to one parameter in the homogeneous isotropic model) and therefore provides two degrees of freedom for fitting observed data, the laminated model was capable of closely matching the observed abutment stresses and surface subsidence. In fact, the laminated model was easily fit to the observed surface subsidence, whereas the subsidence for the homogeneous isotropic overburden was fundamentally different from the observed subsidence.

In the second part of this paper, a new laminated displacement-discontinuity program, LAMODEL, was presented. This new program, in addition to the laminated overburden, also implements a number of innovative features, including topographic stress calculations, various in-seam material models, and variable boundary conditions at the seam level. In order to evaluate the accuracy and utility of the new model, it was used in a case study of a multiple-seam mining situation in steep topography. At this site, the ability of LAMODEL to include topographic stress effects, strain-softening coal, and symmetric boundary conditions greatly increased the realism and accuracy of the model. By correlating the LAMODEL results with the observed ground control problems, mine management will be better able to design and plan for future multiple-seam interactions. Because of the realistic flexibility of the laminated overburden model and the utility of the numerous practical features implemented in the new program, it appears that LAMODEL can provide realistic stress and displacement calculations for a wide range of mining situations.

REFERENCES

Berry DS [1960]. An elastic treatment of ground movement due to mining - part I. Isotropic ground. J Mech Physics of Solids *8*:280-292.

Berry DS, Sales TW [1961]. An elastic treatment of ground movement due to mining - part II. Transversely isotropic ground. J Mech Physics of Solids *9*:52-62.

Cook NGW, Hoek E, Pretorious JPG, Ortlepp WD, Salamon MDG [1966]. Rock mechanics applied to the study of rock bursts. J South Afr Inst Min Metall *66*:436-528.

Crouch SL [1976]. Analysis of stresses and displacements around underground excavations: an application of the displacement discontinuity method. Minneapolis, MN: University of Minnesota, Department of Civil Engineering, Geomechanics Report.

Crouch SL, Fairhurst C [1973]. The mechanics of coal mine bumps and the interaction between coal pillars, mine roof, and floor. U.S. Department of the Interior, Bureau of Mines, OFR 53-73.

Heasley KA, Zelanko JC [1992]. Pillar design in bump-prone ground using numerical models with energy calculations. In: Iannacchione AT, Mark C, Repsher RC, Tuchman RJ, Jones CC, comp. Proceedings of the Workshop on Coal Pillar Mechanics and Design. Pittsburgh, PA: U.S. Department of the Interior, Bureau of Mines, IC 9315, pp. 50-60.

Jaeger JC, Cook NGW [1979]. Fundamentals of rock mechanics. London: Chapman and Hall.

Jeran PW, Adamek V, Trevits MA [1986]. A subsidence prediction model for longwall mine design. In: Proceedings of the Longwall U.S.A. Conference. Pittsburgh, PA: pp. 101-112.

Kripakov NP, Beckett LA, Donato DA, Durr JS [1988]. Computer-assisted mine design procedures for longwall mining. Pittsburgh, PA: U.S. Department of the Interior, Bureau of Mines, RI 9172.

Mark C [1990]. Pillar design methods for longwall mining. Pittsburgh, PA: U.S. Department of the Interior, Bureau of Mines, IC 9247.

Plewman RP, Deist FH, Ortlepp WD [1969]. The development and application of a digital computer method for the solution of strata control problems. J South Afr Inst Min Metall *70*(9):33-44.

Salamon MDG [1961]. An introductory mathematical analysis of the movements and stresses induced by mining in stratified rocks. Durham, United Kingdom: King's College, University of Durham, Department of Mining, Research Report *9*:Bull 3.

Salamon MDG [1962]. The influence of strata movement and control on mining development and design [Thesis]. Durham, United Kingdom: University of Durham, Department of Mining.

Salamon MDG [1963]. Elastic analysis of displacements and stresses induced by the mining of seam or reef deposits, part I. J South Afr Inst Min Metall *63*(4):128-149.

Salamon MDG [1964]. Elastic analysis of displacements and stresses induced by the mining of seam or reef deposits, part II. J South Afr Inst Min Metall *64*(6):197-218.

Salamon MDG [1974]. Rock mechanics of underground excavations. In: Proceedings of the 3rd Congress, International Society for Rock Mechanics. Denver, CO: National Academy of Sciences, *1*(b)951-1099.

Salamon MDG [1989a]. Some applications of the frictionless laminated model. In: Proceedings of the 30th U.S. Symposium on Rock Mechanics. Morgantown, WV: West Virginia University, pp. 891-898.

Salamon MDG [1989b]. Subsidence prediction using a laminated linear model. In: Proceedings of the 30th U.S. Symposium on Rock Mechanics. Morgantown, WV: West Virginia University, pp. 503-510.

Salamon MDG [1991]. Deformation of stratified rock masses: a laminated model. J South Afr Inst Min Metall *91*(1):9-26.

Sinha KP [1979]. Displacement discontinuity technique for analyzing stresses and displacements due to mining in seam deposits [Thesis]. Minneapolis, MN: University of Minnesota.

Yang G [1992]. Numerical approach to the prediction of subsidence due to longwall coal mining using a laminated model [Thesis]. Golden, CO: Colorado School of Mines.

Zipf RK Jr., Heasley KA [1990]. Decreasing coal bump risk through optimal cut sequencing with a non-linear boundary element program. In: Hustrulid WA, Johnson GA, eds. Proceedings of the 31st U.S. Symposium on Rock Mechanics. Golden, CO: Colorado School of Mines, pp. 947-954.

RETREAT MINING WITH MOBILE ROOF SUPPORTS

By Frank E. Chase,[1] Allen McComas,[2] Christopher Mark, Ph.D.,[3] and Chester D. Goble[4]

ABSTRACT

Mobile roof supports (MRS's) are shield-type support units mounted on crawler tracks. MRS's are used during retreat mining and eliminate the setting of roadway, turn, and crosscut breaker posts that are required during pillar recovery operations. Mobiles are a more effective ground support than timbers, and their usage enhances the safety of section personnel and reduces material handling injuries. MRS usage is rapidly increasing, and approximately 40 U.S. coal mines have successfully employed this relatively new technology. This paper addresses the practical aspects of MRS usage in underground coal mines.

During this study, nearly one-half of the U.S. mines that have utilized mobiles were visited. This report depicts the more common pillar extraction methods that operators have found successful. The "Christmas tree" and outside lift methods are described and illustrated. Roof control plans that do not require breaker posts or allow pillar extraction with fewer than four mobiles are also examined. In addition, operators' experiences with setting pressures, loads, and rates of loading during pillar extraction are addressed. Mining and support strategies to more effectively control hillseams, weak roof, and gob overrides are also discussed.

[1]Geologist, Pittsburgh Research Center, National Institute for Occupational Safety and Health, Pittsburgh, PA.
[2]President, Mobile Mining Supports, Inc., Peach Creek, WV.
[3]Mining engineer, Pittsburgh Research Center, National Institute for Occupational Safety and Health, Pittsburgh, PA.
[4]Vice president, Mobile Mining Supports, Inc., Peach Creek, WV.

INTRODUCTION

Mobile roof supports (MRS's) are shield-type support units mounted on crawler tracks (figure 1). MRS technology was pioneered by the former U.S. Bureau of Mines during the 1980's [Thompson and Frederick 1986]. Commercial units are currently manufactured by J. H. Fletcher and Co., Huntington, WV, and Voest-Alpine Mining and Tunneling, Pittsburgh, PA. Fletcher refers to its units as "Fletcher Mobile Roof Supports" (FMRS). Voest-Alpine has designated its units as "Alpine Breaker Line Supports" (ABLS). For the purposes of this paper, the generic term "MRS," or "mobile," is used to identify both manufacturers' units. In 1988, the Donaldson Mine in Kanawha County, WV, was the first U.S. operation to use mobiles. Since then, approximately 40 U.S. mines in 5 States have utilized mobiles. These States include Illinois, Kentucky, Pennsylvania, Virginia, and West Virginia. Mobiles have been employed in more than 15 different U.S. coalbeds ranging from 1.7 to 4 m (5.5 to 13 ft) thick. MRS units are primarily used in coalbeds thicker than 2.4 m (8 ft). Currently, there are approximately 100 units in use in the United States. Mobiles have been used primarily during full and partial pillar recovery operations. However, the first longwall face shield recovery operation to utilize mobiles instead of walking shields was in a southern West Virginia coal mine in 1996. Operators and others have also been discussing mobile employment in longwall headgates and tailgates.

MRS's provide improved safety to section personnel compared with a conventional timber plan. However, the first fatality on an MRS section occurred in 1995 in Mingo County, WV. During the fatality investigation, questions arose regarding (1) pillar extraction methods, (2) setting pressures, (3) loads and rates of loading on the machines, and (4) proper positioning of mobiles and face personnel. In order to determine the current state of the art in MRS usage, researchers from the Pittsburgh Research Center visited 20 U.S. mines with different geologic and mining conditions. Personnel with practical hands-on experience were questioned at each operation, and operational advantages and issues were discussed. In addition, all Mine Safety and Health Administration (MSHA) approved MRS roof control plans were examined. The findings are summarized below.

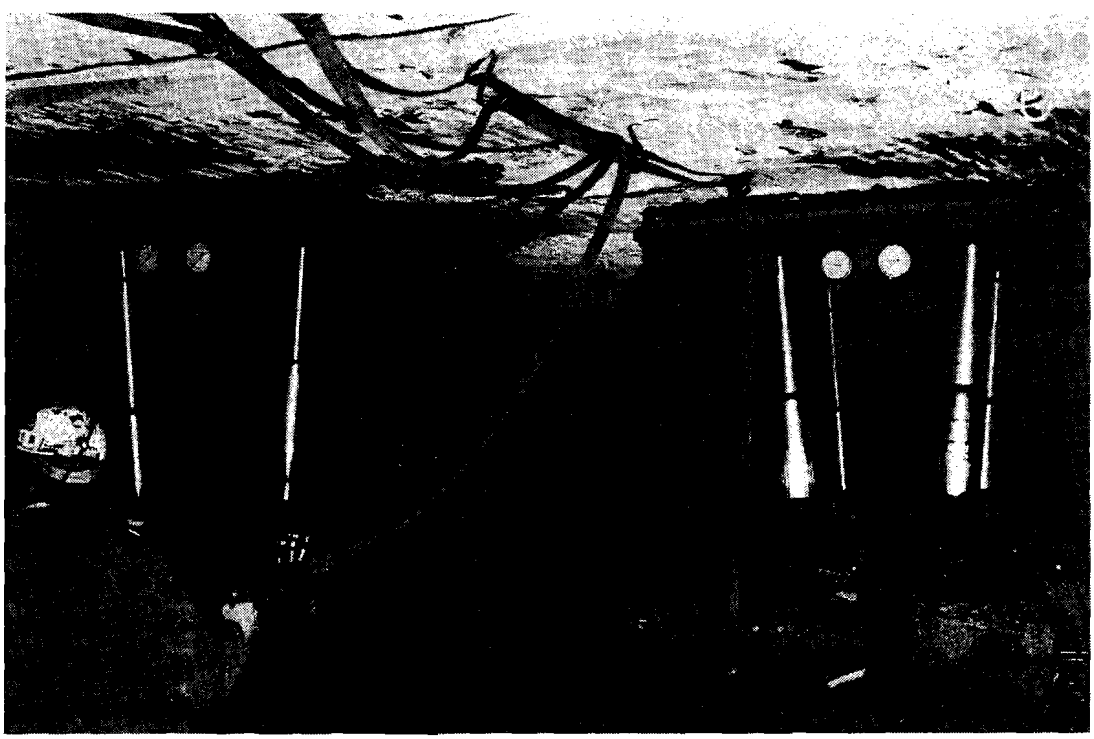

Figure 1.—Full pillar extraction using mobile roof supports.

SAFETY ADVANTAGES

MRS's are used in lieu of roadway, turn, and crosscut breaker posts during pillar recovery operations. Eliminating the setting of these posts enables miners to remain further outby the pillar line and reduces their exposure to gob overrides and rib spalling. Mobiles are active supports, whereas wooden posts are strictly passive. Mobiles also provide better roof coverage. Roof coverage depends on the manufacturer; however, the unit with the least canopy dimensions provides 3.3 m^2 (36 ft^2) of pressurized roof coverage, compared with less than 0.1 m^2 (1 ft^2) for a wood post. The improved stability of mobiles is also a major advantage. Wood posts will fail, sometimes with little or no warning, at less than 2.5 cm (1 in) of convergence. Mobiles will displace approximately 2.5 cm (1 in) before yielding and have the ability to yield through a few meters of displacement without becoming unstable. Mobiles are much better suited to handle eccentric load conditions (i.e., horizontal and lateral loading), which are common during pillar extraction, compared with wood posts, which suffer reduced stability for anything but pure axial (vertical) loads [Barczak and Gearhart 1997]. Gob sliding and rib rolls will commonly kick out breaker and turn posts.

MRS units are available in two different support capacities. With one exception, all U.S. mines employ mobiles that can exert up to approximately 5,338 kN (600 tons) of force against the roof. These units each have a load-bearing capacity equivalent to six 20-cm (8-in) diameter hardwood posts [Barczak and Gearhart 1997]. One deep-cover operation in Virginia is using mobiles that have a 7,118-kN (800-ton) support capacity. Based on the above, MRS's are superior to wood posts for pillar extraction. At every operation visited, personnel expressed the opinion that mobile usage enhances pillar line stability and safety.

Mobiles reportedly reduce material handling injuries and free personnel for other less strenuous assignments. In a mine visited in Mingo County, WV, the operator noticed a significant reduction in back injuries with mobile usage. Prior to mobiles, scores of posts 3.4 m (11 ft) long and weighing 80 kg (175 lb) had to be set to recover each pillar. Because of reduced roadway clearance, shuttle cars were constantly knocking out the posts, which then had to be reset. Three miners were required to set each post. One miner had to climb a stepladder to drive in the wedges. This miner summarized by saying "we're not setting posts, we're planting trees." In another mine visited in Mingo County, WV, 105 posts were typically set for every pillar mined, compared with only 8 breaker posts when mobiles were employed. The mine worked three shifts, and it required one miner on each shift to haul in enough timbers to keep up with pillar line advancement. This same operator reported a reduction in cost of $0.65/t ($0.60/st) over conventional timbering and an 18% increase in production. A reduction in cost of $2.20/t ($2.00/st) was reported by an operator in Boone County, WV. Mobiles also increase the self-esteem of reassigned miners. Miners have traded in their axes and bow saws for more modern technology.

PILLAR EXTRACTION METHODS

CHRISTMAS TREE METHOD

The "Christmas tree" method (also called left-right, fishbone, or treetopping) is the most commonly used full pillar extraction method with MRS's (see figures 2*A* through *D*). This method is generally employed under deep cover when pillars on 18- or 24-m (60- or 80-ft) centers are required to maintain necessary pillar stability factors. Figures 2*A* through *D* depict a common sequence in which lifts are extracted during barrier and production pillar extraction. As shown in figure 2*A*, mobile unit 4 is trammed approximately 2.1 m (7 ft) outby and pressurized prior to mining lift 2. Prior to mining lift 3 (figure 2*B*), unit 3 is trammed 4.3 m (14 ft) outby and pressurized. This process continues until the breakers are set, as indicated in figure 2*B*. After the breakers are set, unit 3 is moved to position F and unit 4 is trammed to position G. When referring to a particular mobile, units 1 through 4 are designated as shown in figure 2*B* by convention. After mining the barrier pillar, the mobiles tramming down the entry are referred to as the "No. 1" (left side) and "No. 2" (right side) units. Mobiles maneuvered through the crosscut are designated as the "No. 3" (pillar line side) and "No. 4" (solid pillar side) units.

The size and shape of the pillar remnants, back wing, and pushout stump (figures 2*C* and *D*) can vary from pillar to pillar. The riskiest process during pillar extraction is pushout removal. Some operators routinely try to extract 60% or more of the pushout, conditions permitting; others do not attempt to remove the pushout. This decision is based on mining conditions, past experiences with equipment entrapments, and safety considerations. In general, the more competent the roof, the more likely the pushout is removed. Operators who typically remove the push will abandon it if the stump shows signs of excessive

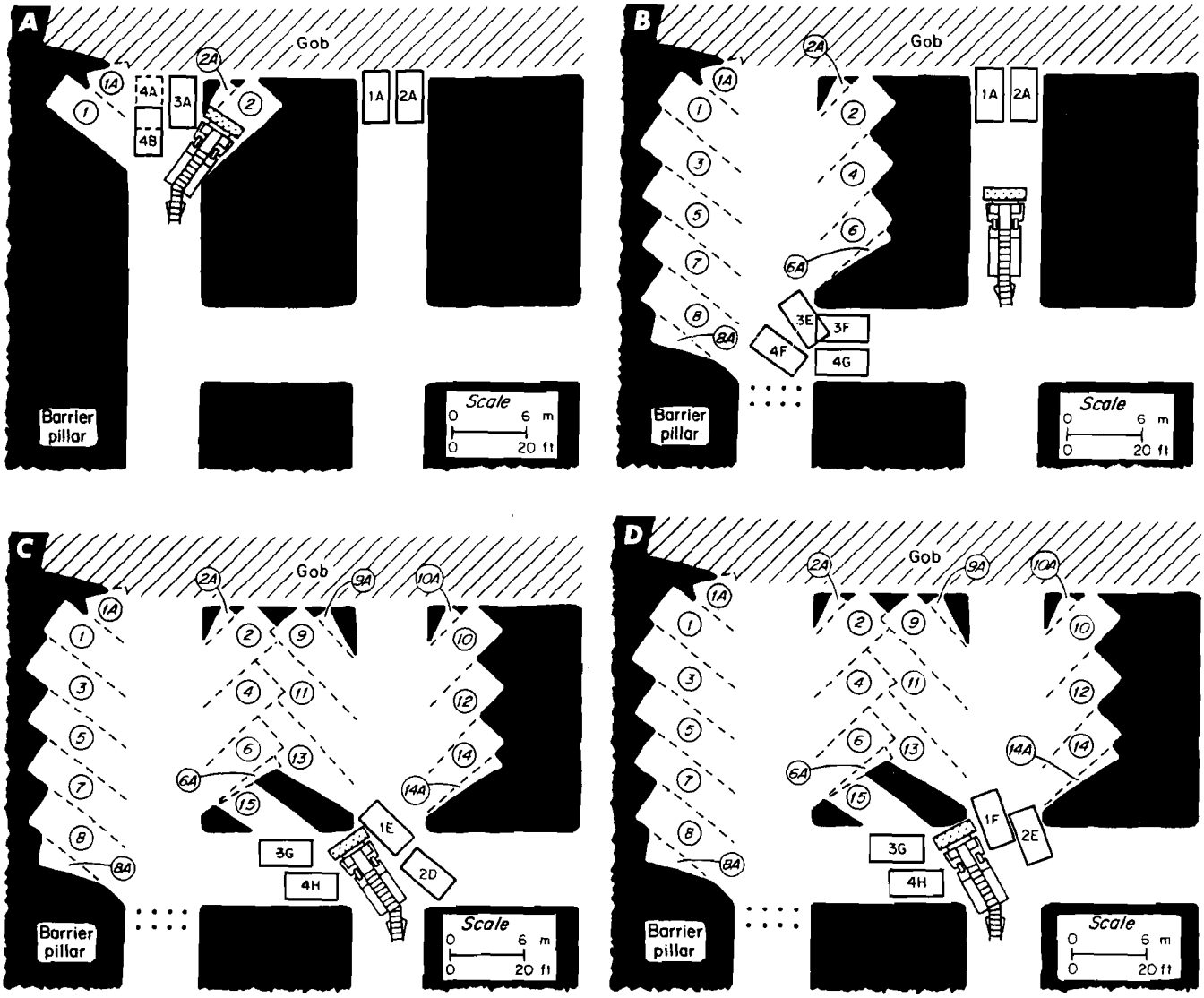

Figure 2.—Christmas tree extraction method. *A*, lifts 1-2A. *B*, lifts 1-8A. *C*, lifts 1-push; pushout removal with units 1 and 2 in tandem. *D*, lifts 1-push; pushout removal with units 1 and 2 staggered.

weight. It should be noted that when attacking the pushout, most operators situate the mobiles so that the roadway is from 3.7 to 4.3 m (12 to 14 ft) wide. The clearance is so restrictive that the ripper head has bent mobile canopies. Bit marks were also observed on a few canopies. If the push is wider than the ripper head, the sump will normally be taken through the middle of the push.

Based on operators' experiences and underground data obtained by Hay et al. [1997], the area most prone to roof falls during pillar extraction is the intersection. Operators sometimes refer to the intersection as the "critical area." During the study conducted by Hay et al. [1997], units 1 and 2 were situated in the entry just inby the intersection during back wing and pushout removal. Significant roof deflection and higher roof bolt loads were monitored, compared with an adjacent instrumented intersection, where timbers were used to extract a pillar. Therefore, Hay et al. [1997] concluded that units 1 and 2 should be placed in the intersection as much as possible to protect miners and equipment. It is important to note that MRS units 1 and 2 were positioned inby the intersection when the 1995 fatality occurred in Mingo County, WV (figure 3). The fatal accident happened during the mining of the last lift in the pillar. To enhance intersection stability, some operators position mobiles 1 and 2 in tandem, as shown in figure 2*C*, prior

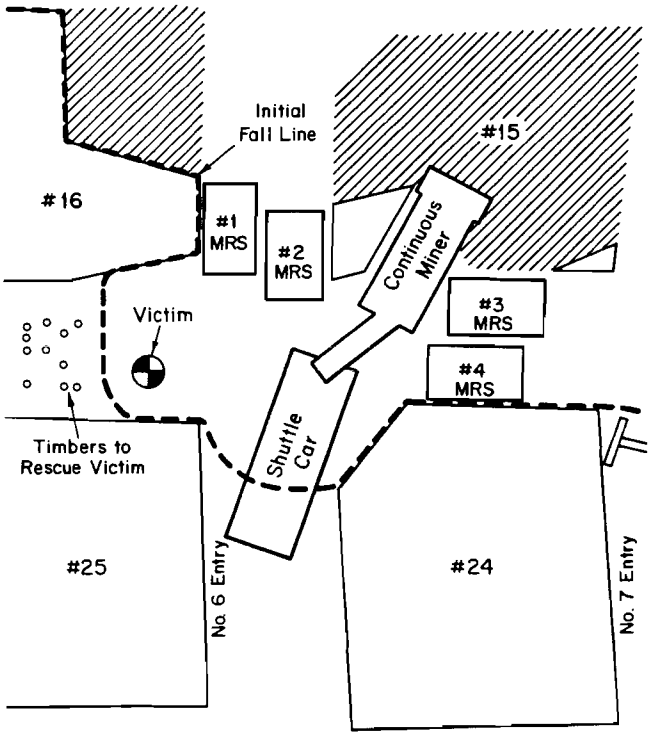

Figure 3.—MSHA drawing of fatal roof fall accident [Vance et al. 1995].

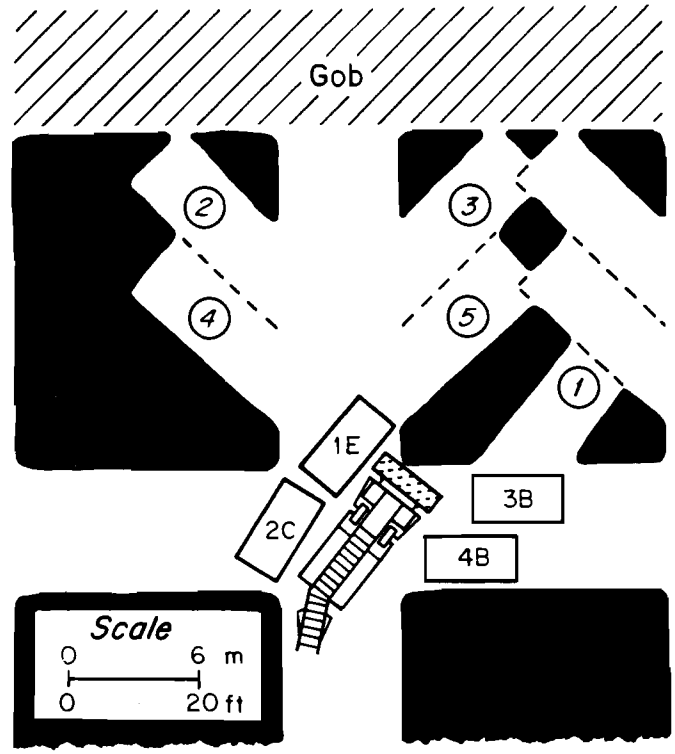

Figure 4.—Modified Christmas tree method.

to pushout removal. Other operators stagger units 1 and 2 side by side in the intersection as much as possible (see figure 2*D*). In figures 2*C* and *D*, lift 11 is a 14-m (46-ft) extended cut. In certain MSHA districts, the length of an extended cut (measured from the rib-side column of bolts) cannot exceed 14.8 m (40 ft).

A variation of the usual Christmas tree lift sequence is illustrated in figure 4, where lift 1 is taken from the back wing (also called bottom of the block). Mobile units 3 and 4 are then moved to locations 3B and 4B and pressurized. Some operators indicated that this positioning enhances intersection stability prior to the mining of the left and right wings (lifts 2-5). However, some State and Federal roof control specialists expressed the concern that the removal of the back wing lift first actually reduces intersection stability, which is critical.

OUTSIDE LIFT METHOD

The extended-cut outside lift method (figures 5*A* through *C*) generally has been used under less than 120 m (400 ft) of cover. Entry spacings are typically about 15 m (50 ft) with crosscuts on 25-37 m (80-120 ft) centers. One complaint from operators concerning this method is that the smaller pillars contain less coal; therefore, the equipment spends more time moving from pillar to pillar. As a result, some operators prefer that the pillars be as long as possible, with the major constraint being ventilation on development. A few operators have oriented the pillars in what is sometimes referred to as the "laid-down" position. In other words, the long axis of the pillar is perpendicular, not parallel, to panel development. This panel design increases the number of stoppings and roof bolts required on development, but is sometimes chosen because it reduces belt move and haulage time.

Some operators prefer the outside lift method because most power cables exit continuous miners in a right rear position. Therefore, miner operators tend to position themselves on the right side of the continuous miner. During the outside lift pillar extraction, the miner operator's positioning gives him or her an excellent line of vision. A few operators believe that this method is safer than the Christmas tree method because the continuous miner operator is less tempted to move further forward to observe the mining of the left wing.

Under weak roof conditions, some operators also prefer the outside lift method because the unsupported span (width) of the mined-out area is smaller compared with the area opened up with the Christmas tree method. In addition, the outside lift method provides added protection to the continuous miner because a solid coal pillar is nearby. Further support can be

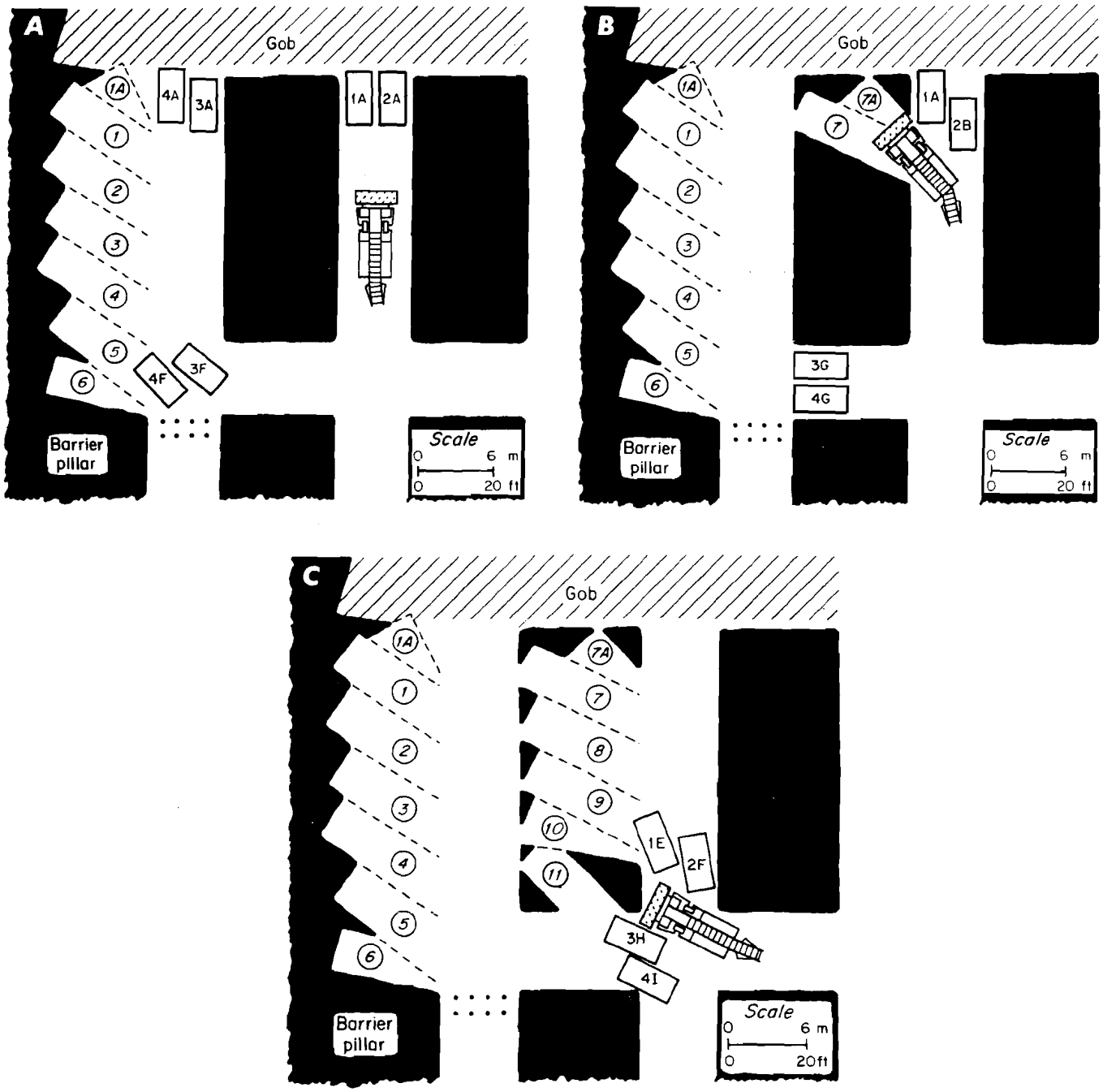

Figure 5.—Outside lift method. *A*, lifts 1-6; *B*, lifts 1-7A; *C*, lifts 1-push.

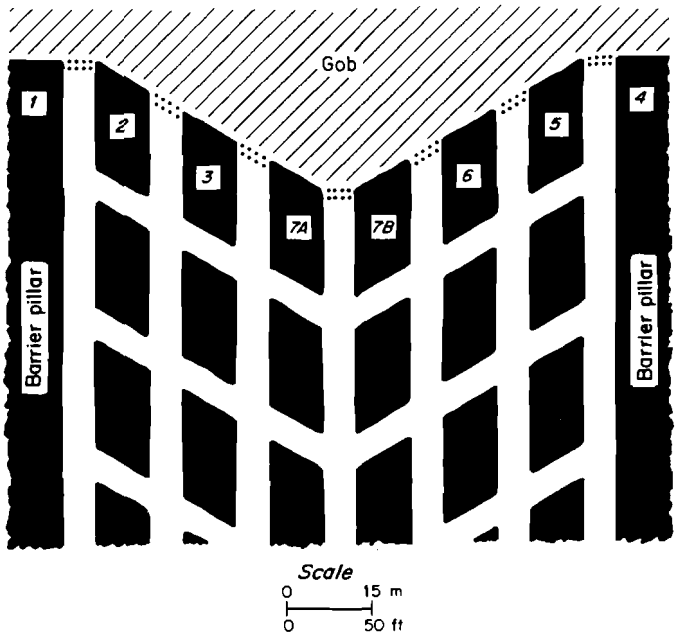

Figure 6.—Herringbone panel design.

obtained under weak roof conditions if remnants are left at the back end of the lifts. One disadvantage to the outside lift method compared with Christmas treeing is that the lift lengths are usually longer (deeper). Prolonged exposure while mining deeper lifts subjects the continuous miner to greater risk.

EXTRACTION WITH CONTINUOUS HAULAGE

The Christmas tree and outside lift methods have been used in combination to extract the parallelogram-shaped pillars (figure 6) that are developed using continuous haulage. Crosscuts are driven on approximately 60° angles to facilitate the movement of bridges and carriers. This panel configuration has been referred to as the "herringbone" or "turkey foot" design. Common entry centers range from 16 to 18 m (52 to 58 ft), with crosscuts on 25- to 27-m (81- to 90-ft) centers. Barrier and production pillars can be extracted as shown in figure 6, or pillars can be mined from right to left, then from left to right. After the mining of lifts 1 and 1A (figure 7*A*), unit 4 is trammed 2.1 m (7 ft) outby and pressurized. Lifts 2 and 2A are then removed from pillar 2. These lifts are removed to reduce the length of lift 7 shown in figure 7*B*. Mobile units 3 and 4 are positioned and pressurized at locations E and F, respectively, during breaker installation (figure 7*A*).

If poor ground conditions occur, they normally develop in the center or belt entry because the center pillars being mined are surrounded by gob on three sides, as shown in figure 7*C*. Figure 7*C* also displays mobile positioning during pushout removal in pillar 7B. A single pushout is usually removed from either pillar 7A or 7B. The push is taken from whichever fender is least loaded. The other fender (pillar 7A remnant) is left intact to function as a breaker during equipment removal. If both fenders exhibit severe loading, no pushout is taken. A laid-down version of this design has also been tried by one operator. A high incidence of roof falls in the belt entry prompted this operator to change to three-way belt entry intersections (figure 8). Three U.S. operators have employed mobiles in conjunction with continuous haulage. In one operation, shift production exceeded 5,400 t (6,000 st) during barrier pillar slabbing.

PARTIAL PILLAR RECOVERY

Mobiles were used during partial pillar recovery operations in two mines visited. Managers at one mine chose partial pillaring because the shale roof was so weak that they believed that full pillar extraction was not feasible. At this operation, pillars were initially developed on 30-m (100-ft) centers. On retreat, the pillars were "L-slabbed," with 7- to 10-m (20- to 30-ft) cuts taken from the entry and crosscut (figure 9). The remnant stumps measured approximately 19 by 19 m (62 by 62 ft). Two continuous miners were used on the section, each working with a pair of mobiles. As a row of pillars was extracted, one of the miners worked from the crosscut, while the other moved from entry to entry. Mine officials were quite satisfied with the results obtained from this method.

In the other mine practicing partial recovery, a massive sandstone roof subjected the mobiles to excessive loading during full pillar recovery. At this operation, a 4.9-m (16-ft) wide diagonal split was cut through a 9- by 9-m (30- by 30-ft) pillar, which left two triangular stumps. Miners call these stumps "coal cribs" because they provide enough short-term support for the equipment to be moved safely to the next pillar before they yielded and crushed out.

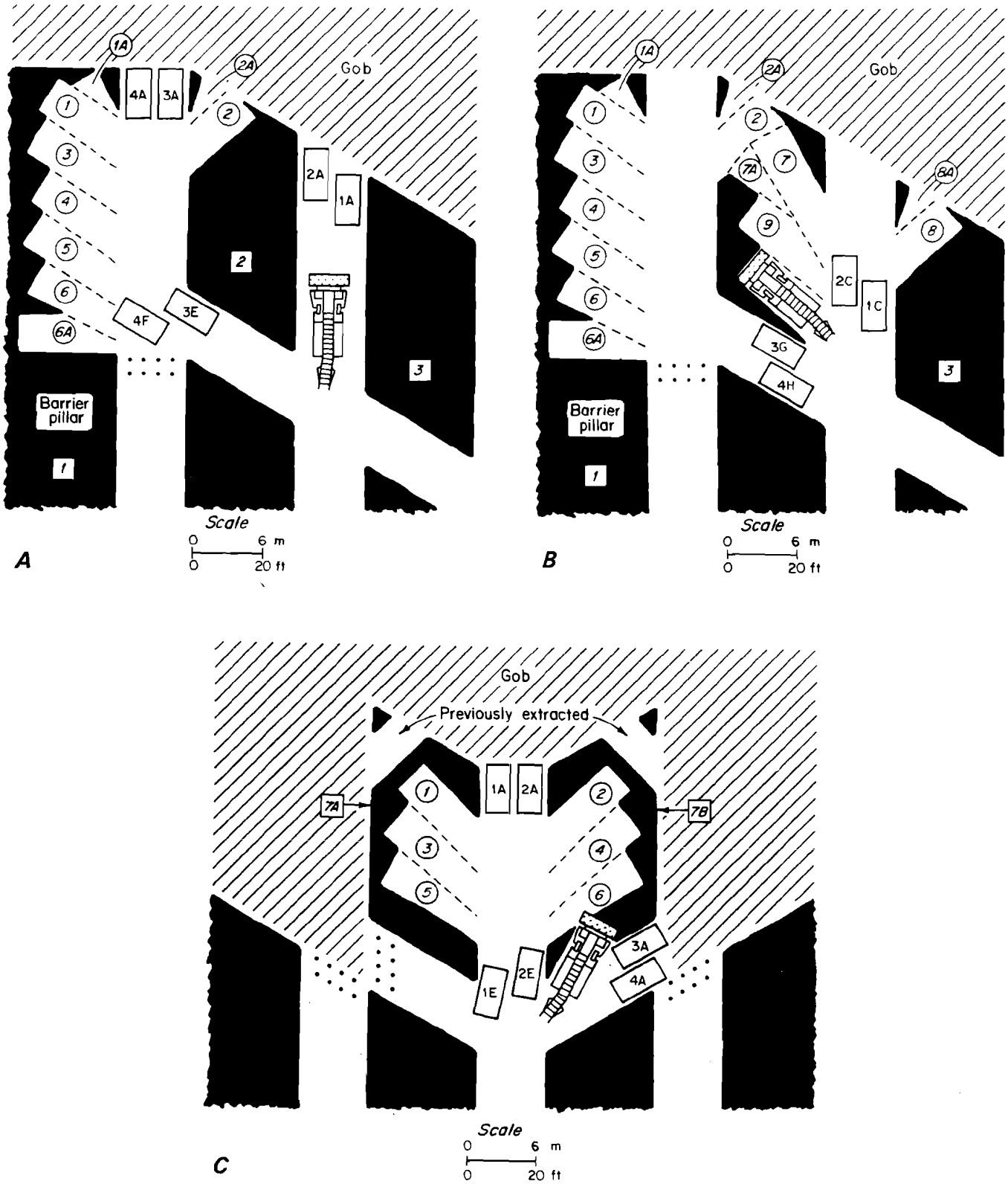

Figure 7.—Herringbone design: *A*, lift sequence for pillars 1 and 2; *B*, lift sequence for pillars 1-3; *C*, lift sequence for pillars 7A and 7B.

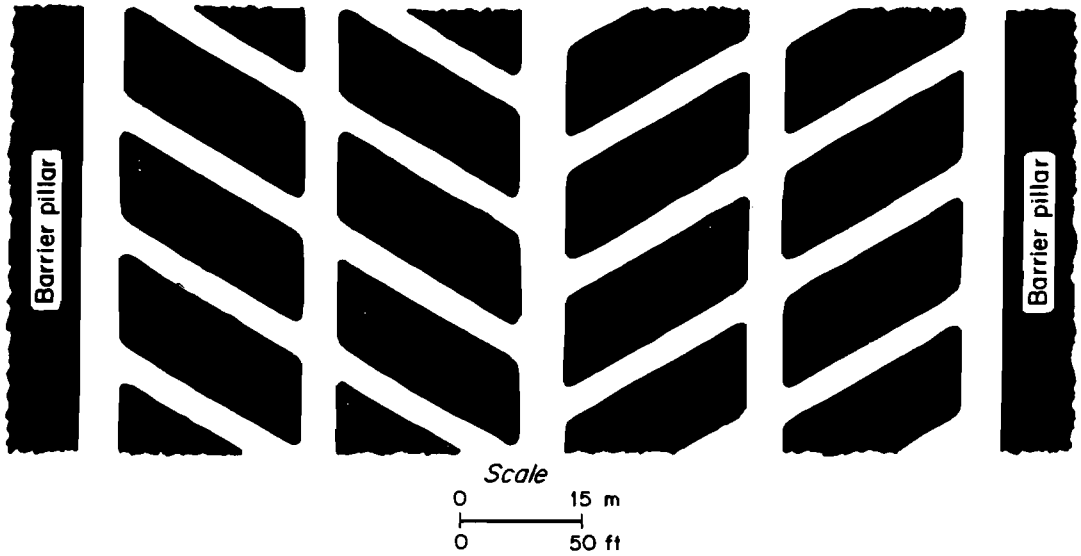

Figure 8.—Three-way intersection belt entry design.

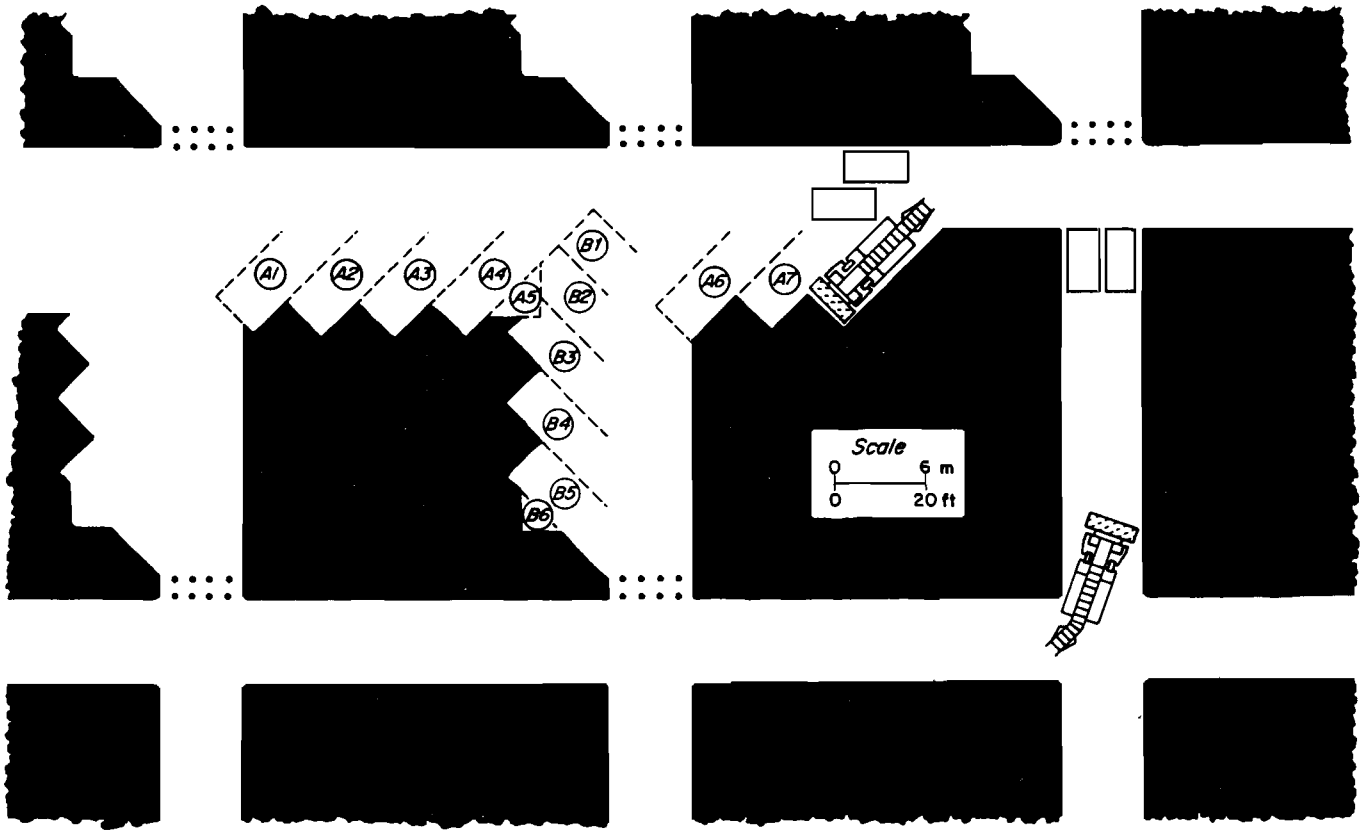

Figure 9.—Partial pillar extraction by slabbing.

OPERATIONAL ISSUES

ROOF FALLS

Roof falls or major rib rolls (side hits) can foul or bury mobiles. "Fouling" is a common term used by miners when mobiles are covered up and it requires less than 2 hours to recover them. Usually a 3.2-cm (1.25-in) high-strength steel cable or 2.5-cm (1-in) chain is attached to the mobile, and it is pulled out with the continuous miner or another mobile. A few operators with weak roof reported that weak "drawrock" sometimes fell prematurely and fouled the continuous miner while still mining in the lift. To remedy this, two mines that were visited employed fenders that separated the lift being mined from the gob. At an operation in Pennsylvania, the fender was initially fairly substantial, but it was extracted as the lift was completed (figure 10). An operation in Kentucky left 0.6-m (2-ft) fenders between lifts. These fenders were not extracted, and they provided enough support to complete the lift and remove the continuous miner before the fenders crushed out.

Major roof falls that bury mobiles may necessitate extensive cribbing and rebolting to rehabilitate the area, drilling and shooting, and a miner retriever (crab). A common mistake is to lower the canopy of the buried mobile in an attempt to tram it out from under the rock. This practice usually aggravates the problem, and mine operators have suggested that one or two cribs should be set along each side of the mobile before the canopy is lowered. Major roof falls under massive sandstone roof rock, especially during first cave conditions, can subject the mobiles to impact (shock) loads. This shock loading can cause hydraulic cylinders to swell, mushroom, or even bend. This damage occurs when the rock burst valves are unable to release sufficient hydraulic fluid to prevent the excessive buildup of hydraulic pressure. If sufficient fluid is released, the mobile becomes inoperative. Shock loading has also sheared lemniscate pins.

Numerous operators mentioned problems associated with hillseams (also called mountain cracks and surface breaks). Hillseams usually occur under shallow cover in sandstone roof rock. Parallel and intersecting hillseams can segment the roof into huge isolated blocks. Massive roof falls can occur when the coal pillars supporting these blocks are extracted. Several machines have yielded, been buried, or been severely damaged because of hillseams. Mining strategies under these conditions include leaving sufficiently sized pillar remnants to support the roof. Also, because cover is normally shallow, operators room out on 12- by 12-m (40- by 40-ft) centers near the outcrop and do not recover the pillars. One mobile operation in eastern Kentucky was mining under a massive sandstone main roof that would not break. First attempts at retreat mining were terminated due to squeeze conditions. Pillaring plans, which factored in hillseam locations, were later developed. As reported by Unrug et al. [1991], controlled systematic caving was achieved.

OPERATOR TRAINING

All of the coal mine operators visited indicated a need for practical, hands-on training. Training is required around the clock and can take from 2 to 6 weeks depending on the crew and conditions. One of the most common mistakes during training is mobile advancement. Many operators reported that mobiles best work in pairs, thereby providing protection to one

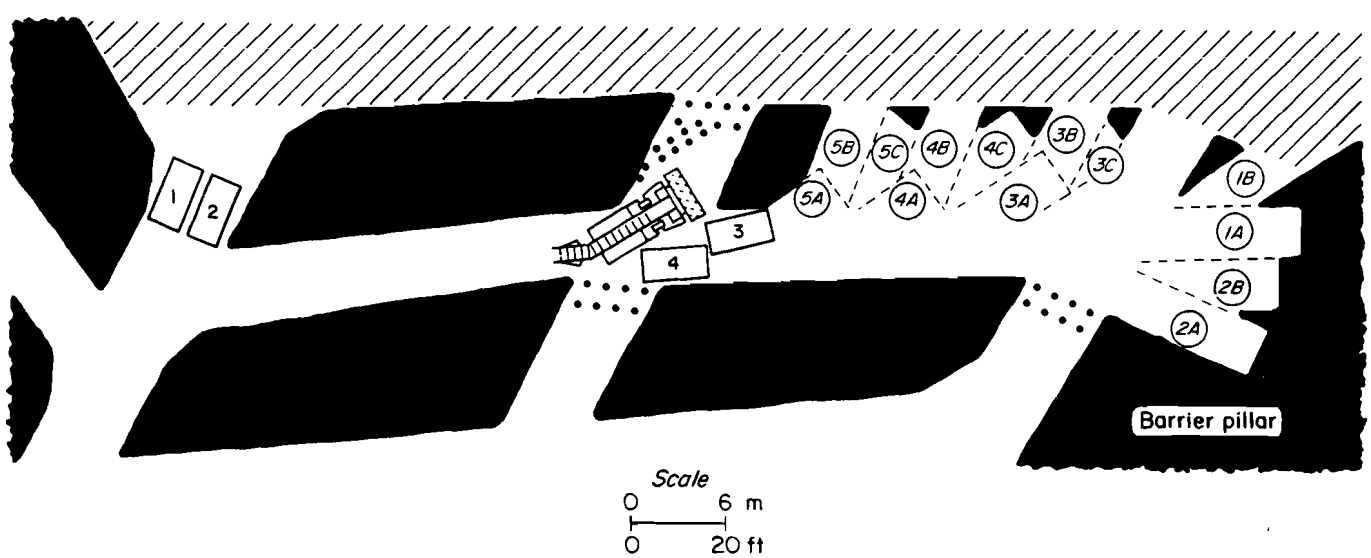

Figure 10.—Outside lift pillar extraction using temporary support fenders.

another. When moving mobiles during the mining of a pillar, it has been recommended that the machine be advanced no more than one-half the length of a canopy, or approximately 2.1 m (7 ft) from the canopy tip of the adjacent machine, and then pressurized. The second mobile, which is now protected by the first, can then be lowered and trammed forward. Mobile operators tend to advance one mobile too far and not leapfrog them, which has caused mobiles to be buried. Also, the canopy should not be lowered more than necessary to clear roof obstructions during advancement.

OPERATOR POSITIONING

After section personnel become familiar and comfortable with mobiles, it is not uncommon to hear miners say that "a mobile can pick up the whole mountain." It is important that miners do not position themselves in potentially hazardous areas because of this overconfidence and false sense of security. Leaning against the mobiles or standing in the intersection during the later stages of pillar recovery has been discouraged. During the final stages of recovery, some operators have made it a company policy that mobile and other nonessential section personnel be outby the intersection, in the entry of the next pillar row to be mined. At one mine visited, the superintendent remarked that "all it took was one gob override outby the canopies to convince the miners to stay out of the intersection."

PRESSURE GAUGES

Two pressure gauges are mounted on each mobile (figure 1). These gauges are visually monitored by operating personnel to determine loads and rates of loading on the units. Since the first fatality on an MRS section, considerable emphasis has been placed on the size of gauges. Some mobile operators have mentioned that it is necessary to stand close to the mobiles to read standard gauges. Other operators expressed that even the 10-cm (4-in) diameter gauges are of adequate size and can be read easily from 9 m (30 ft) away. Gauges are constantly monitored to determine loads and load development rates on the mobiles. Common sense modifications, which have made gauges easier to read, include the mounting of flood lights to illuminate the gauges and/or the adherence of reflective tape on the gauges' glass covers to mark a critical load threshold. At one operation, the positioning of the reflective tape depends on the roof rock type being mined under. The Spokane Research Center, MRS manufacturers, and others are currently working to develop lighting systems that can be seen from farther distances. Green, yellow, and red pulsating lights will indicate different total load levels or stages of loading. Additionally, a light-emitting diode bar graph will indicate rates of loading on individual units. Prototype lighting systems will initially be placed on the MRS units during the underground testing phase.

MACHINE RELIABILITY

During this study, operators indicated that mobiles were very reliable. Most operators cited cut power cables due to roof spalling or rib rolls as the most frequent cause of downtime. When mining in thicker reserves, high ribs are usually more hazardous and troublesome than the roof. At one mine visited, a 3-m (10-ft) high rib rolled onto the continuous miner's deadman switch while the miner was deep in a lift. While recovery efforts were underway, the roof deteriorated and a major roof fall occurred. Also, cable handling and hanging is more cumbersome in high coal, and concern has been expressed regarding the mobile operator's positioning when cables are detached from the mine roof after the lift has been taken. Breakaway cable-holding devices have recently become available. Dialog has begun with equipment manufacturers on permissible battery-powered mobiles, which has greatly interested mine operators.

RECOVERY AND PRODUCTION CONCERNS

Mobile usage has enabled a few operators to retreat mine reserves that could not be mined previously due to poor ground conditions. A mine operator in Boone County, WV, mentioned that previous attempts to retreat mine using a timber plan had failed because of poor roof conditions. He stated that caving would occur so quickly that it endangered the miners. Attempts to pillar using mobiles have proven successful in controlling premature caving. Another operator noted that past pillaring attempts with a conventional timber plan had failed because of weak floor conditions. The timbers punched into the floor, and the section would go on a squeeze. These same reserves were later successfully pillared using mobiles, which exert less ground-bearing pressure than wood posts because the crawler tracks distribute the load to the mine floor more uniformly. Coal recovery rates as high as 85% to 95% have been reported when using mobiles.

Mobile usage also assists operators in meeting production goals. Contrary to popular opinion, most of the mines contacted reported that shift production is usually higher on advance than during retreat when timbers are used. This is especially true when supersections are used on development. One major coal producer estimated that during retreat mining with timber supports, 20% less coal is mined per shift than during panel development. Some of the production decrease is attributable to downtime while setting timbers, practicing caution, and waiting for the roof to cave. Most of the operators indicated

that when mobiles are employed, shift production can improve to approximately 90% to 115% of what it is during panel development. Decreased production during retreating operations has prompted some operators to run supersections with mobiles or continuous haulage in conjunction with mobiles. A few operators using the extended-cut outside lift method have reported a slight production decrease when they switched to mobiles. This occurred because the pillars are typically smaller and, therefore, contain less coal, and considerable time is lost tramming the units. These operators have continued mobile usage, however, because of their safety advantages.

PROCEDURAL VARIATIONS

Procedures governing MRS usage are addressed in each mine's roof control plan. In some MSHA districts, if one mobile becomes inoperative, the section is down until the unit is again functional. In these districts, the mine operator should consider having an approved conventional timbering plan so that mining can continue. At one mine visited, a faulty solenoid on a mobile idled the pillar line. The section squeezed and all the mobiles were entrapped. In one district, pillaring can continue with three mobiles; however, mining of the back wing and pushout are prohibited. Eight posts or two cribs are set in lieu of the No. 4 machine. Mobile No. 3 and the posts or cribs are set just outside of the intersection in the crosscut prior to mining the left or right wing. The district's position is that this scenario is safer than setting 3-m (10-ft) timbers, and operators have applauded this decision. In four MSHA districts, mines have approved plans to use only two mobiles in conjunction with timbers. Figure 11 shows mobile and post positioning during back wing removal for an outside lift plan. At least one approved combination mobile/timber plan has been approved for the Christmas tree pillar extraction method. Mobile units 1 and 2 are positioned in the same locations, as shown in figure 11. Two rows of posts on 1.2-m (4-ft) centers are also set so that the roadway width into the push is 5 m (16 ft) or less.

In two districts, plans have been approved that do not require entry breaker posts. To prevent miners from wandering into the gob, one of these districts requires a recoverable, permissible, battery-powered pulsating light to be mounted on a tripod at eye level midway down the entry. The other district requires that at least eight roof bolts on 1.2-m (4-ft) centers be installed in lieu of breakers. These bolts must be at least 0.3 m (1 ft) longer than those installed immediately outby and anchored at least 0.3 m (1 ft) into competent strata. In addition, access to the gobbed-out area must be restricted at the outby end of the unmined pillars by devices, such as chain link fencing, roping, or barrier ribbons. Reflectorized warning streamers, at least 5 cm (2 in) wide by 0.9 m (3 ft) long, are suspended from the roof at or near the restrictive devices. The other districts require the setting of eight entry breaker posts. These breakers are usually knocked out with the mobiles prior to mining the first lifts. Most of the operators expressed dissatisfaction with the requirement that entry breaker posts be installed when using mobiles. They insisted that breakers served no function, especially in competent roof, and that setting breakers subjected mine personnel to unnecessary risk. Two operators who believed that breakers were helpful were mining under weak roof. Their decision was based on previous experiences with the gob overriding the breakers, which necessitated the abandonment of lifts.

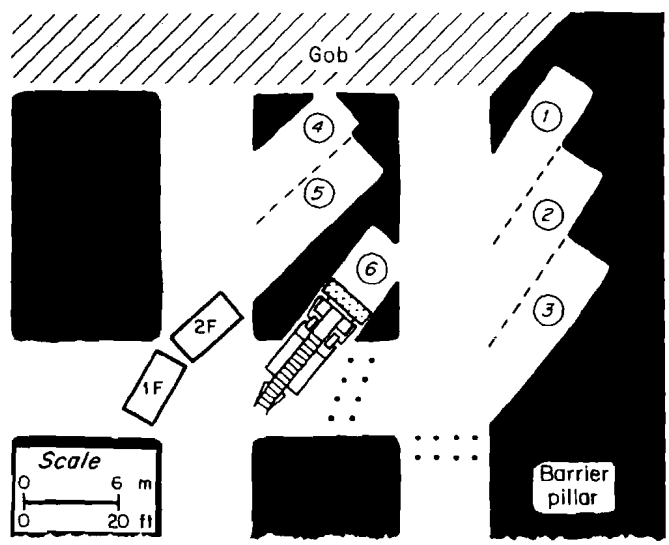

Figure 11.—Combination mobile/timber plan.

SETTING PRESSURES

The active loading capabilities of an MRS can be a significant advantage if properly used. Ideally, the support should be set against the roof with just enough force to close any gaps within the immediate roof structure. Excessive force has damaged the bolted horizon and promoted roof beam failure outby the canopy tip. The Spokane Research Center conducted an extensive field study monitoring MRS and roof bolt loading during pillar extraction [Hay et al. 1997]. Results indicated that adjacent roof bolt loads decreased when the mobiles were pressurized, which was expected. However, when the canopies were lowered, load was transferred to the bolts, and load increases up to 11 kN (2,500 lbf) were recorded. This increase in bolt load did not cause the bolts to yield in this particular mine, but the possibility exists, especially on a pillar line. Hydraulic setting pressures on the instrumented mobiles were normally 10 MPa (1,450 psi).

Setting pressures ranged from 6.9 to 30.3 MPa (1,000 to 4,400 psi) at the mines visited. The support force applied to the roof by an MRS is the product of the hydraulic pressure multiplied by the leg cylinder area. For example, an FMRS with a bore (inside cylinder) diameter of 25.4 cm (10 in) will exert a force of 2,803 kN (315 tons) with a setting pressure of 13.8 MPa (2,000 psi). An ABLS with a bore diameter of 21.8 cm (8.6 in) will require 18.8 MPa (2,730 psi) to provide the same setting force. If the same hydraulic setting pressure is used, the support force is equivalent regardless of the ABLS model or whether the hydraulic cylinders are two- or three-stage [Hatch 1996]. Regarding the FMRS units, the set force is different for two- versus three-stage hydraulic cylinders given the same set pressure [Howe 1996].

Some mines have found that weak shale top can be damaged by high setting forces. Hairline cracks can develop, mechanical bolts can "pop" and fail, and loose rock can become dislodged. At one mine, an MRS operator was injured by spalling shale roof while pressurizing the canopy. The operator was standing close to the machine, and company policy now mandates that MRS operators stand back when the canopy is being set. In addition, the setting pressures were reduced from 13.8 MPa (2,000 psi) to 10.3 MPa (1,500 psi), and no problems have occurred since. It has been recommended that mobile operators periodically check the setting pressure. Pressure bleed-off can occur if the floor is soft or if there is excessive floor gob. If bleed-off occurs, the MRS should be repressurized.

LOADS AND LOADING RATES

Operators cited several factors and conditions that have imposed increased loads on mobiles. In two operations visited, mining had been previously conducted in an upper seam. Excessive machine loading occurred while mining under remnant barrier pillars. Another reported source of mobile loading was underdesigned pillars, which had low stability factors. During retreat mining, pillars are subjected to development, front abutment, and sometimes side abutment loading. If pillars are to be mined safely and efficiently, all anticipated loading conditions should be considered during the design process [Mark and Chase 1997]. MRS loading can also be induced by excessive floor heave.

In general, mobiles operating under weaker shale roof rock have experienced lower loads. Pressure increases after the canopy was set were in the range of 3.4 to 4.1 MPa (500 to 600 psi) and, at this point, the roof normally breaks. Conversely, numerous mobiles operating under massive sandstone roof, which tends to cantilever, have yielded. At one mine visited, mobiles have been used under both sandstone and shale roof rock. The operator stated that, on average, load pressures are 1.4-2.1 MPa (200-300 psi) higher under sandstone roof rock, other factors being equal.

During the mining of a pillar, most of the operators indicated no significant load development on the No. 1 and No. 2 units during the mining of the first few lifts. Hay et al. [1997] monitored increased loads on units 1 and 2 as mining progressed during a lift and as the pillar size was reduced during successive lifts. Operators experienced maximum loading during pushout removal, with pressure increases ranging from 3 to 31 MPa (500 to 4,500 psi). The No. 3 unit sustained the greatest loads and suffered the most damage because of side hits. The No. 4 unit, which is normally situated along an unmined pillar, experienced the least loads and damage. Periodically, some operators switch the No. 3 and No. 4 units. During the mining of the first rows of pillars in a panel, prior to establishing a first cave, most operators reported no significant mobile load development. However, a few operators noted load increases of 2-7 MPa (300-1,000 psi) higher than normal. In order to establish a first cave and minimize outby loading, pillars at these operations are mined as completely as possible,

which included pushout removal. Some of these operators discontinue pushout removal after the first cave.

Technical specialists and operators agree that the critical factor is not the amount of load, but rather the loading rate. Loading rates and magnitudes varied from mine to mine. Most operators commented that the decision to remove section personnel and equipment based on steady, rapid loading conditions is a judgment call based on past experiences. One operator reported that it was time to back out the continuous miner, shut down, and listen when 1.4-2.1 MPa (200-300 psi) pressure increases occurred every 5 min over a 15-min interval. Another operator indicated that if the pressure jumps 1.4 MPa (200 psi) once, and then again, it is time to lower the canopies and tram out because a fall normally always occurs. Other operators cited instances during pushout removal when, in a matter of seconds, 21-28 MPa (3,000-4,000 psi) pressure increases occurred. The continuous miner and personnel were removed, and a fall never occurred. The mobiles later inched their way out. During the mobile field monitoring investigation conducted by Hay et al. [1997], no significant MRS load increase was detected when the canopy of the adjacent mobile was lowered. In other mines, operators noticed immediate increases in the 2-14 MPa (300-2,000 psi) range. Significant load transfer to the adjacent machine can cause it to yield. Whether or not load is transferred is a function of roof geology and the pillars' stiffness. Some operators reported that the pressure gauges seldom showed any change during the mining cycle, and a few operators even observed pressure decreases. No pressure change implies that the force exerted by the roof has not exceeded the setting force applied by the MRS. A decrease in MRS pressure might occur if the machine settled into the floor or roof, or if there was a leak in the hydraulic system.

When mobiles are subjected to consistent load increases, operators practice one of two strategies. Some operators remove section personnel, the continuous miner, and lastly the mobiles prior to the cave. Other operators leave the mobiles in place until after the fall to breaker it off. These operators indicated that when the mobiles start creaking and taking weight, they are performing their function. Even when the yield valves open and the hydraulic fluid is spewing out, these operators insist that it is still not time to lower a canopy. In fact, one of the advantages of an MRS is that it continues to maintain a high support load even though it is yielding. Some operators reported that lowering the canopy removes the support from the roof and allows the roof cave to override the MRS's.

CONCLUSIONS

By replacing roadway, turn, and crosscut breaker posts, MRS usage enhances the safety of section personnel by (1) providing a more effective ground support, (2) reducing worker exposure near the gob edge, and (3) eliminating a major cause of material handling injuries. Compared with wood posts, mobiles provide better roof coverage and improved stability. To achieve the full advantages of mobiles, they must be employed properly. Training and careful attention to standard operating procedures are essential. Through the experience at different mines, strategies have been developed to cope with the hazards posed by hillseams, weak roof, and first falls.

During the later stages of pillar recovery, the area most prone to a roof fall is the intersection. Placement of mobile units 1 and 2 in the intersection during pushout removal enhances roof stability. Positioning of nonessential personnel outby the intersection better ensures their safety.

Mobiles have been employed during full and partial pillar recovery operations. Most pillars are recovered using either the Christmas tree or outside lift method. In some MSHA districts, roof control plans have been approved that do not require breaker posts. A few districts have approved plans that allow pillar extraction with fewer than four mobiles.

Setting pressures in the mines visited ranged from 6.9 to 30.3 MPa (1,000 to 4,400 psi). The most common setting pressure for mobiles is 10 MPa (1,500 psi). In some instances, higher setting pressures have damaged weak shale roof rock. Operators reported that maximum loading occurred during pushout removal. MRS loading is typically higher under sandstone roof rock than shale.

REFERENCES

Barczak TM, Gearhart DF [1997]. Full-scale performance evaluation of mobile roof supports. In: Mark C, Tuchman RJ, comp. Proceedings: New Technology for Ground Control in Retreat Mining. Pittsburgh, PA: U.S. Department of Health and Human Services, Public Health Service, Centers for Disease Control, National Institute for Occupational Safety and Health, IC 9446.

Hatch JW [1996]. Personal communications between J. W. Hatch, Product Manager, Voest-Alpine Mining and Tunneling, Pittsburgh, PA, and F. E. Chase, Pittsburgh Research Center, National Institute for Occupational Safety and Health, Centers for Disease Control, Public Health Service, U.S. Department of Health and Human Services.

Hay KE, Signer SP, King ME, Owens JK [1997]. Monitoring mobile roof supports. In: Mark C, Tuchman RJ, comp. Proceedings: New Technology for Ground Control in Retreat Mining. Pittsburgh, PA: U.S. Department of Health and Human Services, Public Health Service, Centers for Disease Control, National Institute for Occupational Safety and Health, IC 9446.

Howe LC [1996]. Personal communications between L. C. Howe, Product Manager, J. H. Fletcher and Co., Huntington, WV, and F. E. Chase, Pittsburgh Research Center, National Institute for Occupational Safety and Health, Centers for Disease Control, Public Health Service, U.S. Department of Health and Human Services.

Mark C, Chase FE [1997]. Analysis of retreat mining pillar stability (ARMPS). In: Mark C, Tuchman RJ, comp. Proceedings: New Technology for Ground Control in Retreat Mining. Pittsburgh, PA: U.S. Department of Health and Human Services, Public Health Service, Centers for Disease Control, National Institute for Occupational Safety and Health, IC 9446.

Thompson RT, Frederick JR [1986]. Design and field testing of a mobile roof support for retreat mining. In: Proceedings of the 5th International Conference on Ground Control in Mining. Morgantown, WV: West Virginia University, pp. 73-79.

Unrug KF, Tussey IJ, Moore R [1991]. Using mobile roof supports for pillar extraction at Martin County Coal. Min Eng *Oct*:1215-1218.

Vance C Jr., Cybulski JA, Gray WJ [1995]. Report of investigation (underground coal mine): fatal roof-fall accident, Big Branch Mine (ID No. 46-05978), Eastern Mingo Coal Company, Naugatuck, Mingo County, West Virginia. Mount Hope, WV: U.S. Department of Labor, Mine Safety and Health Administration, District 4.

MONITORING MOBILE ROOF SUPPORTS

By Kenneth E. Hay,[1] Stephen P. Signer,[2] Michael E. King,[3] and John K. Owens[4]

ABSTRACT

Researchers from the Spokane Research Center conducted a field study to assess the safety of remotely controlled mobile roof supports (MRS's) in a retreat pillar mining operation. Data were collected to provide the Mine Safety and Health Administration with criteria needed to develop guidelines for MRS use and to determine if precursors could be identified that would alert miners to imminent roof falls.

Two test sites at which two different support methods—MRS's and posts—were used were monitored to obtain information on entry stability. Pressure transducers and string potentiometers were installed on all four MRS's to obtain loading and displacement information. Roof bolt load cells, sonic probes, extensometers, and survey targets were installed in the surrounding entries to obtain information on ground behavior.

Results showed a larger increase in roof bolt loading and roof movement when MRS's were used, especially in the intersection area. Roof bolt loads in the entries showed decreases when the MRS's were set and increases of up to 11.1 kN (2,500 lbf) when the MRS's were unloaded. Unloading of one MRS in a pair did not significantly increase load on the other. MRS's 1 and 2 usually had the higher loads; these loads increased as the pillars on each side were being mined. MRS 3 normally had lower loads than 1 and 2; however, it also experienced some very high loads when in the last position near the pushout. MRS 4 usually had the lowest loads, primarily because it was located near the solid pillar that was not being mined.

[1]Supervisory civil engineer.
[2]Mining engineer.
[3]Electronics technician
[4]Mechanical engineer.
Spokane Research Center, National Institute for Occupational Safety and Health, Spokane, WA.

INTRODUCTION

Mobile roof supports (MRS's) (figure 1), also known as breaker line supports, were developed by the former U.S. Bureau of Mines (USBM) in the 1980's [Thompson and Frederick 1986]. Currently, 2 mining equipment companies manufacture commercial units, and 21 units (4 machines per unit) are in operation in U.S. coal mines. MRS's have been in use in Australia since 1987 [Follington et al. 1992], where they replace posts during full or partial pillar extraction.

MRS's were developed to reduce the high number of injuries and fatalities in retreat pillar mining operations [Chase and Mark 1993]. Most of these accidents occur during the preparation and installation of the required turn and breaker posts used in retreat sections.

The Mine Safety and Health Administration (MSHA) is assessing safety associated with the use of MRS's and has asked us for assistance in establishing guidelines for their use. There is also a need for a method to detect imminent roof failure. Previous methods of using loading on posts and other indicators are no longer applicable when using MRS's.

Use of MRS's requires an understanding of how an active roof support behaves. To further this understanding, the Spokane Research Center conducted a field test in which instruments were installed on four MRS's and in entries surrounding two pillars. One pillar was mined using posts; the other, using an MRS as the support. These instruments included load cells on point-anchor bolts and fully grouted bolts to measure loading and unloading of roof bolt supports, sonic probes to measure displacement in the roof to a depth of 6 m (20 ft), and extensometers and survey targets to measure roof sag. Instruments installed on the MRS's included pressure transducers on all hydraulic lines to measure load on each of the support cylinders and string potentiometers to measure leg closure.

MINE LAYOUT

The field test was conducted at a mine in southwestern West Virginia, where the Lower Cedar Grove Coalbed is being mined. This seam is approximately 2.8 m (10 ft) thick. The Upper Cedar Grove Seam lies 24 to 30 m (80 to 100 ft) directly above the Lower Cedar Grove Seam, and the Hernshaw Seam lies 91 m (300 ft) above. The depth of cover varies from approximately 91 m (300 ft) near the outcrop to over 305 m (1,000 ft).

Figure 1.—Mobile roof supports in operation.

The pillars for the retreat section were developed on 21- by 27-m (70- by 90-ft) centers and 6-m (20-ft) wide entries. Normal roof support consisted of 1.2-m (4-ft) mechanically anchored roof bolts on 1.2-m (4-ft) centers. Breaker posts were still required between the gob and the pillar line.

The test site was located in the second panel being mined with MRS's (figure 2). Each row in the panel had seven or eight pillars, but the number varied depending on whether or not the barrier pillar between the second and first panel had been mined. The test pillars were the third ones from the end of the pillar rows.

The immediate roof is a dark gray shale that contains numerous plant fossils. Its high clay content results in a soft, moisture-sensitive rock with poorly bonded bedding planes. The shale grades upward into a moderately hard, strong sandstone located 1 to 2 m (4 to 6 ft) above the opening.

The pillar recovery method used with the MRS's was "Christmas tree" extraction (figure 3*A*). With posts only, the pillar recovery method was pocket-and-wing (figure 3*B*).

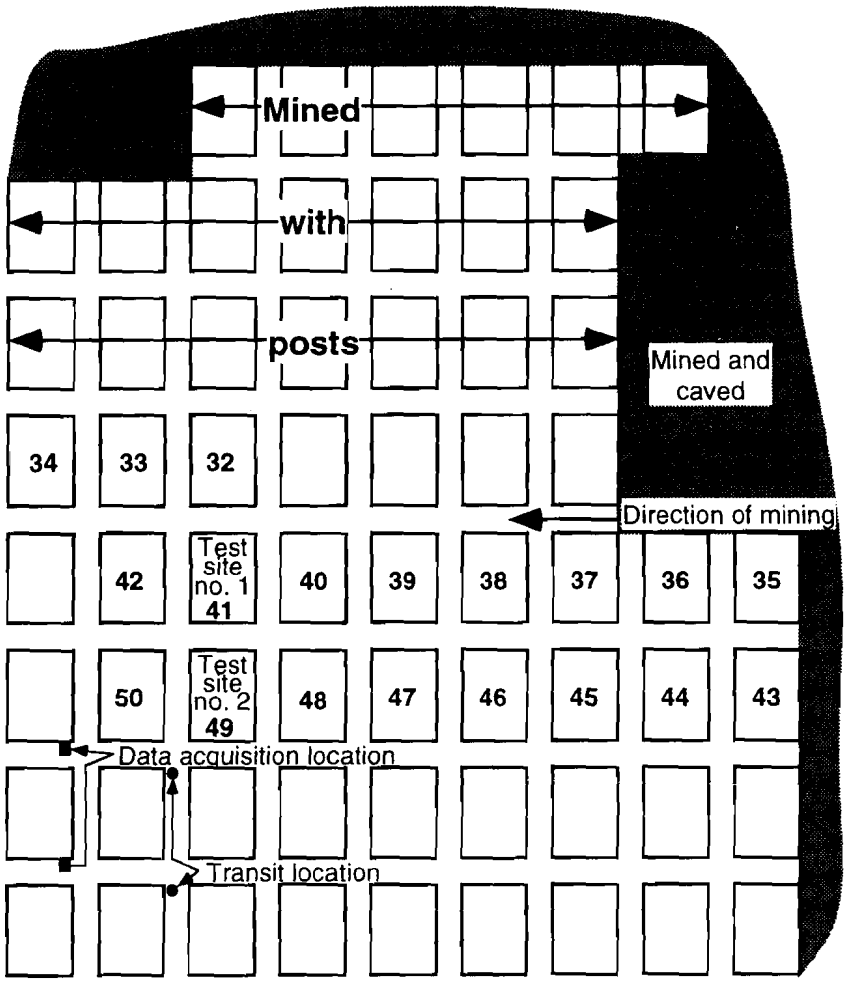

Figure 2.— Retreat panel layout.

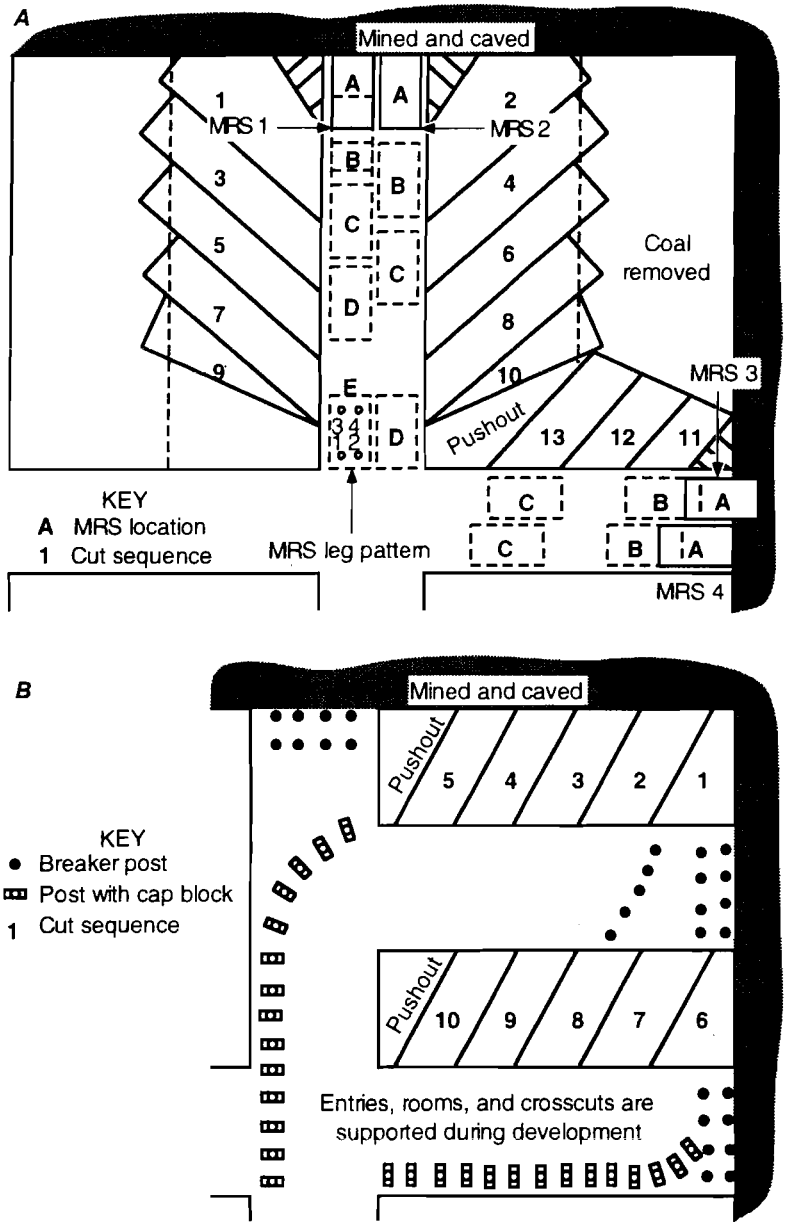

Figure 3.—Mining plan using *(A)* mobile roof supports and *(B)* posts.

MOBILE ROOF SUPPORT INSTRUMENTS

HYDRAULIC PRESSURE TRANSDUCERS

Pressure transducers were installed on the hydraulic lines to obtain information on the loading patterns on each of the four support cylinders, as well as on total loading of each MRS. Displacement devices were also installed to measure leg closure. Results showed that the front and rear hydraulic legs were not consistently set to the same loads, but that similar setting loads occurred in the left and right cylinders of the front and rear legs, which were plumbed together. A dial indicator indicated loading on the front pair and the rear pair of leg cylinders, so that the operator could set the desired load for each pair of cylinders.

During pillar mining in the test area, the hydraulic pressures were normally set at 10,000 kPa (1,450 lbf). Shortly after setting each MRS, the load would decrease on each leg. In one case, on MRS 2, it decreased by approximately 80% of the load (figure 4). This decrease could be attributed to bleed-off of hydraulic pressure, soft roof and/or floor conditions, loose debris (coal and rock) on the floor, transfer of load because of mining, or any combination of these conditions. The data show that the decrease in load became less as the MRS was advanced in the entry. Thus, it would be expected that the load decrease resulted from debris on the floor, because that was the only condition that changed.

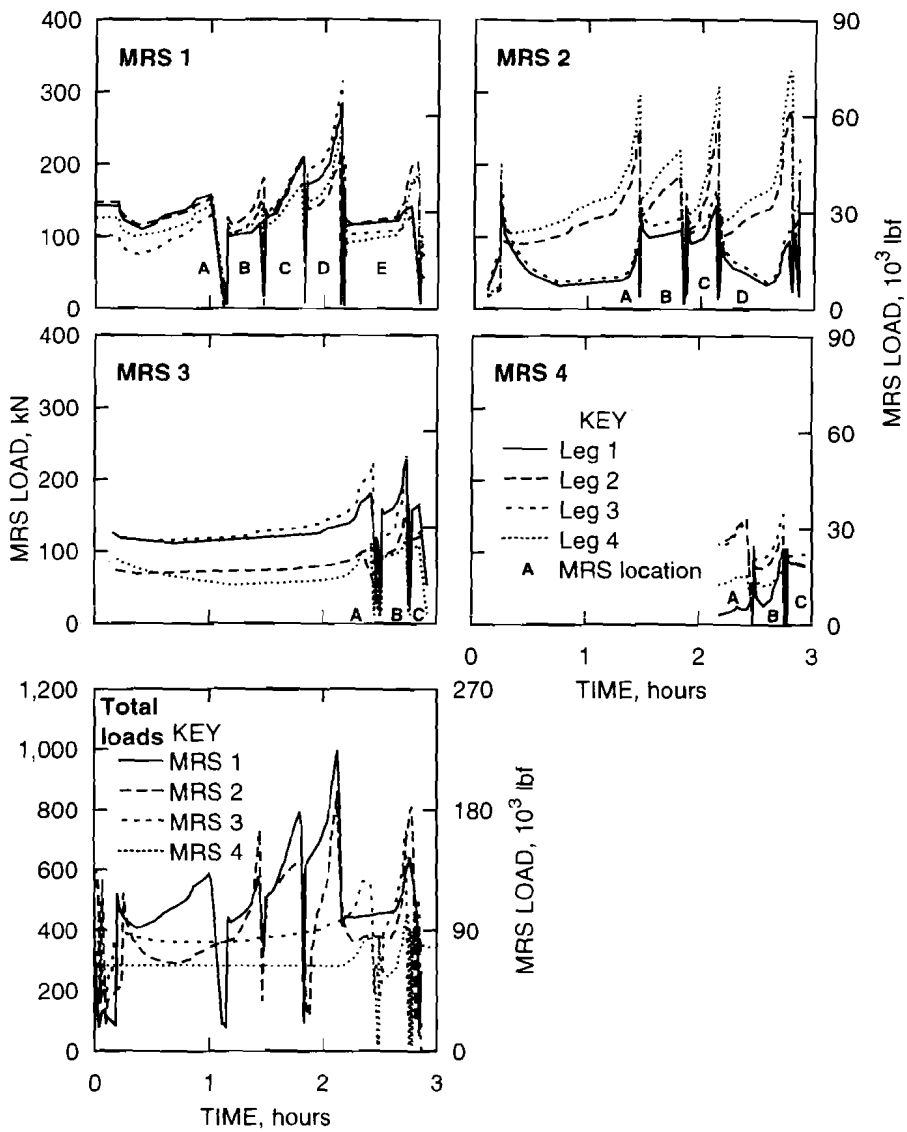

Figure 4.—Loading patterns on mobile roof supports.

The highest loads were attained in the entry with MRS's 1 and 2. Typically, loads on MRS's 1 and 2 increased as mining progressed during a cut and as the pillar size was reduced during successive cuts. The data show that all legs on MRS 1 reached their maximum load at location D in the entry (figure 4). The highest loads were on cylinders 1 and 3, which indicated that loading was greater on the pillar side on the left. On MRS 2, the highest loading occurred at location D in the entry. The highest loads were on cylinders 2 and 4, which were closest to the pillar side on the right. There was no significant increase in loads on MRS's 3 and 4 until the first end cut (6) was being made (figure 3*B*). The maximum loads on MRS's 3 and 4 were almost the same at both the first and second locations. However, on one occasion, while several other pillars were being mined, MRS 3 exceeded the yield load. The instruments were not collecting data at this time. On MRS 3, the highest loads were on cylinders 1 and 3, which were closest to the pillar being mined. MRS 4 had the lowest overall load of the four MRS's.

To determine if unloading of one MRS increased loading on the MRS next to it, loads were compared when MRS 1 was first moved. The unloading of MRS 1 did not increase the load on MRS 2 (figure 5). In evaluating data during other moves of MRS pairs, there were no significant increases in load on one MRS when another was unloaded.

Data were compiled on the MRS loads for a consecutive 7-day period following the first test to identify maximum loads over an extended time (figure 6). Overall, loading was similar to that found at the first test site. MRS's 1 and 2 had higher maximum total loads than MRS's 3 and 4. However, average total loads on MRS 3 were higher than those on MRS's 1 and 2. MRS 4 continued to take less load than the others.

Monitoring of the MRS's continued during most of the panel mining. One month after the first test, another pillar was observed during extraction and was documented in detail to provide information for an analysis of the MRS data. Loading on each of the MRS's was similar to that at the first test site.

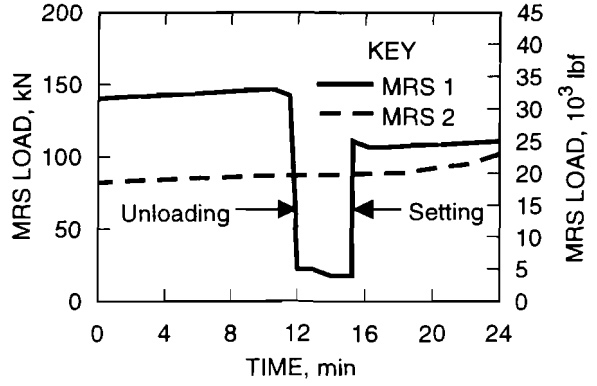

Figure 5.—Effect of MRS 1 unloading on MRS 2.

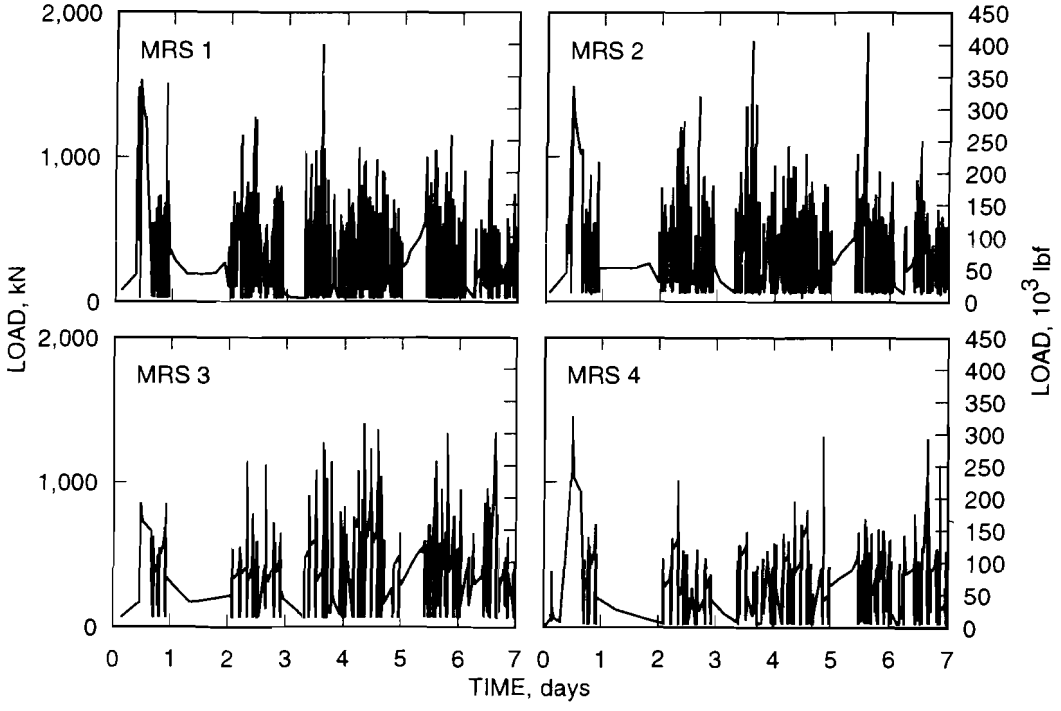

Figure 6.—Total loads on mobile roof supports.

ROOF BOLT LOAD CELLS

Load cells were installed on 1.2-m (4-ft) long, point-anchor roof bolts at 10 locations to determine the impact of MRS setting loads on the roof bolts. These bolts were installed approximately 1 month after normal bolting had been completed. The roof bolts with load cells were centered between existing bolts. Installation tension varied from approximately 25 to 53 kN (5,700 to 12,000 lbf).

These roof bolts were installed in the center of the entry and located between the MRS's at the first MRS set location. During setting of the MRS, the load decreased from about 1.8 to 0.44 kN (400 to 100 lbf) (figure 7). The amount of decrease depended on the position of the MRS's with respect to the position of the roof bolt, the setting load of the MRS at that location, and roof conditions.

During unloading of MRS's 1 and 2 during the first and second moves, load on the roof bolts increased from approximately 1.8 to 3.6 kN (400 to 800 lbf) (figure 8). Similar results were observed when MRS's 3 and 4 were unloaded. This indicates that during unloading, this amount of load was being transferred to the roof bolts. (Note that the monitored roof bolts were installed after the normal bolting cycle; however, it is likely that similar unloading and loading conditions existed on the other roof bolts.) These results confirm that there should be optimum MRS setting loads established that will have the least effect on the existing support and roof strata, yet will still provide adequate support.

The roof bolt load cells showed a significant increase in load when the last lifts were being mined at each test site, from 36 to 48 kN (8,000 to 10,500 lbf) at the MRS site and from 34 to 43 kN (7,500 to 9,500 lbf) at the post site. This increase in load was relative to the load increase on the resin-grouted bolts and roof movement.

ROOF-TO-FLOOR CLOSURE DEVICES (SAGMETERS)

Roof-to-floor closure devices (sagmeters) were installed near the load cells. The purpose was to monitor roof movement and correlate roof-to-floor movement to displacement of the MRS's, as well as to monitor the roof after the MRS's advanced in each of the entries. These readings were then compared with roof movement in the same area when posts had been used.

Results showed a significant amount of closure beginning just prior to moving MRS's 1 and 2 (figure 8) and continuing at a high rate throughout the mining of the pillar. Also, when MRS 1 was moved for the first time, the sagmeters did not show any significant change. This is consistent with figure 5, which shows that the unloading of MRS 1 did not have any effect on the loading of MRS 2. At MRS's 3 and 4, roof response was similar. At the post site, the sagmeters showed a significant rate of movement as the last lift in the first wing was being mined and when mining in the last wing was started.

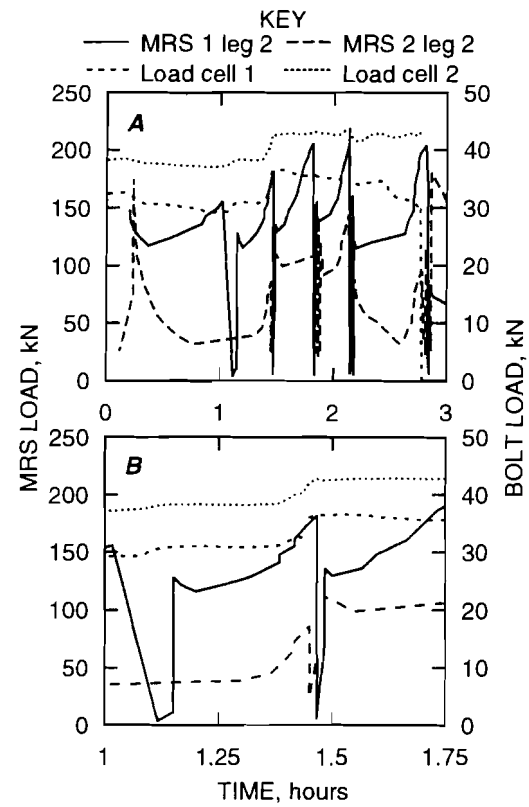

Figure 7.—Loading of MRS 1, MRS 2, and roof bolts for *(A)* entire pillar and *(B)* during one cycle.

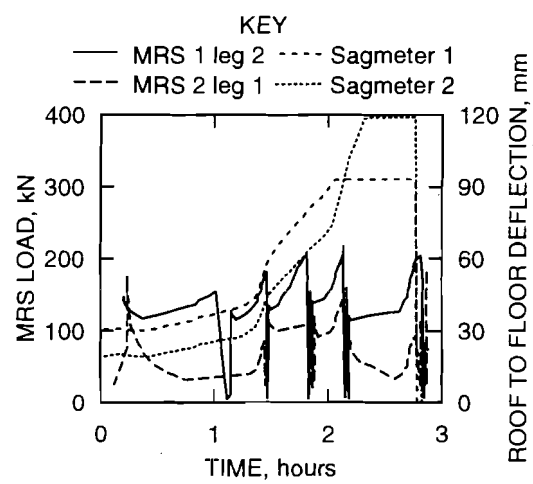

Figure 8.—Loading of MRS 1 and MRS 2, and roof-to-floor closure for entire pillar.

FULL-COLUMN INSTRUMENTED BOLTS

Twelve strain gauges were placed on each of two 1.8-m (6-ft) long, full-column, resin-grouted bolts. One was installed in the center of each of the test site intersections [Signer et al. 1993]. The results showed that strain at both the MRS site and the post site increased rapidly during mining of the last lift (13) and the last wing (10), respectively. Those gauges positioned

135 cm (54 in) above the roof line had exceeded the yield strain. When mining was completed at the test sites, 75% of the strain gauges had exceeded 66% of the yield strain at the MRS site; at the post site, 25% of the strain gauges had exceeded 66% of the yield strain.

SONIC PROBES

Sonic probes were installed to measure roof displacement at increments of 0.3 m (1 ft) to a depth of 6 m (20 ft) above the roof line. One sonic probe was installed in the center of the intersection at each test site. Significantly higher movement was found in the intersection where MRS's were used compared with the intersection where posts were used. Table 1 compares roof movements measured by the sonic probes immediately after the crew completed mining of the pillar and was moving out to the next pillar. There was approximately 4.4 times the amount of movement in the MRS test site, which is consistent with the higher loads recorded on the roof bolts in the intersection area.

Table 1.—Intersection roof displacement

Test site	Movement of roof line with probe end as reference, mm (in)	Maximum separation, mm (in)	Location of maximum separation, mm (in)
Mobile roof support	12.7 (0.500)	3.3 (0.13)	610 (24)
Post	2.9 (0.114)	0.76 (0.03)	914 (36)

SURVEY TARGETS

Survey targets were installed on seven roof bolts and monitored to determine the amount of roof sag in the intersection area at both test sites. From a distance of about 30 m (100 ft), the targets were surveyed with a transit and monitored from the time mining of the pillar was started until mining was completed and miners had left the area. There was only a slight difference between the amount of roof sag at the two sites. The MRS test site showed a slightly higher amount of total roof sag.

SUMMARY AND CONCLUSIONS

1. The location of an MRS is most important during retreat pillar mining. The MRS should be moved as often as possible and kept as close as possible to the continuous miner to reduce the possibility of premature roof caving. It is especially important that the MRS be in the intersection as much as possible to protect miners and equipment, because the results of this test show that the most roof-fall-prone area is the intersection. In this test, the MRS's were not positioned in the intersection.

2. Proper setting loads need to be established to match geologic conditions. It was shown that setting loads were appropriate for the conditions encountered during this test. This conclusion is based on the finding that loads on the roof bolts decreased as the MRS's were set, yet the bolts were still able to support increases in load significantly when the MRS's were released. Other indicators of proper setting loads were that the roof did not break above or around the MRS's and that caving patterns remained the same.

3. There were higher loads on the roof bolts in the intersection area and more roof displacement when MRS's were used. This can be attributed to one or both of the following conditions:

(a) *Type and location of support*: In the MRS test site, MRS's were not positioned in the intersection. In the post test site, posts were installed and left in the intersection.

(b) *Method of mining*: The Christmas tree method was used at the MRS test site, whereas the pocket-and-wing method was used with posts. This may have contributed to some of the difference in roof support loading and displacement.

As stated in item 1 above, the MRS's should be placed into the intersection as much as possible to safeguard miners and equipment.

4. The load loss that occurred immediately after setting the MRS's to the roof can be caused by creep or leaks in the MRS's hydraulic system, soft roof and/or floor conditions, loose coal and rock on the floor, setting pressures that are too high (which causes creep in the roof and floor), or load transfer as a result of mining. A test of the MRS determined that creep was not a significant factor in the MRS system. Of the remaining possibilities, the greatest loss of load would likely be caused by loose coal and rock on the floor, because the loss of load was very rapid immediately after setting. To eliminate this possibility, it is important to clean the floor prior to setting an MRS. This can be done with a continuous miner or the dozer blades on the MRS.

5. A major advantage to using an MRS is that mine personnel no longer need to go into hazardous areas in entries or intersections to install supports as they do when setting posts. Dial gauges are installed on all MRS's to establish setting pressures and to indicate how the MRS's are loading up. Some of this improvement in safety is jeopardized when MRS operators must get close to the MRS to read the dial gauges while they are setting the machine or determining how the MRS's are being loaded. Larger, more visible gauges should be installed to eliminate the necessity of approaching the MRS to read the gauges.

6. Research is continuing to establish optimum setting loads for a variety of conditions, define precursors to roof caving, investigate possible combinations of MRS's and other types of supports, and improve safety when using MRS's.

REFERENCES

Chase FE, Mark C [1993]. Ground control design for pillar extraction. Soc Min Eng preprint 93-282.

Follington IL, Trueman R, Medhurst TP, Hutchinson IN [1992]. Continuous monitoring of mechanized breaker line supports to investigate roof and pillar behavior. In: Proceedings of the 11th International Conference on Ground Control in Mining. Wollongong, New South Wales, Australia: University of Wollongong, pp. 345-357.

Signer SP, Mark C, Franklin G, Hendon G [1993]. Comparisons of active versus passive bolting in bedded mine roof. In: Proceedings of the 12th International Conference on Ground Control in Mining. Morgantown, WV: West Virginia University, pp. 16-23.

Thompson RT, Frederick JR [1986]. Design and field testing of a mobile roof support for retreat mining. In: Proceedings of the 5th International Conference on Ground Control in Mining. Morgantown, WV: West Virginia University, pp. 73-79.

APPENDIX.—LOAD RATE MONITORING SYSTEM

Two pressure gauges mounted on each MRS were monitored continually by mine personnel to determine loads and loading rates on the machines. This loading information is used by MRS operators to determine when to cease mining operations and/or remove miners and equipment from an area before a dangerous fall occurs. The dial gauges could be difficult to read, requiring the MRS operator to approach the MRS to monitor the gauges. Spokane Research Center personnel and equipment manufacturers are currently cooperating in the development of a load rate monitoring (warning) system for the MRS that can be easily seen by all miners in the vicinity of the MRS. The system monitors dynamic loading on the MRS and activates green, amber, and red warning lights on the canopy near the dial gauges. Each light represents a different loading rate on the machine.

The system uses a dedicated embedded processor to monitor pressure inside the four hydraulic jacks associated with the MRS. Loading is proportional to the internal pressure and the surface area of the piston head of the hydraulic cylinder and is determined by the formula

$$F = A \times P, \qquad \text{(A-1)}$$

where F = force in pounds,

A = area, in^2,

and P = pressure, psi.

The embedded processor reads changes in cylinder pressure through four multiplexed data acquisition channels and converts these pressure changes to load rates, which are then displayed by the three load rate indicator lights.

External components of the load rate monitoring system are shown in the back row in figure A-1. From left to right, the components are pressure transducers and connecting cables for monitoring the internal pressure in the hydraulic cylinders; an explosion-proof, MSHA-approved container that houses the internal components of the system; and three colored fluorescent load rate indicator lights with magnetic mounting bases.

The internal components of the explosion-proof container are shown in the foreground of figure A-1. From left to right, these components are the power supply for the internal components, the embedded processor and associated control program, the solid-state control relays for the lights, and intrinsically safe power supplies and barriers for the external components.

As an integrated package, these components can be retrofitted into existing MRS equipment. Further underground studies of MRS loading histories will be performed to determine critical load rate settings for the system and to evaluate its performance.

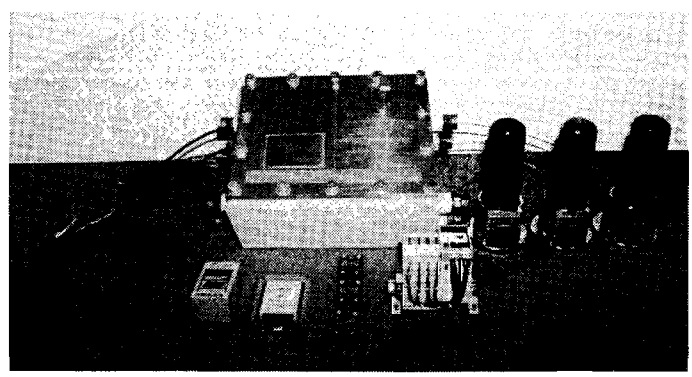

Figure A-1.—Load rate monitoring system components.

FULL-SCALE PERFORMANCE EVALUATION OF MOBILE ROOF SUPPORTS

By Thomas M. Barczak[1] and David F. Gearhart[2]

ABSTRACT

Two mobile roof supports (MRS's), one manufactured by J. H. Fletcher and Co. and one manufactured by Voest-Alpine Mining and Tunneling, were evaluated under controlled load conditions in the Strategic Structures Testing Laboratory at the Pittsburgh Research Center. A unique load frame, called the mine roof simulator, provided a realistic simulation of mining conditions by inducing vertical, horizontal, and lateral loading on the support. The purpose of these tests was to determine the performance capabilities and limitations of the supports and to investigate factors that influence the measurement of loading and loading rate. An evaluation of the support design and load conditions that can cause support failure or loss of support capacity is presented relative to the laboratory tests. In general, lateral loading perpendicular to the longitudinal axis of the canopy is most severe, although horizontal loading in the direction of the longitudinal axis of the canopy can also produce critical loading is some cases. The tests indicate that both setting force and leg pressure measurement are influenced by the staging of the leg cylinders. The implications of these factors on load rate measurement are evaluated. Differences in design philosophy between the two supports are identified and related to support performance. The difference in leg design, two- versus three-stage, had the most impact on support performance. Safety issues pertaining to support operation and maintenance are also discussed. Lastly, MRS capacity and stiffness characteristics are compared with those of conventional timber supports.

[1]Research physicist, Pittsburgh Research Center, National Institute for Occupational Safety and Health, Pittsburgh, PA.
[2]Project engineer, SSI Services, Inc., Pittsburgh, PA.

INTRODUCTION

Mobile roof supports (MRS's) have improved the safety of pillar extraction during secondary mining by providing superior roof control and significantly reducing the materials handling associated with timber posts in pillaring operations. The superior capabilities of the MRS's have promoted pillar extractions in conditions such as weak roof and floor geologies prone to unpredictable caving that were previously too dangerous when using timber posts.

Since the introduction of MRS's in the United States in 1988, MRS technology has matured, with installations in more than 40 coal mines. Overall, MRS's have experienced widespread success. Few failures have been reported; these are typically attributed to lack of operating experience or severe conditions, such as those associated with the first or large areas of caving strata. Only one fatality has occurred on a mobile section; however, the fatality was not attributed to failure of the mobile supports. Nevertheless, some questions arose during the fatality investigation in 1995 regarding the performance capabilities of MRS's and the capability to assess ground instabilities from MRS loading.

In an effort to evaluate their support design, but unrelated to the fatality investigation, the two manufacturers of MRS's, J. H. Fletcher and Co., Huntington, WV, and Voest-Alpine Mining and Tunneling (VAMT), Pittsburgh, PA, made arrangements to have their supports tested at the Pittsburgh Research Center. One support from each manufacturer was evaluated at the Center's Strategic Structures Testing Laboratory through full-scale testing in the unique *mine roof simulator* load frame. Although the supports that were tested are similar in operating range and capacity, the Fletcher support utilized three-stage leg cylinders, whereas the VAMT support utilized two-stage leg cylinders. This difference in leg design should be considered when making comparisons of support performance, particularly the stiffness of the support.

A series of tests was conducted under controlled load conditions, which provides a better understanding of the performance capabilities and limitations of MRS's and factors that influence the measurement of loading and loading rate. This paper presents the results of these laboratory studies and compares differences in design philosophies and evaluates their impact on support performance. The supporting capabilities of MRS's is compared with those of conventional timber posts and cribs. Safety issues relative to support maintenance and operation are also discussed.

STRATEGIC STRUCTURES TESTING LABORATORY

The Strategic Structures Testing Laboratory is a unique laboratory where full-scale mining equipment and roof support structures can be tested in a controlled environment. Figure 1 shows an MRS in the laboratory's mine roof simulator load frame. This unique load frame is designed to simulate the loading induced on support structures due to the behavior of rock masses during mining. The load frame can provide controlled roof and floor movements to simulate the closure of the mine opening while generating up to 13,334 kN (3 million lb) of vertical force and 7,117 kN (1.6 million lb) of horizontal (shear) force.

The test procedure for the MRS evaluation was as follows:

1. The MRS was positioned in the proper orientation to allow the load frame to induce vertical, horizontal, or lateral loading on the support.
2. The MRS was actively set against the load frame platens using the internal hydraulic power to establish the initial load condition.
3. Subsequent loading was applied by controlled displacement of the load frame's lower platen to simulate closure of the mine entry. Three different load vectors were evaluated through applied vertical, horizontal, and lateral displacements, as depicted in figure 2.
4. The support response to the applied loading was measured through strain gauges and pressure transducers

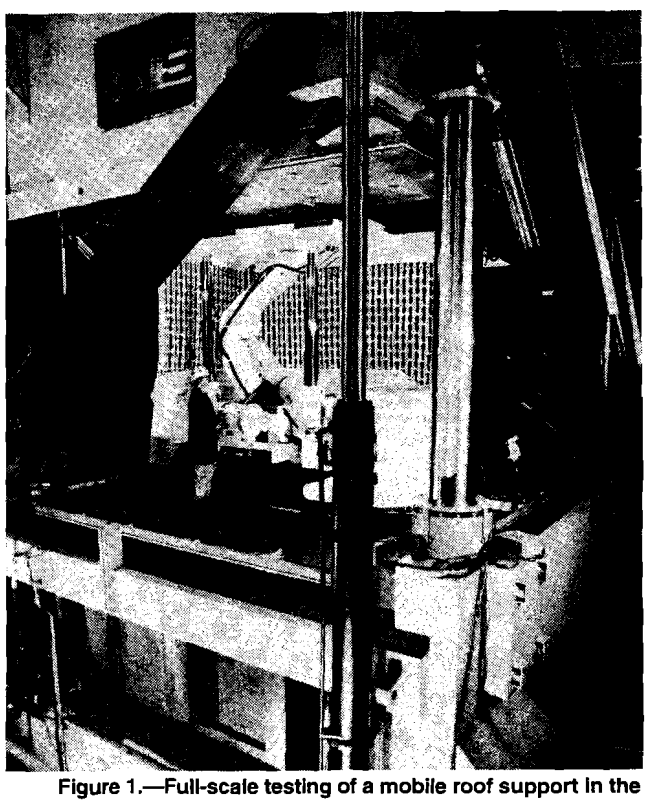

Figure 1.—Full-scale testing of a mobile roof support in the unique mine roof simulator load frame.

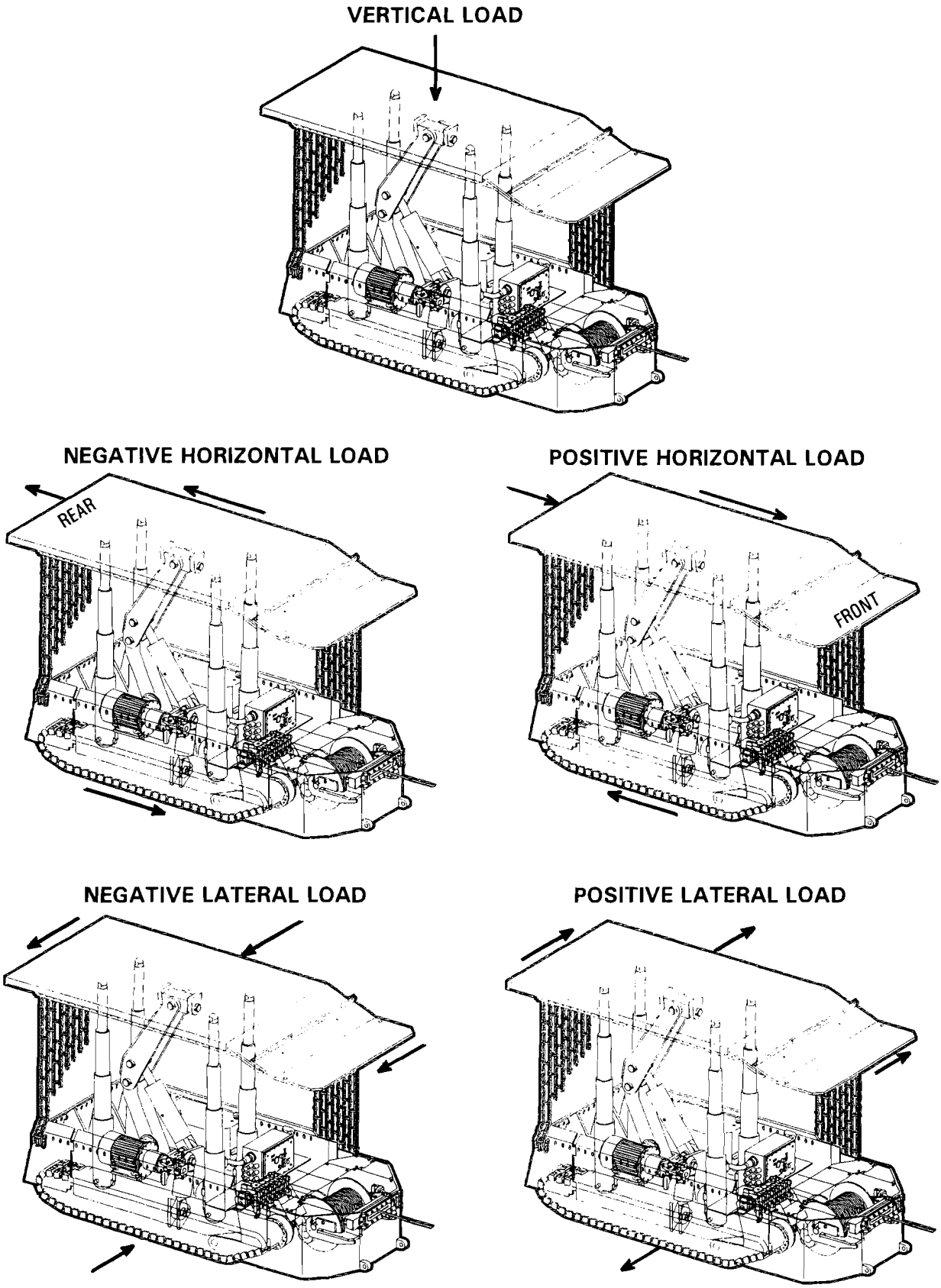

Figure 2.—Vertical, horizontal, and lateral loading applied to the mobile roof supports by the mine roof simulator.

installed on the various MRS components. A typical instrumentation arrangement is shown in figure 3.

Parameters investigated included (1) setting pressure, (2) support height, (3) load vector (direction of loading), and (4) canopy contact configuration. Additionally, a variety of eccentric crawler frame contact configurations were evaluated with the Fletcher support. The testing effort focused on the following studies:

1. *Rated support capacity:* Determination of maximum support capacity in relation to the support's rated design capacity.

2. *Stiffness characteristics:* Measurement of support resistance and component responses to roof movements in the vertical, horizontal, and lateral directions.

3. *Setting force:* Evaluation of setting force as a function of leg staging and hydraulic pump pressure.

4. *Load and load rate measurement:* Evaluation of factors that affect the measurement of roof load and loading rate.

5. *Conditions that reduce support capacity:* Identification of load conditions that reduce support capacity.

6. *Critical load conditions:* Identification of load conditions that maximize component loading and those that produce critical loading where the structural integrity of the supports could be jeopardized.

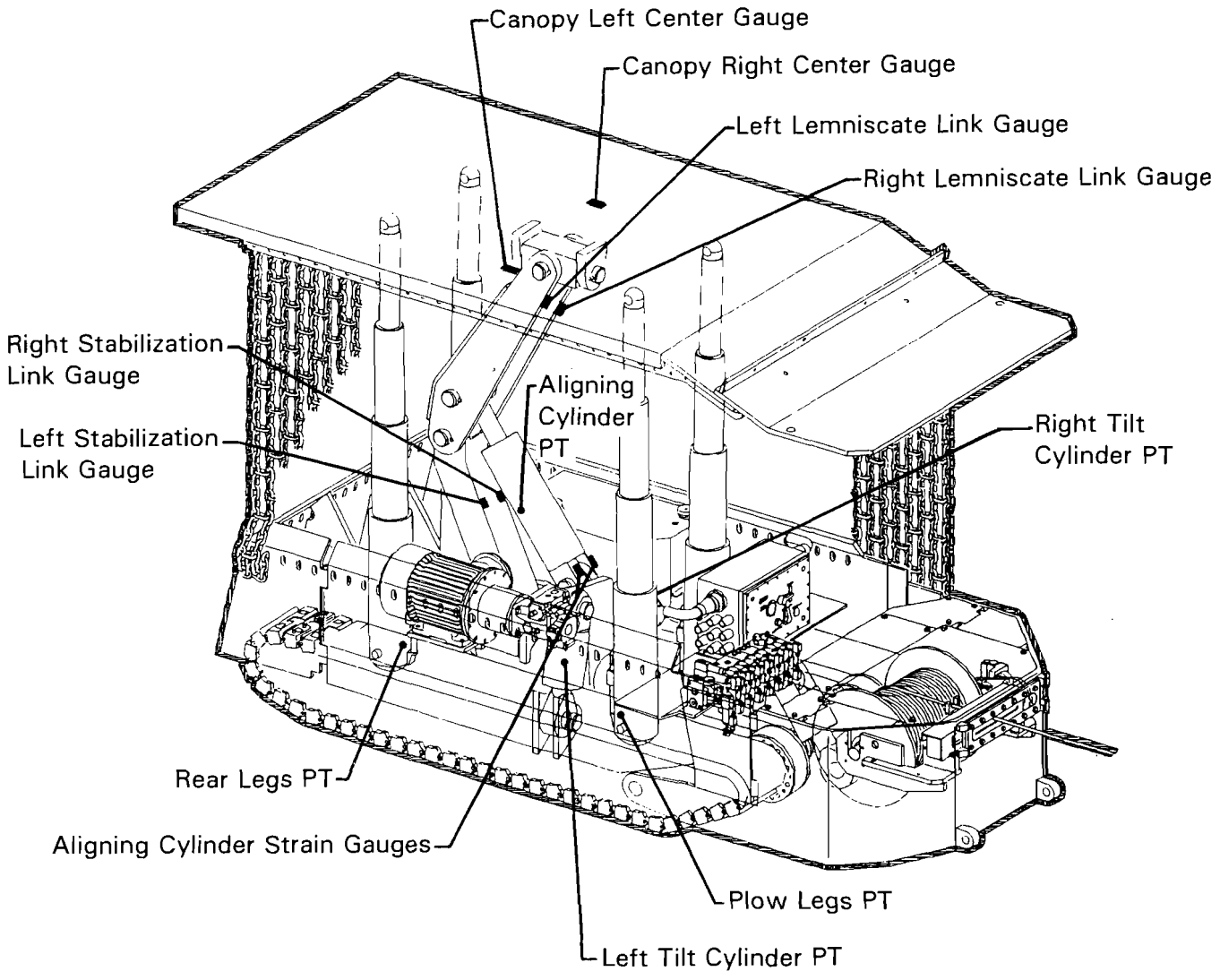

Figure 3.—Instrumentation installed on the VAMT support to assess support performance. PT = pressure transducer.

MOBILE ROOF SUPPORT DESCRIPTION AND BASIC DESIGN PHILOSOPHIES

The VAMT support tested during this study was a model 185/380-540. The Fletcher support was a model MRS-13 with 1.45 m (57 in) to 3.71 m (146 in) operating height. These support designs are representative of the support philosophies of the two manufacturers, although both manufacturers offer a variety of machines and designs to operate in mining heights ranging from 1.17 m (46 in) to 3.96 m (13 ft).

The similarities in support design for the two supports evaluated in this study are as follows:

- Both supports were rated at 5,338 kN (600 tons) of support capacity and designed to operate in high seams at heights up to 3.81 m (12.5 ft). The maximum capacity is controlled by hydraulic yielding of the leg cylinders.
- The canopy is connected to the base frame by four hydraulic leg cylinders and a lemniscate assembly. The hydraulic cylinders provide the (vertical) support capacity or resistance to roof-to-floor convergence. The lemniscate assembly acts to minimize horizontal canopy movement during raising and lowering of the support and provides resistance to horizontal and lateral loading.
- The connection of the lemniscate assembly to the canopy is articulated to permit pitch and roll rotations of the canopy independent of the lemniscate assembly to allow full contact in uneven roof and floor conditions.
- An internal hydraulic power supply provides active setting of the support against the mine roof and floor with independent control of the front and rear legs.
- Ground contact is established through the crawlers with the crawler frame designed to support the full 5,338 kN (600 tons) of roof load.

There are four significant differences in design philosophy between the two supports tested: (1) a flat-plate canopy construction versus a sloped-edge canopy construction, (2) a tilt-frame lemniscate assembly versus a rigid link lemniscate assembly, (3) internal versus exposed lemniscate assembly, and (4) a two- versus a three-stage leg cylinder design.

The Fletcher support utilized a canopy construction that is sloped at the edges, whereas the VAMT support utilized a flat-plate canopy design. The rationale for Fletcher's sloped-edge design is to accommodate edge and point loading with reduced deflection and stress at full load. The sloped edges are also intended to facilitate moving the support in uneven or jagged roof strata. A result of this design is increased canopy stiffness as the edge plates reduce the size and significantly stiffen the top canopy plate. The flexibility of the flat-plate canopy utilized in the VAMT support is illustrated in figure 4, where deflections as great as 7.6 cm (3 in) were observed over the length of the VAMT canopy when the support was loaded with a single contact placed near the canopy tip. The flat-plate concept typically provides greater roof coverage due to roof contact across the full width and length of the canopy structure. However, the greater roof contact will not necessarily translate into larger support loads, since the roof typically behaves as some sort of beam with support loading controlled by roof displacements and not the dead weight of the rock mass. The larger canopy can result in higher stress developments due to greater bending moments when the canopy is not uniformly loaded.

Another major design difference pertained to the lemniscate assembly. The VAMT support utilized a lemniscate assembly connected to a tilt frame that permits single degree-of-freedom rotation of the lemniscate assembly due to lateral loading (see figure 5). The rotation is controlled by hydraulic cylinders called tilt cylinders. This design minimizes stress development in the lemniscate assembly due to lateral loading, but allows lateral translation of the canopy once the yield pressure of the tilt cylinders is reached. The Fletcher MRS as tested did not incorporate a tilt frame for the lemniscate assembly and relies on the strength of the lemniscate structure and connecting joints to resist lateral loading. The consequence of this design is significantly larger stress development in the lemniscate assembly due to lateral loading; however, the lateral translation of the canopy as a function of applied load is less than that of the VAMT tilt-frame design, particularly when the yield pressure of the tilt cylinders is reached.

The VAMT support also utilized a hydraulic cylinder, called an aligning cylinder (see figure 6), for the top lemniscate link, versus a rigid steel link in the Fletcher support. The aligning cylinder limits horizontal load development, thereby minimizing stress development in the lemniscate assembly due to horizontal loading. When yield pressure is reached, the aligning cylinder yields through a 60-mm (2.4-in) stroke, permitting an equivalent horizontal displacement of the canopy relative to the base. When the rear legs are retracted, the aligning cylinder returns to its initial stroke and restores the canopy to its initial horizontal position.

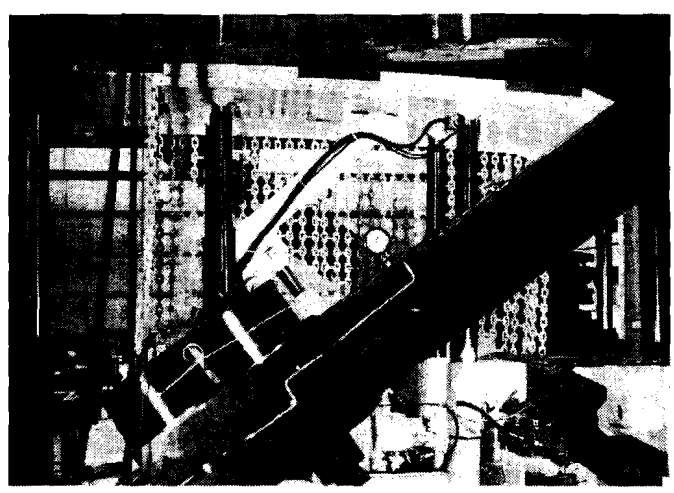

Figure 4.—Deflection of the VAMT canopy under partial contact loading.

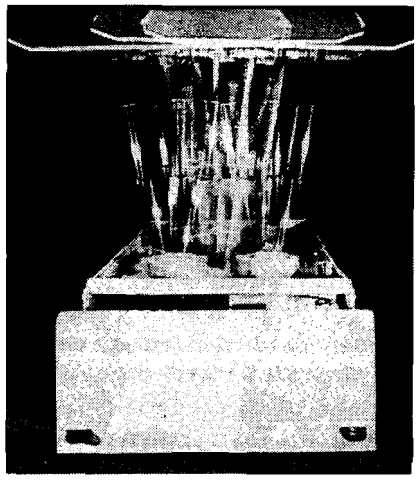

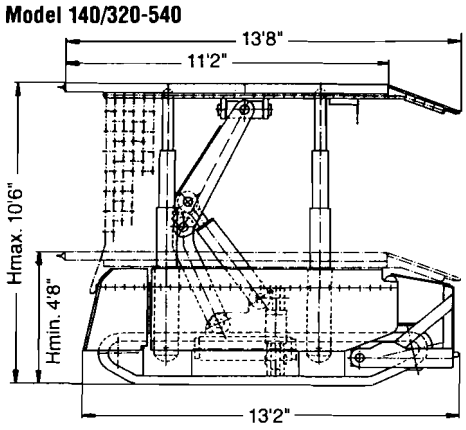

Figure 5.—Tilt-frame lemniscate assembly utilized on the VAMT support.

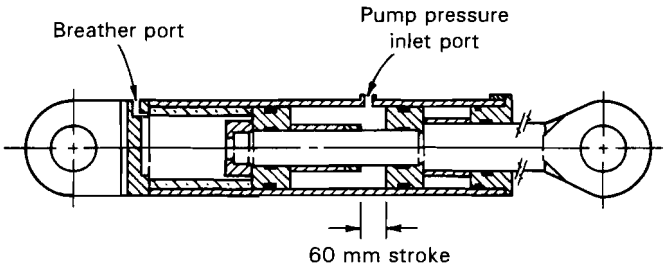

Figure 6.—Aligning cylinder designed to control horizontal loading on the VAMT support.

The position of the lemniscate assembly also differed for the two supports tested. The caving shield protruded beyond the rear of the canopy in the Fletcher support, whereas the entire lemniscate assembly was internal (within the confines of the canopy) on the VAMT support. The VAMT support utilized a chain curtain to resist gob flushing into the support. Fletcher contends that the external position of the caving shield provides increased protection to machine components from gob material and can act as a wedge to help to push the support from heavily caved areas. The exposed caving shield can also cause additional loading on the lemniscate assembly due to gob loading.

The Fletcher support that was tested utilized three-stage leg cylinders, as opposed to two-stage leg cylinders in the VAMT support. The rationale for the three-stage design is to enhance operating range. A consequence of the three-stage design is larger diameter leg cylinders, which impacts the operating pressure and several performance parameters, as described later in this paper.

ASSESSMENT OF LABORATORY TEST RESULTS

MAXIMUM SUPPORT CAPACITY

The maximum support capacity is controlled by hydraulic yielding of the leg cylinders, with a yield valve controlling the maximum pressure in the *bottom* stage of the leg cylinders. Normally, the left and right legs in the front and rear set are hydraulically connected together. As a result, the yield valve with the lowest operating pressure will control both legs in the set. The yield pressure required to provide a designated support capacity is a function of the effective area of the bottom stage of the leg cylinder. For example, the required yield pressure to produce 5,338 kN (600 tons) of support capacity was 26.3 MPa (3,820 psi) for the Fletcher support and 36.3 MPa (5,263 psi) for the VAMT support. This difference is due to the difference in leg diameters: 25.4 cm (10 in) for the Fletcher and 21.8 cm (8.6 in) for the VAMT support. The measured yield settings were approximately 38.4 MPa (5,575 psi) for the VAMT support, providing a maximum support capacity of 5,649 kN (635 tons), and 27.6 MPa (4,000 psi) for the Fletcher support, providing a maximum support capacity of 5,604 kN (630 tons).

STIFFNESS CHARACTERISTICS

Stiffness is a measure of how much roof movement is required to produce load resistance in the support. The stiffness characteristics of the support are evaluated for vertical, horizontal, and lateral displacements of the canopy relative to the base. Horizontal and lateral displacements are imposed in both a positive and negative direction (see figure 2). A comparison of the vertical, horizontal, and lateral stiffness at a 2.4-m (96-in) operating height is presented in table 1. As seen in the table, both supports are much stiffer vertically than horizontally or laterally; this means that much more roof movement is required to produce equivalent support resistance to the applied displacement in the horizontal or lateral direction than for roof-to-floor convergence. It should also be noted that the initial horizontal and lateral stiffness of the support is

sensitive to translational freedom in the various joints of the lemniscate assembly and the gear train of the crawler drive assembly. The stiffnesses shown in table 1 represent the support response once this translational freedom has been removed.

Table 1.—Comparison of support stiffness at a 2.4-m (96-in) operating height

Load vector	Support stiffness, kN/cm (kips/in) [1]	
	VAMT support [2]	Fletcher support [3]
Vertical displacement	3,002 (1,714)	2,140 (1,222)
Horizontal displacement [4] . . .	[5]271 (155); [6]137 (78)	315 (180)
Lateral displacement	[7]91 (52)	[8]137 (78); [9]39 (22)

[1]Stiffness measured when no leg stage is fully extended.
[2]Two-stage leg cylinder support design.
[3]Three-stage leg cylinder support design.
[4]Horizontal stiffness shown for horizontal displacement toward the plow of the support.
[5]Initial stiffness prior to pressure development in the aligning cylinder.
[6]Stiffness after aligning cylinder begins to develop pressure.
[7]Initial stiffness prior to yield of tilt cylinders. Load applications that would produce yielding of the tilt cylinders were not evaluated.
[8]Initial stiffness during first 1.3 cm (0.5 in) of lateral movement.
[9]Stiffness beyond initial 1.3 cm (0.5 in) of lateral movement.

Vertical Stiffness

Vertical stiffness is a measure of support resistance to roof-to-floor convergence. It is controlled almost entirely by the stiffness of the hydraulic leg cylinders. Vertical stiffness depends on the height of the support and decreases with increasing height (figures 7*A* and 7*B*). Therefore, the supporting force at a high operating height will be less than at a lower operating height for the same roof-to-floor convergence. Using the VAMT support as an example, the supporting force at a height of 3.8 m (148 in) is only 38% of the supporting force at a height of 2.4 m (96 in) for the same roof-to-floor convergence.

When none of the leg stages are fully extended, the support stiffness is constant from set to yield, and the setting pressure does not have a significant effect on the support stiffness. When the support is set with the bottom stage fully extended, the support capacity as a function of displacement is bilinear. The initial stiffness is high, since the effective column length is reduced to that of the upper stage of the leg cylinders, and decreases once the upper stage force exceeds that of the lower stage *setting* force. An example for the VAMT support with two-stage leg cylinders is shown in figure 8*A*, where the stiffness decreases at about 4,226 kN (950 kips) of loading, which is where the bottom stage is dislodged from its mechanical stop when set at 28.96 MPa (4,200 psi) setting pressure. Figure 8*B* shows an example of the change in stiffness for a Fletcher support with three-stage leg cylinders when both the bottom and middle stages were fully extended. The initial stiffness was reduced when the top stage force exceeded the setting force of 2,829 kN (636 kips) developed in the second stage.

As expected, the VAMT support was stiffer in response tovertical loading than the Fletcher support (see table 1). This is primarily due to the two-stage leg cylinder design in the VAMT support, compared with the three-stage leg cylinder design in the Fletcher support. All other things being equal, a three-stage leg cylinder will *always* be less stiff than a two-stage leg cylinder, because the stages act in series with the equivalent stiffness reduced as the number of stages increases, as shown in equation 1 for a three-stage leg cylinder. Equation 1 also indicates that the equivalent stiffness is never greater than the least stiff member. The stiffness of individual stages is governed primarily by the area and stroke of the cylinder, decreasing in stiffness as the area decreases or the stroke increases. Thus, the stage with the smallest diameter will be the least stiff stage and is likely to control the equivalent stiffness of the entire leg:

$$\frac{1}{K_E} = \frac{1}{K_1} + \frac{1}{K_2} + \frac{1}{K_3}, \qquad (1)$$

where K_E = equivalent stiffness of the leg cylinder,

K_1 = stiffness of stage 1,

K_2 = stiffness of stage 2,

and K_3 = stiffness of stage 3.

When both supports are set at the same leg *pressure*, they will reach yield load at nearly the same displacement. For example, with a setting pressure of 17.3 MPa (2,500 psi) at the 2.4-m (96-in) operating height, the VAMT support will reach yield load (5,338 kN (1,200 kips)) after 0.94 cm (0.37 in) of roof-to-floor convergence, compared with 0.86 cm (0.34 in) for the Fletcher support (see figure 9). However, when set to the same setting *force*, the Fletcher support will require 40% more displacement to reach yield load (see figure 10).

Horizontal Stiffness

Horizontal stiffness is a measure of support resistance to forward or rearward displacements of the canopy relative to the base. The action of the lemniscate assembly primarily controls the horizontal stiffness of MRS's, since the leg cylinders are nearly vertical and do not provide much resistance to horizontal loading. Horizontal stiffness is at least an order of magnitude less than the vertical support stiffness.

As previously indicated, the initial horizontal stiffness is controlled by translational freedom in the connecting joints of the lemniscate assembly and gear train of the drive motors. For example, up to 1.91 cm (0.75 in) of horizontal displacement of the canopy relative to the base was required in the VAMT support before any significant load resistance was generated. The horizontal stiffness of the support is also height-dependent, decreasing at increasing heights, as shown in the example in figure 11 for the Fletcher support.

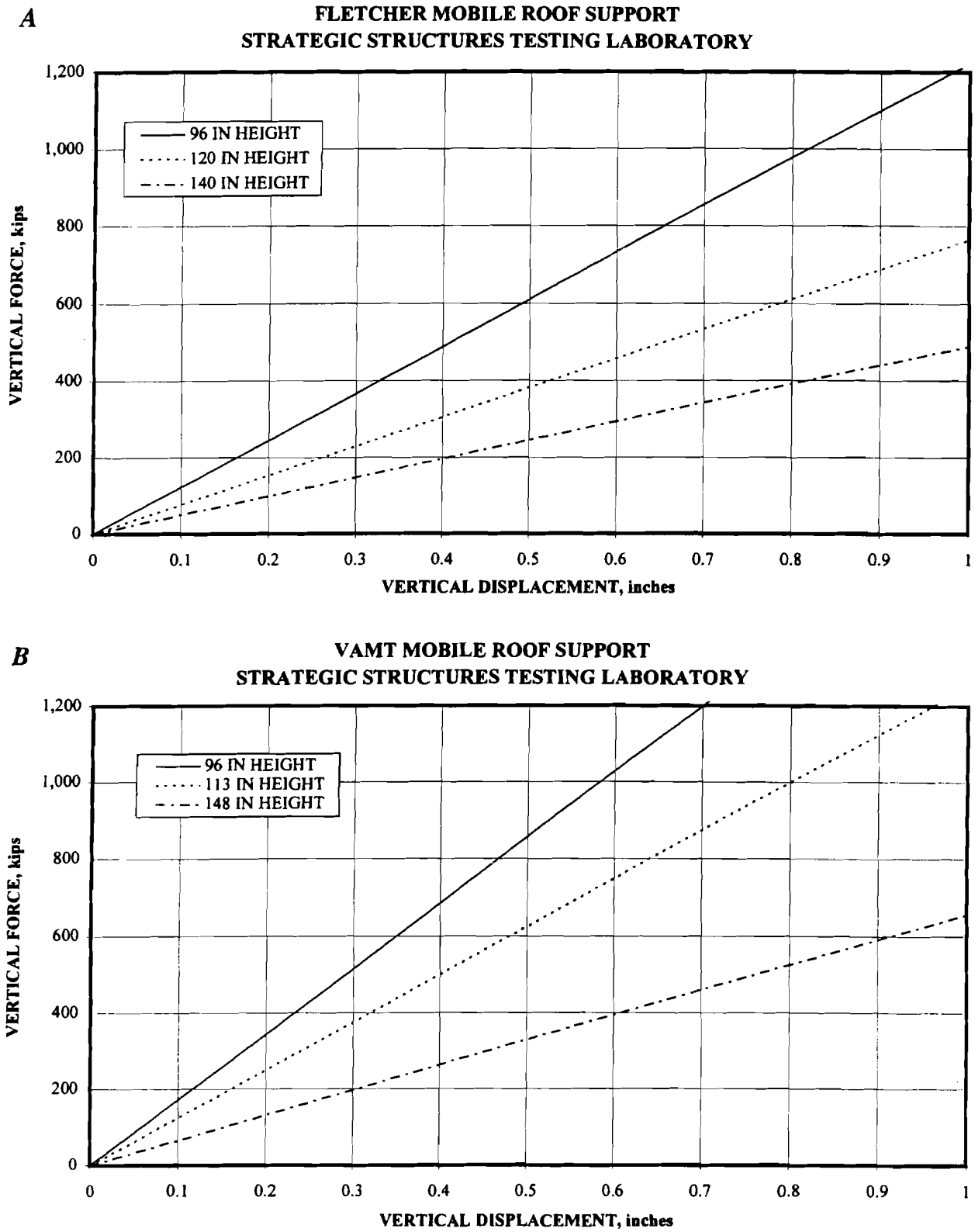

Figure 7.—Effect of support height on vertical stiffness. *A*, Fletcher support; *B*, VAMT support.

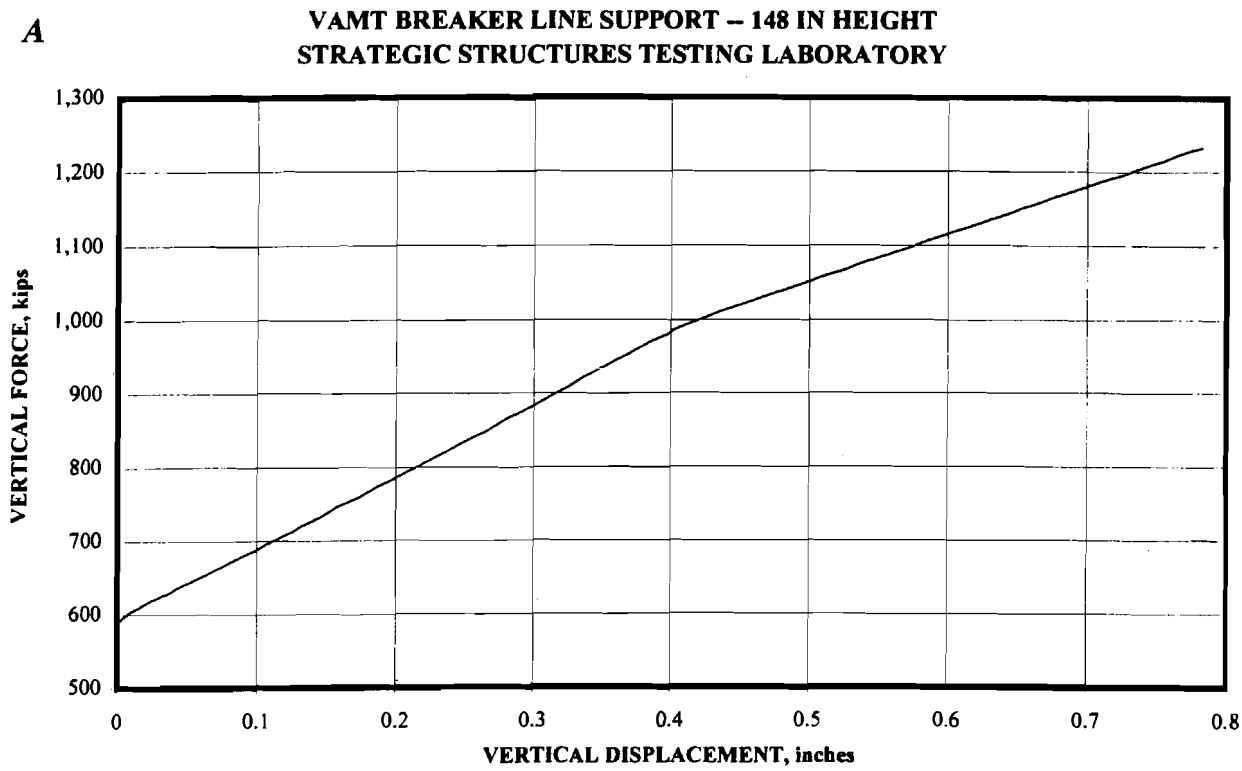

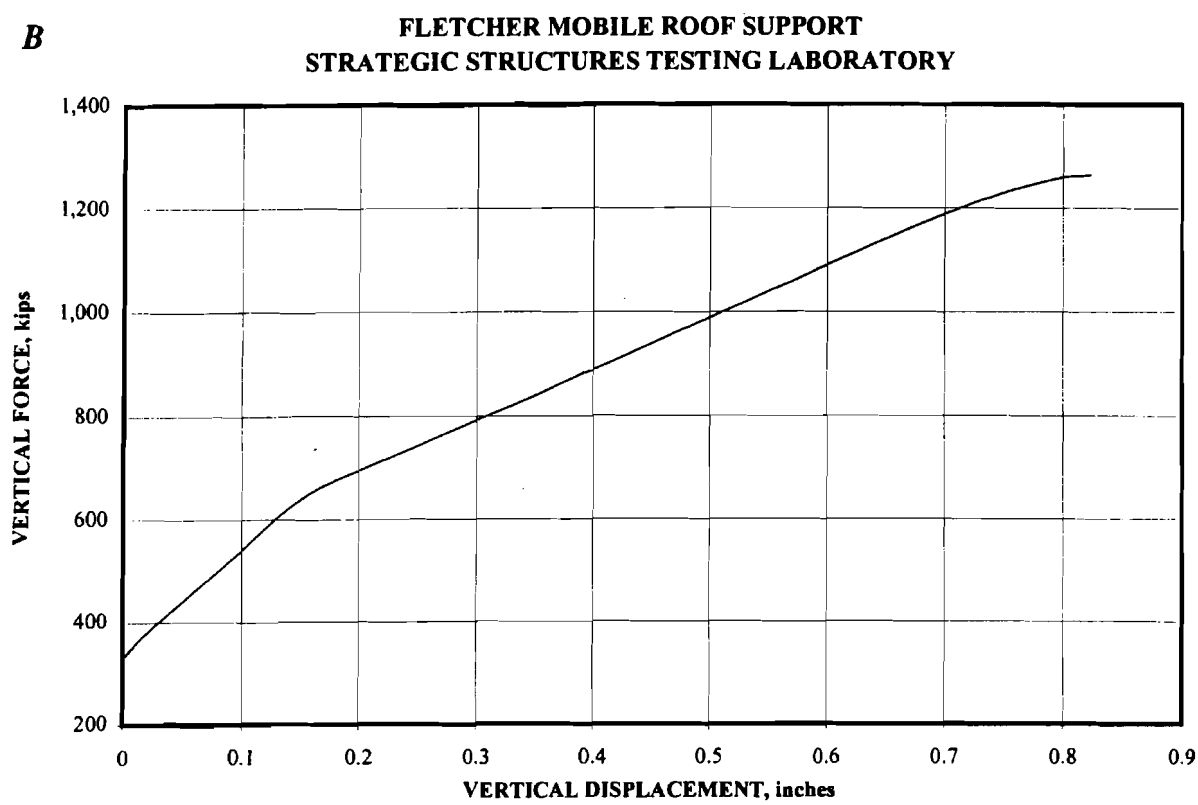

Figure 8.—*A*, Decrease in vertical stiffness on the VAMT support when bottom stage is fully extended at 0.4 in of displacement. *B*, Reduction in Fletcher support stiffness when both bottom and middle stages are fully extended at 0.15 in of displacement.

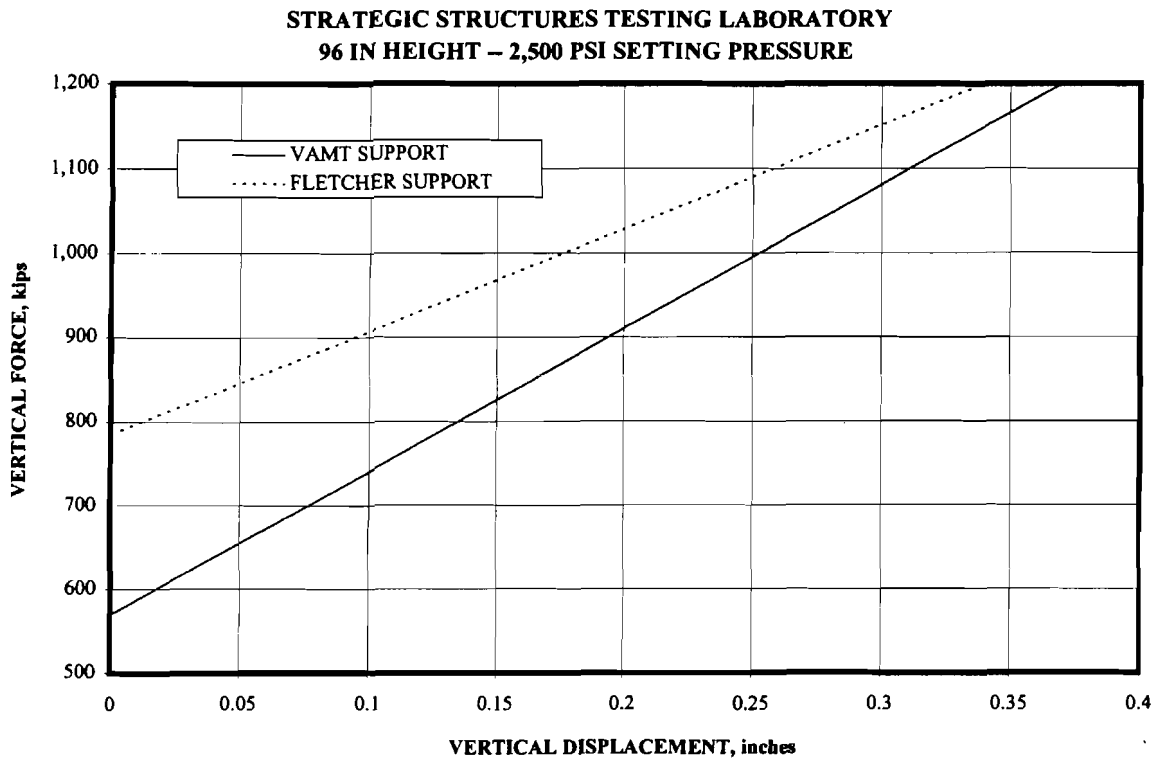

Figure 9.—Both the VAMT and Fletcher supports reach yield load at nearly the same displacement when set to the same leg pressure.

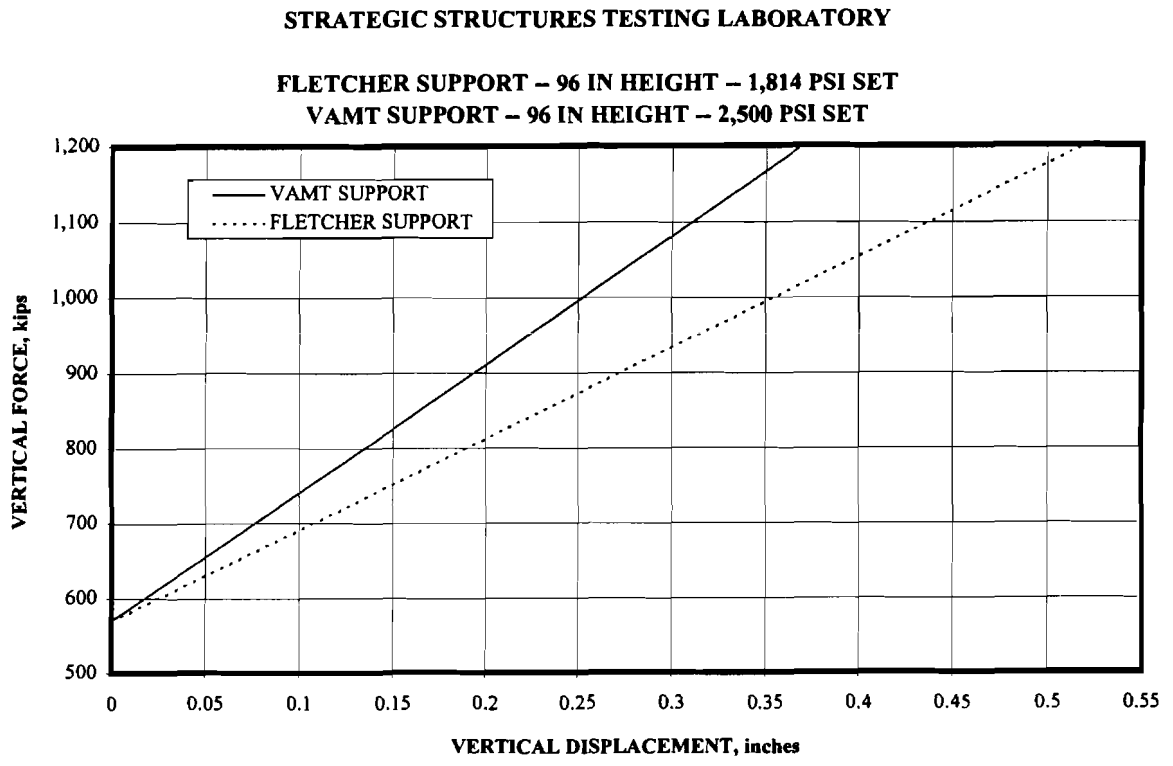

Figure 10.—Roof-to-floor convergence required to produce yield load in Fletcher and VAMT supports when both set to the same setting force.

Unlike the Fletcher support, which utilizes rigid lemniscate links, the horizontal force in the VAMT support, which utilizes a hydraulic aligning cylinder to limit the maximum horizontal loading, is a bilinear function of horizontal displacement. The horizontal stiffness at a particular height is reduced by as much as 50% when the aligning cylinder begins to develop load (see figure 12). For the example shown in figure 12 (horizontal displacement of the canopy toward the

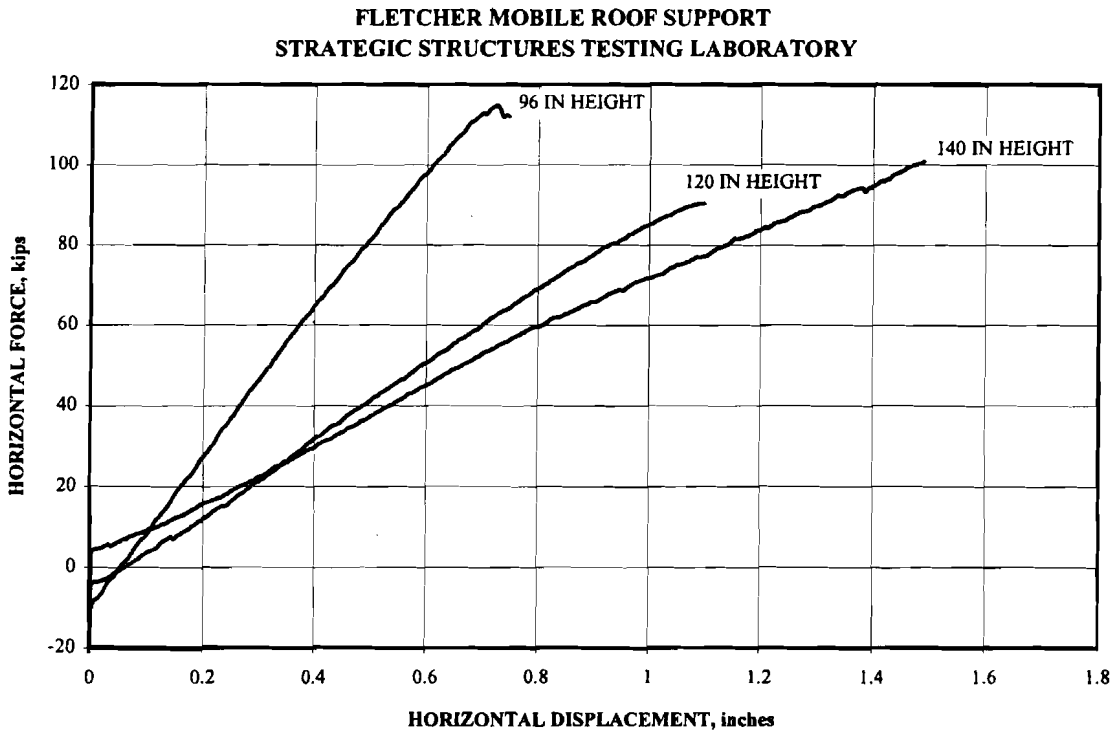

Figure 11.—Horizontal stiffness increases at decreasing support heights.

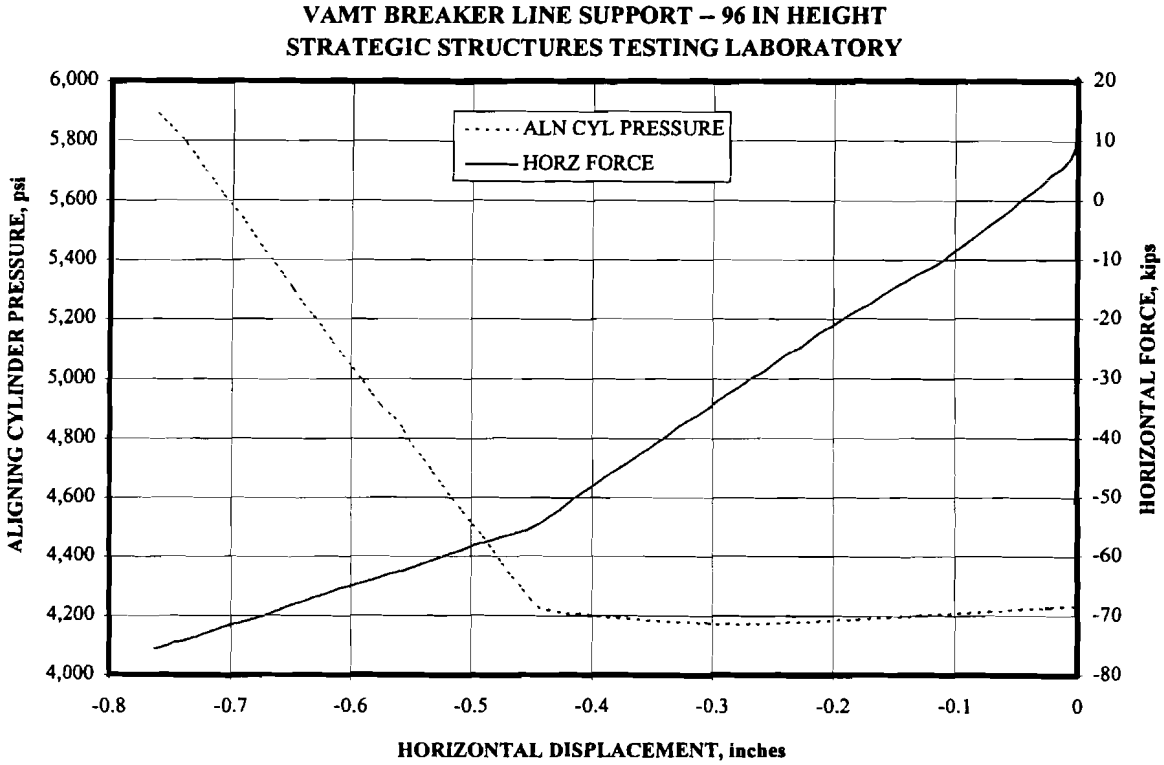

Figure 12.—Reduction in horizontal stiffness when pressure develops in the aligning cylinder.

caving shield), the initial horizontal stiffness is 233 kN/cm (133 kips/in), followed by a stiffness of 116 kN/cm (66 kips/in) after the aligning cylinder pressure began to increase. The horizontal stiffness of the Fletcher support is 2.3 times that of the VAMT support when the aligning cylinder is controlling horizontal load development.

Lateral Stiffness

Lateral stiffness is a measure of support resistance to applied left or right displacements of the canopy relative to the base. Thus, the direction of loading is across the width of the canopy versus along its length in horizontal stiffness evaluations. Lateral stiffness, as shown in figure 13, is also height-dependent.

For supports equipped with a tilt-frame lemniscate assembly such as the tested VAMT support, lateral stiffness is controlled primarily by the tilt cylinders, which control rotation of the lemniscate tilt assembly. The lateral stiffness of the Fletcher support tended to be bilinear with a high initial stiffness during the first 1.3 cm (0.5 in) of lateral movement, followed by a reduced stiffness for lateral movements beyond this, as shown in figure 14. The decrease in stiffness was greatest at the 2.4-m (96-in) operating height, with a 70% reduction in stiffness when the lateral movement exceeded 1.3 cm (0.5 in). The bilinear nature of the lateral stiffness is probably due to the interaction of the leg cylinders and the lemniscate assembly. This bilinear behavior was not observed in the VAMT support. As shown in table 1 , the Fletcher support is stiffer than the VAMT support initially, whereas the VAMT support is stiffer than the Fletcher support when the lateral movement exceeds 1.3 cm (0.5 in).

The lateral stiffness is less than the horizontal stiffness by a factor of 3 for the VAMT support and a factor of 2.3 (initial stiffness) or a factor of 8 (final stiffness) for the Fletcher support at a 2.4-m (96-in) operating height.

ASSESSMENT OF SETTING FORCE

Setting force is defined as the force exerted against the mine roof and floor by actively setting the support using the internal hydraulic power. The setting force is determined by the effective leg area times the hydraulic pressure with the total setting force equal to the sum of all four leg cylinder forces. The effective leg area depends on the staging of the leg cylinders. Figure 15 compares the setting force as a function of hydraulic leg pressure with no stages fully extended for the Fletcher and VAMT supports. Because the VAMT support has smaller diameter leg cylinders—21.8 cm (8.6 in) compared with 25.4 cm (10 in) for the Fletcher support—greater pressures are required to produce equivalent setting forces. For example, approximately 17.4 MPa (2,530 psi) of pressure is required to produce 3,558 kN (800 kips) of setting force with the Fletcher support, whereas 24.1 MPa (3,500 psi) would be required to produce an equal setting force with the VAMT support.

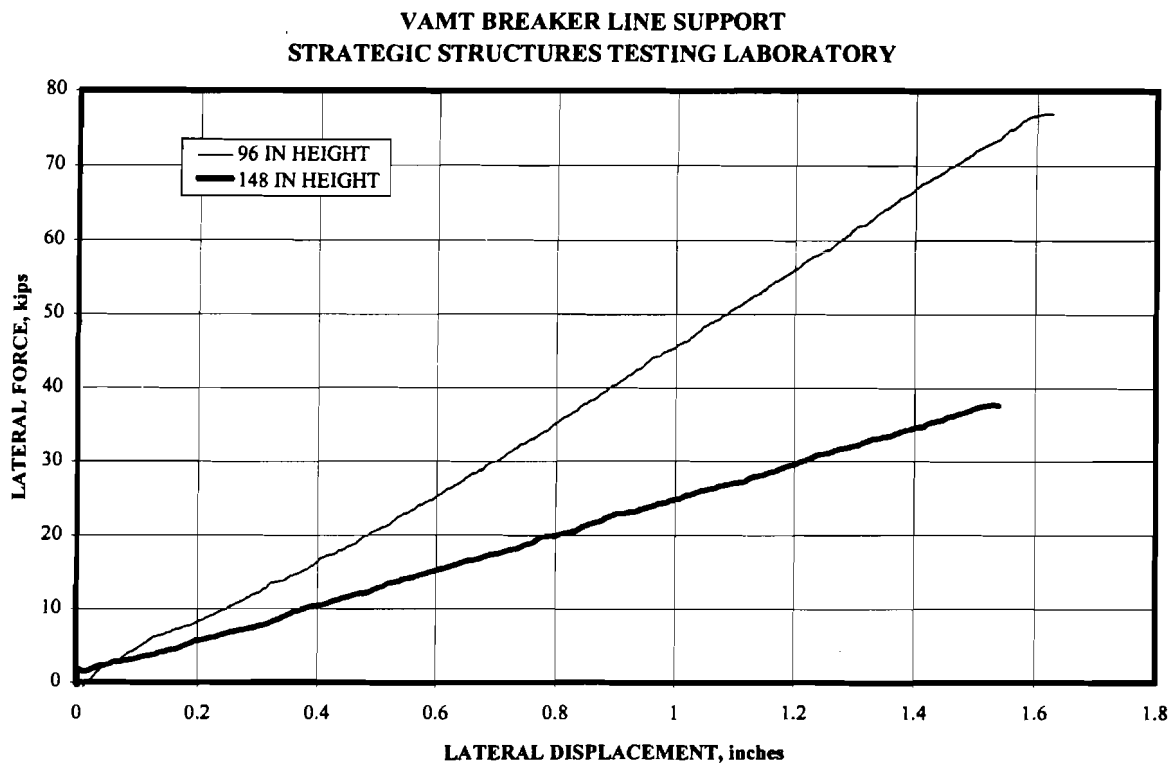

Figure 13.—Effect of height on lateral support stiffness. Left-to-right lateral displacement of the canopy.

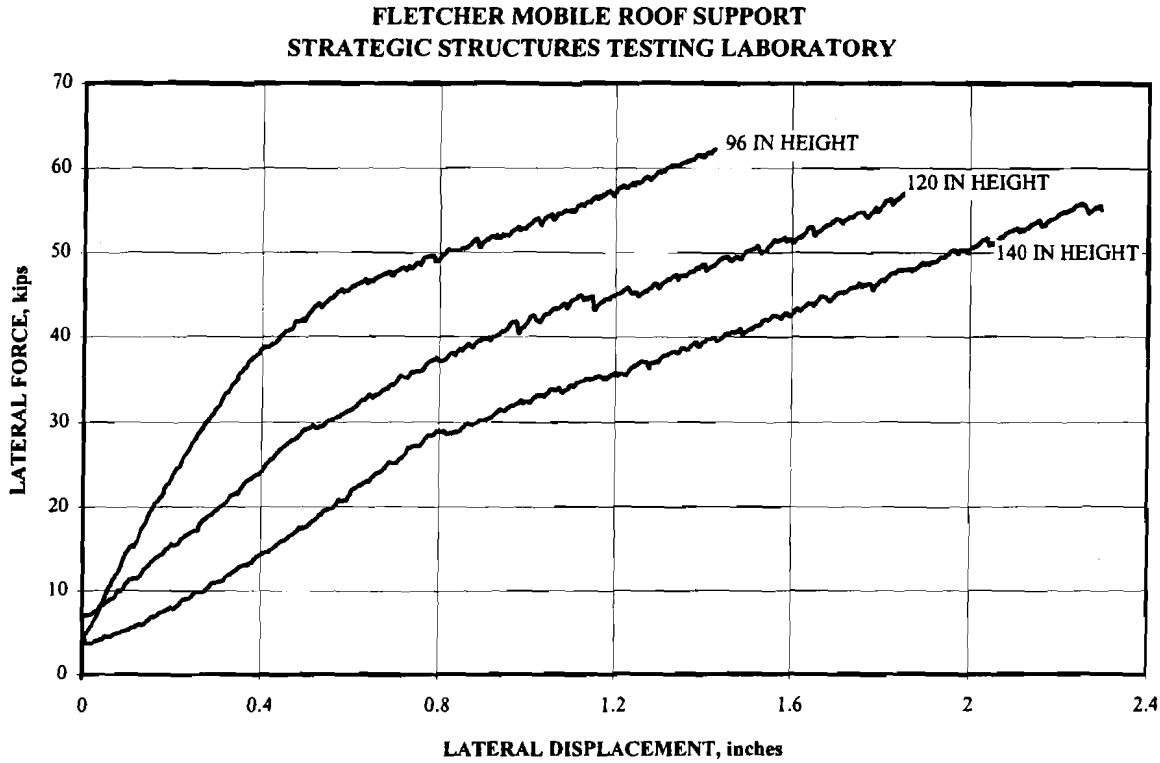

Figure 14.—Bilinear stiffness response to lateral loading.

The VAMT support utilized a two-stage leg cylinder, whereas the Fletcher support utilized a three-stage leg cylinder. Table 2 shows the reduction in setting force due to leg staging for the VAMT and Fletcher supports. As shown in the table, setting force can be reduced by as much as 70% for three-stage leg cylinders when the bottom and middle stages are fully extended. Because variances can also exist in each leg of the support with regard to staging, setting forces between the values shown in table 2 are possible. Thus, a wide range of setting forces can be provided for both supports even if the hydraulic setting pressures remain constant from set to set. An example of this is shown in figure 16.

Table 2.—Reductions in setting force due to leg staging

Leg stage condition	Reduction in setting force, %	
	Fletcher support [1]	VAMT support [2]
No stages fully extended	0	0
Bottom stage fully extended . . .	45	42
Bottom and middle stage fully extended	70	NAp

NAp Not applicable.
[1]Three-stage leg cylinder design.
[2]Two-stage leg cylinder design.

The effect of leg staging on setting force development can be explained by examining the operation of the leg during setting and the associated leg mechanics, as depicted in figure 17 for a three-stage leg cylinder. Operationally, when the support is raised, the bottom stage is designed to extend to full extension first, followed by the middle and top stages. Likewise, when the support is lowered, the bottom stage retracts first, followed by the middle and top stages. The setting force will always equal the force developed in the stage with the largest diameter that is *not* fully extended, equaling the pump pressure times the area of that stage.

When the support is initially raised from a collapsed position to a height greater than the bottom leg extension, the setting force is diminished in proportion to the area reduction of the next stage, as depicted in table 2. On subsequent setting events, the setting force depends on whether full extension of leg stages is required due to changes in operating height. Once a support is extended to an operational height with a diminished setting force due to the bottom or middle stage being fully extended, the setting force will be restored to its maximum capability if the support is reset at *any* lower height, provided the bottom stage has not been fully retracted, and the setting force again will be diminished if the support is reset at an equal or greater height.

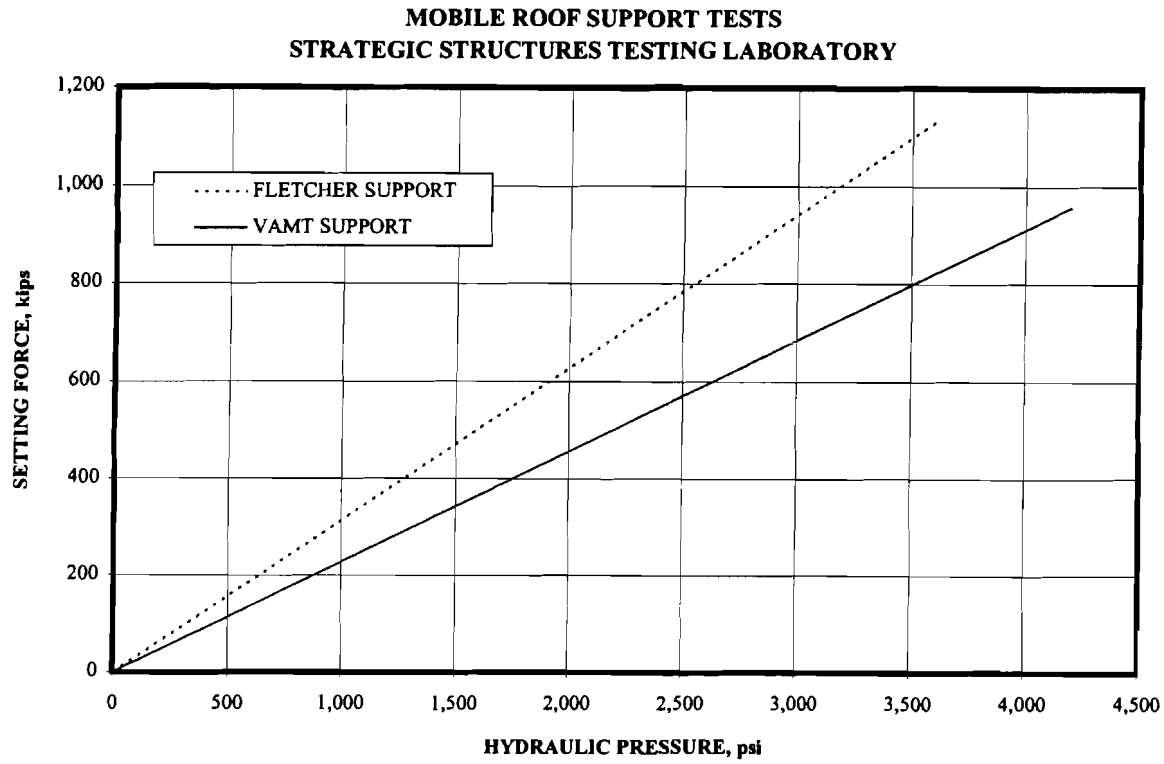

Figure 15.—Comparison of setting forces as a function of leg pressure with no stages fully extended for Fletcher and VAMT supports.

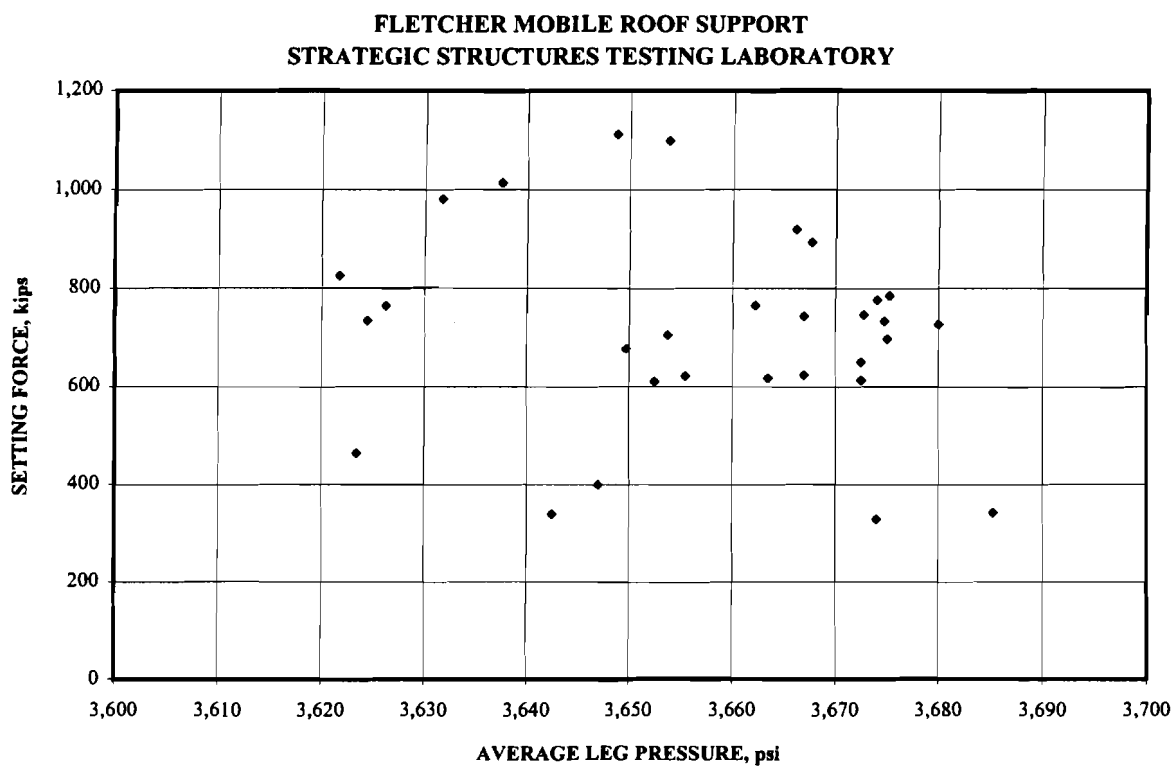

Figure 16.—Range of measured setting forces for maximum pump pressures.

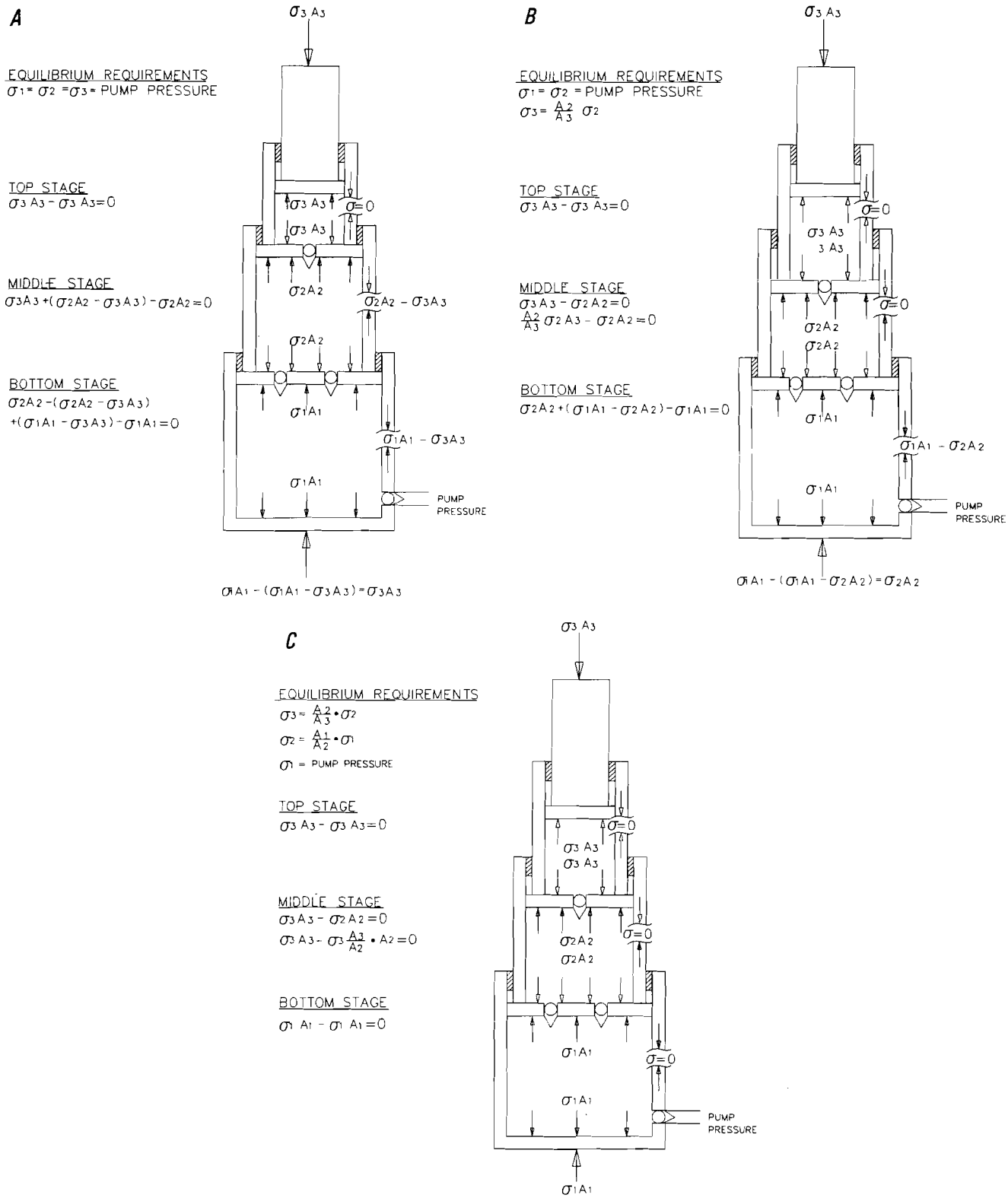

Figure 17.—Leg mechanics. *A*, bottom and middle stages fully extended; *B*, bottom stage fully extended; *C*, no stage fully extended.

An example is shown in figure 18 for a three-stage leg cylinder. Behavior of a two-stage leg cylinder can be deduced by elimination of the middle stage. Initially, the support is set at a height (H_{INT}) that causes the bottom stage to be fully extended, providing a diminished setting force. In preparation for the next cycle, the support is lowered, during which the bottom stage is partially retracted while the upper stages remain extended. When the support is reset (second cycle) at a lower operating height, full extension of the bottom stage is not required since the upper stages remain extended from the previous cycle. As a result, the setting force is restored to its maximum capability, equaling the setting pressure times the area of the bottom stage. Two scenarios are examined for the third cycle. In both cases, the support is reset at a higher operating height than the second cycle. In the first case, the support is raised to a height greater than the initial height. In this case, the bottom stage is fully extended once again and the setting force is once again diminished. However, if the support is raised to a height on the third cycle that is less than the initial height, full extension of the bottom stage is not required and full setting capacity is maintained.

In summary, during underground operation, the setting force will *always* be reduced on the mining cycle that establishes a *new maximum operating height* after an initial operating height that causes full extension of the bottom stage. All other cycles should provide full setting capability because extension of the bottom stage will not be required. Operationally, the probability of achieving maximum setting forces can be enhanced by establishing a maximum operating height as soon as possible. Ideally, when the support is initially taken underground, it can be brought to a location that is higher than where it will be placed into operation during pillar extraction, and fully extended. This will ensure full setting forces for all load cycles, provided the support is not lowered to the point where the bottom stage is fully collapsed, which would then cause retraction of the upper stages. In this case, a new maximum operating height would have to be established to prevent reductions in setting force.

FACTORS AFFECTING LOAD AND LOAD RATE MEASUREMENTS

Since the dial gauges on the support measure pressure in only the bottom stage of the leg cylinder, an assessment of load and loading rates can only be determined through the full load cycle when none of the stages are fully extended. If the bottom stage or bottom and middle stages (three-stage cylinder design) are fully extended, the dial gauges will not record changes in pressure until the setting forces in the extended stages are overcome by additional load development in the upper stages. When this condition occurs, roof loading during a beginning portion of the loading cycle will go undetected by the dial pressure gauges. The period of undetected roof loading depends on the setting pressure and will increase with increasing setting pressure in a particular support.

Using the VAMT support as an example, if the support is set with 29.0 MPa (4,200 psi) of hydraulic pressure with the bottom stage fully extended, a force of approximately 4,226 kN (950 kips) is generated in the bottom stage against the mechanical stops and 2,558 kN (575 kips) is generated in the upper stage acting on the mine roof. Because the bottom stage is fully extended, the dial gauges will remain inactive until the roof load acting on the support increases by 1,668 kN (375 kips) to cause the force in the upper stage to exceed 4,226 kN (950 kips) and cause the bottom stage to be moved off of its mechanical stops, resulting in an increase in pressure.

Figure 19 shows the magnitude of roof loading that is not recorded by the dial pressure gauges when one or more leg stages are fully extended as a function of the setting pressure. As seen in the figure, the unrecorded roof loads increase linearly with increasing setting pressure. As expected, the magnitude of unrecorded roof loading is much greater for the Fletcher three-stage leg cylinders than for VAMT two-stage leg cylinders because the bottom stage area is 35% larger in the Fletcher support, creating a higher setting force in the bottom stage compared with the VAMT support at the same hydraulic setting pressure. Additionally, when the bottom and middle stages are fully extended, the load difference between the top and bottom stages governs the unrecorded roof load. As shown in figure 19, unrecorded roof load ranged from approximately 445 kN (100 kips) at 6.9 MPa (1,000 psi) of setting pressure to as high as 1,690 kN (380 kips) at full pump pressure for the VAMT support and 609 kN (137 kips) at 6.9 MPa (1,000 psi) of setting pressure to 2,202 kN (495 kips) at full pump pressure when the bottom stage of the Fletcher support is fully extended. When both the bottom and middle stages are fully extended, 3,509 kN (789 kips) of roof loading can go undetected by the dial gauges when the Fletcher support is set to full pump pressure.

Therefore, a false sense of loading and loading rate can be interpreted from the pressure gauges when the bottom leg stage is fully extended. This can result in unreliable information for operators that utilize support loading to assess roof stability and impending roof caving. Full extension of the bottom stage can occur at heights greater than 50% of the operating range for a two-stage leg cylinder and at heights greater than 33% of the operating range for a three-stage leg cylinder (assuming equal stroke of the leg stages). However, the inaccurate information occurs only when a new maximum operating height is attained; therefore, the probability of inaccurate information depends on the mining conditions.

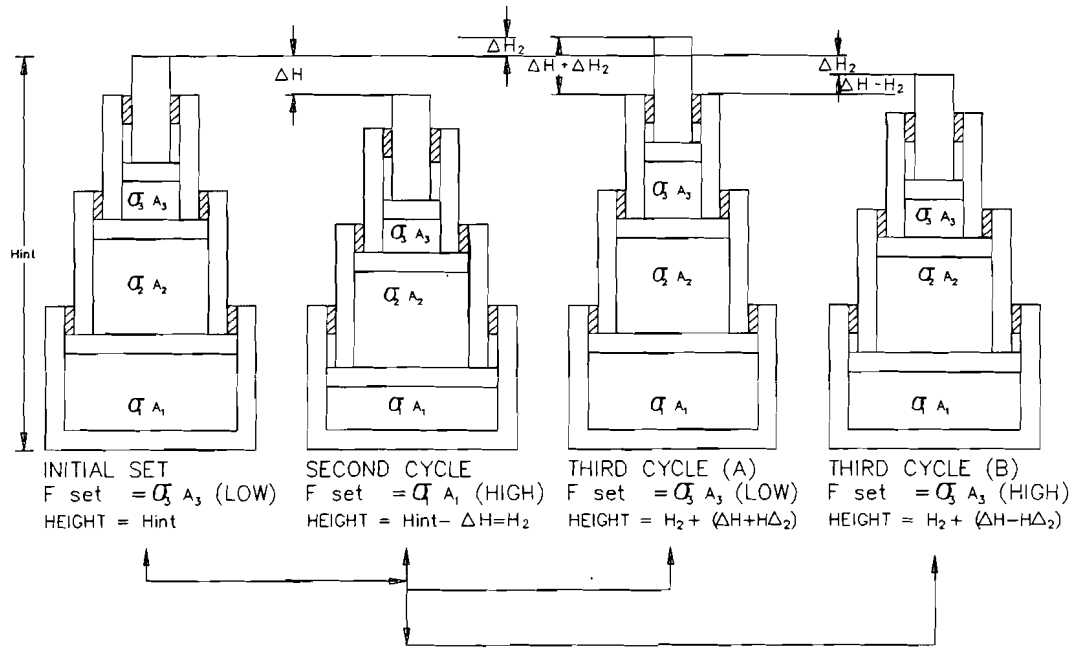

Figure 18.—Conditions that produce diminished setting force and unrecorded roof loads.

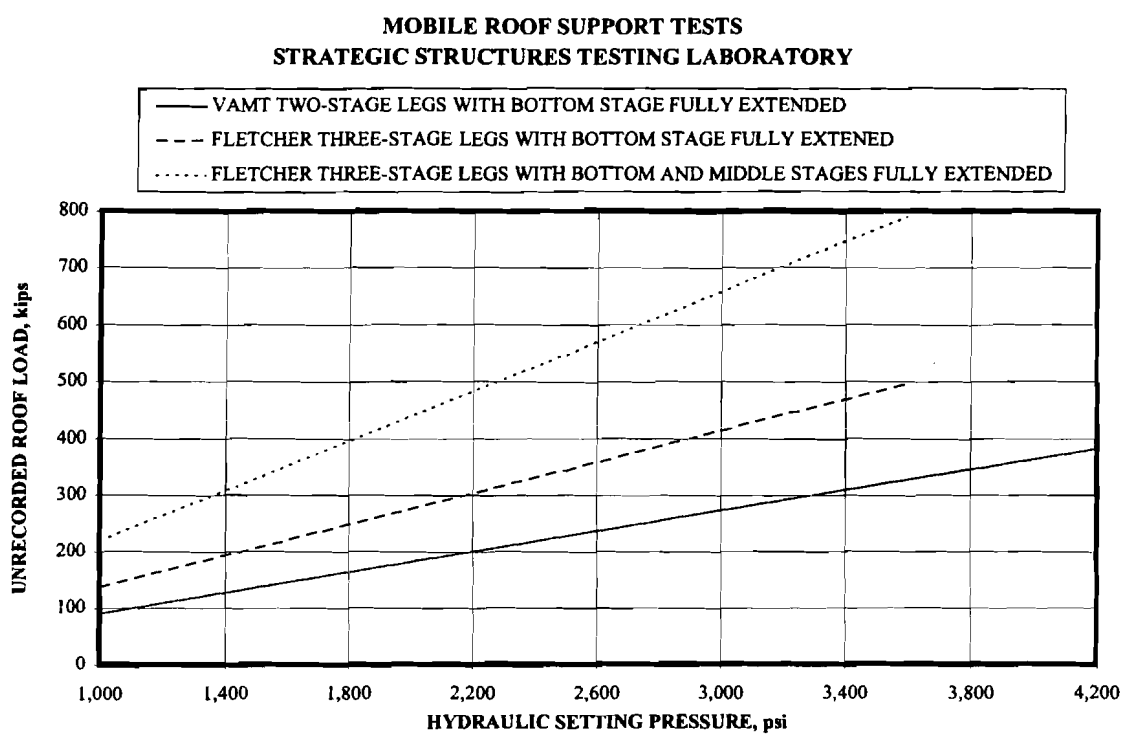

Figure 19.—Unmeasured roof load when one or more of the stages are fully extended as a function of setting pressure in the leg cylinders.

CONDITIONS THAT REDUCE SUPPORT CAPACITY

One cause of reduced support capacity is the bleed-off of hydraulic pressure from the leg cylinders under static loading conditions. Bleed-off rates of 69 kPa (10 psi) to 138 kPa (20 psi) per minute were common to both supports tested. As shown in figure 20, approximately 356 kN (80 kips) of load resistance was lost in 30 min because of loss of leg pressure under static loading for the VAMT support.

Horizontal loading can either increase or decrease support capacity depending on the change in leg pressures between the front and rear set of legs and the reaction of lemniscate assembly. Leg cylinders that are inclined toward the direction of the horizontal displacement will generally increase in pressure; those inclined away from the direction of the horizontal displacement will generally lose pressure. The net pressure change between the front and rear set of legs will generally determine whether the support capacity will be reduced or increased. However, the reaction of the lemniscate assembly must also be considered. For horizontal displacement of the roof acting to push the canopy toward the caving shield, the lemniscate assembly develops an upward reaction at the canopy connection, which increases support capacity. Likewise, when the horizontal displacement is toward the plow, a downward reaction is developed at the canopy connection, which reduces support capacity.

For the two supports tested, horizontal displacement produced the most change in support capacity at the lower heights because of the greater leg inclination. Figure 21 depicts the effect of horizontal loading on support capacity for the VAMT and Fletcher supports at a 2.4-m (96-in) operating height. As shown in the figure, support capacity was reduced for horizontal roof displacement toward the caving shield end of the canopy, and support capacity was increased when the horizontal canopy displacement was toward the plow. A maximum reduction in support capacity of 334 kN (75 kips) was observed for the VAMT support as a result of 2.0 cm (0.78 in) of horizontal roof displacement toward the rear of the canopy. Figure 22 is an example of an *increase* in VAMT support capacity despite a *reduction* in leg pressures on both the front and rear set due to the reaction of the lemniscate assembly.

Lateral displacements of the canopy in both directions tended to produce a loss of leg pressure that resulted in loss of support capacity. An example is shown in figure 23 for the Fletcher support. Support capacity was reduced by 378 kN (85 kips) on the VAMT support for left-to-right lateral displacement of the canopy at a 2.4-m (96-in) operating height with no significant loss of leg pressure (see figure 24), which suggests a negative reaction by the lemniscate assembly.

Figure 25 compares the effects of horizontal and lateral loading on support capacity at a 2.4-m (96-in) operating height for the Fletcher and VAMT supports. As shown in the figure, reductions in support capacity were greater for horizontal loading than lateral loading for both supports.

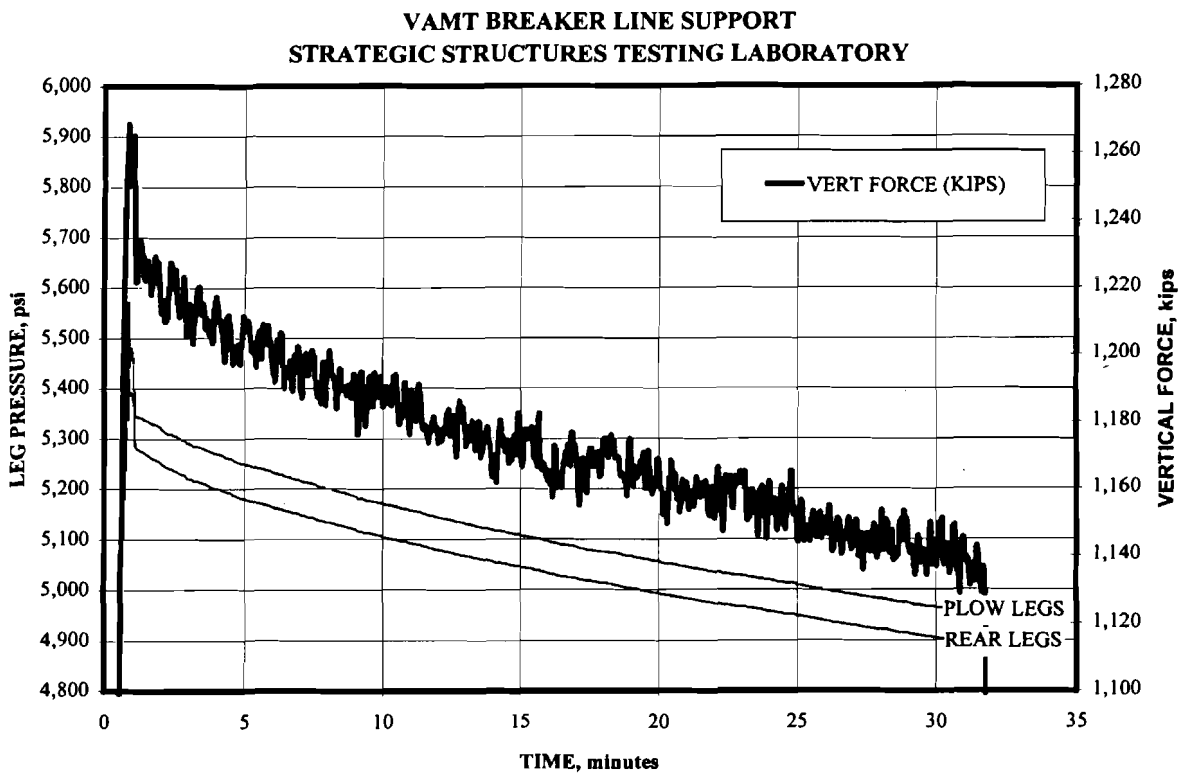

Figure 20.—Reduction in support capacity due to bleed-off of leg pressures after leg yielding.

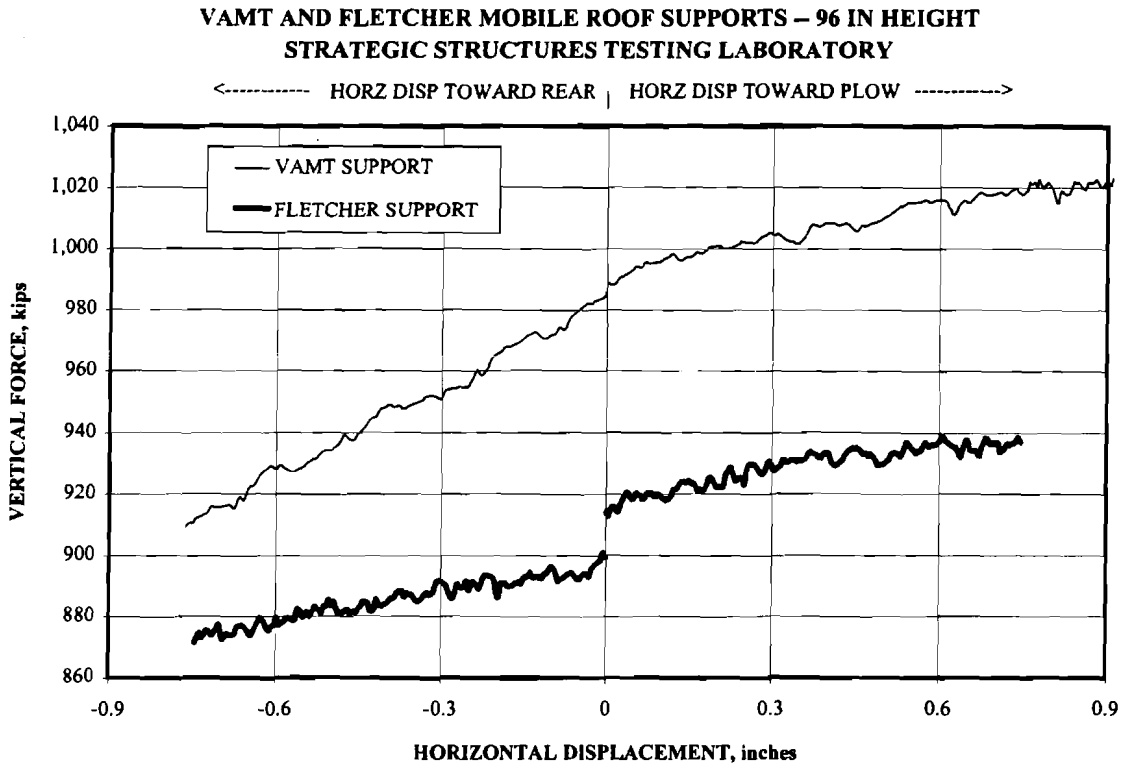

Figure 21.—Increase in support capacity for horizontal displacement toward the plow and decrease in support capacity for horizontal displacements toward the rear.

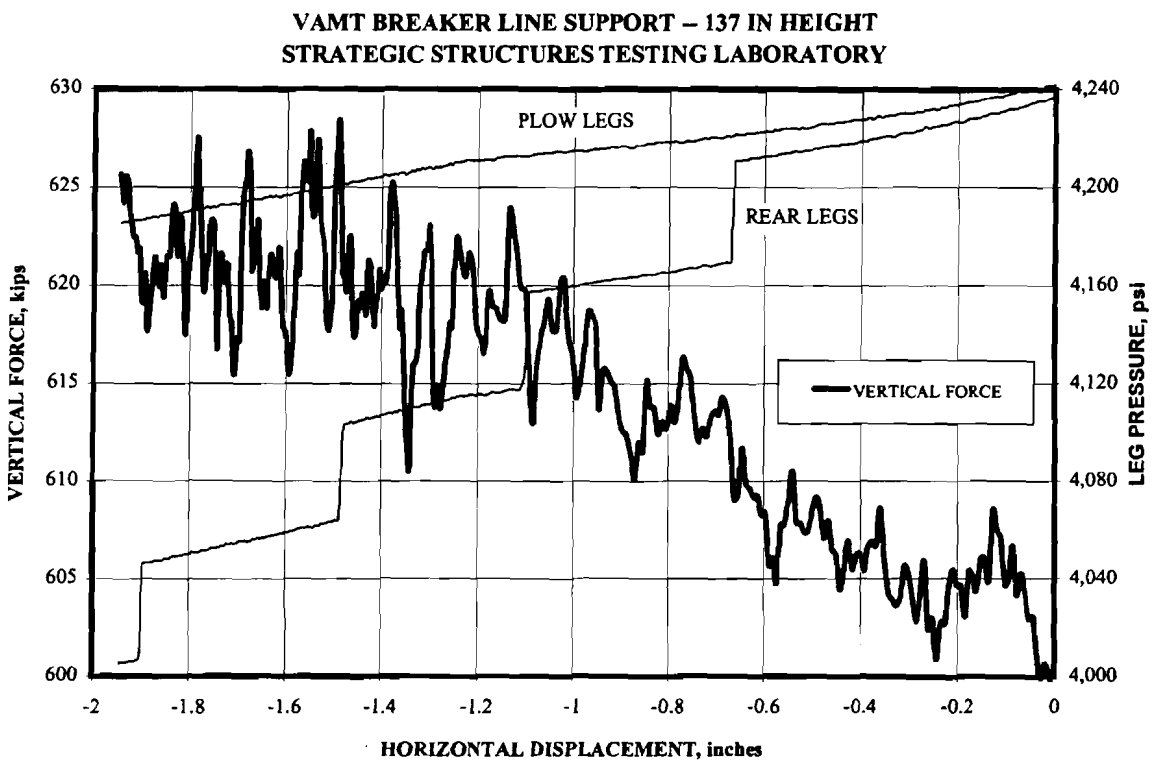

Figure 22.—Increase in support capacity despite a reduction in leg pressures.

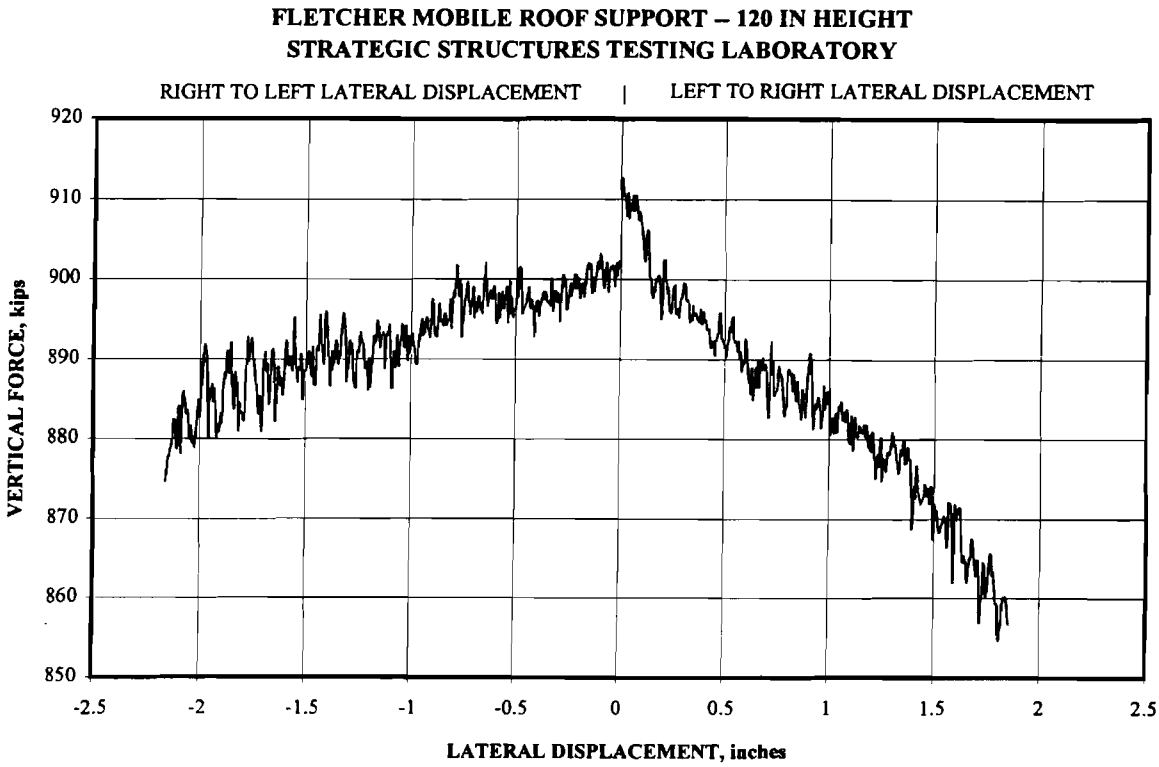

Figure 23.—Reduction in support capacity as a function of direction of lateral loading.

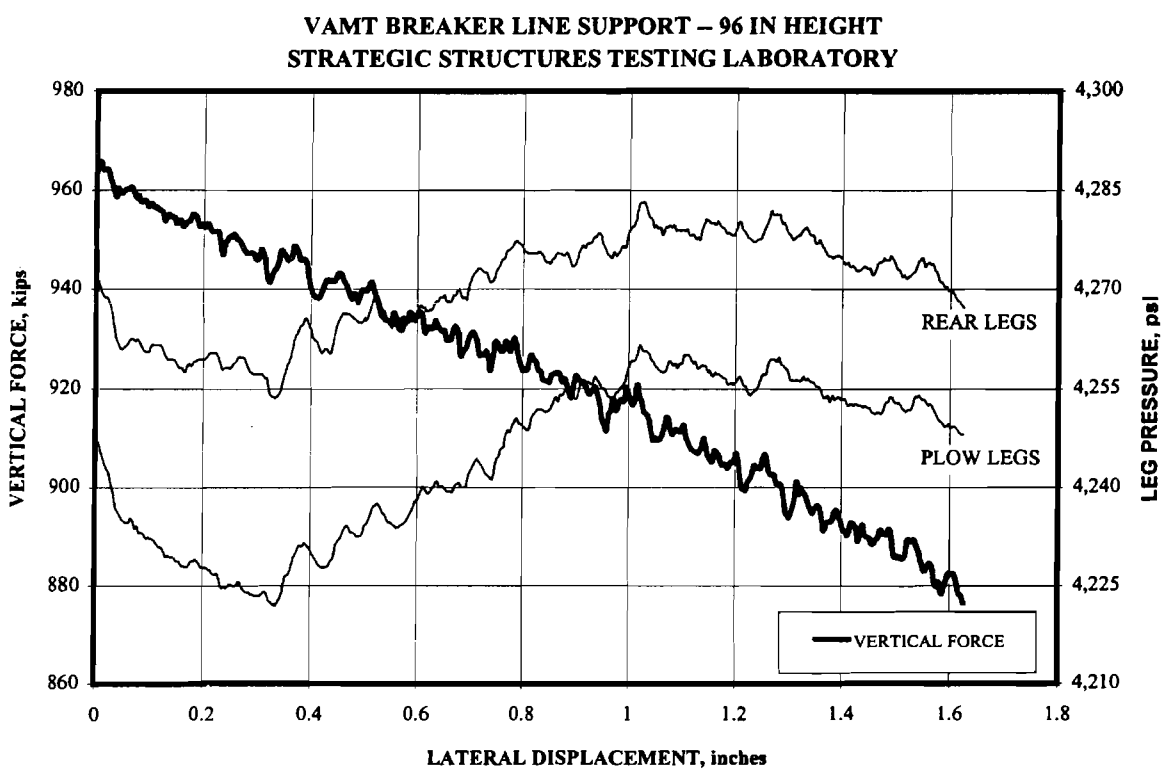

Figure 24.—Reduction in support capacity due to lateral loading with no significant loss of leg pressure.

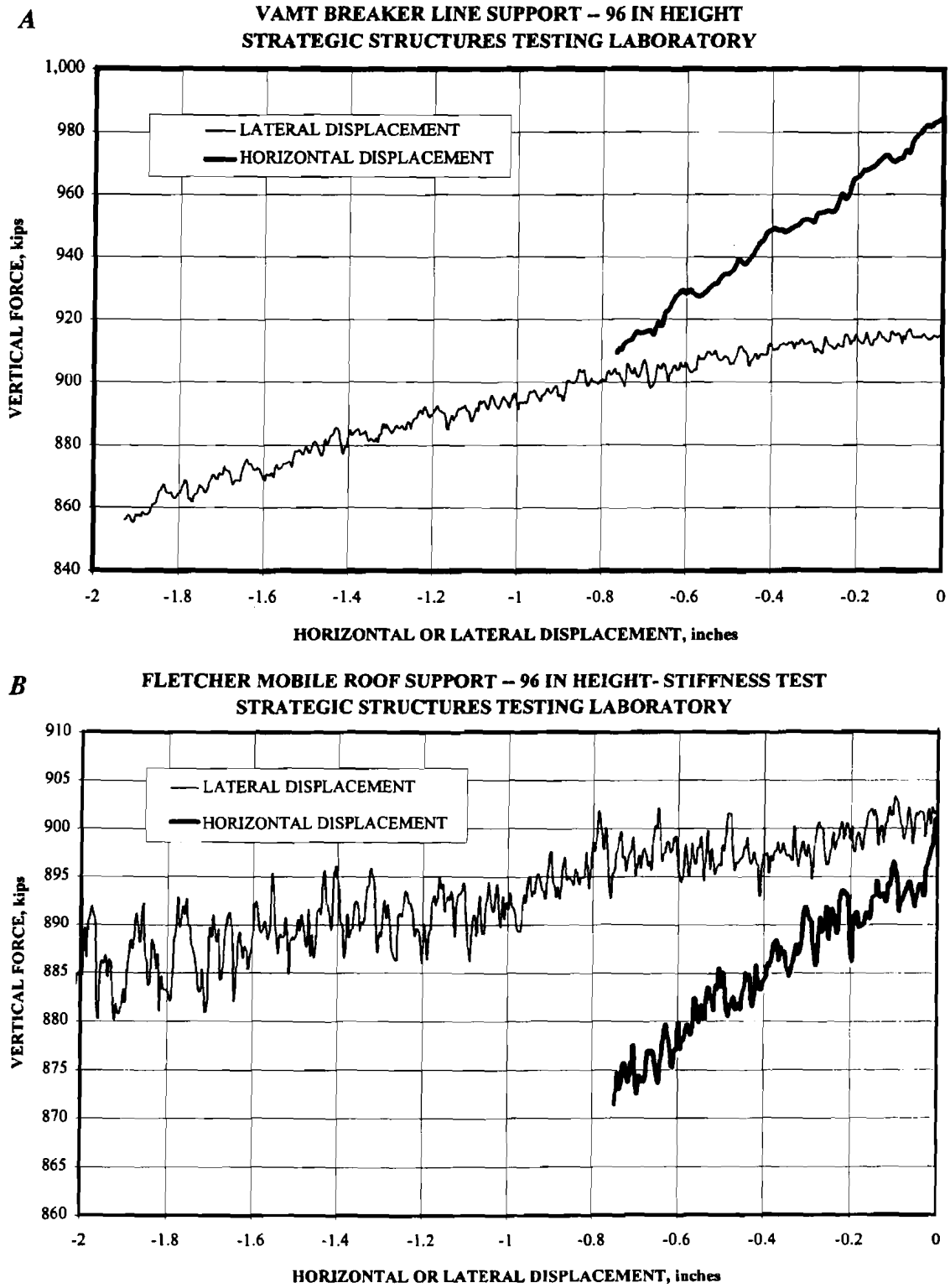

Figure 25.—Comparison of the effects of horizontal and lateral loading on reductions in support capacity. *A*, VAMT support; *B*, Fletcher support.

CRITICAL LOAD CONDITIONS

In general, the worst-case load condition for MRS's is lateral loading that causes lateral displacement of the canopy relative to the crawler frame. All of the rotational joints within the support structure are designed with a single rotational degree of freedom. Because lateral loading produces rotations along axes perpendicular to this rotational degree of freedom, it is the most severe load condition.

Depending on the stiffness of the lemniscate assembly, horizontal loading can also produce critical loads in the lemniscate assembly components. VAMT uses a hydraulic cylinder in lieu of a rigid lemniscate link to limit stress development in the lemniscate assembly due to horizontal loading.

The worst-case load conditions for canopy and base structures are partial contact configurations that induce bending. The associated stress development will be a function of the stiffness of the structure in relation to the applied loading.

STRUCTURAL INTEGRITY OF THE VAMT AND FLETCHER SUPORTS

Obviously, the effects of the above critical load conditions will be specific to a particular support design. A summary evaluation of the structural integrity of the VAMT and Fletcher supports based on measured component strains follows. However, it should be noted that the strain gauges were intended to assess load transfer through the various support components and were not necessarily positioned to measure maximum loading in any one component. All components were evaluated on both supports, except the crawler frame on the VAMT support.

VAMT Support

Highly loaded components on the VAMT support were the aligning cylinder and the canopy.

The amount of horizontal force acting on the support required to produce pressure development in the aligning cylinder varied from 178 to 467 kN (40 to 105 kips) for support heights ranging from 2.4 to 3.8 m (96 to 148 in). Once pressure development begins, only another 67 to 89 kN (15 to 20 kips) is required to produce a yield pressure of 40 MPa (5,800 psi) in the aligning cylinder. An example is shown in figure 26. In this case, 245 kN (55 kips) of horizontal loading acting to displace the canopy toward the rear of the support was required to produce pressure development in the aligning cylinder, and approximately 89 kN (20 kips) of additional horizontal loading produced a pressure of 40 MPa (5,800 psi). In this example, the displacement required to initiate pressure development in the aligning cylinder was 1.14 cm (0.45 in), with 0.76 cm (0.3 in) of additional displacement required to produce a maximum pressure of 40 MPa (5,800 psi) in the aligning cylinder (see figure 27).

A malfunction of the aligning cylinder occurred during a test in which the cylinder was yielded in compression under the application of horizontal displacement of the canopy toward the plow. At the completion of the test when the pump pressure was applied to the cylinder during the retraction of the rear legs, hydraulic fluid under considerable p ure blew out of the breather port on the base of the cylinder, indicating that the lower piston seals had been damaged. Strain data were recorded during the test from two strain gauges located on the clevis that connects the cylinder to the tilt-frame assembly. The strain responses are displayed in figure 28. An examination of the strain data suggests that the damage occurred at approximately 13 cm (5.1 in) of horizontal displacement of the canopy relative to the base. The sharp increase in strain that occurred just prior to this suggests that the cylinder was fully stroked. However, an analysis of the lemniscate geometry indicates that approximately 23 cm (9 in) of horizontal canopy movement is required to compress the aligning cylinder through its full 60 mm (2.4 in) of stroke. An examination of the damaged cylinder by VAMT revealed that the cylinder was radially deformed (ballooned), suggesting that the failure was caused by excessive hydraulic pressure. However, the strain data indicate that there were not sufficient forces acting to generate hydraulic pressure that would damage the cylinder. Therefore, the cause of the failure has not been satisfactorily determined. A new aligning cylinder was installed, and testing resumed. Subsequent tests at less-than-yield pressure were successfully conducted with no malfunctions of the aligning cylinder. However, at the discretion of VAMT, the new aligning cylinder was *not* tested under conditions that caused full compression or extension of the cylinder.

The worst load case for the canopy was concentrated loading at the center or at one end of the canopy. However, it is important to note that the strain gauges were located midway between the front and rear leg connections, which is where the maximum bending moment is for the "contact at center" and "contact at both ends" configurations, but not for the other contact configurations. An assessment of stress at full support capacity can be made by extrapolating the canopy strains shown in figure 29 to 5,338 kN (1,200 kips) of support loading utilizing a modulus of elasticity of 206,850 MPa (30×10^6 psi) for steel. The "contact at center" configuration produces a stress of 625 MPa (90,600 psi) at 5,338 kN (1,200 kips) of support capacity. Assuming a yield strength of 690 MPa (100,000 psi) for the steel, this configuration is close to producing permanent deformation in the canopy. A contact located 15.2 cm (6 in) from the canopy tip is projected to produce a stress of 393 MPa (57,000 psi) at the measured strain locations at full support capacity. However, the maximum bending moment is located farther back toward the rear leg in this loading condition, and the maximum stress is known to be greater than that measured in this test.

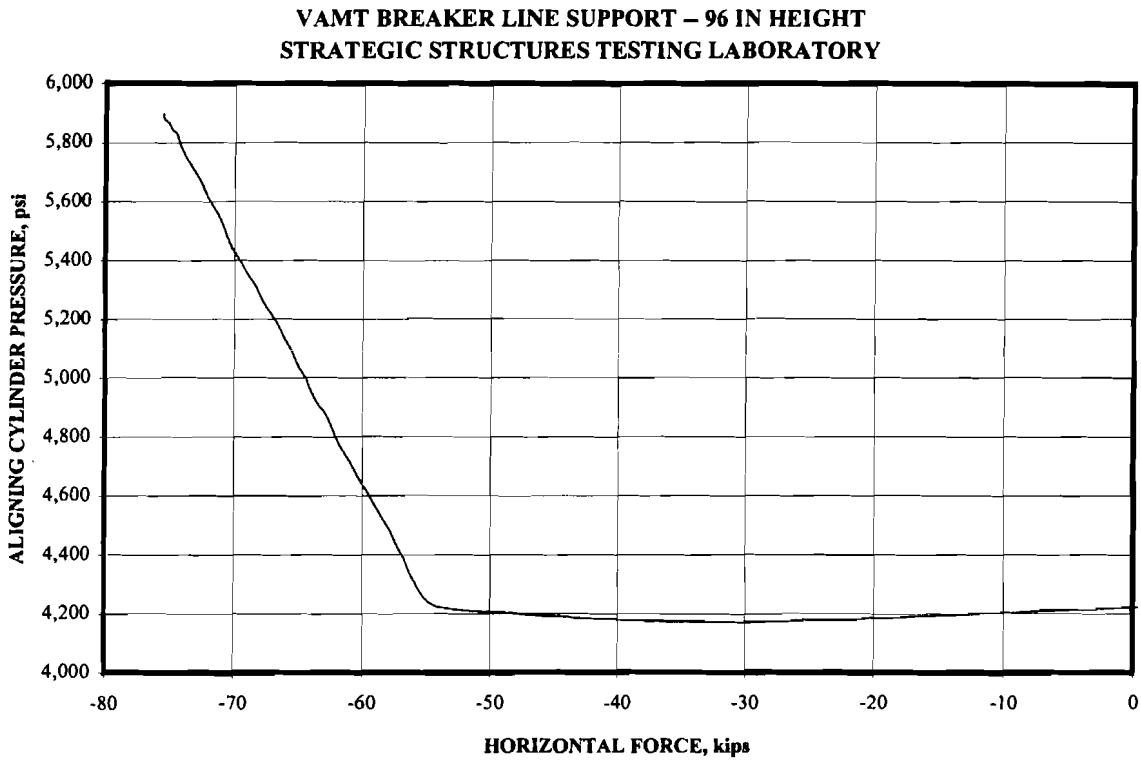

Figure 26.—Horizontal force required to initiate load development and yield pressure in the aligning cylinder.

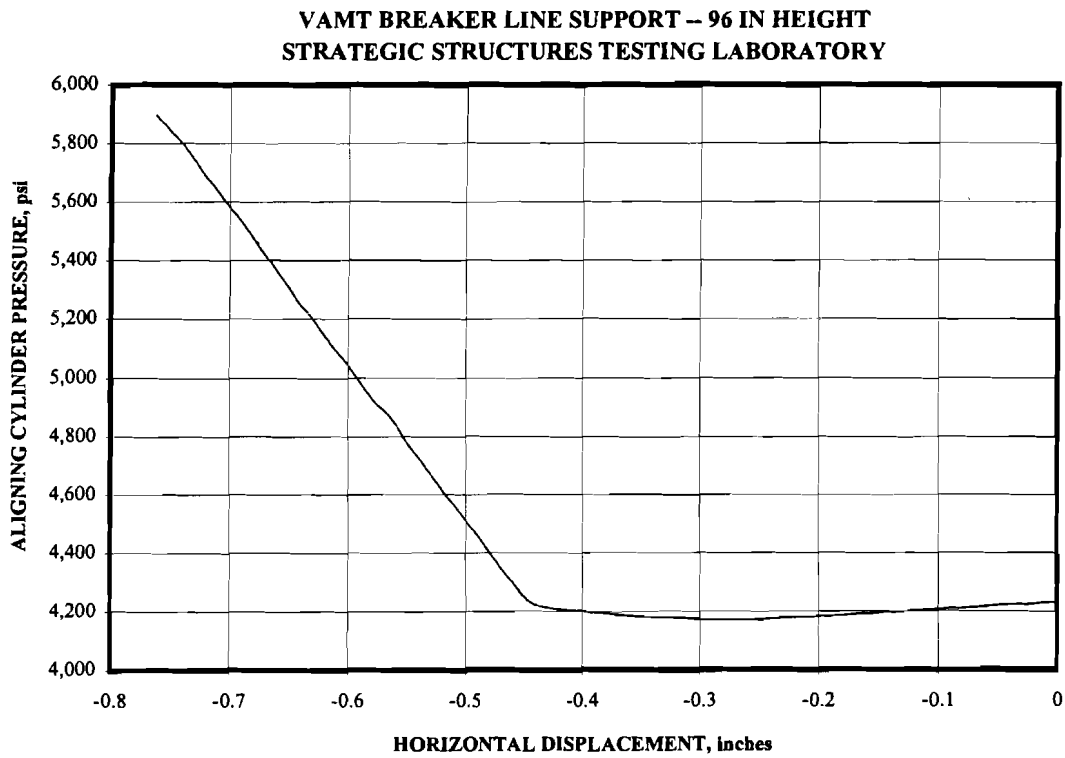

Figure 27.—Horizontal displacement required to initiate load development and yield pressure in the aligning cylinder.

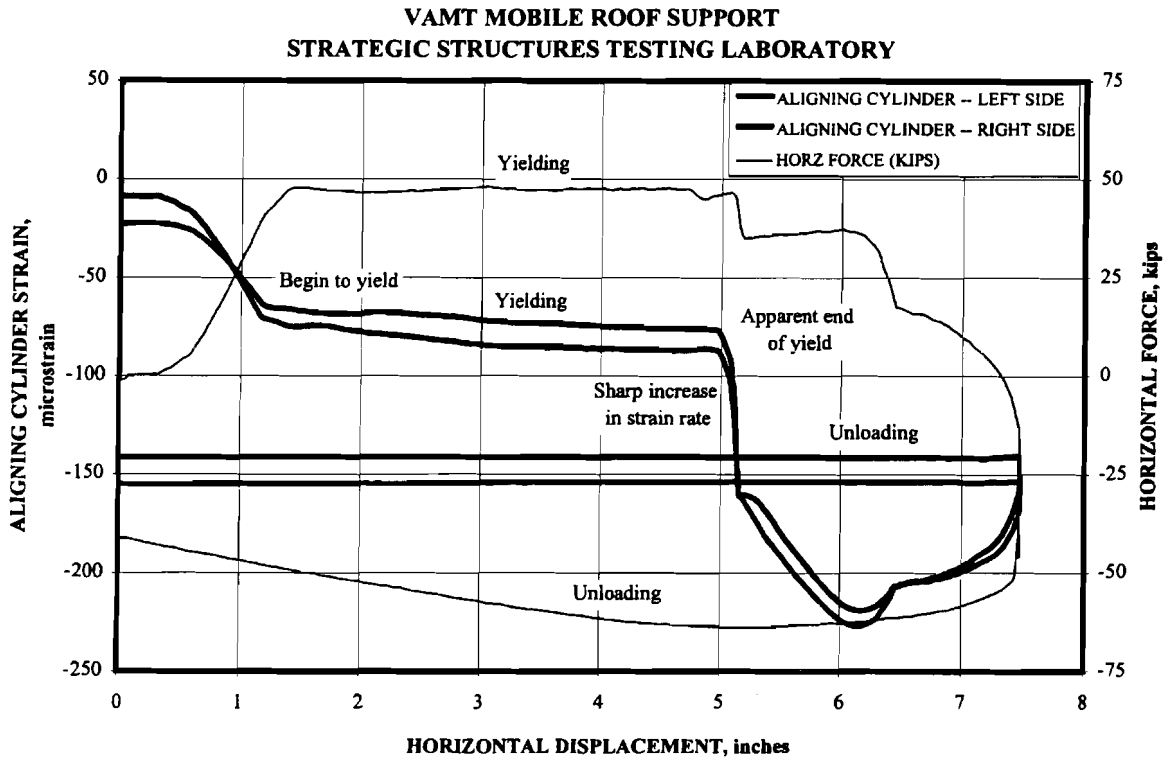

Figure 28.—Malfunction of aligning cylinder during horizontal displacement toward the plow.

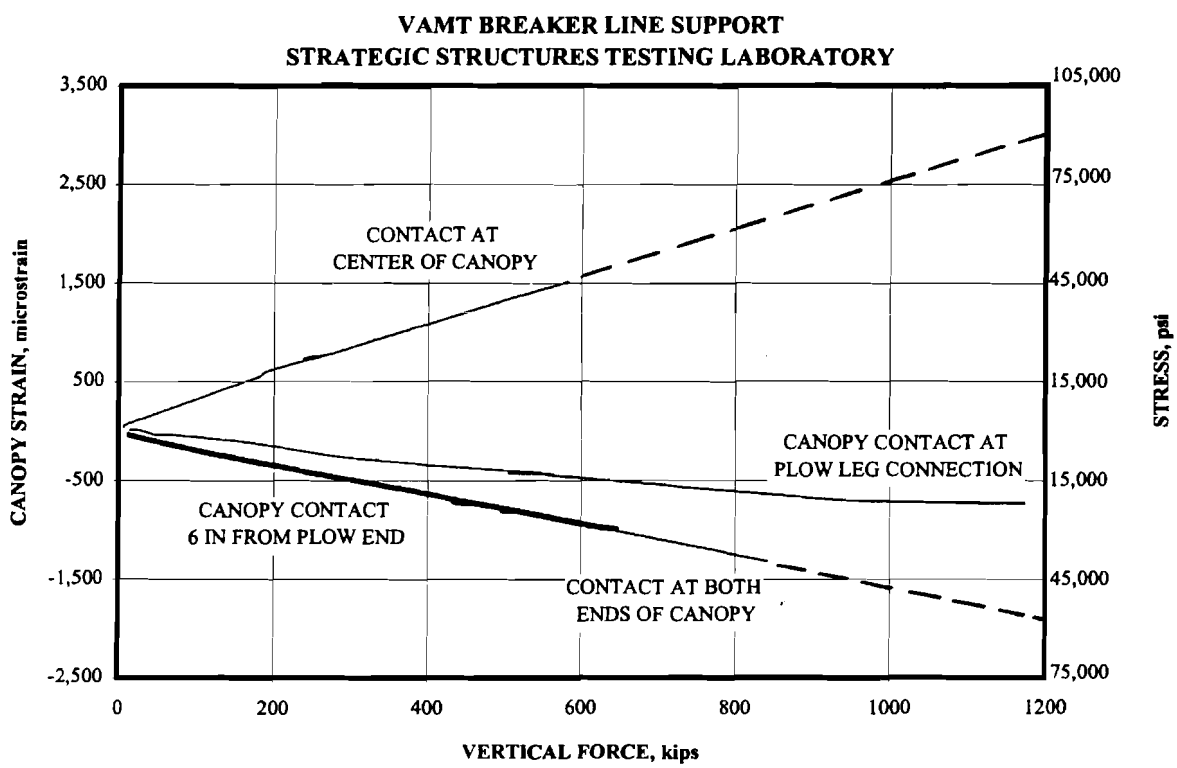

Figure 29.—Extrapolation of measured canopy strains to evaluate stress development at maximum support capacity.

Fletcher Support

The most highly stressed components in the Fletcher support were the bottom lemniscate link and sections of the base (crawler) frame. An objective of the testing was to determine loading limitations for these components. The following limitations are based on extrapolation of test data, where a margin of safety was maintained during load application. No failures of any component were observed under the test conditions.

Lateral loading of 267 kN (60 kips) produced a stress of 207 MPa (30,000 psi) in the bottom lemniscate link. Assuming a 690 MPa (100,000 psi) yield strength, extrapolation of the test data indicates that permanent deformation of the link would occur if the lateral load exceeded 556 kN (125 kips).

Horizontal loading of 400 kN (90 kips) produced stresses as high as 310 MPa (45,000 psi) in the base cross frame member at a 3.1-m (120-in) support operating height. Extrapolation of these data suggests that the maximum horizontal loading capability for the base cross frame member at the 3.1-m (120-in) operating height is approximately 934 kN (210 kips), assuming a 690-MPa (100,000-psi) yield strength. At the 3.6-m (140-in) height, horizontal loading of 445 kN (100 kips) produced stresses as high as 393 MPa (57,000 psi). Extrapolation of these data suggests that the maximum horizontal loading capability for the cross frame member at the 3.6-m (140-in) operating height is approximately 778 kN (175 kips).

This analysis is conducted for full canopy and base contact. Eccentric load conditions on the crawler frame or canopy did not dramatically increase measured component strains.

OTHER OPERATIONAL AND MAINTENANCE SAFETY CONSIDERATIONS

Any MRS will become unstable if any of the lemniscate pins fail. Since critical stresses can be developed within the range of possible horizontal and lateral loading, these pins should be periodically inspected. Additionally, before any of the lemniscate pins are removed, the canopy and lemniscate assembly should be supported to prevent both vertical and *horizontal* movement. Unrestrained movement of the canopy can result in serious injury or death.

Caution should be used when working around the support while it is pressurized. Oil leaking at these pressures can cause serious bodily damage. Likewise, pressure should be relieved before any hydraulic component is removed.

COMPARISON OF MOBILE ROOF SUPPORTS WITH TIMBER POSTS

The most obvious difference between MRS's and conventional timber posts is their size and effective roof coverage. Roof coverage depends on the manufacturer and support model, ranging from 3.3 to 7.9 m^2 (35 to 85 ft^2). In comparison, a wood post will provide less than 0.1 m^2 (1 ft^2) of roof coverage; thus, several timber posts are required to replace a single MRS.

MRS's can provide an active load of up to 4,448 kN (500 tons) to the mine roof; wood posts are strictly passive supports. The load-bearing capacity of one MRS is about the same as six 20-cm (8-in) diameter hardwood posts, as shown in figure 30. The stiffness of an MRS varies by support design and is height-dependent for a specific support. In general, an MRS operating at less than 75% of its maximum height is stiffer than a single 20-cm (8-in) diameter post with no headboard or two 20-cm (8-in) diameter posts with headboards. Figure 31 compares the stiffness of the Fletcher and VAMT supports with that of conventional timber posts and wood cribs. Comparisons with smaller diameter posts can be made by reducing the stiffness of the post in proportion to the reduction in cross-sectional area.

Another significant advantage of an MRS is that it will continue to provide close to its full rated capacity after reaching yield load and can maintain this load capacity until the full leg stroke is exhausted. Thus, whereas MRS's can provide support through a meter or more of closure, timber posts can fail at less than 2.5 cm (1 in) of convergence and have no residual strength after failure.

MRS's are also much better suited than timber posts to handle eccentric load conditions caused by horizontal and lateral roof or floor movements, gob loading, and rib rolls, which are common during pillar extraction and often kick out breaker and turn posts. In general, timber posts suffer reduced stability for anything but pure axial (vertical) loads.

CONCLUSIONS

Full-scale testing of MRS's at the Strategic Structures Testing Laboratory provided a wealth of information pertaining to their performance capabilities and limitations. The tests were conducted in the unique mine roof simulator load frame under controlled conditions that simulate in-service load conditions.

The basic design of the VAMT breaker line support and the Fletcher MRS tested in this study is similar. Design differences that impacted support performance included the lemniscate assembly, the canopy construction, and the leg cylinder design.

The VAMT support incorporated a tilt frame with hydraulic cylinders to control horizontal and lateral loading; the Fletcher support utilized rigid lemniscate links to resist horizontal and lateral loading. The tilt concept limits stress development in the support structure, but permits greater translation of the canopy relative to the base, thereby allowing greater roof movements to occur, particularly when the hydraulic tilt cylinders have yielded. The advantages and disadvantages of these designs from a ground control perspective have not been evaluated.

Differences in the leg cylinder design caused most of the differences in support performance. The Fletcher support utilized a three-stage leg cylinder; the VAMT support, a two-stage leg cylinder. Consequences of the three-stage leg design were (1) reduced support stiffness, (2) greater reductions in setting force when both the bottom *and* middle stages are fully extended, and (3) larger unrecorded roof movements, particularly when both stages are fully extended. The advantage of the three-stage leg design is greater operating range, providing a lower support profile for transporting and tramming underground.

A critical issue pertaining to the measurement of support loading and loading rate is the effect of the staging of the leg cylinders. When the bottom stage of the leg cylinders is fully extended, the dial pressure gauges do not respond to increases in support load until the setting force established in the bottom stage is overcome by pressure development in the upper stages. The unrecorded roof load is greater at high setting pressures and is minimized at low setting pressures. Operationally, the bottom stage will be fully extended when the support is first raised to a height that exceeds the bottom stage stroke and, on subsequent cycles, whenever a new maximum operating height is established. Therefore, when possible, it is recommended that the support be taken initially to a location with a height greater than the expected operating height during pillar extraction, and fully raised. This will eliminate the problem of unrecorded roof loading. However, if this practice is followed, the support should be lowered as little as possible when moving the support to the section and during cycle changes. If the support is lowered sufficiently to cause the bottom stage to fully collapse, the probability of unrecorded roof loading will increase.

Setting forces also greatly depend on leg cylinder staging and are diminished by as much as 70% for the Fletcher support with three-stage leg cylinders when the bottom and middle stages are fully extended. Setting pressure as measured by the dial gauges will not always reflect the true setting force. The same circumstances that cause unrecorded roof loading also cause diminished setting forces. It is desirable to avoid diminished setting forces because the effectiveness of the support to act as a breaker line for roof caving may be reduced for low setting forces. When comparing supports of different design, it is important to remember that the smaller diameter leg cylinder will provide less setting force for the same hydraulic pressure than supports with larger diameter leg cylinders. This is one reason that the VAMT support operates at higher pump pressure than the Fletcher support.

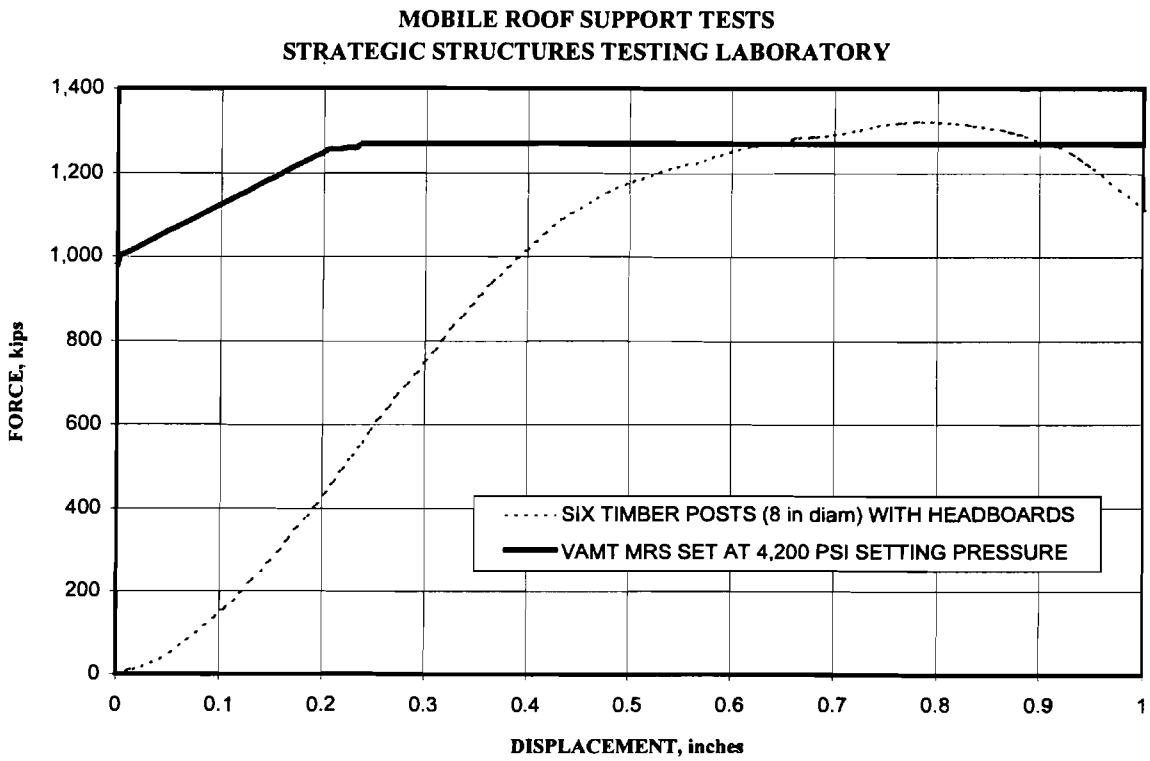

Figure 30.—One VAMT support provides about the same capacity as six high-quality timber posts.

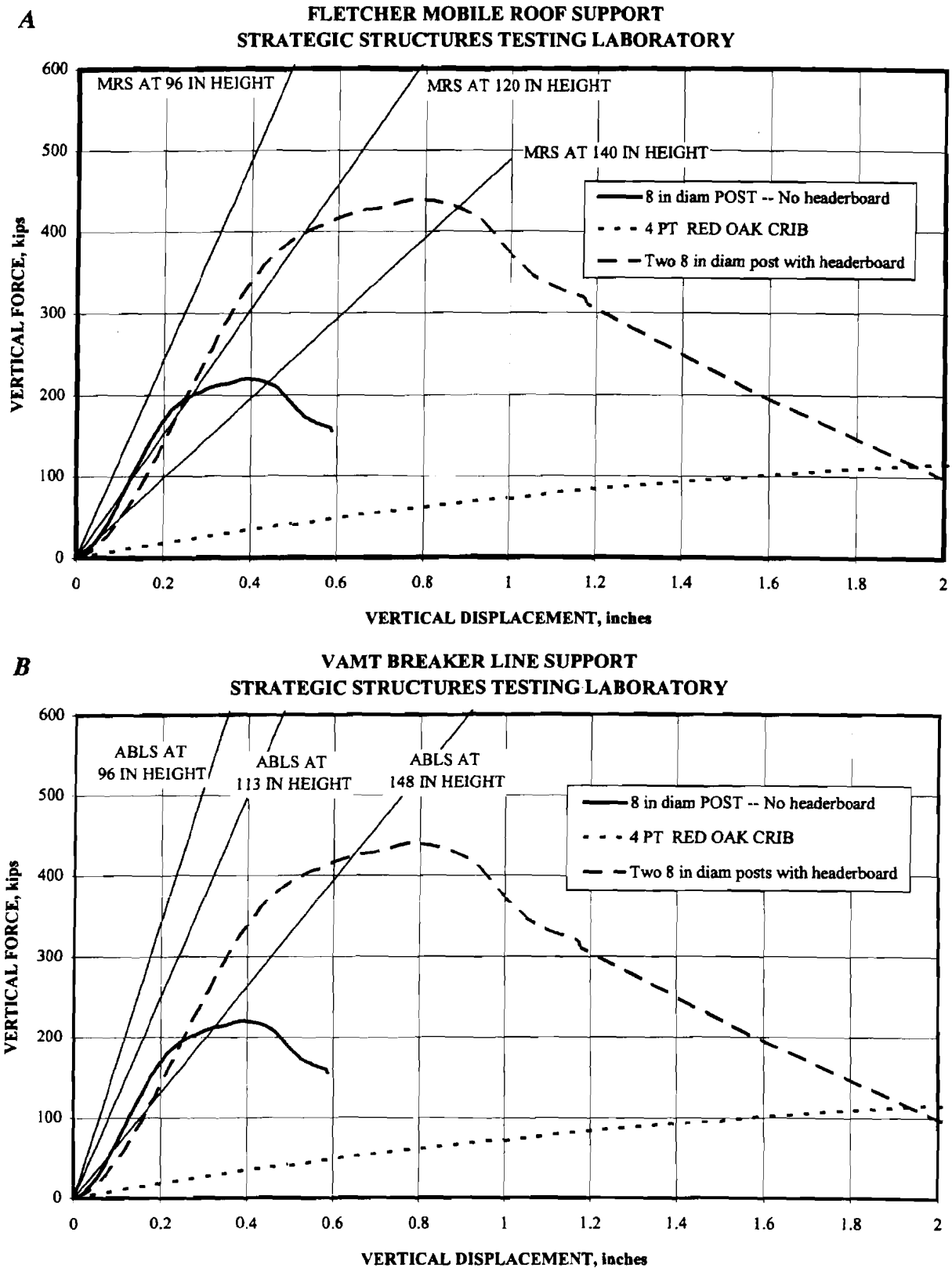

Figure 31.—Comparison of support stiffness with that of conventional timber posts. *A*, Fletcher support; *B*, VAMT support.

Both the Fletcher and VAMT supports were found to be structurally sound for *typical* load conditions. The canopy is likely to be the most highly stressed component on the VAMT support for most load conditions. Partial contact can cause stresses as high as 690 MPa (100,000 psi).

When horizontal or lateral loading is present, the lemniscate assembly and cross frame between the base crawler frames are likely to be the most highly stressed parts of the Fletcher support. Lateral loads in excess of 556 kN (125 kips) can cause damage to the bottom lemniscate link, and horizontal loads in excess of 778 kN (175 kips) can cause damage to the cross frame member. Unfortunately, there is no way to assess the magnitude of horizontal and lateral loads underground without installing additional instrumentation on the support.

The aligning cylinder on the VAMT support was damaged when it was yielded in compression by approximately 13 cm (5 in) of horizontal displacement of the canopy relative to the base. The probability of such large horizontal displacements during underground use is not known, but it is likely that this is an extreme load condition that will *not* occur during *normal* mining cycles. The cause of the failure was not satisfactorily determined. The damaged cylinder was replaced, and subsequent tests at less-than-yield pressure were conducted without any failures.

Because any support is unstable if the lemniscate link pins fail, all supports should be periodically inspected for damage or excessive deformation in the pin clevises. Furthermore, the canopy should be supported to prevent vertical and horizontal movement prior to removal or repair of an any lemniscate pin, regardless of the support manufacturer.

MRS's provide superior supporting capabilities compared with conventional timber posts. Each mobile support has a load-bearing capacity of approximately six timber posts and equivalent stiffness to two or more posts. MRS's provide significantly greater roof coverage and are much more stable for the types of eccentric loading that is common during pillar extraction. Furthermore, the active loading capability provides a more effective breaker line by minimizing initial roof movements that can lead to roof instability or caving inby the supports.

• ☆U.S. GOVERNMENT PRINTING OFFICE: 1997-508-248